REPORT DOCUMENTATION PAGE

AFRL-SR-BL-TR-98-

0785

1. AGENCY USE ONLY (Leave Blank)	2. REPORT DATE	3. REPORT TYPE AND DATES COVERED
	December, 1994	Final

4. TITLE AND SUBTITLE
USAF Summer Research Program - 1994 High School Apprenticeship Program Final Reports, Volume 15A, Wright Laboratory

5. FUNDING NUMBERS

6. AUTHORS
Gary Moore

7. PERFORMING ORGANIZATION NAME(S) AND ADDRESS(ES)
Research and Development Labs, Culver City, CA

8. PERFORMING ORGANIZATION REPORT NUMBER

9. SPONSORING/MONITORING AGENCY NAME(S) AND ADDRESS(ES)
AFOSR/NI
4040 Fairfax Dr, Suite 500
Arlington, VA 22203-1613

10. SPONSORING/MONITORING AGENCY REPORT NUMBER

11. SUPPLEMENTARY NOTES
Contract Number: F49620-93-C-0063

12a. DISTRIBUTION AVAILABILITY STATEMENT
Approved for Public Release

12b. DISTRIBUTION CODE

13. ABSTRACT *(Maximum 200 words)*
The United States Air Force High School Apprenticeship Program's (USAF- HSAP) purpose is to place outstanding high school students whose interests are in the areas of mathematics, engineering, and science to work in a laboratory environment. The students selected to participate in the program work in an Air Force Laboratory for a duration of 8 weeks during their summer vacation.

14. SUBJECT TERMS
AIR FORCE HIGH SCHOOL APPRENTICESHIP PROGRAM, APPRENTICEDHIP, AIR FORCE RESEARCH, AIR FORCE, ENGINEERING, LABORATORIES, REPORTS, SCHOOL, STUDENT, SUMMER, UNIVERSITIES

15. NUMBER OF PAGES

16. PRICE CODE

17. SECURITY CLASSIFICATION OF REPORT	18. SECURITY CLASSIFICATION OF THIS PAGE	19. SECURITY CLASSIFICATION OF ABSTRACT	20. LIMITATION OF ABSTRACT
Unclassified	Unclassified	Unclassified	UL

UNITED STATES AIR FORCE

SUMMER RESEARCH PROGRAM -- 1994

HIGH SCHOOL APPRENTICESHIP PROGRAM FINAL REPORTS

VOLUME 15A

WRIGHT LABORATORY

RESEARCH & DEVELOPMENT LABORATORIES

5800 Uplander Way

Culver City, CA 90230-6608

Program Director, RDL
Gary Moore

Program Manager, AFOSR
Major David Hart

Program Manager, RDL
Scott Licoscos

Program Administrator, RDL
Gwendolyn Smith

Program Administrator, RDL
Johnetta Thompson

Submitted to:

AIR FORCE OFFICE OF SCIENTIFIC RESEARCH

Bolling Air Force Base

Washington, D.C.

December 1994

HSAP FINAL REPORT TABLE OF CONTENTS i-xiv

<u>APPENDICIES:</u>

HSAP FINAL REPORTS

PREFACE

Reports in this volume are numbered consecutively beginning with number 1. Each report is paginated with the report number followed by consecutive page numbers, e.g., 1-1, 1-2, 1-3; 2-1, 2-2, 2-3.

Due to its length, Volume 15 is bound in two parts, 15A and 15B. Volume 15A contains #1-26. Volume 15B contains reports #27-52. The Table of Contents for Volume 15 is included in both parts.

This document is one of a set of 16 volumes describing the 1994 AFOSR Summer Research Program. The following volumes comprise the set:

VOLUME	TITLE
1	Program Management Report
	Summer Faculty Research Program (SFRP) Reports
2A & 2B	Armstrong Laboratory
3A & 3B	Phillips Laboratory
4	Rome Laboratory
5A & 5B	Wright Laboratory
6	Arnold Engineering Development Center, Frank J. Seiler Research Laboratory, and Wilford Hall Medical Center
	Graduate Student Research Program (GSRP) Reports
7	Armstrong Laboratory
8	Phillips Laboratory
9	Rome Laboratory
10	Wright Laboratory
11	Arnold Engineering Development Center, Frank J. Seiler Research Laboratory, and Wilford Hall Medical Center
	High School Apprenticeship Program (HSAP) Reports
12A & 12B	Armstrong Laboratory
13	Phillips Laboratory
14	Rome Laboratory
15A&15B	Wright Laboratory
16	Arnold Engineering Development Center

SRP Final Report Table of Contents

SRP Final Report Table of Contents

SRP Final Report Table of Contents

SRP Final Report Table of Contents

SRP Final Report Table of Contents

SRP Final Report Table of Contents

SRP Final Report Table of Contents

SRP Final Report Table of Contents

SRP Final Report Table of Contents

Author	University/Institution Report Title	Arnold Engineering Development Center Directorate	Vol-Page
Ryan B Bond	Tullahoma High School , Tullahoma , TN Modeling Engine Test Facility Cells in Vissim	Sverdrup	16 - 1
Robert B Cassady	Coffee County Cen High School , Manchester , TN Mach-Flow Angularity Probe Calibration	Calspan	16 - 2
Thomas L Clouse	Coffee County Central HS , Manchester , TN Workstation Inventory Control Program	Sverdrup	16 - 3
Michael L Fann	Tullahoma High School , Tullahoma , TN The Conversion of Millivolts Measured from Thermoc	Sverdrup	16 - 4
Derek E Geeting	Shelbyville Central High , Shelbyville , TN Lighting Calculation Study and Software Evaluation	SSI	16 - 5
Jennifer A Groff	Franklin County Sr High School , Winchester , TN The Use of Labview for Serial Data Transmission	Sverdrup	16 - 6
James J Lemmons	Coffee County Central HS , Manchester , TN Out of Band Filter Calibration Technology Project	Bionetics	16 - 7
Lana L Matthews	Coffee County Central HS , Manchester , TN A Study of Hydrocarbon Combustion: Stoichiometry	Sverdrup	16 - 8
Steve G Pugh	Shelbyville Central HS , Shelbyville , TN An Analytic Capability for Predicting Sability of	Sverdrup	16 - 9
Kristopher S Ray	Shelbyville Central High Schoo , Shelbyville , TN Power Systems Analysis	SSI	16 - 10

1. INTRODUCTION

The Summer Research Program (SRP), sponsored by the Air Force Office of Scientific Research (AFOSR), offers paid opportunities for university faculty, graduate students, and high school students to conduct research in U.S. Air Force research laboratories nationwide during the summer.

Introduced by AFOSR in 1978, this innovative program is based on the concept of teaming academic researchers with Air Force scientists in the same disciplines using laboratory facilities and equipment not often available at associates' institutions.

AFOSR also offers its research associates an opportunity, under the Summer Research Extension Program (SREP), to continue their AFOSR-sponsored research at their home institutions through the award of research grants. In 1994 the maximum amount of each grant was increased from $20,000 to $25,000, and the number of AFOSR-sponsored grants decreased from 75 to 60. A separate annual report is compiled on the SREP.

The Summer Faculty Research Program (SFRP) is open annually to approximately 150 faculty members with at least two years of teaching and/or research experience in accredited U.S. colleges, universities, or technical institutions. SFRP associates must be either U.S. citizens or permanent residents.

The Graduate Student Research Program (GSRP) is open annually to approximately 100 graduate students holding a bachelor's or a master's degree; GSRP associates must be U.S. citizens enrolled full time at an accredited institution.

The High School Apprentice Program (HSAP) annually selects about 125 high school students located within a twenty mile commuting distance of participating Air Force laboratories.

The numbers of projected summer research participants in each of the three categories are usually increased through direct sponsorship by participating laboratories.

AFOSR's SRP has well served its objectives of building critical links between Air Force research laboratories and the academic community, opening avenues of communications and forging new research relationships between Air Force and academic technical experts in areas of national interest; and strengthening the nation's efforts to sustain careers in science and engineering. The success of the SRP can be gauged from its growth from inception (see Table 1) and from the favorable responses the 1994 participants expressed in end-of-tour SRP evaluations (Appendix B).

AFOSR contracts for administration of the SRP by civilian contractors. The contract was first awarded to Research & Development Laboratories (RDL) in September 1990. After completion of the 1990 contract, RDL won the recompetition for the basic year and four 1-year options.

2. PARTICIPATION IN THE SUMMER RESEARCH PROGRAM

The SRP began with faculty associates in 1979; graduate students were added in 1982 and high school students in 1986. The following table shows the number of associates in the program each year.

Table 1: SRP Participation, by Year

YEAR	Number of Participants			TOTAL
	SFRP	GSRP	HSAP	
1979	70			70
1980	87			87
1981	87			87
1982	91	17		108
1983	101	53		154
1984	152	84		236
1985	154	92		246
1986	158	100	42	300
1987	159	101	73	333
1988	153	107	101	361
1989	168	102	103	373
1990	165	121	132	418
1991	170	142	132	444
1992	185	121	159	464
1993	187	117	136	440
1994	192	117	133	442

Beginning in 1993, due to budget cuts, some of the laboratories weren't able to afford to fund as many associates as in previous years; in one case a laboratory did not fund <u>any</u> additional associates. However, the table shows that, overall, the number of participating associates increased this year because two laboratories funded more associates than they had in previous years.

3. RECRUITING AND SELECTION

The SRP is conducted on a nationally advertised and competitive-selection basis. The advertising for faculty and graduate students consisted primarily of the mailing of 8,000 44-page SRP brochures to chairpersons of departments relevant to AFOSR research and to administrators of grants in accredited universities, colleges, and technical institutions. Historically Black Colleges and Universities (HBCUs) and Minority Institutions (MIs) were included. Brochures also went to all participating USAF laboratories, the previous year's participants, and numerous (over 600 annually) individual requesters.

Due to a delay in awarding the new contract, RDL was not able to place advertisements in any of the following publications in which the SRP is normally advertised: *Black Issues in Higher Education, Chemical & Engineering News, IEEE Spectrum* and *Physics Today*.

High school applicants can participate only in laboratories located no more than 20 miles from their residence. Tailored brochures on the HSAP were sent to the head counselors of 180 high schools in the vicinity of participating laboratories, with instructions for publicizing the program in their schools. High school students selected to serve at Wright Laboratory's Armament Directorate (Eglin Air Force Base, Florida) serve eleven weeks as opposed to the eight weeks normally worked by high school students at all other participating laboratories.

Each SFRP or GSRP applicant is given a first, second, and third choice of laboratory. High school students who have more than one laboratory or directorate near their homes are also given first, second, and third choices.

Laboratories make their selections and prioritize their nominees. AFOSR then determines the number to be funded at each laboratory and approves laboratories' selections.

Subsequently, laboratories use their own funds to sponsor additional candidates. Some selectees do not accept the appointment, so alternate candidates are chosen. This multi-step selection procedure results in some candidates being notified of their acceptance after scheduled deadlines. The total applicants and participants for 1994 are shown in this table.

Table 2: 1994 Applicants and Participants

PARTICIPANT CATEGORY	TOTAL APPLICANTS	SELECTEES	DECLINING SELECTEES
SFRP (HBCU/MI)	600 (90)	192 (16)	30 (7)
GSRP (HBCU/MI)	322 (11)	117 (6)	11 (0)
HSAP	562	133	14
TOTAL	1484	442	55

4. SITE VISITS

During June and July of 1994, representatives of both AFOSR/NI and RDL visited each participating laboratory to provide briefings, answer questions, and resolve problems for both laboratory personnel and participants. The objective was to ensure that the SRP would be as constructive as possible for all participants. Both SRP participants and RDL representatives found these visits beneficial. At many of the laboratories, this was the only opportunity for all participants to meet at one time to share their experiences and exchange ideas.

5. HISTORICALLY BLACK COLLEGES AND UNIVERSITIES AND MINORITY INSTITUTIONS (HBCU/MIs)

In previous years, an RDL program representative visited from seven to ten different HBCU/MIs to promote interest in the SRP among the faculty and graduate students. Due to the late contract award date (January 1994) no time was available to visit HBCU/MIs this past year.

In addition to RDL's special recruiting efforts, AFOSR attempts each year to obtain additional funding or use leftover funding from cancellations the past year to fund HBCU/MI associates. This year, seven HBCU/MI SFRPs declined after they were selected. The following table records HBCU/MI participation in this program.

Table 3: SRP HBCU/MI Participation, by Year

YEAR	SFRP		GSRP	
	Applicants	Participants	Applicants	Participants
1985	76	23	15	11
1986	70	18	20	10
1987	82	32	32	10
1988	53	17	23	14
1989	39	15	13	4
1990	43	14	17	3
1991	42	13	8	5
1992	70	13	9	5
1993	60	13	6	2
1994	90	16	11	6

6. SRP FUNDING SOURCES

Funding sources for the 1994 SRP were the AFOSR-provided slots for the basic contract and laboratory funds. Funding sources by category for the 1994 SRP selected participants are shown here.

Table 4: 1994 SRP Associate Funding

FUNDING CATEGORY	SFRP	GSRP	HSAP
AFOSR Basic Allocation Funds	150	98*1	121*2
USAF Laboratory Funds	37	19	12
HBCU/MI By AFOSR (Using Procured Addn'l Funds)	5	0	0
TOTAL	192	117	133

*1 - 100 were selected, but two canceled too late to be replaced.
*2 - 125 were selected, but four canceled too late to be replaced.

7. COMPENSATION FOR PARTICIPANTS

Compensation for SRP participants, per five-day work week, is shown in this table.

Table 5: 1994 SRP Associate Compensation

PARTICIPANT CATEGORY	1991	1992	1993	1994
Faculty Members	$690	$718	$740	$740
Graduate Student (Master's Degree)	$425	$442	$455	$455
Graduate Student (Bachelor's Degree)	$365	$380	$391	$391
High School Student (First Year)	$200	$200	$200	$200
High School Student (Subsequent Years)	$240	$240	$240	$240

The program also offered associates whose homes were more than 50 miles from the laboratory an expense allowance (seven days per week) of $50/day for faculty and $37/day for graduate students.

Transportation to the laboratory at the beginning of their tour and back to their home destinations at the end was also reimbursed for these participants. Of the combined SFRP and GSRP associates, 58% (178 out of 309) claimed travel reimbursements at an average round-trip cost of $860.

Faculty members were encouraged to visit their laboratories before their summer tour began. All costs of these orientation visits were reimbursed. Forty-one percent (78 out of 192) of faculty associates took orientation trips at an average cost of $498. Many faculty associates noted on their evaluation forms that due to the late notice of acceptance into the 1994 SRP (caused by the late award in January 1994 of the contract) there wasn't enough time to attend an orientation visit prior to their tour start date. In 1993, 58 % of SFRP associates took orientation visits at an average cost of $685.

Program participants submitted biweekly vouchers countersigned by their laboratory research focal point, and RDL issued paychecks so as to arrive in associates' hands two weeks later.

HSAP program participants were considered actual RDL employees, and their respective state and federal income tax and Social Security were withheld from their paychecks. By the nature of their independent research, SFRP and GSRP program participants were considered to be consultants or independent contractors. As such, SFRP and GSRP associates were responsible for their own income taxes, Social Security, and insurance.

8. CONTENTS OF THE 1994 REPORT

The complete set of reports for the 1994 SRP includes this program management report augmented by fifteen volumes of final research reports by the 1994 associates as indicated below:

Table 6: 1994 SRP Final Report Volume Assignments

	VOLUME		
LABORATORY	SFRP	GSRP	HSAP
Armstrong	2	7	12
Phillips	3	8	13
Rome	4	9	14
Wright	5A, 5B	10	15
AEDC, FJSRL, WHMC	6	11	16

AEDC = Arnold Engineering Development Center
FJSRL = Frank J. Seiler Research Laboratory
WHMC = Wilford Hall Medical Center

APPENDIX A -- PROGRAM STATISTICAL SUMMARY

A. Colleges/Universities Represented

Selected SFRP and GSRP associates represent 158 different colleges, universities, and institutions.

B. States Represented

SFRP -Applicants came from 46 states plus Washington D.C. and Puerto Rico. Selectees represent 40 states.

GSRP - Applicants came from 46 states and Puerto Rico. Selectees represent 34 states.

HSAP - Applicants came from fifteen states. Selectees represent ten states.

C. Academic Disciplines Represented

The academic disciplines of the combined 192 SFRP associates are as follows:

Electrical Engineering	22.4%
Mechanical Engineering	14.0%
Physics: General, Nuclear & Plasma	12.2%
Chemistry & Chemical Engineering	11.2%
Mathematics & Statistics	8.1%
Psychology	7.0%
Computer Science	6.4%
Aerospace & Aeronautical Engineering	4.8%
Engineering Science	2.7%
Biology & Inorganic Chemistry	2.2%
Physics: Electro-Optics & Photonics	2.2%
Communication	1.6%
Industrial & Civil Engineering	1.6%
Physiology	1.1%
Polymer Science	1.1%
Education	0.5%
Pharmaceutics	0.5%
Veterinary Medicine	0.5%
TOTAL	100%

Table A-1. Total Participants

Number of Participants	
SFRP	192
GSRP	117
HSAP	133
TOTAL	442

Table A-2. Degrees Represented

Degrees Represented			
	SFRP	GSRP	TOTAL
Doctoral	189	0	189
Master's	3	47	50
Bachelor's	0	70	70
TOTAL	192	117	309

Table A-3. SFRP Academic Titles

Academic Titles	
Assistant Professor	74
Associate Professor	63
Professor	44
Instructor	5
Chairman	1
Visiting Professor	1
Visiting Assoc. Prof.	1
Research Associate	3
TOTAL	192

Table A-4. Source of Learning About SRP

SOURCE	SFRP		GSRP	
	Applicants	Selectees	Applicants	Selectees
Applied/participated in prior years	26%	37%	10%	13%
Colleague familiar with SRP	19%	17%	12%	12%
Brochure mailed to institution	32%	18%	19%	12%
Contact with Air Force laboratory	15%	24%	9%	12%
Faculty Advisor (GSRPs Only)	--	--	39%	43%
Other source	8%	4%	11%	8%
TOTAL	100%	100%	100%	100%

Table A-5. Ethnic Background of Applicants and Selectees

	SFRP		GSRP		HSAP	
	Applicants	Selectees	Applicants	Selectees	Applicants	Selectees
American Indian or Native Alaskan	0.2%	0%	1%	0%	0.4%	0%
Asian/Pacific Islander	30%	20%	6%	8%	7%	10%
Black	4%	1.5%	3%	3%	7%	2%
Hispanic	3%	1.9%	4%	4.5%	11%	8%
Caucasian	51%	63%	77%	77%	70%	75%
Preferred not to answer	12%	14%	9%	7%	4%	5%
TOTAL	100%	100%	100%	100%	99%	100%

Table A-6. Percentages of Selectees receiving their 1st, 2nd, or 3rd Choices of Directorate

	1st Choice	2nd Choice	3rd Choice	Other Than Their Choice
SFRP	70%	7%	3%	20%
GSRP	76%	2%	2%	20%

APPENDIX B -- SRP EVALUATION RESPONSES

1. OVERVIEW

Evaluations were completed and returned to RDL by four groups at the completion of the SRP. The number of respondents in each group is shown below.

Table B-1. Total SRP Evaluations Received

Evaluation Group	Responses
SFRP & GSRPs	275
HSAPs	116
USAF Laboratory Focal Points	109
USAF Laboratory HSAP Mentors	54

All groups indicate near-unanimous enthusiasm for the SRP experience.

Typical comments from 1994 SRP associates are:

> "[The SRP was an] excellent opportunity to work in state-of-the-art facility with top-notch people."

> "[The SRP experience] enabled exposure to interesting scientific application problems; enhancement of knowledge and insight into 'real-world' problems."

> "[The SRP] was a great opportunity for resourceful and independent faculty [members] from small colleges to obtain research credentials."

> "The laboratory personnel I worked with are tremendous, both personally and scientifically. I cannot emphasize how wonderful they are."

> "The one-on-one relationship with my mentor and the hands on research experience improved [my] understanding of physics in addition to improving my library research skills. Very valuable for [both] college and career!"

Typical comments from laboratory focal points and mentors are:

> "This program [AFOSR - SFRP] has been a 'God Send' for us. Ties established with summer faculty have proven invaluable."

> "Program was excellent from our perspective. So much was accomplished that new options became viable "

> "This program managed to get around most of the red tape and 'BS' associated with most Air Force programs. Good Job!"

> "Great program for high school students to be introduced to the research environment. Highly educational for others [at laboratory]."

> "This is an excellent program to introduce students to technology and give them a feel for [science/engineering] career fields. I view any return benefit to the government to be 'icing on the cake' and have usually benefitted."

The summarized recommendations for program improvement from both associates and laboratory personnel are listed below (Note: basically the same as in previous years.)

A. Better preparation on the labs' part prior to associates' arrival (i.e., office space, computer assets, clearly defined scope of work).

B. Laboratory sponsor seminar presentations of work conducted by associates, and/or organized social functions for associates to collectively meet and share SRP experiences.

C. Laboratory focal points collectively suggest more AFOSR allocated associate positions, so that more people may share in the experience.

D. Associates collectively suggest higher stipends for SRP associates.

E. Both HSAP Air Force laboratory mentors and associates would like the summer tour extended from the current 8 weeks to either 10 or 11 weeks; the groups state it takes 4-6 weeks just to get high school students up-to-speed on what's going on at laboratory. (Note: this same arguement was used to raise the faculty and graduate student participation time a few years ago.)

2. 1994 USAF LABORATORY FOCAL POINT (LFP) EVALUATION RESPONSES

The summarized results listed below are from the 109 LFP evaluations received.

1. LFP evaluations received and associate preferences:

Table B-2. Air Force LFP Evaluation Responses (By Type)

		How Many Associates Would You Prefer To Get ? (% Response)											
		SFRP				GSRP (w/Univ Professor)				GSRP (w/o Univ Professor)			
Lab	Evals Recv'd	0	1	2	3+	0	1	2	3+	0	1	2	3+
AEDC	10	30	50	0	20	50	40	0	10	40	60	0	0
AL	44	34	50	6	9	54	34	12	0	56	31	12	0
FJSRL	3	33	33	33	0	67	33	0	0	33	67	0	0
PL	14	28	43	28	0	57	21	21	0	71	28	0	0
RL	3	33	67	0	0	67	0	33	0	100	0	0	0
WHMC	1	0	0	100	0	0	100	0	0	0	100	0	0
WL	46	15	61	24	0	56	30	13	0	76	17	6	0
Total	121	25%	43%	27%	4%	50%	37%	11%	1%	54%	43%	3%	0%

LFP Evaluation Summary. The summarized repsonses, by laboratory, are listed on the following page. LFPs were asked to rate the following questions on a scale from 1 (below average) to 5 (above average).

2. LFPs involved in SRP associate application evaluation process:
   a. Time available for evaluation of applications:
   b. Adequacy of applications for selection process:
3. Value of orientation trips:
4. Length of research tour:
5 a. Benefits of associate's work to laboratory:
   b. Benefits of associate's work to Air Force:
6. a. Enhancement of research qualifications for LFP and staff:
   b. Enhancement of research qualifications for SFRP associate:
   c. Enhancement of research qualifications for GSRP associate:
7. a. Enhancement of knowledge for LFP and staff:
   b. Enhancement of knowledge for SFRP associate:
   c. Enhancement of knowledge for GSRP associate:
8. Value of Air Force and university links:
9. Potential for future collaboration:
10. a. Your working relationship with SFRP:
    b. Your working relationship with GSRP:
11. Expenditure of your time worthwhile:

(Continued on next page)

12. Quality of program literature for associate:
13. a. Quality of RDL's communications with you:
    b. Quality of RDL's communications with associates:
14. Overall assessment of SRP:

Laboratory Focal Point Reponses to above questions

	AEDC	*AL*	*FJSRL*	*PL*	*RL*	*WHMC*	*WL*
# Evals Recv'd	10	32	3	14	3	1	46
Question #							
2	90 %	62 %	100 %	64 %	100 %	100 %	83 %
2a	**3.5**	**3.5**	4.7	4.4	4.0	4.0	**3.7**
2b	4.0	3.8	4.0	4.3	4.3	4.0	3.9
3	4.2	3.6	4.3	3.8	4.7	4.0	4.0
4	3.8	3.9	4.0	4.2	4.3	NO ENTRY	4.0
5a	4.1	4.4	4.7	4.9	4.3	3.0	4.6
5b	4.0	4.2	4.7	4.7	4.3	3.0	4.5
6a	**3.6**	4.1	**3.7**	4.5	4.3	**3.0**	4.1
6b	3.6	4.0	4.0	4.4	4.7	3.0	4.2
6c	3.3	4.2	4.0	4.5	4.5	3.0	4.2
7a	3.9	4.3	4.0	4.6	4.0	3.0	4.2
7b	4.1	4.3	4.3	4.6	4.7	3.0	4.3
7c	3.3	4.1	4.5	4.5	4.5	5.0	4.3
8	4.2	4.3	5.0	4.9	4.3	5.0	4.7
9	3.8	4.1	4.7	5.0	4.7	5.0	4.6
10a	4.6	4.5	5.0	4.9	4.7	5.0	4.7
10b	4.3	4.2	5.0	4.3	5.0	5.0	4.5
11	4.1	4.5	4.3	4.9	4.7	4.0	4.4
12	4.1	3.9	4.0	4.4	4.7	3.0	4.1
13a	**3.8**	**2.9**	4.0	4.0	4.7	**3.0**	**3.6**
13b	**3.8**	**2.9**	4.0	4.3	4.7	**3.0**	**3.8**
14	4.5	4.4	5.0	4.9	4.7	4.0	4.5

3. 1994 SFRP & GSRP EVALUATION RESPONSES

The summarized results listed below are from the 275 SFRP/GSRP evaluations received.

Associates were asked to rate the following questions on a scale from
1 (below average) to 5 (above average)

1. The match between the laboratories research and your field:		4.6
2. Your working relationship with your LFP:		4.8
3. Enhancement of your academic qualifications:		4.4
4. Enhancement of your research qualifications:		4.5
5. Lab readiness for you: LFP, task, plan:		4.3
6. Lab readiness for you: equipment, supplies, facilities:		4.1
7. Lab resources:		4.3
8. Lab research and administrative support:		4.5
9. Adequacy of brochure and associate handbook:		4.3
10. RDL communications with you:		4.3
11. Overall payment procedures:		**3.8**
12. Overall assessment of the SRP:		4.7
13. a. Would you apply again?	Yes:	85%
b. Will you continue this or related research?	Yes:	95%
14. Was length of your tour satisfactory?	Yes:	86%
15. Percentage of associates who engaged in:		
a. Seminar presentation:		52%
b. Technical meetings:		32%
c. Social functions:		03%
d. Other		01%

16. Percentage of associates who experienced difficulties in:

a. Finding housing:	12%
b. Check Cashing:	03%

17. Where did you stay during your SRP tour?

a. At Home:	20%
b. With Friend:	06%
c. On Local Economy:	47%
d. Base Quarters:	10%

THIS SECTION FACULTY ONLY:

18. Were graduate students working with you? Yes: 23%

19. Would you bring graduate students next year? Yes: 56%

20. Value of orientation visit:

Essential:	29%
Convenient:	20%
Not Worth Cost:	01%
Not Used:	34%

THIS SECTION GRADUATE STUDENTS ONLY:

21. Who did you work with:

University Professor:	18%
Laboratory Scientist:	54%

4. 1994 USAF LABORATORY HSAP MENTOR EVALUATION RESPONSES

The summarized results listed below are from the 54 mentor evaluations received.

1. Mentor apprentice preferences:

Table B-3. Air Force Mentor Responses

		How Many Apprentices Would You Prefer To Get ?			
		HSAP Apprentices Preferred			
Laboratory	*# Evals Recv'd*	*0*	1	2	3+
AEDC	6	0	100	0	0
AL	17	29	47	6	18
PL	9	22	78	0	0
RL	4	25	75	0	0
WL	18	22	55	17	6
Total	**54**	**20%**	**71%**	**5%**	**5%**

Mentors were asked to rate the following questions on a scale from
1 (below average) to 5 (above average)

2. Mentors involved in SRP apprentice application evaluation process:
    a. Time available for evaluation of applications:
    b. Adequacy of applications for selection process:
3. Laboratory's preparation for apprentice:
4. Mentor's preparation for apprentice:
5. Length of research tour:
6. Benefits of apprentice's work to U.S. Air force:
7. Enhancement of academic qualifications for apprentice:
8. Enhancement of research skills for apprentice:
9. Value of U.S. Air Force/high school links:
10. Mentor's working relationship with apprentice:
11. Expenditure of mentor's time worthwhile:
12. Quality of program literature for apprentice:
13. a. Quality of RDL's communications with mentors:
    b. Quality of RDL's communication with apprentices:
14. Overall assessment of SRP:

	AEDC	*AL*	*PL*	*RL*	*WL*
# Evals Recv'd	**6**	**17**	**9**	**4**	**18**
Question #					
2	100 %	76 %	56 %	75 %	61 %
2a	4.2	4.0	**3.1**	**3.7**	**3.5**
2b	4.0	4.5	4.0	4.0	3.8
3	4.3	**3.8**	**3.9**	**3.8**	**3.8**
4	4.5	**3.7**	**3.4**	4.2	**3.9**
5	**3.5**	4.1	**3.1**	**3.7**	**3.6**
6	4.3	3.9	4.0	4.0	4.2
7	4.0	4.4	4.3	4.2	3.9
8	4.7	4.4	4.4	4.2	4.0
9	4.7	4.2	3.7	4.5	4.0
10	4.7	4.5	4.4	4.5	4.2
11	4.8	4.3	4.0	4.5	4.1
12	4.2	4.1	4.1	4.8	3.4
13a	**3.5**	**3.9**	**3.7**	4.0	**3.1**
13b	4.0	4.1	3.4	4.0	3.5
14	4.3	4.5	3.8	4.5	4.1

5. 1994 HSAP EVALUATION RESPONSES

The summarized results listed below are from the 116 HSAP evaluations received.

HSAP apprentices were asked to rate the following questions on a scale from 1 (below average) to 5 (above average)

1. Match of lab research to you interest:		3.9
2. Apprentices working relationship with their mentor and other lab scientists:		4.6
3. Enhancement of your academic qualifications:		4.4
4. Enhancement of your research qualifications:		4.1
5. Lab readiness for you: mentor, task, work plan.		3.7
6. Lab readiness for you: equipment supplies facilities		4.3
7. Lab resources: availability		4.3
8. Lab research and administrative support:		4.4
9. Adequacy of RDL's apprentice handbook and administrative materials:		4.0
10. Responsiveness of RDL's communications:		3.5
11. Overall payment procedures:		3.3
12. Overall assessment of SRP value to you:		4.5
13. Would you apply again next year?	Yes:	88%
14. Was length of SRP tour satisfactory?	Yes:	78%
15. Percentages of apprentices who engaged in:		
a. Seminar presentation:		48%
b. Technical meetings:		23%
c. Social functions:		18%

Thermal Stresses in Composite Materials

Christine M. Baker
Northmong High School
Cayton, OH

Final Report For:
High School Apprentice Program
Wright-Patterson Air Force Base

Sponsored by:
Air Force Office of Scientific Research
Bolling Air Force Base, DC

and

Wright Laboratory

August 1994

THERMAL STRESSES IN COMPOSITE MATERIALS

Christine M. Baker

Northmont High School

Abstract

The summer research program entailed not just one project, but a large variety of interesting activities. The primary concern was assisting Mr. Bryan Foos, of the FIVEC office in Wright Laboratory, with the research for his Ph.D. dissertation. His research involves the use of unintrusive extrinsic Fabry-Perot interferometric strain sensors embedded through the lamina thickness of a carbon epoxy composite material to monitor the transverse normal stress / strain. Mr. Foos is also running some complex FORTRAN computer programs on the Ohio State University Cray Supercomputer in order to validate the programs with actual experimentation. Some of the tasks completed this summer have included submitting the programs to the Cray Super computer and performing complex data manipulation from the extensive output produced from running these programs. Mr. Leonard Truett also requested help during the short duration this summer. Mr. Truett, of the FIVS office in Wright Laboratory, needed assistance with a massive amount of data using digital image processing. Other assignments have included writing an instruction manual for a photomicrographic camera and mastering the Nicolet data collection system to be used to acquire data during the testing in the TAVLAB (thermal and vibration lab).

THERMAL STRESSES IN COMPOSITE MATERIALS

Table of Contents

THERMAL STRESSES IN COMPOSITE MATERIALS

Christine M. Baker

I. Introduction

On the first day of the summer research program, Mr. Bryan Foos introduced the various tasks that were hoped to be accomplished during the eight week period. The tasks revolved around the various facets of his Ph.D. dissertation and research, which includes analytical, theoretical, and experimental research. Mr. Foos planned to take a trip to Portugal, as part of the NATO Advanced Studies Institute: Optical Fibre Metrology and Standards. In preparation for this conference, a photomicrographic camera would be used to photograph the fiber optic sensor that will eventually be used in the experimental portion of Mr. Foos' research. Also, the software Nicolet, a data acquisition system, was to be learned to help Mr. Foos with the experimentation portion of his research. There were also many FORTRAN computer programs which we had to run on the OSU Cray Supercomputer. Mr. Foos introduced me to the following computer systems during the eight week tour: DEC5000, Sun Spark Workstation, Macintosh II, and the IBM 386. The internet was to be used frequently for these programs, including ftp, telnet, and the Mosaic software. After running these programs, extensive data manipulation would have to occur in order to draw any valid conclusions from the data in the form of charts, spreadsheets, and graphs. Various software packages that were to be used for these tasks on the Macintosh and the IBM included Excel Spreadsheet and Cricket Graph.

In the first few days of the summer program, observation was the main activity. Since having primarily worked on an IBM in the past, the variety of computers was a

shock. After a short while, a good deal was learned, including operating both Macintosh and UNIX based computers. Within a few days, little to no assistance was needed in operating the computers or running the needed programs.

II. FORTRAN Programs on the Cray Supercomputer

A. Introduction

Mr. Foos planned to run two programs written by Dr. Greg Schoeppner of the Structures Division to determine the internal stresses in finite composite laminates, when subjected to inplane mechanical loading. The process for running these particular FORTRAN computer programs included inputting a batch file through one of the programs, then altering the output and running it through a much larger and complex program. While this process is very time consuming and meticulous, it is also very important to ensure that the data was flawless.

B. Discussion

The FORTRAN computer programs run by Mr. Foos form a grid across a one by one inch section of a test sample. The operator decides at what intervals to form this grid, which is made of x- and y-coordinates. Since most of the strain occurs near the edges of the sample, it is ideal to assign the coordinates so that they are more dense near the edge than in the center, where there is minimal strain. The elements formed by the grid consist of nodal points and these elements are numbered for easy reference. This grid of nodal points and elements is on a two dimensional surface. One then assigns a certain number of layers so that on each layer there is a grid identical to the grid on the surface. However, as the number of layers increased, the thickness of each layer decreased in order to maintain a total thickness of one inch. For each element, the output contains the strain

and stress for each element in that layer, i.e. if there are sixteen layers, then the output contains sixteen sets of strain and stress data for that layer element.

Mr. Foos had run the problem with two layers, however results had been inconclusive as well as obviously incorrect because the thickness direction needed to be discretizd into more than the two layers. He needed the program to be run with four, eight, sixteen, and thirty-two layers in order to find the exact point when the data became realistic. Also, he wanted to change the width of the specimen to one, two and three inches to see the affect on the output. Another variable that was added was the number of elements along the length and width of the grid. The number of elements along the length was alternated between two and four, and the two numbers of elements along the width were alternated between fourteen and twenty. These numbers are the numbers that were on either side of the major axis, so these amounts were actually doubled. This means that if twenty elements along the width was inputted, there were actually forty, with twenty positive and twenty negative.

The input for the programs became more extensive as the number of layers increased, and as the number of other variables increased. In addition, the amount of time needed on the Cray Supercomputer in order to run the program increased as the layers increased; time on the computer, unfortunately, is very expensive.

C. Methodology

The very first step was to get an account on the Sun Spark workstation located in Building 63 of Area B in the WL/FIVS branch (an account was already available on the Cray). Once this was completed, files were transferred from other computers using the ftp command, including sample data files for the first program and batch files for both of the programs. The batch files contain the information for how much memory to use, which

data file to use as input, and what to name the output file. Having samples of these files was helpful, so that one may copy the file for each run on the Cray, and only alter the needed data for the variables.

This data file was copied and altered for each of the separate combinations of variables that were needed, totaling fifty-six, on one of the screens that was opened on the workstation. Then another screen was opened to adjust the batch file. Before each run on the Cray, it was necessary to put which file to use as input, and where to put the output. Then another screen was opened to transfer these files to the Cray by ftp. Lastly, a screen was opened that was the Cray by Telnet. We would run the program there, then reverse the process and transfer the output files back to our local screen. The ftp command was a very quick and efficient way of completing this process. Stated simply, files were taken from the local computer, transferred, run on the Cray and then brought back as output.

These output files were large, but it was possible to do essentially the same steps to run the second program. Again there was a batch file, but this time a data file did not need to be created, because the output from the first program was the input, after a few changes. The second program took much more memory, especially the files with thirty-two layers, which could take up to eighteen minutes to run. The output from this second program was huge, so it was impractical to print out a hard copy. Instead, the data was altered, in order to reduce the printing time and paper waste.

III. Data Manipulation of Extensive Output

A. Introduction

The numbers from the output files mean nothing until they are normalized and graphed. As stated above, the output files from the last program were too large to be printed. Also, the printer was not connected to the Sun Spark Workstation, so the files needed to be transferred to another computer, then somehow condensed in order to be printed, then put into a Microsoft Excel file to be normalized. Then they would be copied into graphing software, usually Cricket Graph on the Macintosh.

B. Discussion and Methodology

The first task was to condense the data into an easily transferable and printable form. This was accomplished easily using the UNIX based VI Editor, which had been learned while manipulating the files in order to run them. The VI Editor, which seems complex when it is first being learned, is actually rather a very useful way of editing files. The data files were copied so that there would be an original, then the copies were edited. These changes consisted mostly of deletions in order to shrink the massive files. Next the data needed to be moved from the SUN onto a computer where it was possible to print. This was accomplished quite easily by transferring the files by FTP onto the personal computer of Mr. Foos. Once downloaded, these files were easy to print using the network printer.

These files were essentially lists of numbers. However, they were arranged in such a fashion that it was impossible to copy the files straight into a spreadsheet. These numbers had to be meticulously copied from the hard copies into a spreadsheet, using Microsoft Excel on the Macintosh II in Structures Division Building 45. Then the spreadsheet was programmed in order to normalize the data. This spreadsheet was easily transferable onto the Cricket Graph software. The stress / strain data was depicted against

the location of the particular nodal element on the y coordinate on the grid. In some of the graphs, the y-coordinate was normalized; this made it possible to overlay graphs of data of which the sample were different widths, because each different width of the samples has different y-coordinates.

IV. Digital Image Processing

Mr. Leonard Truett was working on a project involving the burning rates of methane, premixed flames with several different variables. Using Digital Image Processing, he had approximately 400 pictures of flames which he needed to measure in order to formulate the surface area. A grid was created, then the picture of the flame was overlaid and three points were then recorded on another computer.

The other computer was a laptop IBM, and the data was recorded using Excel. Excel was programmed so that three points could be entered and the surface area of the flame would be calculated. Since the work involved the use of two computers, it was difficult to complete the task alone. The help that was given to Mr. Truett was either entering the data points, or plotting the points and reading the data so that he could enter the points.

V. Photomicrography

A. Introduction

While Mr. Foos was preparing to attend the NATO Conference in Portugal, the occasion arose to use the photomicrographic camera. This camera was used to take the detailed shots needed of the microscopic fiber optic sensor. However, it was discovered that the camera was lacking directions. It only had a few pictures with several parts of the camera pointed out, and most of the pictures were not of the particular model in the laboratory.

After several exasperating experiences with it, eventually the mechanics of the camera were figured out. In order to help others using the camera, an instruction manual was written.

B. Discussion and Methodology

The main emphasis in this instruction manual, as in any manual, is to explain a piece of machinery one understands quite well to one who has never used it. First, the basic instructions of using the camera were written, such as loading the film and focusing the camera. Then more detailed information followed, including the manual operation of the camera from a control panel instead of pushing the buttons on the camera, as one would expect. Once the written information was complete, pictures were taken of the photomicrographic camera and the control panels. These were blown up, then inserted into the text. Also, the parts were numbered on the pictures so that the different components of the camera could be referred to in the text. The manual was then bound and is now a permanent addition to the laboratory manuals.

VI. Technical Library Research

A. Introduction

The Technical Library at Wright-Patterson AFB is in Building 22 Area B. This library contains many scientific journals, publications of seminars, dissertations, and other scientific publications. Many of the publications are on the shelves, while others are on microfilm or in storage. If one cannot find the things that they need, the staff will contact other libraries and bring the item to Wright-Patterson on inter-library loan.

B. Discussion and Methodology

Several days were spent in the Wright-Patterson Technical Library researching various topics not only for Mr. Foos, but for others as well. The first steps for researching, which were completed in advance by Dr. Schoeppner, include searches on the computer data bases that are in the library. Lists of articles, journal entries and papers organized by topic have general outlines of what is contained in each entry. These lists can then be printed and used to find the hard copies. After deciding which of the articles on the lists would be useful, which was done by Dr. Schoeppner, the next step is to look through the lists of journals available at the Wright-Patterson Technical Library. These articles can easily be found and copied. Others are available on microfilm, which is easy to copy, while still others can be retrieved from storage. The items that aren't available in the library can be requested by filling out the appropriate paper work.

VII. Nicolet

The Nicolet Multipro is a high speed data acquisition system used on the IBM. Mr. Foos is using it to collect data from the fiber optic sensors embedded through the thickness of the test coupons to measure transverse normal strain directly. The task was to learn the program and then either assist Mr. Foos in his actual experimentation or relay the information quickly on how to use the program for him to use himself. The program was actually pretty straightforward, because it was formatted in Windows style. There were thick manuals to pore through, and although operation the program was not difficult, the most challenging aspect was understanding the oscilloscope, because I had never used one before, except for a display in the laboratory.

VIII. Nontechnical Activities

In addition to learning a large amount of technical information in this program, there was a large amount of nontechnical knowledge acquired in the duration of the program. For example, every Wednesday there were Walleyball games after work, which is volleyball played inside a racquetball court. Frequently, after the games we would go running together. There was also the opportunity to acquire knowledge first hand of the intricate workings of committees, through the WL/IF Picnic Committee, of which Mr. Foos was in charge. Besides the endless array of phone calls and arranging meetings, there was ample opportunity to participate in and learn from the organizational skills of Mr. Foos and from his accomplished abilities of dealing with people in disagreement.

Near the end of the program, a problem arose with my AFROTC Type I scholarship. A medical discharge was issued for the reason of a history of headaches. The first action taken to help with re-obtaining the scholarship was to write a letter from Mr. Foos briefly outlining the type of work being done and how headaches have never interfered with the challenging tasks. After a request for a waiver was rejected by a medical review board, more action was needed to counter the unfortunate turn of events. With the help of Mr. Foos, several of the administrators were visited to ask for assistance in this matter. First, we went to Dr. George Kurylowich, of WL/FIVEC, who suggested some more letter writing, which was accomplished soon after. We then went to the office of Colonel Herklotz, who was unavailable due to a TDY trip so we spoke to Solomon Metres, of WL/FI. He knew of someone that might help, and said that he would contact him, and speak with Colonel Herklotz regarding this matter. Then we proceeded to the office of Colonel Herrelko, WL/CC, where we left a message regarding the matter. Unexpectedly, within twenty minutes we received a call to come and speak with him. After an hour and a half, Colonel Herrelko had made many calls around the nation and at

Wright-Patterson AFB to assist in this concern. This matter is still pending, and may not be resolved for a substantial period of time. We then spoke to Mr. George Kline (branch chief of WL/FIVE), and Mr. Dick Colclough, the division chief of WL/FIV, and then to Mr. Al Basso (who was also one of the walleyball players and avid runner), also of WL/FIV, to let them know what had transpired to date with the AFROTC scholarship and ask for advice on what to do.

IX. Conclusions

This eight week program was a very fun and interesting summer job, as well as a very educational experience. Besides learning a large amount of technical information, I also had a really enjoyable time with Mr. Foos, and with his friends on base. I feel that I will definitiely be more prepared than other first year college students in the use of a large variety of computers. This program is an excellent one, and I am very appreciative to Mr. Foos for the opportunities presented to me in the duration of the summer.

Analysis of a Three-Penetrator EPIC Calculation Using PATRAN

Jennifer R. Bautista
High School Apprentice
Warheads Branch, Computational Mechanics Section

Wright Laboratory Armament Directorate
WL/MNMW
Eglin AFB, FL 32542-5434

Final Report for:
High School Apprenticeship Program
Wright Laboratory Armament Directorate

Sponsored by:
Air Force Office of Scientific Research
Bolling Air Force Base, Washington, DC

August 1994

Analysis of a Three-Penetrator Concrete Penetration Using PATRAN

Jennifer R. Bautista
High School Apprentice
Warheads Branch, Computational Mechanics Section
WL/MNMW

Abstract

To investigate the effects of simultaneous impact of multiple penetrators into a concrete target, a scaled model of a Hardened Target Ordnance Package (HTOP) hard concrete penetration was modeled using the EPIC hydrocode. The intent of the calculation was to determine if a wave synergism would occur in the "tripak" problem, incurring more damage to the concrete target than a single penetrator might. The tripak problem was modeled using EPIC, and the output was processed, using PATRAN, into graphics noting pressure, stress, strain, damage, and temperature of the target at six intervals during the calculation.

Contents

Analysis of a Three-Penetrator EPIC Calculation Using PATRAN

Jennifer R. Bautista

Introduction

A hydrocode models physical problems by solving the equations of conservation of mass, momentum, and energy, subject to equations of state and constitutive laws that relate stress to strain. The EPIC hydrocode is used by members of the Computational Mechanics Section of the Warheads Branch to simulate warhead formation, impact, and response. This report documents my work with Mr. Nixon concerned with the analysis of a large 3D calculation of a three penetrator event. My project included the creation of detailed visual representations for stress, strain, pressure, damage, and temperature fields for the calculation. I also generated time history plots for data gathered at various locations through out the target and penetrators.

Tripak Test Setup

The "tripak" problem that was modeled using the EPIC hydrocode is a scaled model of the Hardened Target Ordnance Package (HTOP) which consists of three 270 lb. rocket boosted penetrators designed to impact and pierce concrete and other hard targets. In the event of failure of the dispense package, the penetrators would impact the target simultaneously in close proximity to each other. The problem was modeled to explore the possibility of wave synergisms that might occur in the penetration.

The tripak problem was not an exact scaled model of the HTOP package; the penetrators were approximately 1/6 HTOP scale, and although the results cannot be directly applied to HTOP performance, they provide useful qualitative information about multiple penetrator effects. The penetrators had a 6 caliber radius (CRH) tangent ogive nose with a button (0.234" diameter, 0.078" long, see Figure 1). HTOP also has a 6 CRH

nose shape but does not have a button. HTOP length to diameter (L/D) ratio is approximately 8:1, and the test items had L/D-9:4. The test projectiles were filled with an explosive simulant. The tripak configuration was housed in a thin aluminum canister (Figure 2), meant to facilitate the launch process. The targets were 3 feet thick concrete, and were poured in 30 inch diameter galvanized culvert pipes. The targets were designed to approximate semi-infinite blocks to the penetrators.

Shots were planned to be at 900 ft/sec, the delivery vehicle's terminal velocity, and at zero obliquity. The tripak was fired from a 155 mm Howitzer sleeved down to a 4 inch bore. The shot line was 10 to 20 feet from the target, and any velocity information was gathered using high speed video and radar. (See Figure 3)

The Calculation

The EPIC 94 calculation was run on Eglin AFB's Cray-YMP located at the Freeman Computing Sciences Center over a series of weeks; due to its complex nature, the calculation was stopped and started several times. The computation, involving 73030 nodes and 450000 elements, dealt with the impact from time 0 to 0.655711E-03 seconds. Output was requested at six of the 5420 cycles in the calculation: cycle 496 (time = 0.100050E-03), cycle 1544 (time = 0.229695E-03), cycle 1867 (time = 0.265205E-03), cycle 2822 (time = 0.371839E-03), cycle 3242 (time = 0.419568E-03), and 5420 (time = 0.655711E-03). The penetration was at 0 degrees obliquity to match the experiment. Calculations at other impact conditions could be made to study the effects of convergence or divergence of the warheads but were deemed as too expensive at this time. These data dumps were turned into pictures of the calculational geometry with contours of the appropriate data overlaid on this model. Time history data was written continuously during the calculation and this was used to generate time history plots of pressure at various locations in the problem. Two-dimensional axisymmetric calculations will be made to supplement this tripak computation.

Methodology

The EPIC hydrocode outputs two different types of neutral files for postprocessing in PATRAN: results files and model files. (Figure 4) The model files draw the geometry of the penetrator and target; the results files contain the information that draws the contours of pressure, stress, strain, damage, and temperature that occur in the target and penetrator. This particular calculation's output was extremely large; the files were processed through a program called *extr.f* , created by Mike Nixon, that extracted all internal information about nodes and elements, leaving the essential external nodes and elements. In PATRAN, the target was constructed according to the model file; for each category (pressure, stress, strain, damage, and temperature) the results file was referred to and the column number that corresponded to the category was specified. "AHIDE" was turned off, and the model was rendered to show the contours. For convenience in shortening a repetitive process a PATRAN session file can be created (Figure 5). For use in analysis, four different views of the model were created: -90, 0, 30 -30, -60 30 (Figures 6-9). A Silicon Graphics utility, *snapshot*, was used to capture *.rgb* files, the graphics displaying the model. A sequence of appropriate plots can be grouped together to form an animation using the SGI *movie* utility. This would show the progression of a variable during the calculation. All of these pictures are to be used by Mr. Nixon to do detailed analysis of the calculation and will be compared to actual data gathered during the experiment on range C-64.

Results and Conclusions

The results of the simulation and postprocessing: 102 color files detailing pressure, stress, strain, damage, and temperature; four files for pressure, stress, strain, and damage, and one file for temperature for each of the six cycles.

Conclusions drawn from analysis of the calculation: no apparent synergism occurs in the multiple penetrator impact. Obvious lines of radial damage occur in a triangular

pattern corresponding to the formation of the penetrators. Additional calculations may be performed to explore convergence or divergence of multiple penetrators. This scaled model is still under study and conclusions are preliminary; my mentor, Mike Nixon, and Lt. Kevin Conner, a test engineer from the Computational Mechanics Branch, will be preparing this study for inclusion in a forthcoming technical report on the tripak problem.

Acknowledgments

I owe many thanks to those responsible for giving me the opportunity to work in the lab for three summers and to those who provided so much assistance and guidance in my three years. Most of all, I'd like to thank my mentor, Mike Nixon, for his invaluable instruction, support and guidance. He truly is my mentor, in the truest sense of the word. I praise him for teaching us, as well as instilling in us a sense of responsibility and independence. My two "partners in crime" deserve thanks for all that they've given me; Mike Dooley and Josh Weaver made my summer truly enjoyable. Thanks to the Sverdrup contractors in our section, Bizhan Aref and Randy Anderson, for their help, friendship, and encouragement. I owe lots to the other members of our section, Dr. Bill Cook, John Collins, Ed Bradley, Dr. Harbans Sidhu, and our chief, Maj. Howard Gans. They helped tremendously. Kudos to the Air Force Research and Development Laboratories and Eglin AFB's HSAP program -- Don Harrison, Mike Deiler, Dr. Norm Klausutis, and Glenda Apel -- for the best three summers of my life. It's been great.

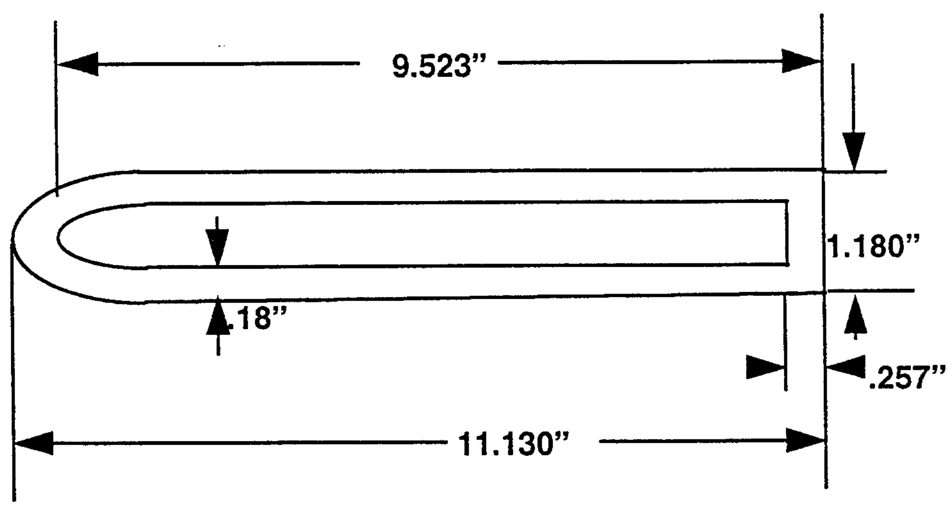

Figure One: Scaled HTOP Penetrator Dimensions

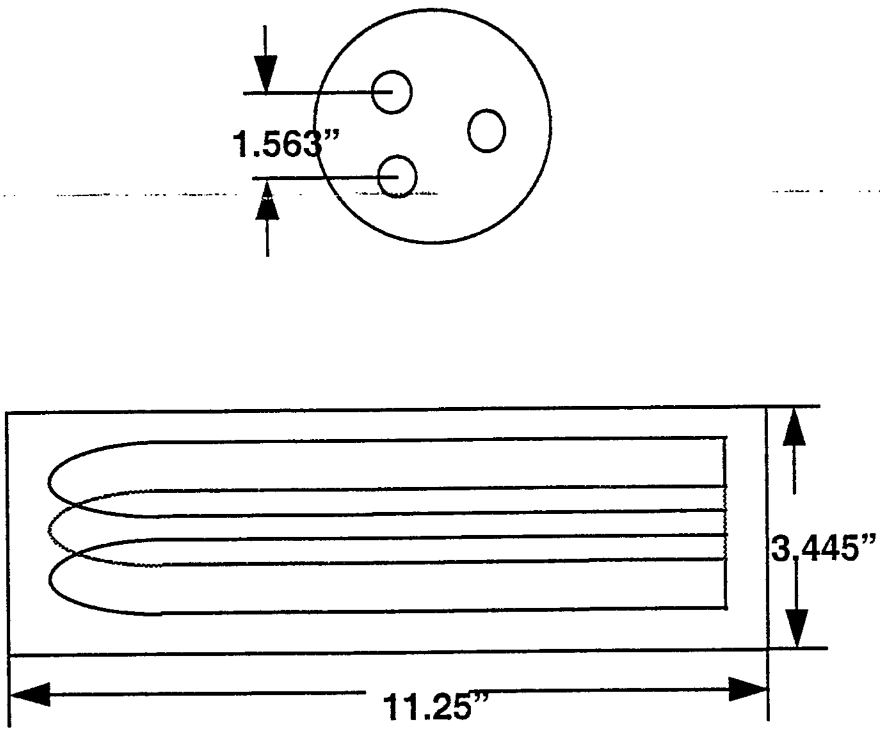

Figure Two: Tripak Configuration

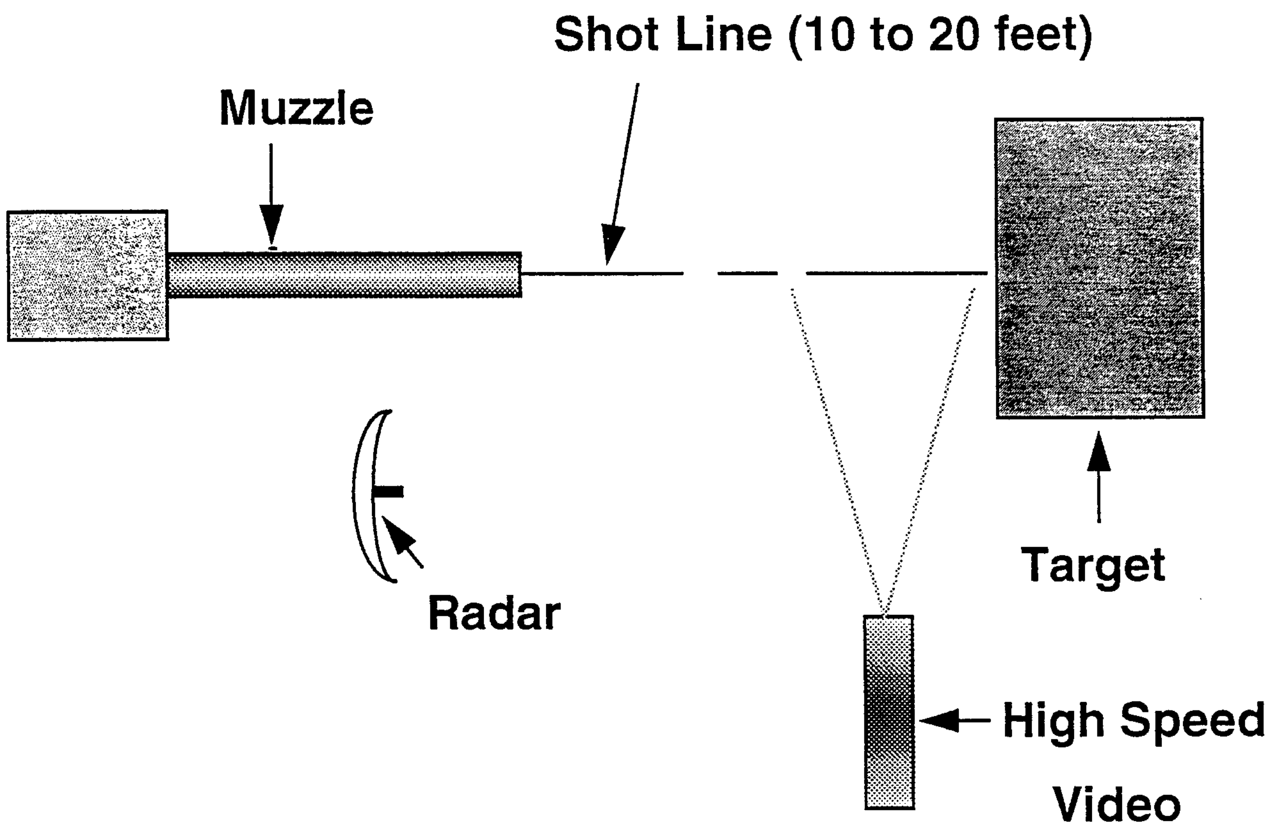

Figure Three: Test Setup

```
    25217          3
0.3792030E+020.4881431E+020.1025296E-150.1025296E-130.7000001E+020.0000000E+00
    25218          3
0.4881103E+020.6652543E+020.1036445E-150.1036445E-130.7000001E+020.0000000E+00
    25219          3
0.4767930E+020.7668682E+020.7725470E-160.7725470E-140.7000001E+020.0000000E+00
    25220          3
0.5020371E+020.8062098E+020.7968238E-160.7968238E-140.7000001E+020.0000000E+00
    25221          3
0.3703962E+020.4869355E+020.9897415E-160.9897415E-140.7000001E+020.0000000E+00
    25222          3
0.4789622E+020.6618410E+020.1047759E-150.1047759E-130.7000001E+020.0000000E+00
    25223          3
0.4789622E+020.6618410E+020.1047759E-150.1047759E-130.7000001E+020.0000000E+00
    25224          3
0.4667194E+020.7629655E+020.7780880E-160.7780880E-140.7000001E+020.0000000E+00
    25225          3
0.4667194E+020.7629655E+020.7780880E-160.7780880E-140.7000001E+020.0000000E+00
    25226          3
0.4922199E+020.8026311E+020.7815586E-160.7815586E-140.7000001E+020.0000000E+00
```

Figure Four: Sample of Results File

```
PATRAN,SIZE:16/12,SIZE:8/10,SIZE:10/10,SIZE:20/48
G
1
5
1
2
c5420x.mdl
N
Y
END
```

Figure Five: Sample PATRAN Session File

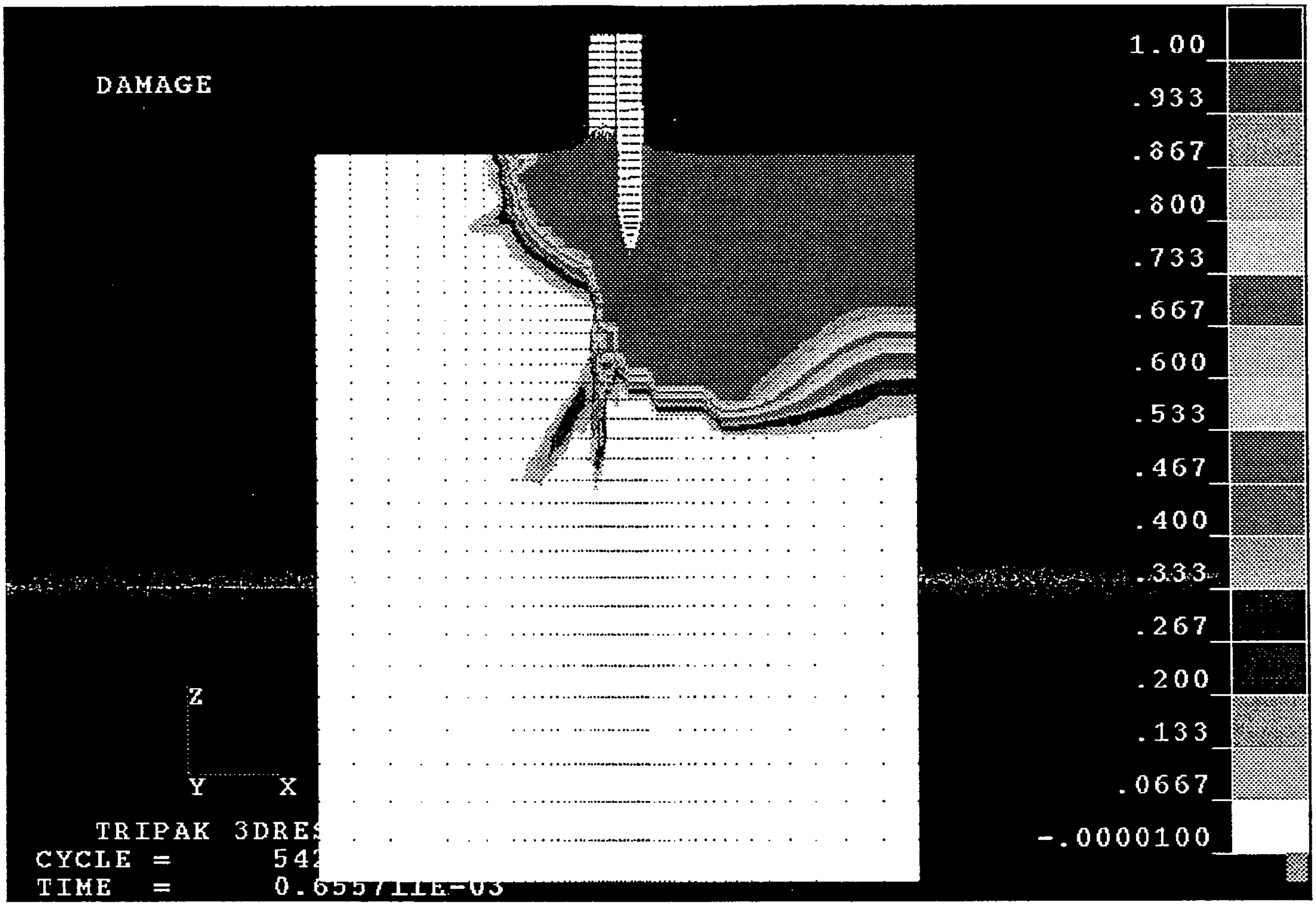

Figure Six: Damage, Cycle 5420, View -90

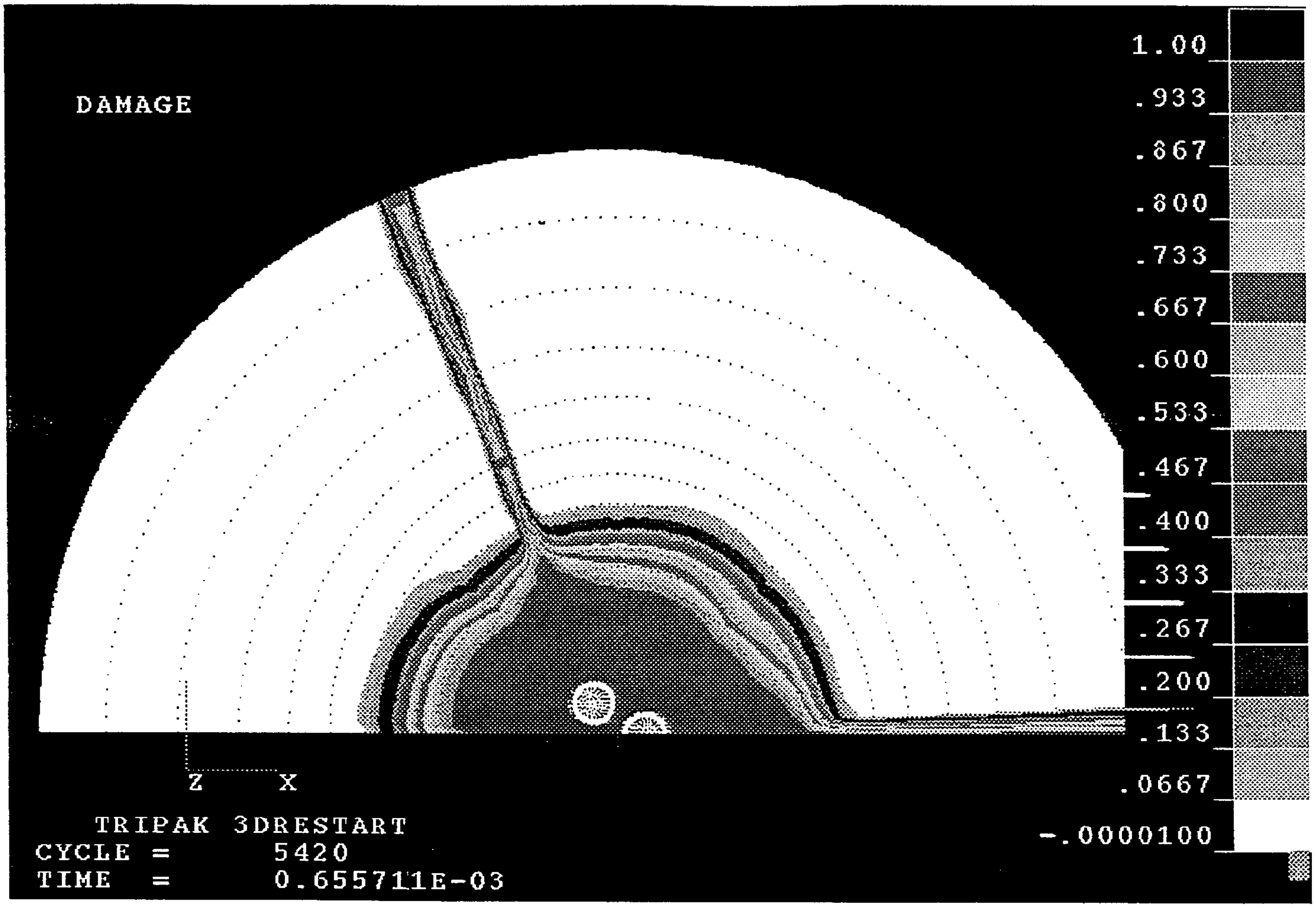

Figure Seven: Damage, Cycle 5420, View 0

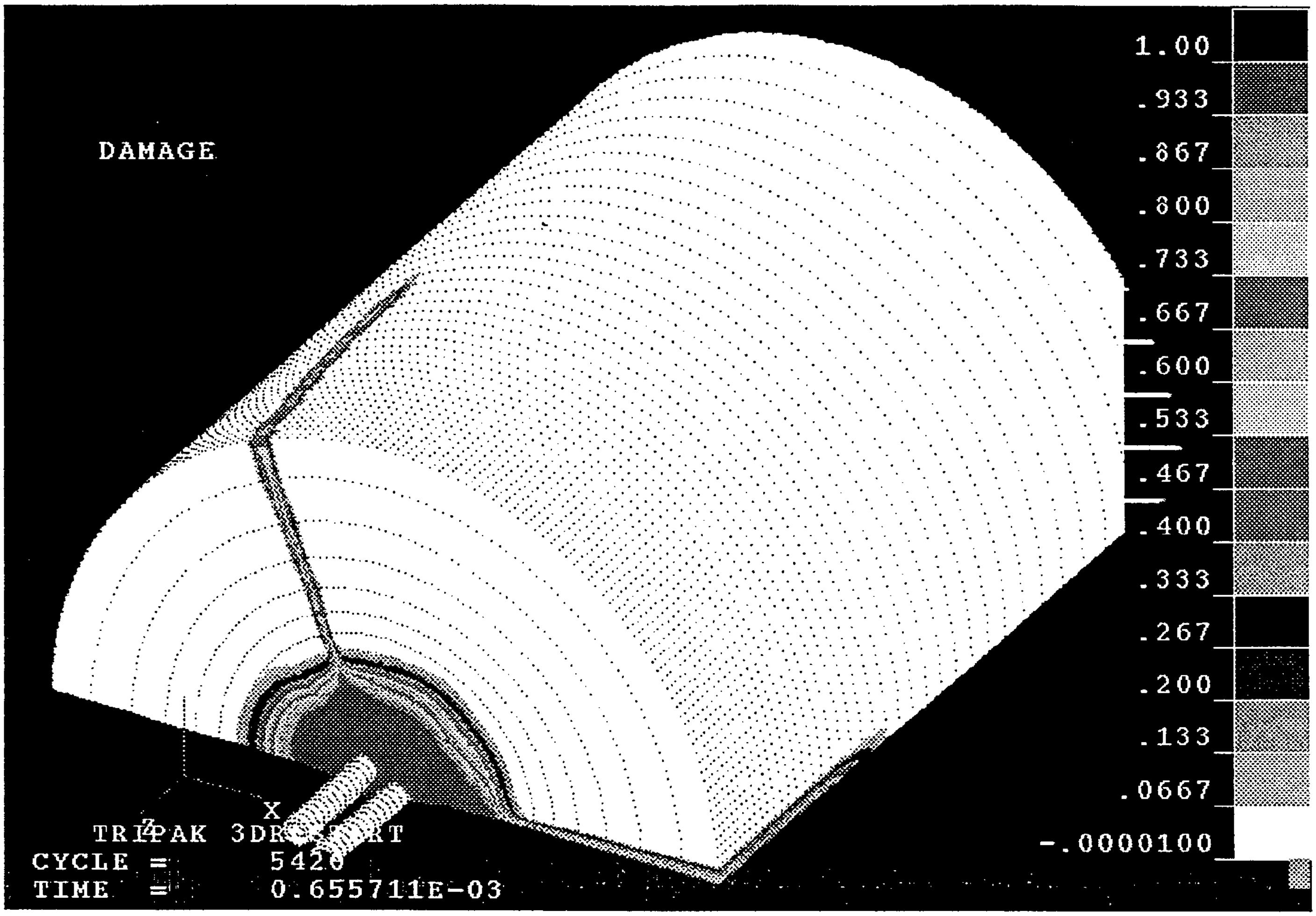

Figure Eight: Damage, Cycle 5420, View 30 -30

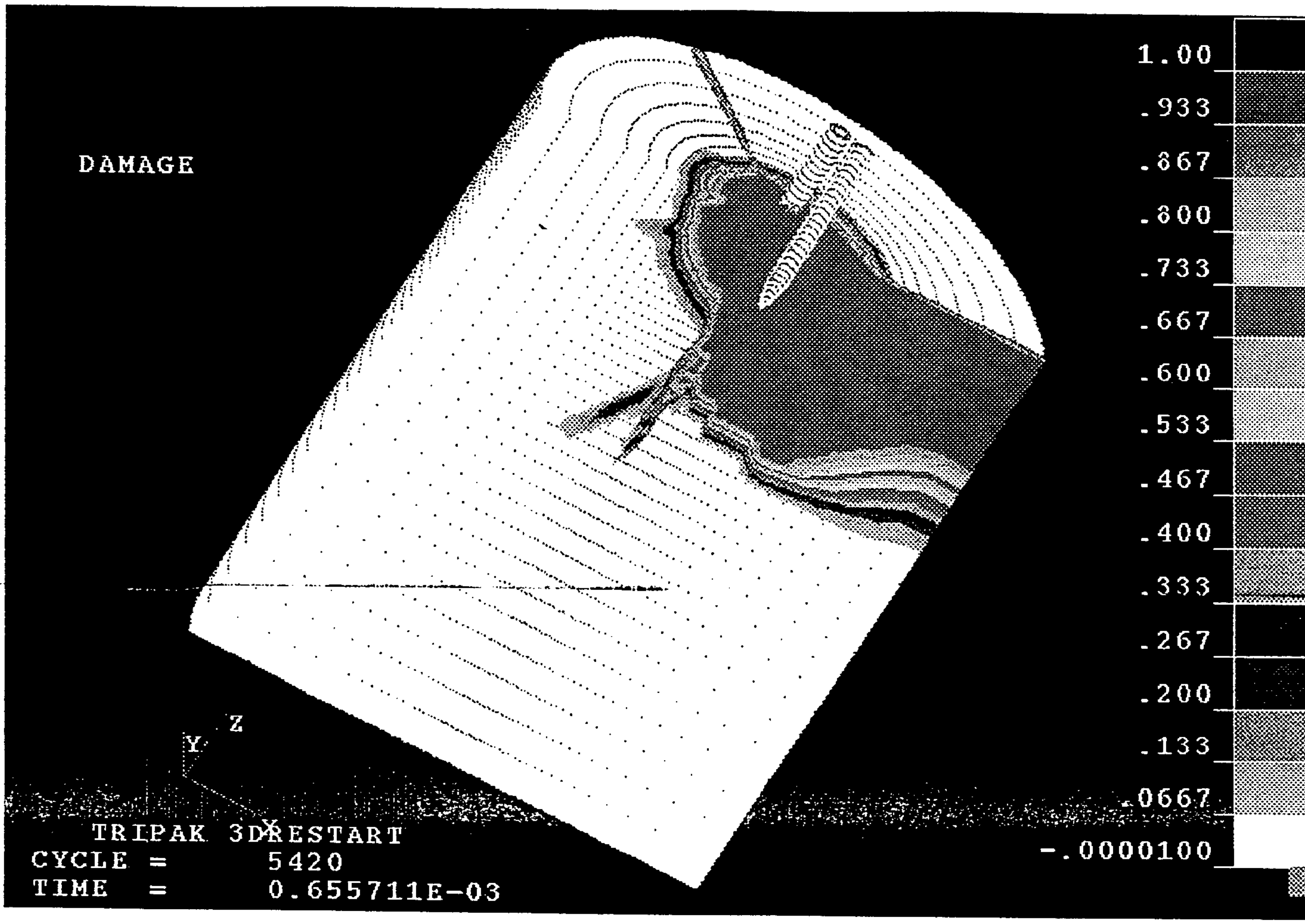

Figure Nine: Damage, Cycle 5420, View -60 30

A STUDY OF SILK COATINGS ON THIN FILMS

Jessica M Behm

Fairmont High School
3301 Shroyer Rd
Kettering, Ohio 45429

Final Report for:
High School Apprentice Program
Wright Laboratory

Sponsored by:
Air Force Office of Scientific Research
Wright Patterson Air Force Base

and

Wright Laboratory

September 1994

A STUDY OF SILK COATINGS ON THIN FILMS

Jessica M. Behm
Fairmont High School

Abstract

The coatings of silkworm silk on thin films was studied. A 9.3M LiBr and several concentrations of silk solutions were made to determine the effect of lasers on thin films covered with these solutions. Experimental results indicated that these solutions will need to be altered to gain the expected results.

A STUDY OF SILK COATINGS ON THIN FILMS

Jessica M. Behm

Introduction

The study of silkworm silks for the coatings thin films has increased. The are now being used for many laser hardening projects. There are many advantages in using silk and silk solutions. This material is readily available, has a natural helical or beta sheet structure which permits chromofores to be easily attached , and can reflect or absorb laser light. The goal of this research is to design a silk coated thin film to reflect and absorb certain wavelengths of laser light.

Methodology

Three colors of silkworm cocoons (white, yellow, and green) were separated and cut into 5 by 5 mm pieces. They were then boiled in Milli-Q water for two days or until the silk became denaturized. The water was changed two to three times during this process. The silk was then dried in an incubator overnight at 37° C. The dried silk was then put into different concentrations of solutions (.01g of silk, 0.1g of silk, and 1.0g of silk per 10 ml of 9.3 M Lithium bromide) was then put in an incubator at 40° C for three hours. Microscope slides were cut into thirds and boiled in ethanol. A dry slide was placed in the spincoater. The vacuum was turned on and set the spin time at 10 seconds. The spincoater's rpms were set at speeds of 25, 50, 80, and 100. For each speed two samples were taken. Each of the three concentrations

were tested for spread. The slides were covered by a drop 3/4 the size of the slide. The slide were left to dry for four weeks. Another solution was made containing 2ml of ethanol, 0.01g of silk, and 10ml of 9.3 LiBr, which was added to speed up the drying process.

Results

After four weeks, the slides were not dry. Although the lower concentrations did not dry completely, they did dry more than the higher concentrations. Other lower concentrations were not tried due to the failure of necessary equipment.

Conclusion

The conclusions drawn from this experiment show although silk is readily available, the processing of silk to a form useful for research is time-consuming. The solutions will need to be made from very small ratios of silk to large ratios of LiBr. And even then, testing the films will be difficult to find to correct wavelength of reflection or absorption. The calculations to find the theoretical concentrations needed at specific wavelengths should be researched before the time is taken to experiment by trial and error.

References

1. D. Kaplan, Adams, Farmer, and Vinery, Silk Polymers-Materials Science and Biotechnology, Library of Congress Cataloging-in-Publication Data AMS, 1993.

Analysis of Spectrum Loading of SCS-6/Timetal®21s

Timothy B. Booher
Tippecanoe High School
Tipp City, OH

Wright Laboratory Materials Directorate
Wright-Patterson AFB, OH 45433-7817

Final Report For:
High School Apprentice Program
Wright-Patterson Air Force Base

Sponsored by:
Air Force Office of Scientific Research
Bolling Air Force Base, DC

and

Wright Laboratory

August 1994

Analysis of Spectrum Loading of SCS-6 / Timetal®21s

Timothy B. Booher

Wright Laboratory Materials Directorate, Wright-Patterson Air Force Base, OH 45433-7817 (USA)

Introduction:

Titanium matrix composites (TMCs) are being considered as materials for structural applications in advanced aerospace applications which involve exposure to both mechanical and thermal cycling at high temperatures. TMCs offer many advantages over superalloy components in high temperature structural applications. Nickel superalloys have worked well in the past, but they are heavy and in current applications are being used at temperatures within a few hundred degrees of their melting temperatures. TMCs offer the potential to replace these alloys with ones that offer higher temperature capability, lower density, and higher stiffness.

At present, however, certain problems exist in the application of TMCs. Besides the high cost of the materials, the titanium alloys suffer from a severe interstitial embrittlement during air exposure at elevated temperatures. Within the Timetal®21S material, high temperate air exposure promotes an alpha precipitation within the normally beta matrix (oxygen is a potent alpha stabilizer). This severely reduces the ductility of the material as well as its fatigue resistance. In composite form, the embrittlement can be so severe that the matrix ductility can drop below the theoretical minimum ductility required for load transfer between fiber and matrix. Also, the oxidizing environment will attack the fiber coatings, typically C or TiB_2, leading to a reduction in the strength of the fiber and a brittle reaction zone at the fiber / matrix interface.

Another problem that exists in TMCs is the reduction in load carrying capacity when the material is not loaded parallel to the fibers. The strength, especially creep

strength, of the composite degrades severely for transverse loading. This limits the application of these materials.

Due to their high temperature capabilities, proposed applications of TMCs often entail both mechanical and thermal cyclic loading. Emphasis is therefore placed on an accurate prediction of the thermomechanical fatigue (TMF) life of these components. Due to the differences found between the coefficients of thermal expansion between the fiber and the matrix, internal stresses are generated during thermal cycling and must be accounted for in addition to those normally produced in mechanical loading. Accurate analysis, therefore, is contingent upon the stress or strain in the fiber and matrix as well as the total applied stress.

Analysis

PROGRAM:

Since the analysis includes both thermomechanical loading and temperature-dependent material properties, a unified constitutive modeling program is necessary. These factors are placed into the FORTRAN program, FIDEP (Finite Difference Code for Elastic-Plastic Analysis).

FIDEP is a PC-compatible user-friendly computer code developed in-house at the Materials Directorate, Wright Laboratory, Ohio, for the purpose of predicting micromechanical stresses in metal matrix composites under complex thermal and mechanical loading histories. The program incorporates different loading histories, micromechanical models, and constitutive models in a modular form to allow for easy implementation of new requirements.

In this simulation, an axisymmetric concentric cylinder model (CCM) was used. This allowed the central core to represent the fiber, while the outer anular region represented the matrix, and the outermost region represented the 90. The geometry of this situation allows for a relatively simple analysis of the advanced three-dimensional stress state in both the fiber, matrix, and 90. This model also permits both axial and radial loading.

The following assumptions are made in the analysis. The temperature distribution is uniform and is quasi-static. A perfect bond exists between the constituents of the composite so that there is no slippage or separation of the

constituents. The concentric cylinders are in generalized plane strain and are subjected to axisymmetric loadings and displacements so that the shear stresses are zero. The constituent properties are isotropic. The fiber is linearly elastic.

MATERIAL MODEL:

In order to reflect various aspects of inelasticity including plasticity, creep and thermal recovery, it was necessary to use a unified viscoplastic constitutive model. The unified inelastic-strain theory consisting of a Bodner-Partom flow rule with modifications can adequately model the response of Timetal®21s. This theory avoids simplifying assumptions about inelastic strain as the sum of plastic and creep components and therefore has adequate description of complex behavior of a material under plasticity-creep interaction conditions.

The total strain (ε^{tot}) is defined as the sum of:

$$\varepsilon_{ij}^{tot} = \varepsilon_{ij}^{el} + \varepsilon_{ij}^{in} + \varepsilon_{ij}^{th}$$

The elastic stress "ε_{ij}^{el}" is contingent on the elastic modulus "E", current stress state "σ", and Poisson's ratio "ν". The thermal strain components are equal to the product of the coefficient of thermal expansion "α" and the difference of the current and reference temperatures. The Bodner-Partom flow rule controls the formation of the inelastic strains "ε_{ij}^{in}" and is described below:

In comparison to other unified inelastic strain formulations, this theory describes the directional (kinematic) hardening with a special directional hardening term. Other theories represent directional hardening phenomena with a "back-stress" modified equivalent stress. Introduction of the directional hardening term alters the Bodner-Partom flow rule by replacing the previously known variable "drag-stress" with the sum of isotropic and directional hardening terms, Z^I and Z^D, respectively. These two hardening terms enter into the inelastic strain rate equation or flow law:

$$\varepsilon_{ij}^{in} = D_0 \cdot \exp\left\{-\frac{1}{2} \cdot \left[\frac{(Z^I + Z^D)^2}{3 \cdot J_2}\right]^n\right\} \cdot \frac{S_{ij}}{\sqrt{J_2}}$$

D_0 is the limiting strain rate, s_{ij} are the components of deviatoric stress, and

$$J_2 = \frac{s_{ij}s_{ij}}{2}.$$

The evolution of Z^I and Z^D have similar empirical forms. Each equation consists of a hardening term, a thermal recovery term, and a temperature rate term. The isotropic hardening evolution equation with these three terms is:

$$\dot{Z}^I = m_1 \cdot (Z_1 - Z^I) \cdot \dot{W}^{in} - A_1 \cdot Z_1 \cdot \left(\frac{Z^I - Z_2}{Z_1}\right)^{r_1} + \left[\left(\frac{Z^I - Z_2}{Z_1 - Z_2}\right) \cdot \frac{\partial Z_1}{\partial T} + \left(\frac{Z_1 - Z^I}{Z_1 - Z_2}\right) \cdot \frac{\partial Z_2}{\partial T}\right] \cdot T$$

and the inelastic work rate is given by:

$$\dot{W}^{in} = \sigma_{ij} \cdot \dot{\varepsilon}_{ij}$$

The initial isotopic hardening, $Z^I(0)$, is Z_0. The material parameters associated with the isotopic hardening evolution are m_1, Z_0, Z_1, Z_2, A_1, and r_1. The thermal differential terms $\frac{\partial Z_1}{\partial T}$ and $\frac{\partial Z_2}{\partial T}$ appropriately scale the isotropic hardening variable when inelastic deformation and thermal recovery do not occur during nonisothermal conditions, thus preventing ZI from passing through maximum or minimum values with temperature changes.

The scalar product of the state variable "bij" and a unit stress vector uij yields the magnitude of the directional hardening term:

$$Z^D = \beta_{ij} u_{ij},$$

where:

$$\dot{\beta}_{ij} = m_2 \cdot \left(Z_3 u_{ij} - \beta_{ij}\right) \cdot \dot{W}^{in} - A_2 \cdot Z_1 \left(\frac{\sqrt{\beta_{kl}\beta_{kl}}}{Z_I}\right)^{r_2} v_{ij} + \frac{\beta_{ij}}{Z_3} \frac{\partial Z_3}{\partial T} \cdot \dot{T}$$

$$u_{ij} = \frac{\sigma_{ij}}{\sqrt{\sigma_{kl}\sigma_{kl}}}$$

and:

$$v_{ij} = \frac{\beta_{ij}}{\sqrt{\beta_{kl} \cdot \beta_{kl}}}$$

The initial directional hardening variable, $Z^D(0)$ is set to zero. The material constants associated with the directional hardening evolution equation are m_2, Z_3, A_2, and r_2. The temperature differential term $\frac{\partial Z_3}{\partial T}$ appropriately scales the directional hardening variable when inelastic deformation and thermal recovery do not occur during nonisothermal conditions. In particular, without these differential terms the directional hardening accrued at one temperature may exceed the limiting value Z_3 at another temperature, which is not physically realistic.[1]

LIFE PREDICTION MODEL

The end result of this modeling is the implementation of the data into a life prediction model that can determine the number of loads, that the specimen can sustain before failure occurs.

The life fraction model consolidates data from a variety of isothermal and TMF tests. Damage is considered to accumulate simultaneously due to independent mechansims, each represented in the model by a fraction of the total life. When the sum of the life fractions from each meachanism equals one, the failure can be predicted.

LOAD CONDITIONS

A TMF test capability was developed to conduct simulations of seven simplified phases of a generalized hypersonic flight profile. Two different loading cycles of interest were cruise and orbital cycles. The orbital mission is displayed is figure 1 and the cruise mission is displayed in figure 2.

Seven points were selected to represent each different phase of the flight profile. To accurately determine which difference between each pair of points produced the most dramatic effect on the life of the specimen, seven phases were selected, one phase connected each pair. The in-phases (denoted by IP) in figures 3-8 reach

---

[1] For further information see Kroupa IMPLEMENTATION OF A NONISOTHERMAL UNIFIED INELASTIC-STRAIN THEORY INTO ADINA6.0 FOR A TITANIUM ALLOY (1993).

maximum load and temperature simultaneously, while the out-of-phases (denoted by OP in figure 3-4,9-11) reach maximum load and minimum temperature simultaneously.

The temperature and load spectrum for each phase is shown in figures 5-11. The spectrum flight profile consists of a non-isothermal load cycle distributed with temperatures over a selected spectrum.

PLOTS AND DISCUSSION

Of interest were the peak values of the separate stresses of the fiber and matrix. The program MIN-MAX was utilized to remove these values from the out-put data files.

A few representative stress-strain plots were chosen to display the results of the analysis. It is apparent that some undergo ratcheting while others stay within a steady pattern. Ratcheting is the term that defines the movement along the absissa of cyclic patterns (see figure 13, in comparison to figure 12). The ratcheting is due to an increase in the strain rate with time-dependent behavior.

Some plots are also chosen that display the individual stresses of the fiber, matrix, and 90 verses time steps. These plots are useful in the sense that they provide a solid comparison of each individual micromechanical stress. It was these values that were placed into the MAX-MIN program. This made the values described in these graphs very important to the life-prediction program.

Closure

The practice of mathmatical modeling has proven useful in such cases as this one. By simplifying complex material models in this manner, both time and money are saved. These results will be further tested with more complex, less simplified models until the degree of error is at a minimum.

Once these values are gathered, and sent to a senior scientist who will alalyze them in the life prediction model discussed above. From this model, the results will then be placed into applications relating to a hypothetical hypersonic flight vehicle, where they will be subjected to temperatures and environments similar to the one described in this paper.

Orbital Mission

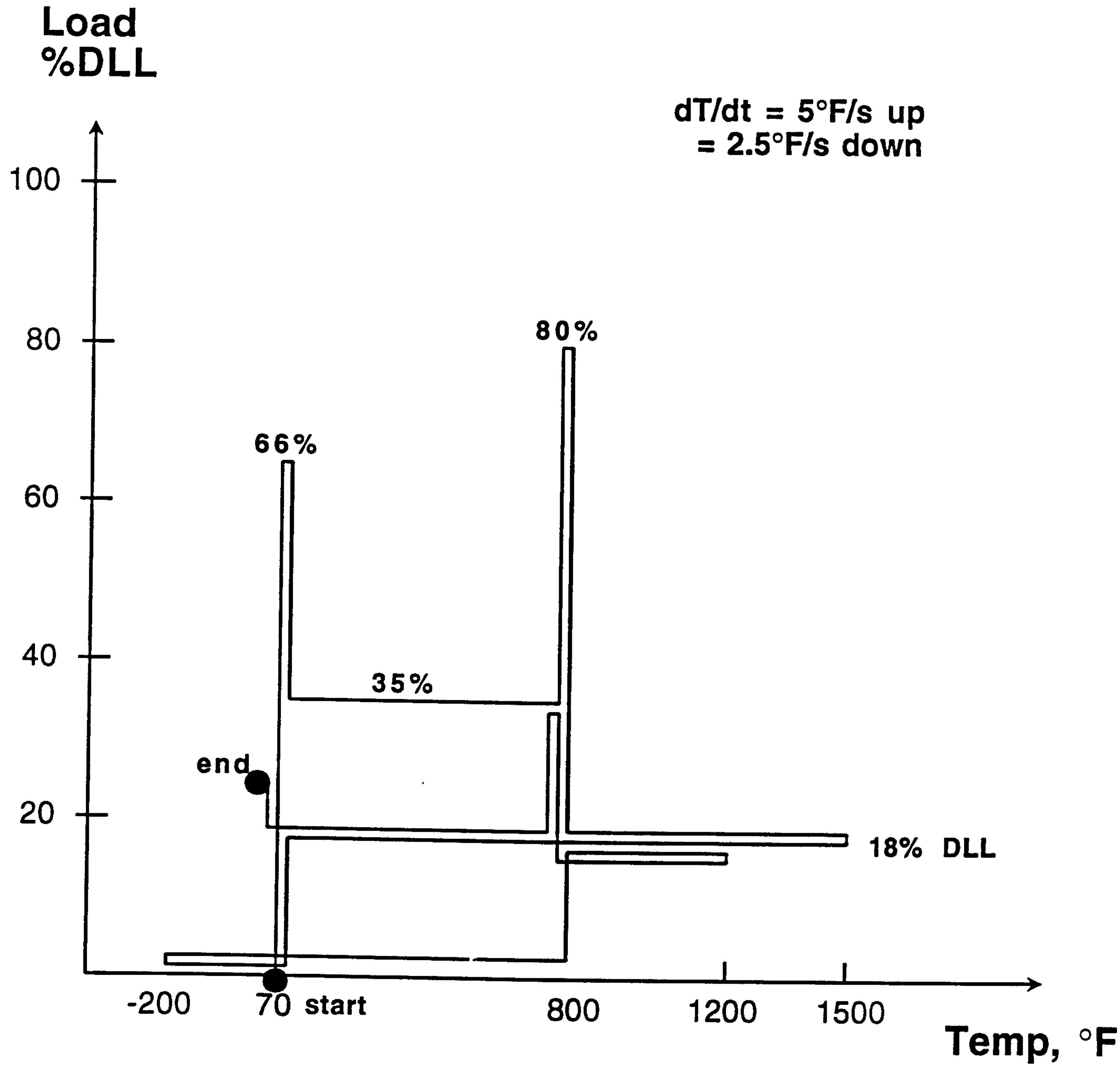

Figure 1

Cruise Mission

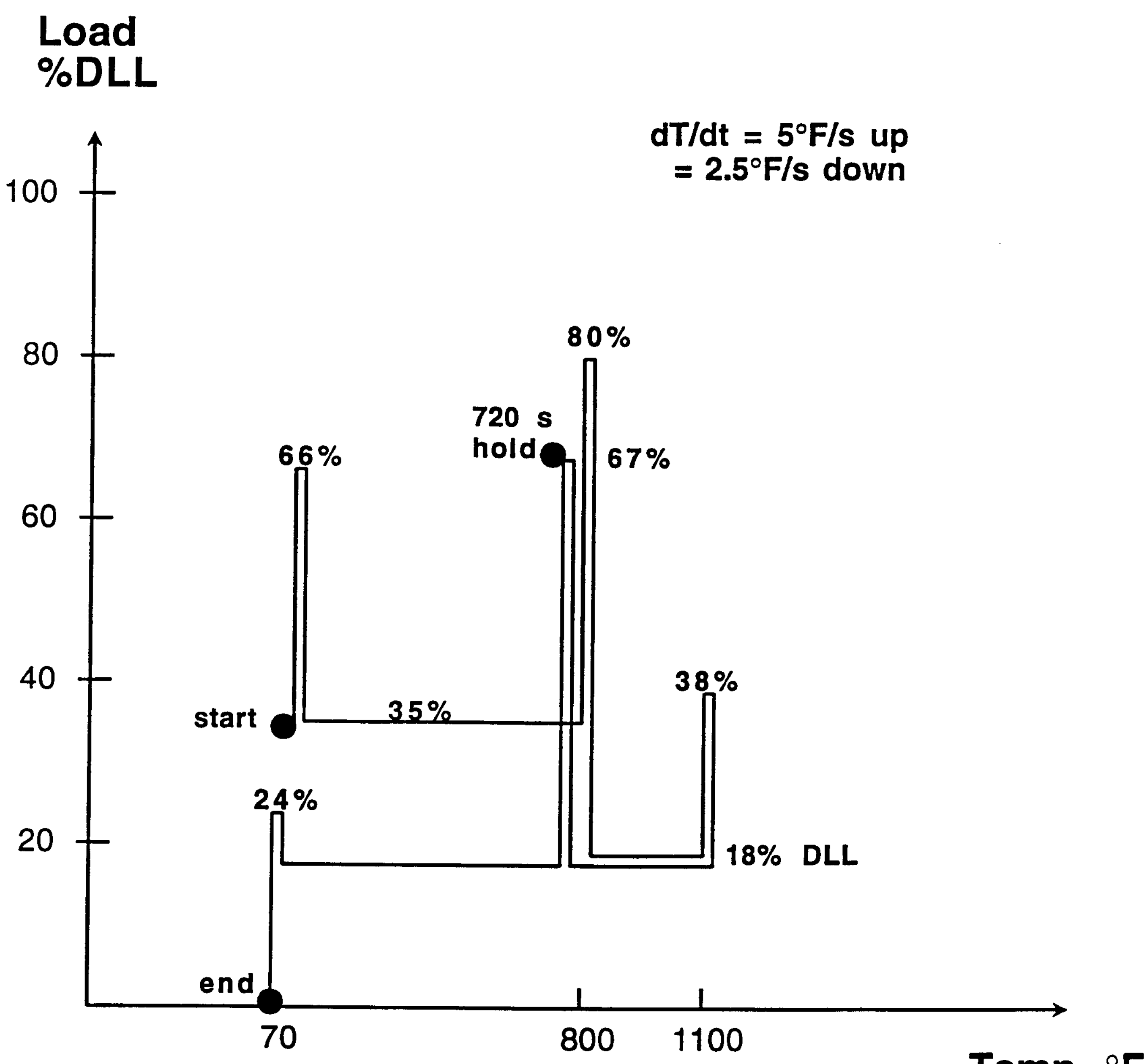

Figure 2

Orbital Mission

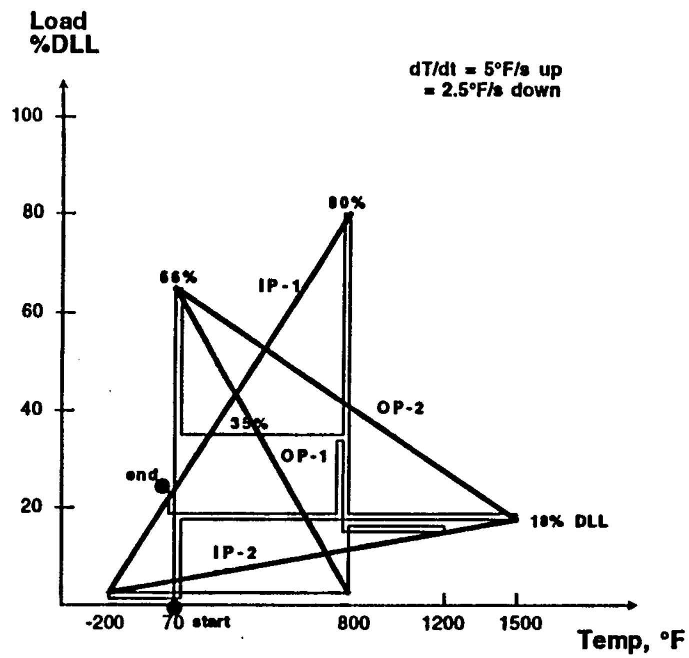

Figure 3

Cruise Mission

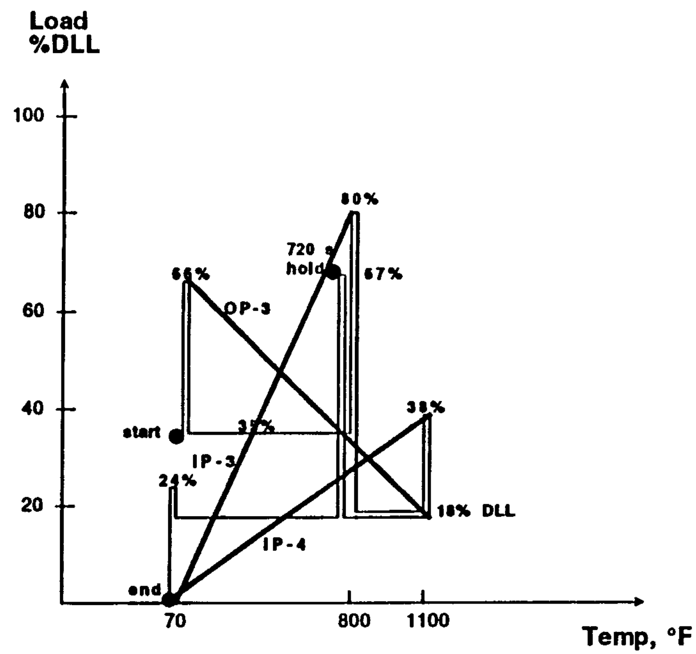

Figure 4

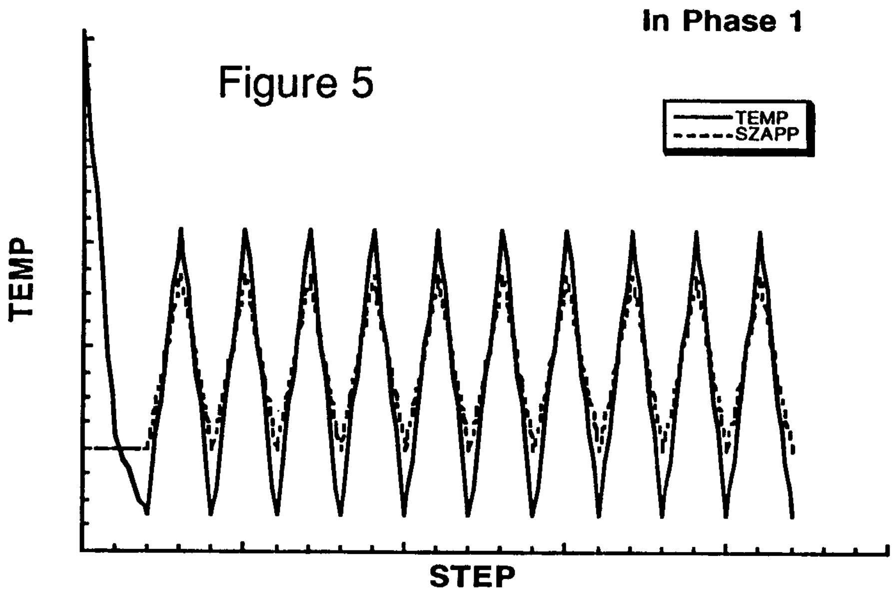

Figure 5

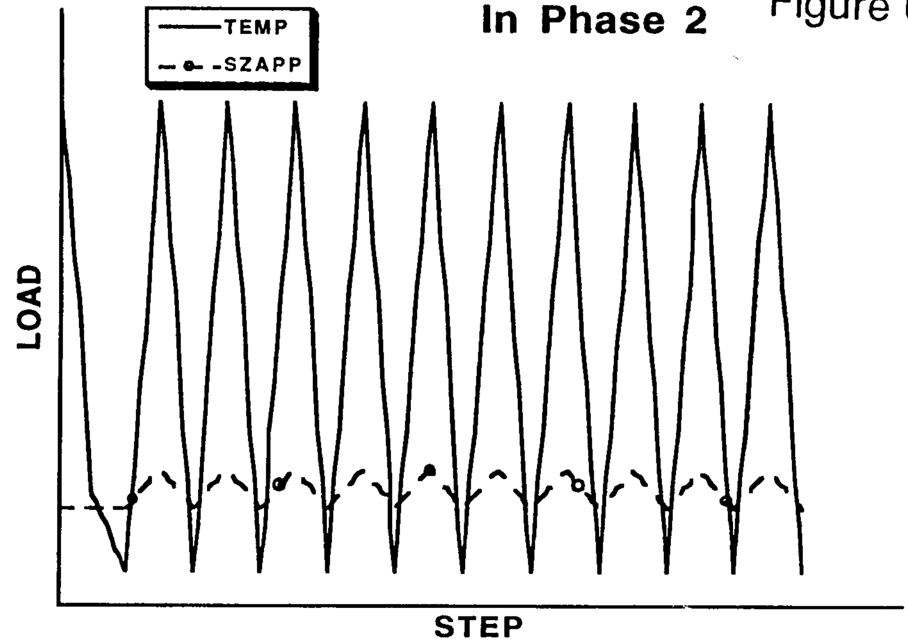

Figure 6

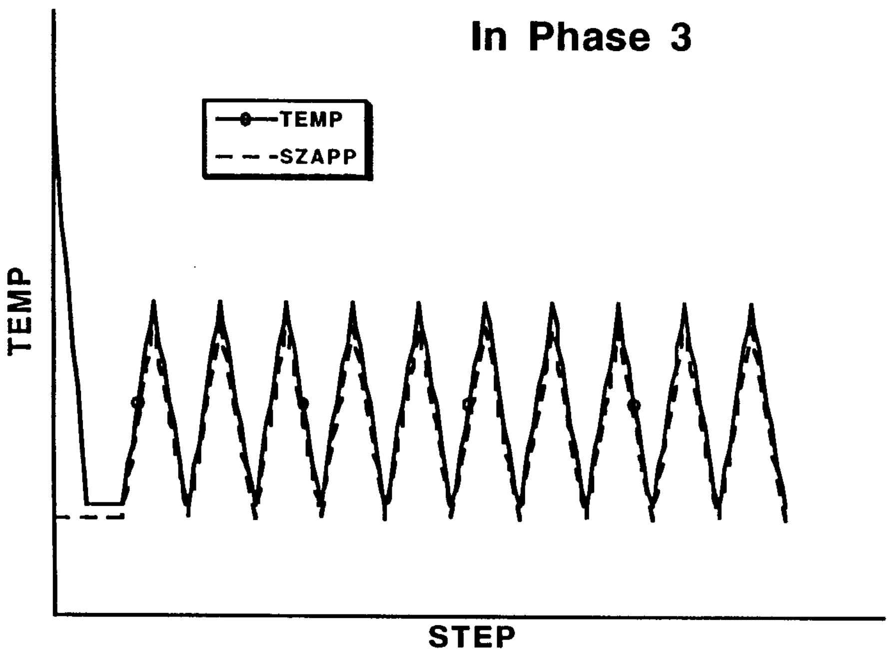

Figure 7

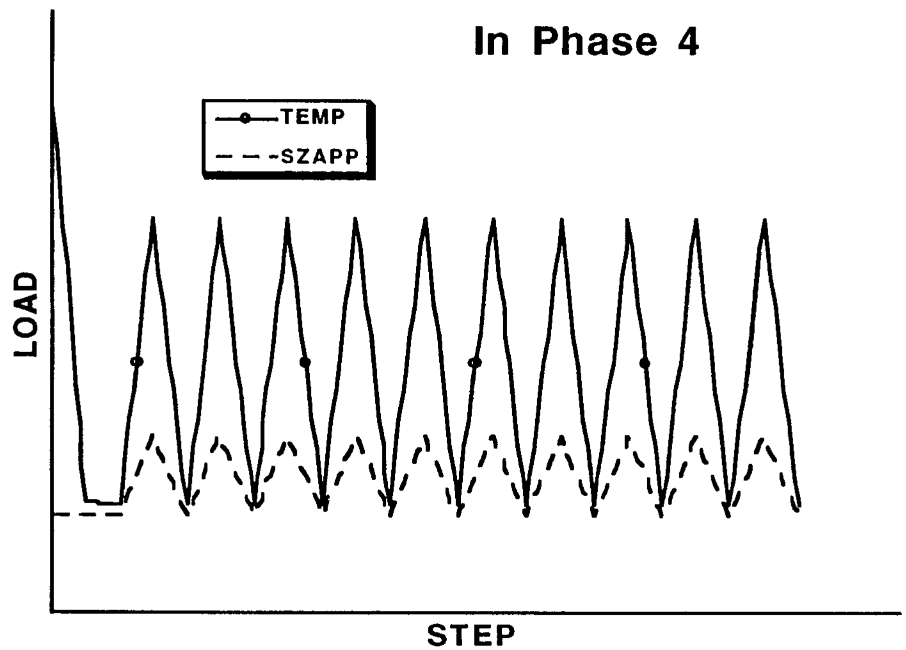

Figure 8

Figure 9

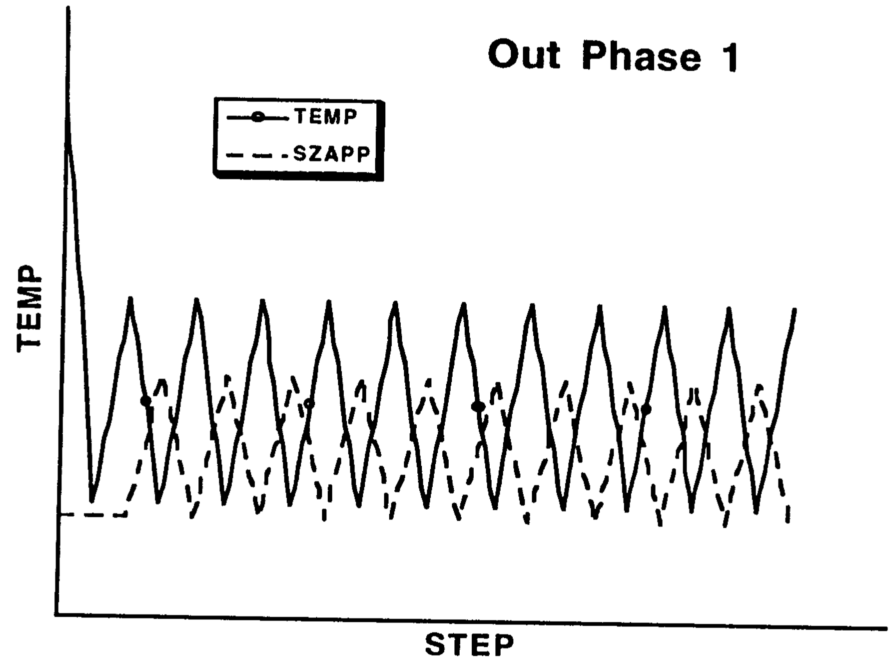

Figure 10

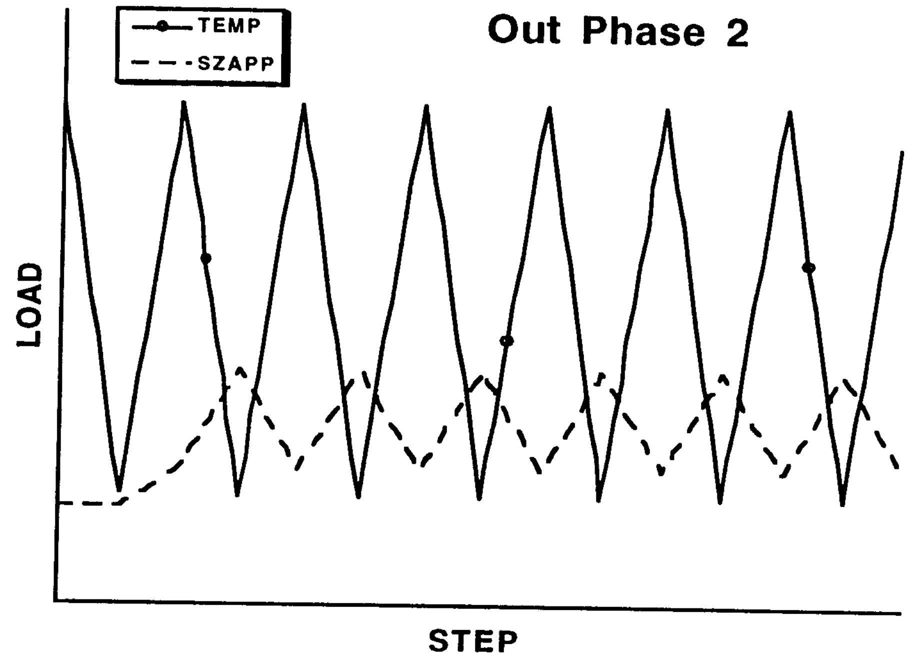

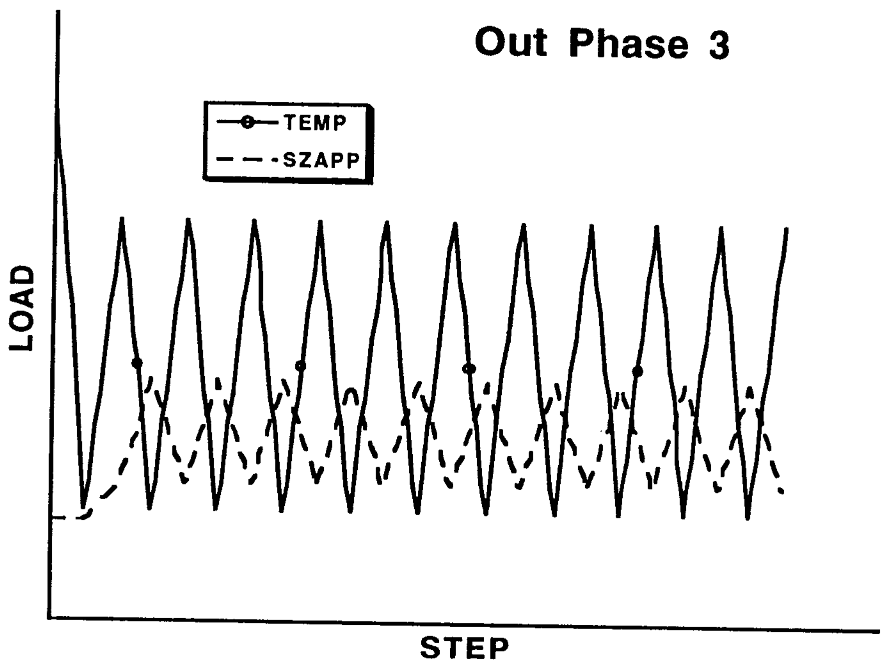

Figure 11

Figure 12

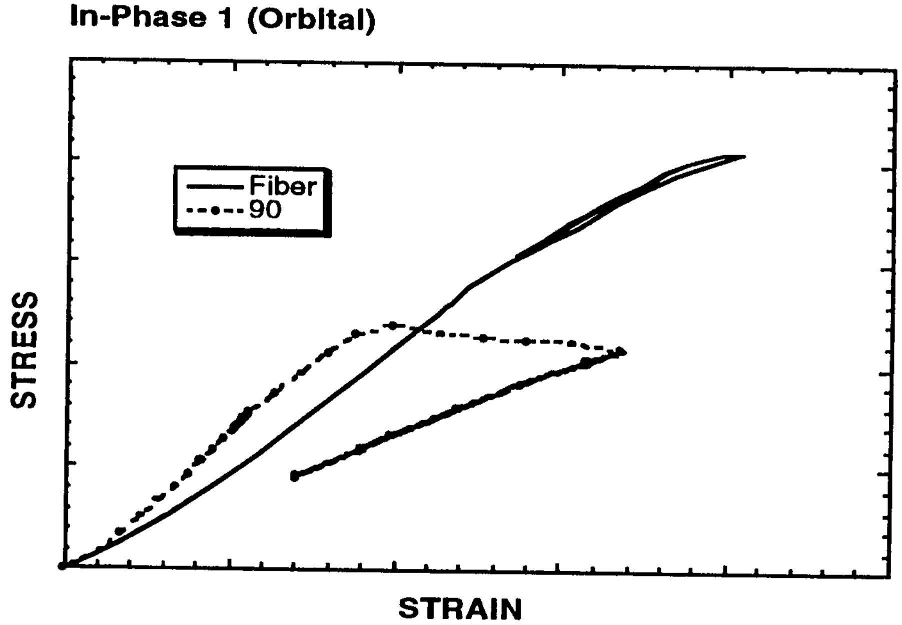

Figure 13

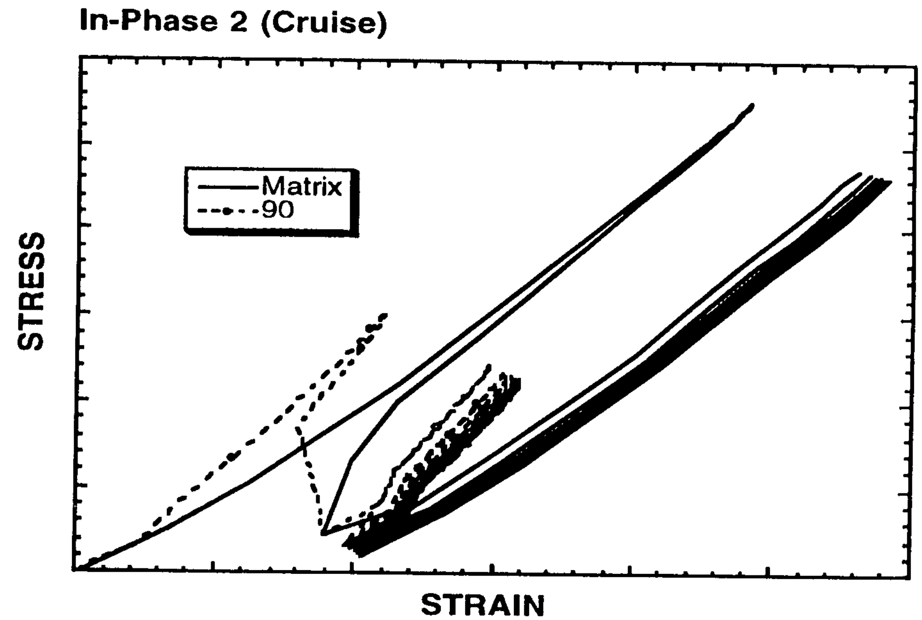

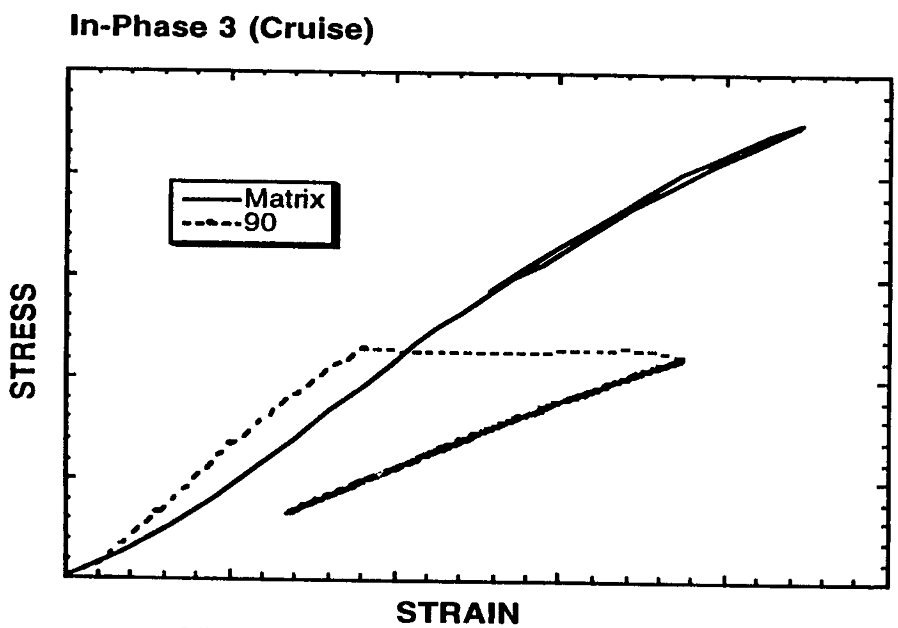

Figure 14

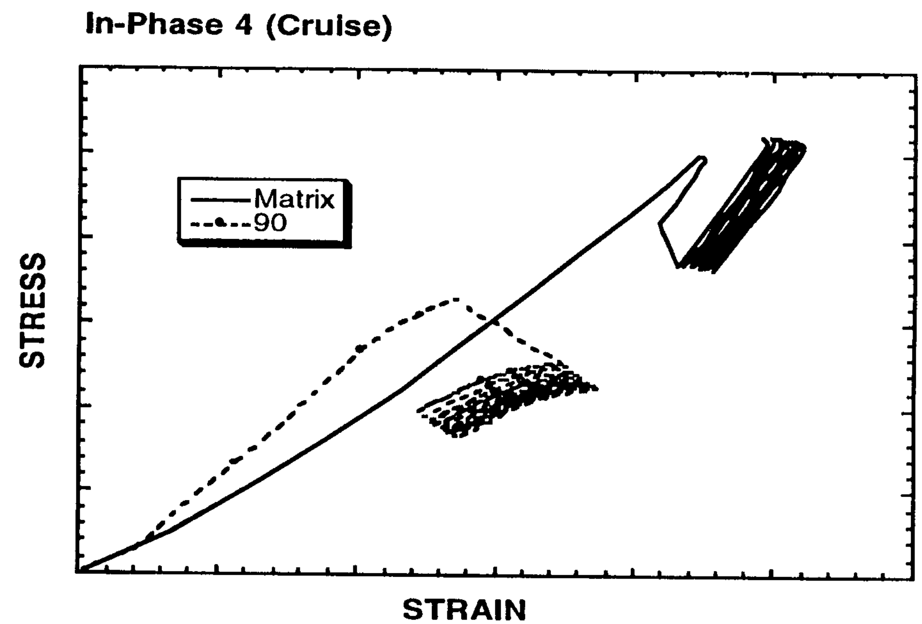

Figure 15

Figure 16

Out-Phase 1 (Orbital)

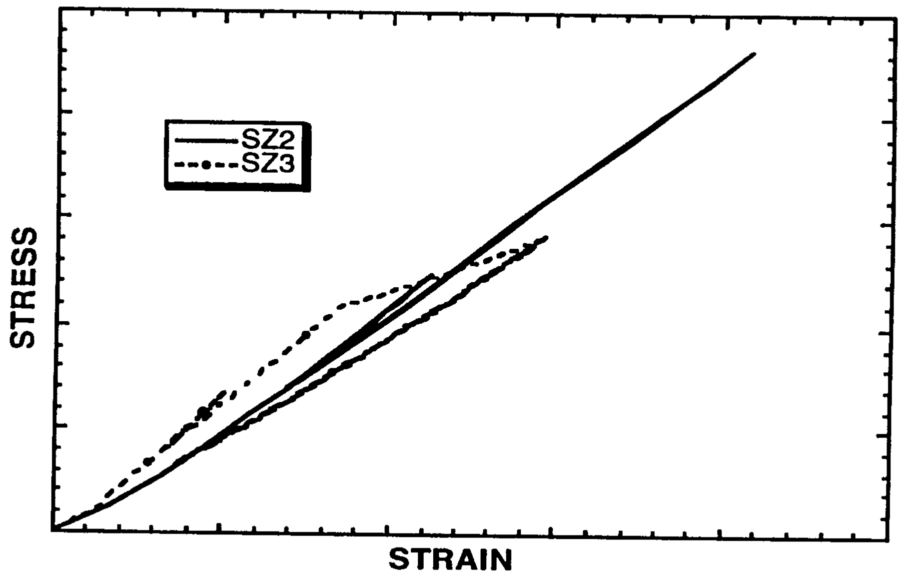

Figure 17

Out-Phase 2 (Orbital)

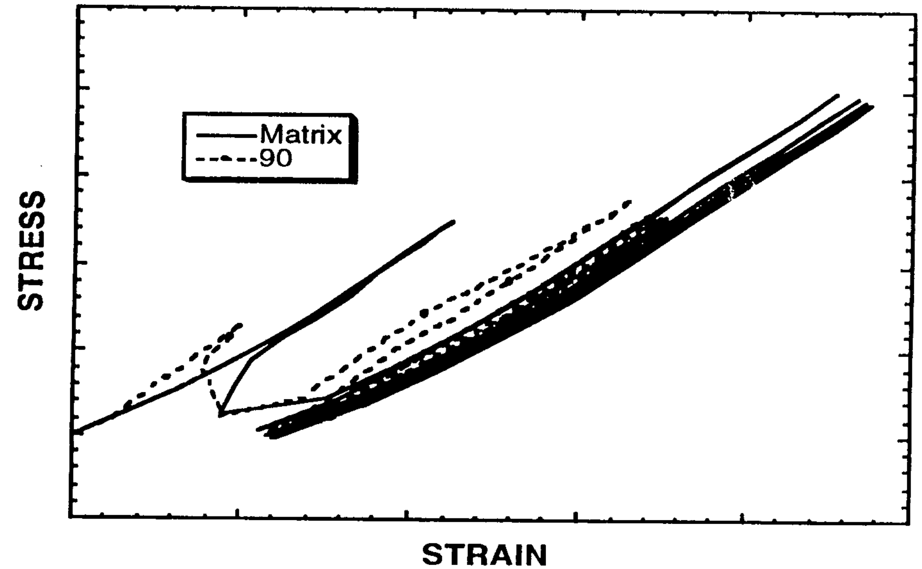

Out-Phase 3 (Cruise)

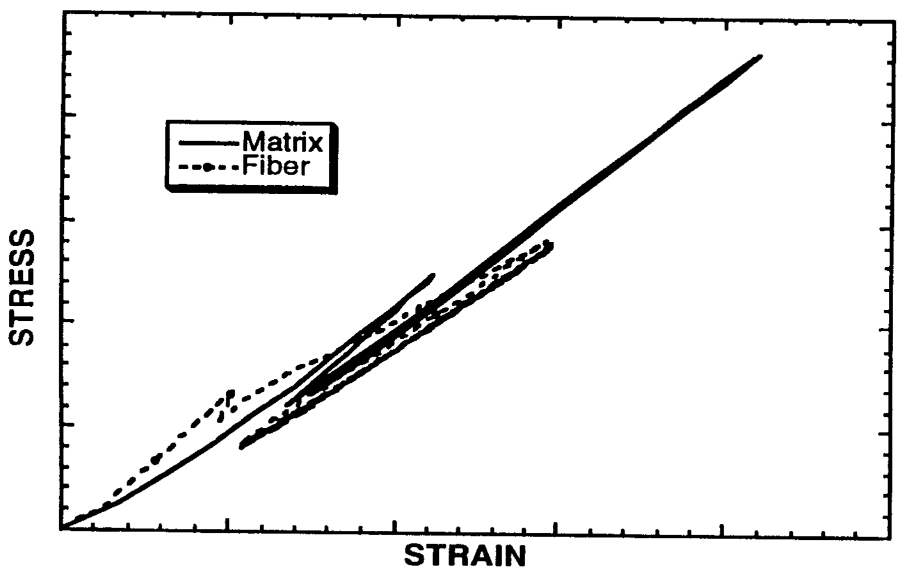

Figure 18

CHEMICAL DECOMPOSITION USING NON-THERMAL DISCHARGE

Kimberly N. Cabral
Mentors: Capt. Randy Drabczuk
and
Heather Petresky

Choctawhatchee High School
110 NW Racetrack Road
Ft. Walton Beach, Florida 32547

Final Report for:
High School Apprenticeship Program
Wright Laboratory

Sponsored by:
Air Force Office of Scientific Research
Bolling Air Force Base, DC
and
Wright Laboratory

August 1994

CHEMICAL DECOMPOSITION USING NON-THERMAL DISCHARGE

Kimberly N. Cabral
Choctawhatchee High School

Abstract

Chemical decomposition produced by a non-thermal discharge process was studied to establish the efficiency of a coaxial reaction tube. Gaseous toxicant TCE was combined in a flow with O_2 and H_2O vapor to form the working gas. The working gas flow passed through the reaction tube, and concentrations of the gas were monitored on input and exhaust ports. Electrical power and concentration reductions (%) were utilized to calculate the process efficiency. Parameters were varied to examine their affect on the efficiency. The varied parameters included flow rate, TCE concentration, power, and frequency of applied electrical voltage. Efficiency is defined as the ratio of a theoretical energy per molecule to the input energy divided by the number of TCE molecules destroyed. Experimental results in the 1-watt range indicate a higher efficiency and show a direct relation between efficiency and flow rate, and efficiency and concentration.

Introduction

As time progresses, pollution proliferates. It has become a problem of particular concern to the government and various industrial organizations [5]. The Environmental Protection Agency (EPA) and Clean Air Act Amendments of 1990 encourage organizations to develop methods to greatly reduce their toxic and hazardous emissions [2,10,13]. For example, several hundred of about 4600 Air Force sites contain noxious wastes, and about 57% have six remaining years to comply with federal standards [5].

Chlorocarbon trichloroethylene , or TCE (C_2HCl_3), is an environmental toxicant. It has been utilized as a decaffeinator until the same general time as the National Cancer Institute (based on a study) detected cancerous tumors in mice that were exposed to it, and some of these tumors spread to the lungs [8]. TCE is, in fact, very harmful to the human health. It can provoke nausea and narcotic effects, cause dermatitis and severe damage to the liver and kidneys, and if exposure is at very high concentrations, the results may be as extreme as coma and death [11]. Currently, TCE is primarily utilized to degrease metals and often contaminates ground water at concentrations between 10 and 15 parts per million (ppm) [5]. In this way, TCE is of great concern to the Air Force.

There are presently sparging towers in use to extract TCE from ground water. In these sparging towers, a gas and liquid, flowing in opposite directions, are introduced by means of a fritted glass to make bubbles which collect TCE. The new gas containing TCE is then emitted from the system via H_2O mist [5]. Sparging is only nascent to the removal process of TCE, however, and it solves one problem while actually creating another. A product is undoubtedly released into the atmosphere which remains noxious and aberrant to EPA standards. An additional technique is necessary to eliminate the TCE and prevent its effects on the atmosphere. The technique should alter the chemical properties of TCE subsequent to its removal from ground water, thus forming innocuous compounds.

NOx is another contaminant of great concern to the Air Force. (The term NOx refers to compounds of nitrogen and oxygen.) There are two general types of NOx: thermal and fuel. Thermal NOx is formed when nitrogen in combustion air is dissociated and recombines with oxygen. Fuel NOx occurs in the oxidation of chemically-bound nitrogen in fuel [2,12].

NOx is severely harmful due to its many possible forms. It plays an active role in photochemical smog, PAN(acronym for peryoxacetal nitrate and ozone) production, acid rain formation and ozone layer depletion [2,12]. Photochemical smog is created when NOx reacts with various hydrocarbons to create alcohols, ketones, aldehydes, formaldehydes and acrolein [2]. PAN is a photochemical oxidant, which means it is a stronger oxidizing agent than oxygen in air and an assailant of chemicals not usually attacked by atmospheric oxygen [8,12]. In a reaction involving NOx and H_2O vapor, HNO_2 and HNO_3 are formed, otherwise known as acid rain, which is damaging to human health when inhaled [2,3]. Because acid rain mists attack calcium carbonate (limestone and marble are composed of calcium carbonate), they contribute to the atrophy of buildings, statues, etc. [8].

NOx is generated in various ways. Some of the NOx in the atmosphere is generated by lightning [2,4]. NOx emitted in processes such as combustion of fossil fuels (petroleum, coal, natural gas) for electricity and industrial processes, and incineration of wastes where air is heated to temperatures greater than 1100^{0}C, is most frequently in the form of NO [3,8,12]. NO endangers human health when inhaled, damages vegetation and degrades materials through acid decomposition [12]. Once in the air, NO can be oxidized to form NO_2.

NO_2 , like NO, is harmful to humans and aids in the decay of materials [12]. In the presence of sunlight and other pollutants, NO and O are formed from NO_2 [2]. If these react with atmospheric oxygen, ozone is formed. Ozone is a photochemical oxidant detectable by most people at a concentration as low as 0.02 ppm due to its strong chlorine-like odor. [8].

One of the many possible solutions to the dilemma of ridding toxic waste in gaseous form is the non-thermal discharge process (NTDP). Thus far, NTDP has successfully destroyed TCE, ethyl acetoacetate, dimethyl methylphosphonate, soman, formaldehyde, malthion, benzene, hydrogen cyanide, carbon tetrachloride, and freon 12 [2]. It may also be applicable to NOx and SOx [2,6]. Even better, any compound that is effectively oxidized by oxygen atoms may be eliminated with this process, and different pollutants can possibly be removed simultaneously [9,15].

There are many types of NTD processes, including glow, pulsed corona, electrified packed bed, surface, and silent electric. The silent electric non-thermal discharge method is the type discussed in this

paper. It is termed "silent" electric because glass is used to deter intervention of outside particles with the plasma; also, the discharge is actually silent as compared to an apparatus in which the discharge occurs between two conducting plates [6].

In NTDP, electricity (as opposed to heat) is applied to excite electrons [5]. Energy from a high voltage supply is dispensed to electrodes and is coupled into the non-thermal plasma. Within the plasma, electrons in the energy range of 5-10 eV (or 50,000-100,000 ^{0}K) attack the background gas [7]. At atmospheric pressures, the breakdown of the background gas gives way to numerous microdischarges which have a life span of approximately 100 nanoseconds [2]. Radicals such as atomic oxygen and excited-state oxygen are created and decompose the pollutant gas. Harmless compounds such as H_2O and CO_2 are then formed [1,2,5,15]. Because the main focus is on exciting the electrons rather than directly heating the gas, NTDP is efficient in saving energy and capital.

The Air Force has environmental problems that may be alleviated with this process. A further investigation of NTDP may bring about favorable results.

Discussion of Experimentation

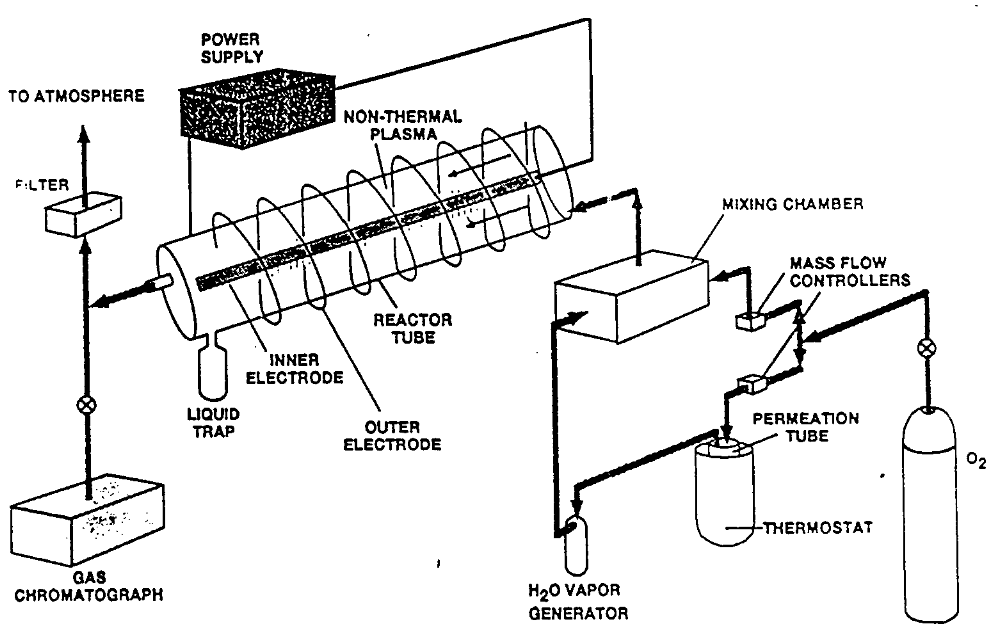

Figure 1. Experimental Setup

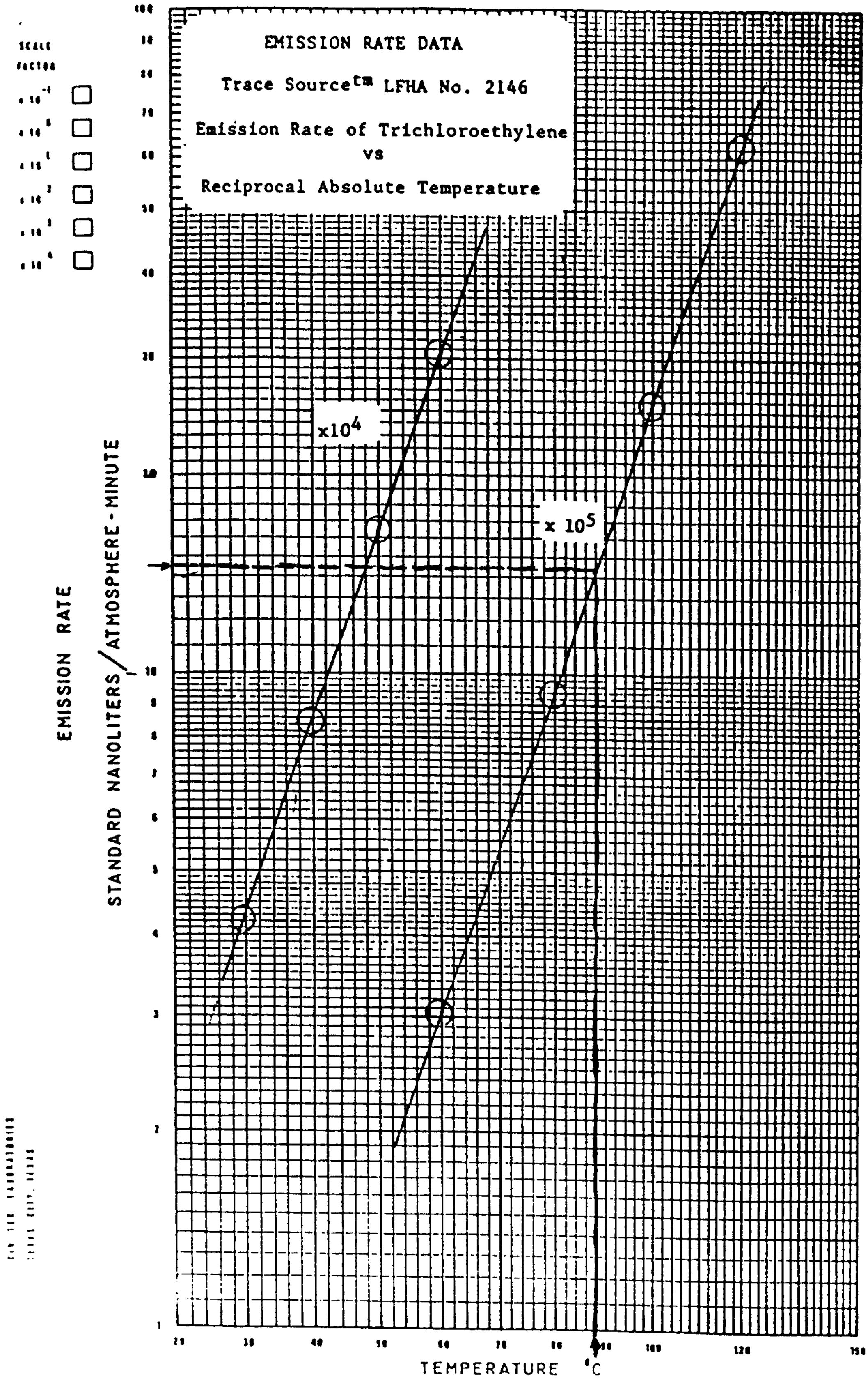

Figure 2. Emission Rate Data [11]

Figure 1 shows the setup of the experimental apparatus. Oxygen (the diluent gas) travels from the tank to two areas, one of which is the thermostat or "bath" (a Scientific Isotemp Immersion Circulator). Inside the bath is a stainless steel permeation tube, and inside the permeation tube, TCE liquid and vapor encompass a membrane. Oxygen enters one end of this membrane and travels a circular path. Some TCE enters the membrane and the oxygen then collects it [11]. A stable gas mixture of O_2 and TCE is thus created.

The amount of TCE which will permeate is determined by the temperature of the bath (which is adjusted with the attached regulator). The necessary temperature can be found in reference to the desired concentration of TCE from the equation

$$C = \frac{E}{F},$$

where C = concentration

E = emission rate

F = flow rate. **[11]**

Assume the desired concentration of TCE is 4800 ppm. The flow rate is 300ml/min and the emission rate is unknown. E is solved using the equation

$$4800 = \frac{E}{300}.$$

Thus, E = 1440000.

Based on the emission rate, the temperature can now be determined, using Figure 2 [11]. 14.4×10^5 (changed to accommodate the table) is found in the left axis. Following 14.4 horizontally until it merges at a point with 10^5 will give the required temperature: 88^0 C.

Reverting to Figure 1, the gas from the permeation tube continues to the water vapor generator, or bubbling chamber, where water vapor is added to the stream. TCE + O_2 + H_2O vapor travels to the mixing chamber.

The second stream of oxygen from the tank (sometimes referred to as "dry O_2") goes directly to a mass flow controller and then to the mixing chamber, where it combines with the TCE + O_2 + H_2O flow.

From the mixing chamber, the gas passes through the input valve to the 200ml coaxial reaction tube. The Elgar system, a commercial power supply, provides the tube with the electricity via voltage transformer. Diagnostics are used to measure the current and voltage in the tube. Microdischarges occur in the flow as it continues down the tube.

The coaxial reaction tube is made of glass. The inner tube contains salt water (to serve conducting purposes) and a wire brush, which is an electrode. Around the outer tube is bound a copper coiling to serve as the other electrode. (The electricity enters one free end of the copper coiling and the wire brush [14]. Microdischarges, then, occur in the gap between the two glass tubes.)

Connected to the output of the reaction tube is a trap that collects any excesses (liquids) formed in the reaction, such as chloroacetic and dichloroacetic acids [2]. Samples of the gas after reaction with the applied voltage and frequency are taken from the output valve.

Voltage was applied with an Elgar 400SD Model 1001SL, and viewed with a connected Nicolet system (Nicolet 4094C Digital Oscilloscope and Nicolet XF-44) in waveforms. The Nicolet system also showed the microdischarges occurring inside the tube. Actual measurements of current and charge were captured by the Nicolet, recorded on a floppy disk, and transferred to Vu Point II, an analysis software used to calculate power in the tube.

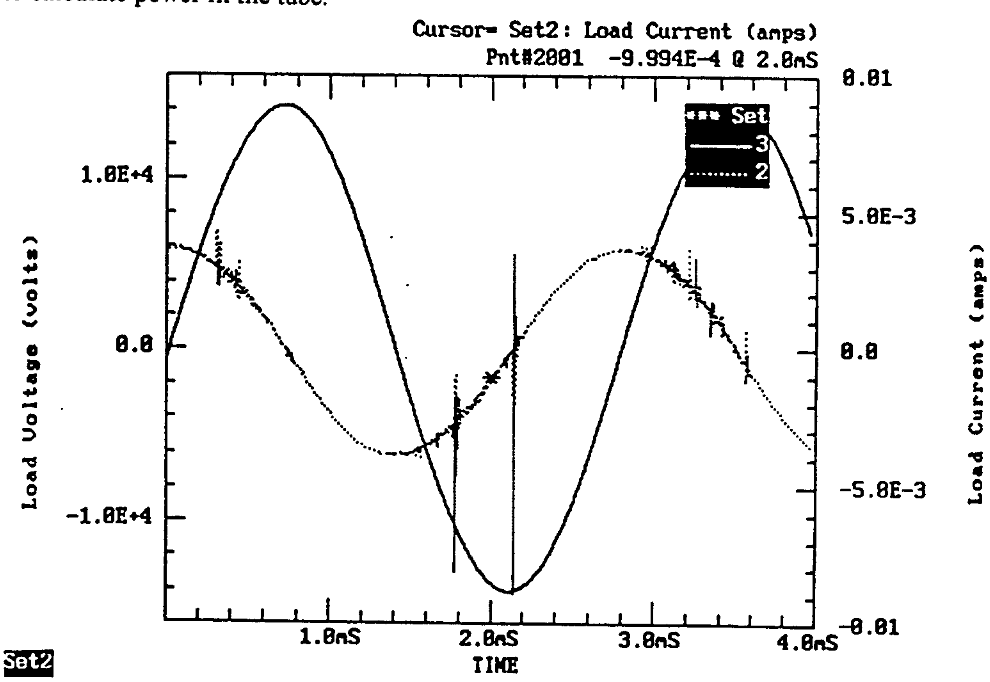

Figure 3. Voltage vs. Current

Voltage and current are represented in Figure 3, which comes from the mentioned Vu Point II program. The darker, more uniform line is the voltage. Microdischarges are seen in the current waveform as the spike-like structures. This particular reading was taken at a voltage of 170 with the power at 1.1 watts.

Each test series included three input and four output gas samples. After a sample was taken, it was injected into a Perkin-Elmer Sigma 300 FID/HWD Chromatograph, which separated the gas into concentrations of oxygen, water vapor and TCE. An attached Hewlett-Packard 3390A Integrator showed the results of the reading as a function of time in minutes (see Figure 4). On the left (the input sample) the first peak represents oxygen, detected at 0.25 minutes. Following oxygen is water vapor at 1.13 minutes. The last peak seen is TCE at 7.47 minutes. Below the peaks in the typed section is the word "area," which denotes the relative concentration. There is a notable difference between the TCE area of the input sample and that of the output sample. (Note: the objective here was not to destroy all of the TCE but to find, after several tests, which parameters were the most efficient.)

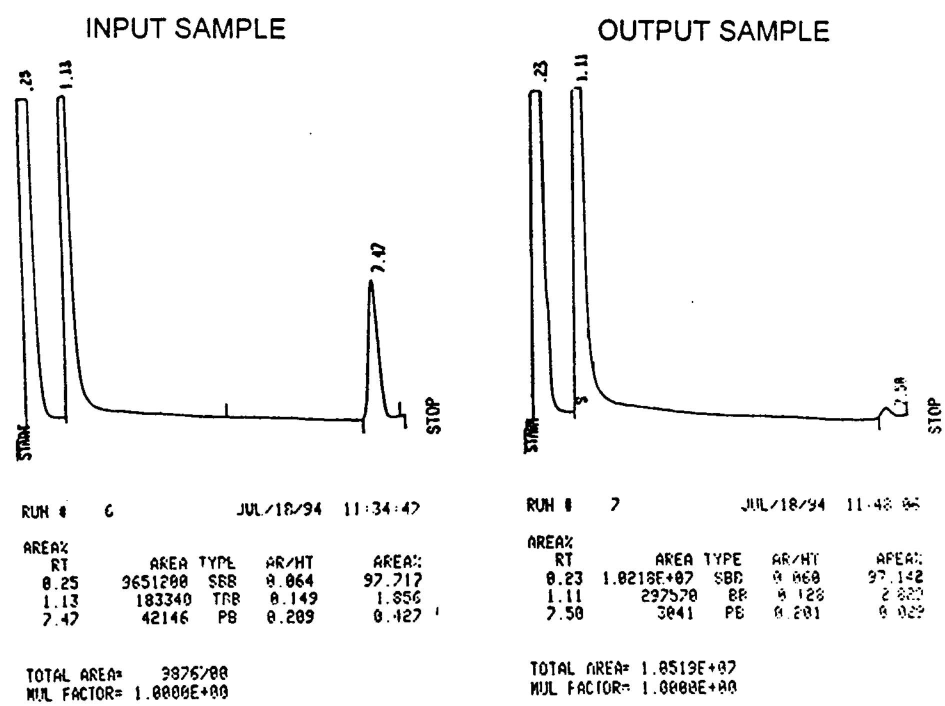

Figure 4. Integrator Readouts

After the three input and four output samples were taken, the percent reduction of TCE and the efficiency of the system was calculated. Percent reduction (R) here is defined as 1 minus the output area (X_{out}) divided by the average of input area (X_{in}), multiplied by one hundred.

$$R = \left(1 - \frac{X_{out}}{X_{in}}\right) \bullet 100$$

The efficiency of the system refers to the ratio of a theoretical energy per molecule to the input energy, divided by the number of TCE molecules destroyed.

$$E\% = \frac{\alpha R F X_{in}}{1.5 \times 10^{7} P}$$

where $\alpha =$ 5 eV per molecule

$R =$ reduction (%)

$F =$ flow rate (ml/min)

X_{in} = the concentration of TCE (ppmv)

P = power (watts)

Results

Applied Elgar voltage can be seen in Figure 5. Initially, the intention was to apply the voltage at specific points on the graph to create more of a linear, diagonal setting; however, the microdischarges in the tube were unpredictable and the original stratagem was altered. Applied voltage had to be varied to keep the tube power constant, rather than the tube power varying and the applied voltage remaining constant. Basically, the more radical action took place between 170 and 190 volts. Most samples were taken in the 160-170 volt range because anything lower than 160 destroyed virtually no TCE. Voltage settings above 170 created massive discharges which could cause damage to experimental equipment. In the 160-170-volt range, the tube power ranged from 0.5 to 1.5 watts.

The extent of TCE destruction based on the power from the tube can be seen in Figure 6. TCE reduction is greater as the power exceeds 0.7 watts, which referring to Figure 5, is within the range where the system is most effective.

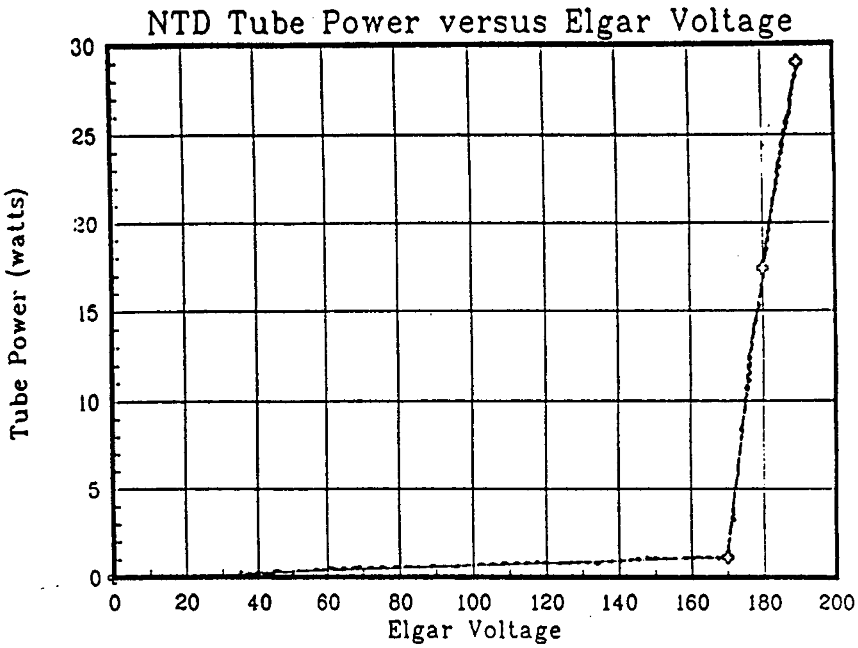

Figure 5.

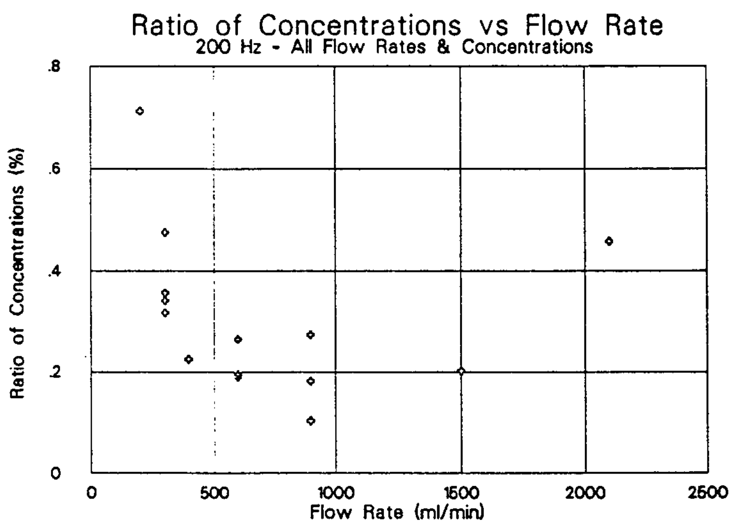

Figure 6.

In the experiment, the main objective involved discovering what trends developed by changing different parameters. The range of parameters were flow rates from 200-2100 ml/min, TCE concentration from 1000 to 4800 parts-per-million (volume), power (as mentioned) 0.5 to 1.5 watts, frequencies 200, 360 and 540 Hz. From these, the TCE reduction ranged from 10 to 90%. For each data set both the efficiency and reduction were calculated. The several trends noted and examined can be observed in the following section.

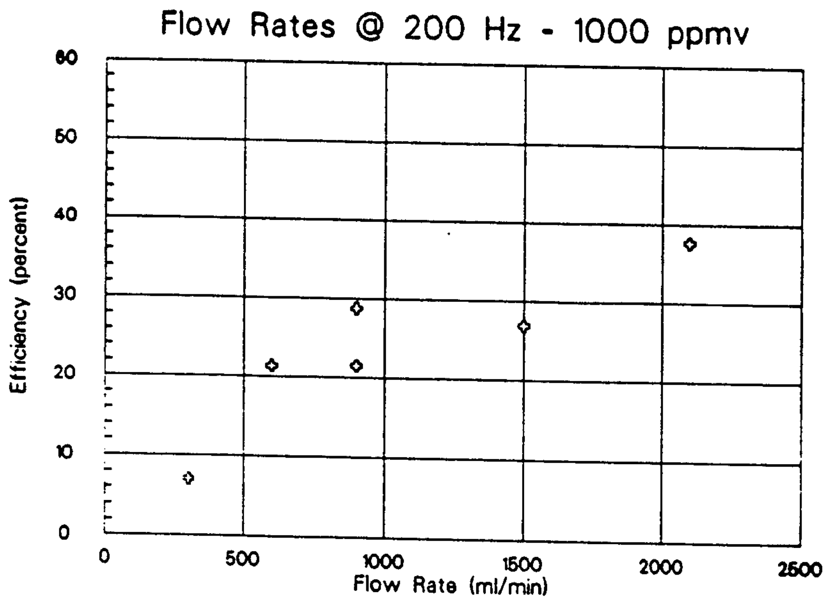

Figure 7.

Figure 7 shows efficiency plotted as a function of flow rate at 200 Hz and a 1000 ppmv concentration. The results indicate a correlation between flow rate and efficiency: as the flow rate increases, the efficiency also increases.

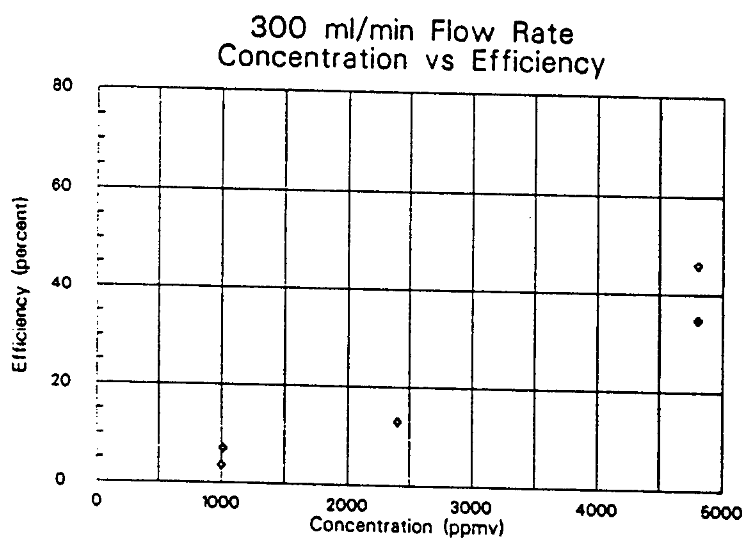

Figure 8.

Figure 8 represents efficiency compared with the input concentration in variation. These preliminary results reveal the concentration and efficiency increase simultaneously.

The three nearly-linear trends in Figure 9 represent the different concentrations of TCE. Again, efficiency increases with flow rate. The increased slope of each line with regard to the increase in concentrations support the results from Figure 7 and Figure 8.

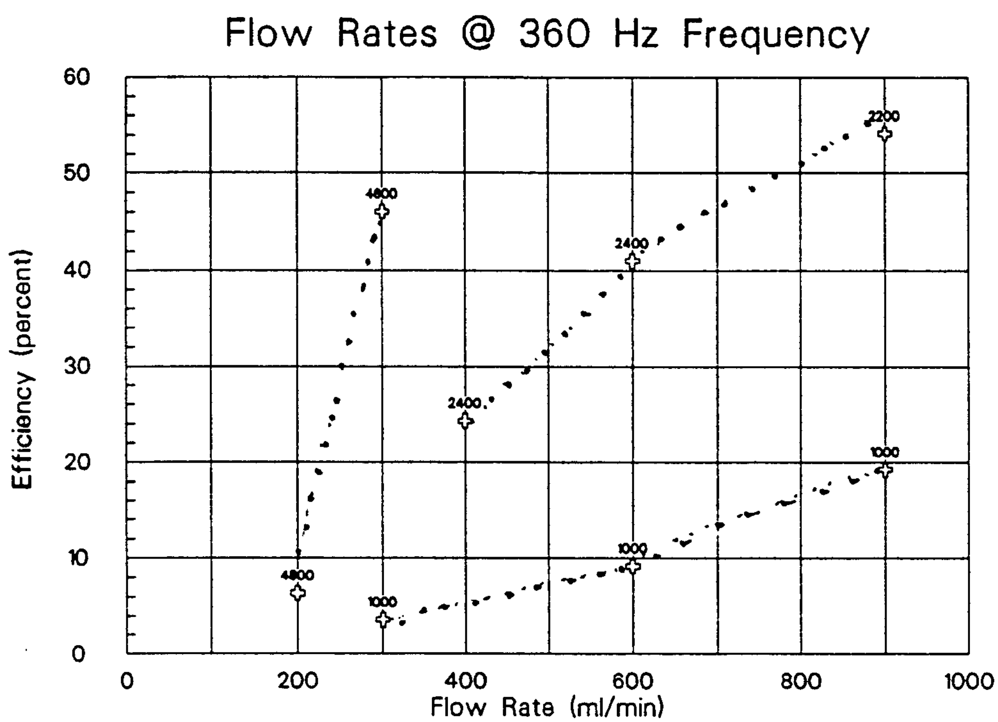

Figure 9.

An additional method of analyzing overall results of the non-thermal discharge technique often involves a comparison of flow rate to the ratio of concentration (in percentage). (The ratio of concentration equals the concentration of the outputs divided by the ratio of inputs. So, for example, if the output concentration is equal to 10,000 ppm and the input 100,000 ppm, then the result is a 0.1 or 10% ratio, resulting in a 90% reduction.) This can be seen in Figure 10.

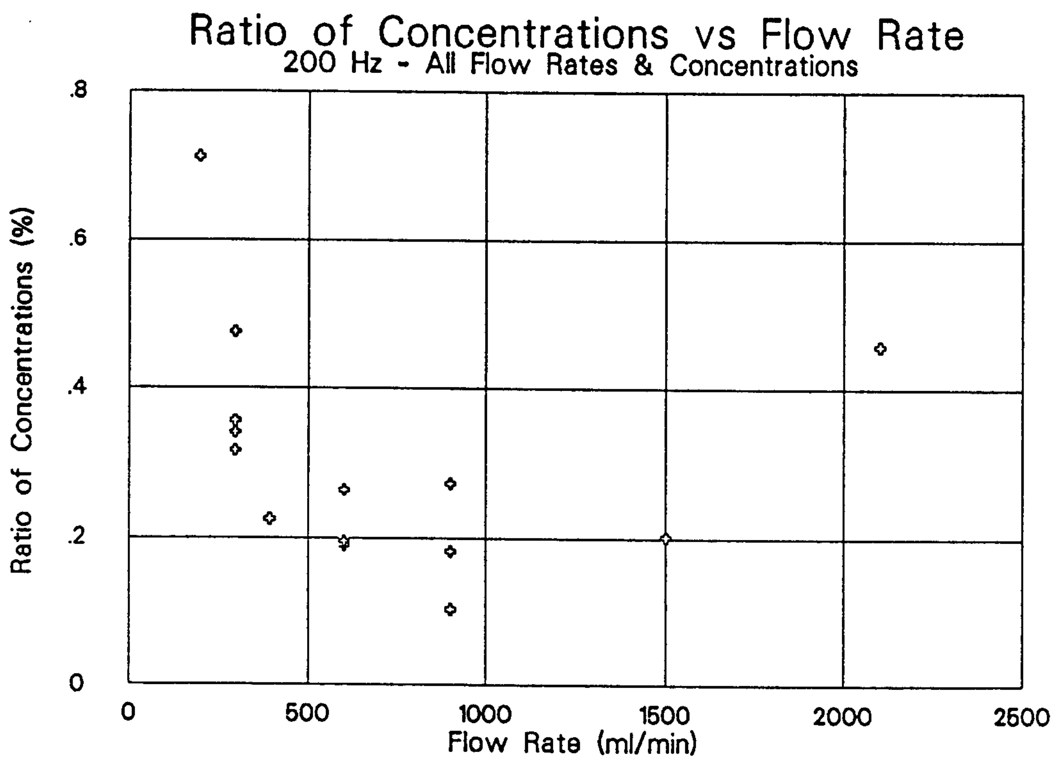

Figure 10.

Results indicate that at a flow rate of 900 ml/min, the ratio of concentration is at its lowest (meaning a greater percent reduction). However, if the flow rate is beyond 900 ml/min, the ratio of concentration increases (or the percent reduction decreases). Perhaps this can be explained with a notion of what may occur in the coaxial reaction tube.

Looking at the diagram below, assume the power and TCE both traverse the entire length (L).

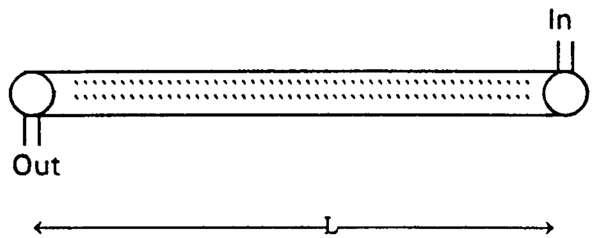

If only a portion (a) of the tube is causing chemical decomposition to occur, then power is wasted in length L-a.

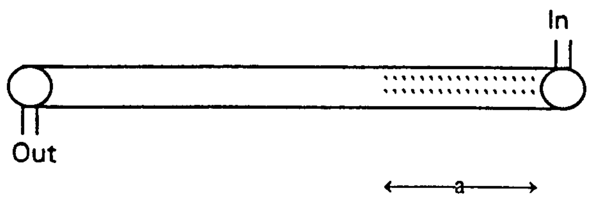

The most efficient use of the tube (which would yield the highest percent reduction) would occur when a=L, or the entire tube is functioning in the destruction of TCE. Likewise, if the flow is increased to a rate surpassing the desired a=L, the percent reduction would decline because the TCE molecules would be traveling more rapidly, and some would escape destruction due to the inability of the NTDP to destroy them all.

Conclusions

In conclusion, preliminary results impart the efficiency increased with flow rate and concentration, and the power variation was unable to be studied. Efficiency may also be affected by the extent of tube usage (in aspects of its length or geometry).

As far as a conclusion of my summer, I can certainly say I had an excellent, edifying experience at Site A-15. From a technical point of view, I learned how to use many types of equipment. I became very familiar with the Gas Chromatograph, as the experimentation called for the taking of numerous input and output samples. The integrator was also a close friend of mine, as I recorded information from its printouts in the laboratory notebook and from them calculated the percent reduction and efficiency of the NTDP.

I took part in the setup of the experimentation process, including manipulation of concentration and flow of TCE. I learned how to figure the required temperature of the Immersion Circulator, based on a certain desired concentration, and adjusted and regulated them as well. I altered the Model 247C Channel Readout, connected to the mass flow controllers, to affect the amount of TCE flowing in the system. In addition, I learned the use of the Elgar and Nicolet systems, dealing with voltage and frequency, and how to use the Vu-Point II computer program that found power based upon the equation $P=V \cdot I$.

There is no doubt I have learned much about the experimentation process. It is not as to-the-point as I had known before. There is much trial and error involved, most definitely with something relatively new. Many times, one component of the experiment affects all components, which delays time if a change occurs, but also opens eyes to new information. It is important for me to have learned the reality of true experimentation.

One of the most intruiging things I have learned deals with correlating information. I can finally see how some of the things from school applies to everyday life and I know, for example, the incentive behind all of the classroom chemistry experiments and mathematical equations.

The apprenticeship program has benefited me greatly. I am pleased to have had the opportunity to be involved and likewise look forward to it in the coming year.

Acknowledgments

Thank you, very much,

Heather Petresky for answering my many questions and always being there to help (I appreciate it!)

Randy Drabczuk for having me as an apprentice and also helping me

Alan Nejezchleb for all of the help at the lab

Keith Jamison and **Alex Cash** for explaining the complicated stuff

Steve Federle for giving me help with computers

Janice for giving all kinds of help

Glenn Rolader for the many references

Gail Filer for being so generous

----and everyone else at Site A-15 for their hospitality

Dr. Klausutis, Don Harrison, Mike Deiler for making HSAP terrific

Glenda Apel for being a superb person...even with all of my questions via telephone

List of References

[1] B.M. Penetrante, S.E. Schultheis, "Preface," Non-thermal Plasma Techniques for Pollution Control, vol G34(A), pp. v-xx, 1993.

[2] "Commercialization of Dual Use Technologies," submitted to Department of AF WL/MNK, Eglin AFB, FL, part I: Technical Disposal, pp.1-20+, 1994.

[3] J.D. Spengler, M. Brauer and P. Koutrakis, "Acid Air and Health," Environ. Sci. Technol., 24(7), pp. 946-953,1990.

[4] Jen-Shih Chang, "Energetic Electron Induced Plasma Process for Reduction of Acid and Greenhouse Gases in Combustion Flue Gas," Non-thermal Plasma Techniques for Pollution Control,, vol. G34(A), pp.1-20, 1993.

[5] J.O. Kolawole and G.E. Rolader, "Non-thermal Plasma Oxidation of TCE in Ground Water," Technical Information Memorandum, TIM-1-507, 1993.

[6] J.D. Skalny, V. Sobek, P.Lukak, "Negative Corona Induced Decomposition of CCl_2F_2," Non-thermal Plasma Techniques for Pollution Control, vol.G34(A), pp.151-165, 1993.

[7] J.J. Coogan, G.K. Anderson, M. Kang, J.P. Piccola and L.A. Rosocha, "Silent Discharge Plasma Destruction of Hazardous Wastes," Non-thermal Discharge, Working Session, pp. 15-16.

[8] J.R. Holum, Topics and Terms in Environmental Problems. New York: John Wileg & Sons, Inc., 1997; pp.1-5, 419-480+.

[9] L.A. Rosocha, "Non-thermal Discharge Session Summary," in First International EPRI/NSF Symposium on Advanced Oxidation, vol. 1: Executive Summary, pp. 23-26, 1993.

[10] L.E. Hancock, Systems Management and Development, section 15, pp. 1-21+, 1994.

[11] LFH Permeation Sources; Kin-Tec Laboratories, inc., Texas, pp. 1-11, 1986.

[12] M.B. Chang, M.J. Kushner and M.J. Rood, 'Gas-Phase Removal of NO from Gas Streams via Dielectric Barrier Discharges," Envirn. Sci. Technol., vol 26(4), 1992.

[13] Senichi Masuda, "Report on Novel Dry DeNOx/ DeSOx Technology for Cleaning Combustion Gases From Utility Thermal Power Plant Boilers," Non-thermal PlasmaTechniques for Pollution Control, vol G34(B), p.131, 1994.

[14] S.F. Windham, "Electrical Measurement and Modeling of a Plasma Discharge Tube." Alabama: Auburn University, 1993; pp.1-7+.

[15] W.C. Neely, E.I. Newhouse, E.J. Clothiaux and C.A. Gross, "Decomposition of Complex Molecules Using Silent Electric Discharge Plasma Processing," Non-thermal Plasma Techniques for Pollution Control, vol. G34(B), pp. 309-319, 1993.

ACCURACY VERIFICATION EXERCISE FOR THE COMPOSITE HIGH ALTITUDE MANEUVERING PBV PROGRAM (CHAMP)

Robyn M. Carley

Fort Walton Beach High School
400 SW Hollywood Blvd.
Fort Walton Beach, FL 32548

Final Report for:
High School Apprenticeship Program

Sponsored by:
Air Force Office of Scientific Research
Bolling Air Force Base, Washington, DC

and

Wright Laboratories

August 1994

ACCURACY VERIFICATION EXERCISE FOR THE COMPOSITE HIGH ALTITUDE MANEUVERING PBV PROGRAM (CHAMP)

Robyn M. Carley
Fort Walton Beach High School

Abstract

CHAMP version 1.2.0, software used for imaging and modeling, had not been quantitatively tested after distribution. Using elementary test cases for which the theoretical intensity values could be calculated, the output of the CHAMP software was analyzed for accuracy. Five geometric shapes were used, and the intensities of the objects were measured with range decreasing over 100 km. Testing methods, errors discovered, and methods and results of correction are discussed.

ACCURACY VERIFICATION EXERCISE FOR COMPOSITE HIGH ALTITUDE MANEUVERING PBV PROGRAM (CHAMP)

Robyn M. Carley

Introduction

The Composite High Altitude Maneuvering PBV software, otherwise known as CHAMP, is an InfraRed (IR) signature modeling and imaging program used primarily for scene generation in the Kinetic Kill Vehicle Hardware in the Loop Simulation (KHILS) Facility. The most recent version, Version 1.2.0, was distributed to Wright Laboratory in April 1994. The simulations which use this software require high levels of accuracy because of the applications of the output. Such applications include evaluation of the functioning of sensors and seekers (the eyes of missiles) for the military. To verify the accuracy of the latest CHAMP version, a scenario was developed, tested, and compared with theoretical answers using the comparison feature of total signature intensity (TSI). Total signature intensity refers to the total image IR "brightness." This number is independent of range and can be calculated using Planck's Equation.

Using five simple geometric shapes (disk, sphere, plate, rectangle, and cylinder) in seven positions (30^{o} rotation increments from 0^{o} to 180^{o}) data was collected on images from ranges 100 to 0 km. The total radiance of each image was multiplied times the range squared times the IFOV (instantaneous field of view) squared to acquire the TSI. The TSI of each image of a shape, no matter what degree of rotation or range the shape possesses, should be equal to the theoretical value for TSI. This number is computed using Planck's Equation and the emissive qualities of blackbody, a theoretical material with ideal radiance aspects. Using KHOROS, an image processing tool, the output was extracted from CHAMP and compared to the theoretical "truth". Errors were discovered, and the data was analyzed. When no user input discrepancies were found, the computer program was examined. The problem appeared to be with the waveband integrator for Planck's Equation within the CHAMP code. After changing the code to increase the number of integration points per micron, the test cases were re-run. Inaccurate results persisted, and further examination discovered flaws in PIXMAP, a pixelizer program that performs CHAMP's imaging operations. Correcting the technique that PIXMAP used to integrate and calculate the intensity of the image corrected the flaw. Taking into account the way CHAMP draws rounded objects that creates answers slightly smaller than the "truth", and after implementing the corrections to CHAMP and PIXMAP, this software now runs with a high degree of accuracy.

Discussion of Problem

CHAMP and its accompanying software have many uses within the Seeker Technology branch of the Armament Directorate at Wright Laboratories. When an updated version was distributed, many of the changes in the software had direct applications to the projects for KHILS. The software was accepted, but it had not gone through quantitative accuracy testing. Tasks involving CHAMP, such as Hardware in the Loop tests, require high levels of accuracy, and levels for the new software were unknown. Therefore, the initial problem following installation was to outline plans for accuracy testing. By using simple test cases whose theoretical "truth" could be easily hand-calculated, the accuracy of the new software could be efficiently measured.

A second problem occurred when inconsistencies were detected early in the exercise. While some TSIs stayed constant, for many of the objects the TSI oscillated at different ranges, or increased as range decreased. Re-running the tests produced identical results, and all input data was checked to rule out the possibility of user input discrepancies. To find and correct these errors, the problem was described to a CHAMP developer who analyzed the CHAMP program code and recommended solutions.

Methodology

The testing procedure began with written objectives. Certain features were defined and kept constant throughout the testing, while others were changed. The test cases dimensions are listed in the following table.

OBJECT NAME	DIMENSIONS (M)
Cylinder	0.1 diam X 1.0 len
Disk	0.1 diam
Plate	0.1 X 0.1
Rectangle	0.1 wid X 0.1 len
Sphere	0.1 diam

The test models were then created on the computer using CHAMP's formats for polygon, dynamics, and input files. Polygon files are the user defined parameters for four-sided polygons. Seven dynamics files were created to define the seven different rotations of the objects (0^o, 30^o, 60^o, 90^o, 120^o, 150^o, 180^o).

Within the dynamics files (stored as degree.dyn), each spatial position (for the object **and** sensor) is defined and assigned a time in seconds. Each object was defined at the origin, and remained stationary, while the sensor moved from 100 km out on the positive X axis in to the origin. Each dynamics file was identical except for different object pointing vectors.

Defined within the input file are: runtime options, library file pathnames, sensor specifications, external source specifications, engine specifications, material property specifications, surface geometry specifications, and temporal specifications.

- OPTIONS : In the options section previewer and plume options may be selected. Other than having the previewer on, this section did not affect the test cases and will not be discussed.
- PATHNAMES : The library file pathnames tell CHAMP where to find different files from which statistics about thermodynamic properties, reaction rates, and other things are read. These affect the way CHAMP creates images and their intensities. These files are distributed with the code and may be copied and modified, but were kept constant throughout the accuracy testing.
- SENSOR : Sensor specifications defined are waveband, filter, and FOV (field of view). The waveband was set to 3-5 microns, the filter left at the CHAMP default (square), and the FOV was 150 microradians.
- SOURCES/ENGINES : The testing used neither external sources (like the sun or earth) nor engines (since they were immobile objects).
- MATERIAL : The material used in all of the testing was "blackbody". "Blackbody" is an ideal, theoretical IR material. It absorbs radiant energy completely, and therefore it must emit completely. Consequently, none of the testing would be affected by reflection or imperfect absorption.
- SURFACES : In the surface geometry specifications, CHAMP has a format that allows the user to create target objects out of spheres, paraboloids, cylinders, cones, disks, polygonfiles, engines, and flowfields. For each of the five objects, one object was defined in this section. The cone and paraboloid were excluded from the testing due to the difficulty of hand calculating their intensities using Planck's Equation Engines and flowfields were excluded because these features are irrelevant for this exercise. Within the surface geometry format, the user can define the number of material layers, the material name, the material thickness, a surface option flag, a base and apex (or center and edge) temperature, spatial coordinates and facing directions, dimensions (in meters) and the number of interpolation points throughout the object (if it is rounded). All of the test cases had one material layer made out of "blackbody" in a layer .005 meters thick at a constant temperature of 450^{o}. The spatial coordinates varied due to shape and size differences. The disk was tested with 2 parallel and 24 radial interpolation points, the sphere with 8 parallel and 24 radial interpolation points, and the cylinder with 4 parallel and 24 radial interpolation points.
- TEMPORAL : Almost the most important feature to be defined in the input file is the temporal feature. In this feature, initial and final times (in seconds) are assigned along with an increment time. Then a dynamics files is listed to tell where the trajectory for the object is located. CHAMP then calls the dynamics file, and reading the trajectory there defined, finds the positions of the object

at the initial and final times (and any positions between the two). Then using the increment time, the program uses linear interpolation for those increments whose positions are undefined. By using the initial time of 1 second and a final time of 2 seconds with an increment of 0.01, 101 images could be created at 1 km intervals. The date and Greenwich mean time can also be defined in this section, but do not affect the running of CHAMP.

Seven input files were created for each object, one for each rotated position. These files were saved under the names shape[degree].inp.

CHAMP was already installed in the PATH of the computers, so it could be run from anywhere. CHAMP was run, starting with the disk. 101 images were created for disk0.inp. These are filed as disk0[001-101].ply. These "ply" files contain the x-y-z coordinates, radiance, opacity, and temperature of the object from the input file for each time-step. Then PIXMAP was run to convert the three-dimensional "ply" files into two-dimensional pixelized images as seen by the sensor. When PIXMAP is run, the user can define FOV (150 microradians) and image size (128*128 pixels). However, PIXMAP only converts one time-step at a time. To speed up testing, a script file was written for each of the 35 input files, to pixelize all of their data at once. These were called "shape[degree]_run" files.

The output of the _run files were 101 ".img" files. Their information is in a form which an imaging program (such as Saoimage which comes with CHAMP) can then use to display a picture. In addition, PIXMAP outputs an information table to the computer screen for each of the "ply" files it translates. This provides statistics on each image's maximum radiance, total image intensity (equal to total radiance), target range, and x and y resolution of pixels.

While CHAMP and PIXMAP were running, the TSI was calculated using Planck's Equation. Planck's Equation (below) describes the spectral distribution of the radiation from a blackbody. In layman's terms, solving the first two portions of the equation for M and then multiplying by the change in waveband (2) and the area of the target, the TSI is calculated. The "truth" or theoretical TSI for each of the objects is also listed below.

$$M_{e,\lambda}(\lambda,T)=\frac{2\pi hc^2}{\lambda^5[e^{hc/\lambda kT}-1]}=\frac{3.74\times 10^4}{\lambda^5[e^{14,388/\lambda T}-1]}$$

where $M_{e,\lambda}(\lambda,T)$ = spectral radiant emittance in watts per square centimeter of an area and micrometer of radiation wavelength ($W\ cm^{-2}\ \mu m^{-1}$),

λ = emitted wavelength in microns (μm),

T = absolute temperature of the blackbody in Kelvins (K),

h = Planck's constant (6.626176×10^{-4} W sec^2),

c = speed of light ($2.99792438 \times 10^{10}$ cm sec^{-1}),

and k = Boltzmann's constant (1.380662×10^{-23} W sec K^{-1})

Object	Truth
Disk	0.6073
Sphere	0.6073
Cylinder	7.858
Rectangle	7.858
Plate	0.7158

While PIXMAP returned information relating to the images' total radiance, it was not information that could be practically compared to the "truth", nor was it usable (since it was printed to the screen). In order to convert the PIXMAP information into usable, manageable data, a C program called "accv" (short for accuracy verification) was written. This program inputted the ".img" files, added up the number of pixels that were on (giving the total intensity level, or TIL), then outputted this number in a "shape[degree].TIL file. Running "accv.c" resulted in 35 files, a more manageable number than the 3535 PIXMAP ".img" files.

To convert the ".TIL" data into a number comparable to the truth, the image processing software KHOROS was used. KHOROS has a menu full of options to convert data, make graphs, multiply images, and more. By using the menu options, various flexible workspaces can be created to extract and display statistics of images. A KHOROS workspace was created for the verification that read in the ".TIL" files, multiplied their data by the range squared and IFOV squared to get the TSI, and put the resulting information in a three-dimensional graph. There were five graphs, one for every object, and each graph showed all seven rotations of the objects. The graphs recorded the TSI on the Z-axis, the range on the X-axis, and the rotation angle on the Y-axis. Later the workspace was modified to create a matrix corresponding to each graph so the values for specific points could be examined, and the percentage error calculated.

<u>Results</u>

As soon as each graph was printed, obvious errors were discovered. Some objects had an oscillating TSI in certain regions of the graph, some objects had an increasing TSI that appeared to be related to decreasing range, and others merely outputted incorrect values. To eliminate the possibility of user input discrepancies, all aspects of the input files, dynamics files, polygon files, and the accv.c program were

examined and checked for error or inconsistency. No error was found, and re-running CHAMP and PIXMAP gave identical results. At that time, the problem was referred to a CHAMP developer.

The developer wrote programs to examine the data from CHAMP, and the data from PIXMAP. He discovered that CHAMP was outputting inaccurate results. Further analysis detected an error with the method in which CHAMP's waveband integrator functioned. (Because the waveband was 3 to 5 microns, the value for λ had to be the integration from 3 to 5 microns.) Apparently, the integrator did not choose enough integration points for each micron, and the value for λ was not accurate enough. Therefore, the developer went into the code and raised the integrator's resolution to a level of accuracy sufficient for CHAMP's uses.

Once the code was modified, the tests were all rerun. While the results were more consistent with themselves (no oscillations or increases), the data inaccuracy was too high of a percentage for the program to be useful. Once again, the problem went to the developer. Using the same programs he had used to find the integration problem, an error in PIXMAP's functioning was detected. The developer described it as an error in the scan information used in temperature integration of the target. The computer was using dead pixels as part of its integration data, resulting in the radiance coming out lower than the calculated values. The error was corrected by installing an internal check in the PIXMAP code to verify that chosen points are part of the target.

Once again, all of the tests had to be rerun to verify if the modifications were sufficient. By examining the matrixes of all of the test cases, the percentage error was calculated. The rectangle and plate came out to within 1.4% accuracy (consistently low), but the disk, sphere and cylinder were off by as much as 8%. All input sources and relevant files were examined, without finding any source for this anomaly. Finally, an examination of CHAMP's methods of curve fitting provided the answer. CHAMP uses the number of radial integration points to create a model of a curve. When CHAMP uses more integration points, the resolution of the curve is higher, and the output is more accurate. By raising the number of radial integration points from 24 to 96, the inaccuracy for all objects was raised to within at least 98% accuracy, as shown in the table below.

Object	Theoretical Truth	Final CHAMP Output	Percent Error
Disk	0.6073	0.6003	1.2%
Sphere	0.6073	0.6039	0.6%
Cylinder	7.858	7.717	1.8%
Plate	0.7158	0.7746	1.4%
Rectangle	7.858	7.746	1.4%

Conclusion

Although it seemed doubtful at first that testing was needed for CHAMP Version 1.2.0 other than as a preventive action, this testing was indeed necessary for Version 1.2.0 to be used for KHILS and other testing. The problems were minor and easy to repair, CHAMP 1.2.0 will now run within 98% accuracy, and the applications of the new CHAMP version can be used at Wright Laboratories for sensor/seeker testing.

Acknowledgements

Charles Coker, WL/MNGI, was my mentor this summer, and was very helpful and supportive while I performed my testing. He was also the CHAMP developer who found the problems, and then managed to describe them so I could understand them. Dennis Garbo, Eric Olson, and Walt Krawczyk are civilian contractors from SAIC in Shalimar, FL, and they were all very helpful when Charles was busy, or when their training was more in-depth than my mentor's for questions that came up. Emily Martinez, WL/MNGI, worked down the hall and also helped out with less technical problems, specifically where to find certain software or how to word sections of my paper. Alice McCrae was our section secretary, and always there to help. John Provine is the MNGI branch chief, and is very supportive of the whole apprentice program. Don Harrison, Mike Deiler, and Glenda Apel all organize and coordinate the HSAP program at Wright Laboratories, and they made it a very personal and in touch program, as well as a fun, educational, and rewarding experience.

Bibliography

Crow, Dennis. Composite High Altitude Maneuvering PBV (CHAMP) Version 1.2 User's Manual. Aero Optics, Inc. Los Angeles. March, 1994.

Hudson, Richard D. Infrared System Engineering. John Wiley & Sons. New York. 1969. pp 35

THE ADAMS PROJECT

Jason P. Carranza
AAAF-3
Wright-Patterson Air Force Base

Chaminade-Julienne High School
505 S. Ludlow St.
Dayton, OH 45402

Final Report for:
High School Apprenticeship Program
Wright Laboratory

Sponsored by:
Air Force Office of Scientific Research
Bolling AFB Washington DC

August 1994

THE ADAMS PROJECT

Jason P. Carranza
Chaminade-Julienne High School

Abstract

During the summer of 1994, I participated in the Air Force Office of Scientific Research (AFOSR) High School Apprenticeship Program as an apprentice of Charles B. Hicks and Clive L. Benjamin. During the first half of the summer I spent most my time with Mr. Benjamin, learning about the C language and the UNIX operating system. I programmed several mathematical programs in the C programming language on a UNIX-run ALPHA workstation and SUN SPARCStation 2. In addition, I spent time evaluating a new piece of software which was an electronic catalog for reuse. During the second half of the summer with the help of Mr. Hicks, I was able to increase my proficiency in ADA, software engineering, and software design. A problem was given to me by Mr. Hicks, and I was instructed to first design an algorithm to meet the requirements, secondly refine the algorithm to pseudocode, then program it into an ADA development environment, compile, and debug the program. Finally, I repeated the process when modifying the program to meet stricter requirements of Mr. Hicks. This program in return was used in the ADAMS project Mr. Hicks was working on at the time.

THE ADAMS PROJECT

Jason P. Carranza

INTRODUCTION

Programming in any language is a time-consuming, nerve-wrecking, pain-stacking process that is well worth the trouble. One word or symbol can crash an entire program, as I found out. However, if one takes time to first design an algorithm and think things through, the project runs much easier. I spent a good amount of time writing a program for the ADAMS project. I was given two parts of the puzzle to solve: converting a point on a screen to a latitude and longitude coordinate, and finding the slant height between two points given the height of both points. These two programs proved to be challenging, yet interesting. As I was programming these two programs, I had to learn to use the UNIX operating system since it is the environment most programmers use. To make things more complicated, I had to learn to use UNIX on two different workstations: a DEC3400 AXP workstation, and a SUN SPARCStation 2. However in the process, I learned how versatile UNIX was in this type of situation. I could write a program in the VI editor on the ALPHA workstation and then copy the program and work on the same program on the SUN SPARCStation 2 with no compatibility problems. In a working environment as I worked in, this advantage was very helpful.

Discussion of Problem

The ADAMS project dealt with finding a flight path through an area on a map with emitters. My part of the project was to find the latitude and longitude of a particular point given to me. I chose to handle the problem with a record of integers as seen below. Since I used integers, I was able to save memory. This was an important point since the ADAMS program would be run on a personal computer (PC). The use of a float number instead of an integer was also possible, however I was initially unable to think of a way to use a floating point number. It was later pointed out to me that it was possible.

```
type coordinatetype is
record
  deg:integer;
  min:integer;
  sec:integer;
  sign:character;
end record;
```

```
type coordrectype is
record
  lat:coordinatetype;
  long:coordinatetype;
end record;
```

Another piece of the ADAMS project given to me was the problem of finding the slant height in feet between two points of different height. This program proved to be easier than the latitude and longitude program. In this program, I chose to do my calculations with a record of floating point numbers instead of integers. Due to the fact that Mr. Hicks wanted the slant height as an integer, I had to round my final answer to the nearest foot. Because of this, my answer could be up to a half a foot off the exact answer. However, due to the nature of the project it must be noted that this error is insignificant.

Methodology

The first program I started was the latitude and longitude program. This project involved taking an X,Y number and converting it to a legitimate latitude and longitude coordinate with degrees, minutes, and seconds. For example, a map is read into a set screen size (see below). The screen size is 1100 units square, and the X,Y coordinate given is 25 units in the X direction and 35 units in the Y direction. In

screen size=1100 x 1100 units

X,Y = 25,35

addition to the X,Y coordinate, I was also given the latitude and longitude coordinate for two points (see below): the starting point to the extreme lower left handside of the screen (0,0) and a checking point to the extreme upper right-handside of the screen (1100, 1100). In addition to the X,Y points given, I was also given the height of the X,Y point. This fact was used in the solving of the slant height program. With the use of the X,Y point and the two latitude and longitude coordinates, I was able to find the distance from the starting point to the X,Y point in latitude and longitude. After finding the distance to the point, I added that distance to the latitude and longitude

```
                      1100 units x 1100 units
                          --------------. <-checking point
                          |             |    (1100, 1100)
                          |    * X,Y pt |
                          |   /         |
        distance to pt---->/   MAP      |
                          | /           |
                          |/            |
     starting point-> .--------------
          (0,0)
```

coordinates of the starting point. This produced the final answer.

The second program I wrote was a program to find the slant height between two points given the height of both points. Slant height is basically the distance between two points, taking into account the height difference (See below). If one point is at 10 feet and the second one is at 30,000 feet, the distance between the two points would be greater than if the two points were at the same altitude.

```
                    ABOVE VIEW:
                               --------------. <-checking point
                              |     *<-2nd pt|
                              |    /         |
                              |   /          |
                              |  * <-1st pt  |
                              |              |
                              |              |
           starting point-> .--------------
```

```
                HORIZONTAL VIEW:
                                         *<--2nd pt (30,000 feet)
                              \
           1st pt (10 feet)-->*_
                                 \
                              ____\_________
```

To solve this problem, I first converted the two latitude and longitude coordinates to one floating point number. So if I had a longitude of 30 degrees, 30 minutes, and 20 seconds the real or float representation would be 30.505556. Seen on the next page is the mathematical representation of the problem. Tempnum is declared as a type float number. Tempnum is assigned the value of the rest of the statement. When done, tempnum is given a degree representation of the longitude with the decimal part of the number representing the minutes and seconds.

*NOTE:

1 degree=60 minutes

1 minute=60 seconds

INPUT:

```
entered #-->tempnum:=      30        +          (30/60)          +
                           ((20/60)/60)
```

```
code -->tempnum:= (firstpt.long.deg) + (firstpt.long.minute/60.0) +
             ((firstpt.long.second/60.0)/60.0)
```

OUTPUT:

tempnum=30.505556 degrees

After converting the degrees, minutes, and seconds into one number, I proceeded to do the calculations needed to find the slant height. In this process I used two triangles to find the slant height (see next page). First, I found the difference of longitude between the two points. This was stored as the variable, X. Then I found the difference of latitude between the two points. I stored this answer in Y. I then used the Pythagorean theorem to solve for hp1. Hp1 is the distance between the two points, not taking into account the height difference. Now refer to the horizontal view. This diagram takes into account the height difference. Hp1 is used as the bottom length and y2 is the difference between the emitter height and the flight path height. Again using the Pythagorean theorem, I found hp2, or the slant height. Finally, I converted hp2 from degrees to feet.

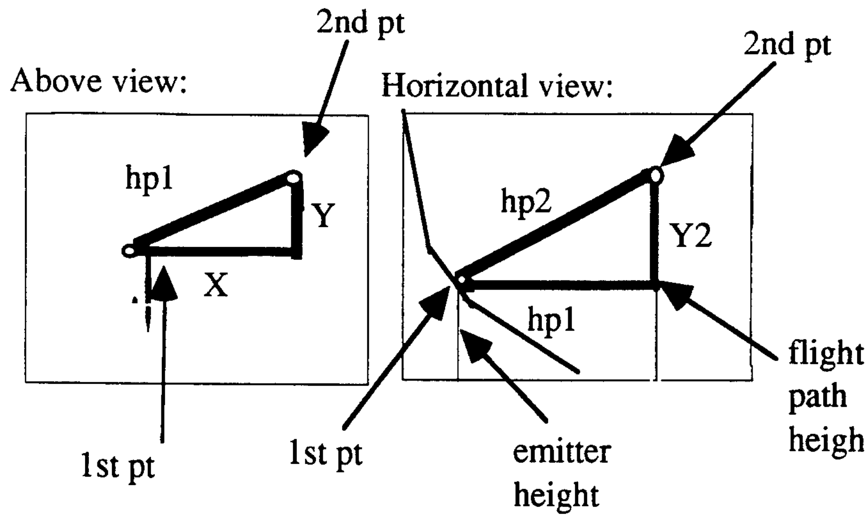

After writing the code to these problems, I had to write a testdriver to check the validity of the program. As I compiled, linked, debugged, and modified the code, I also had to comment it. I found that commenting is an essential part of software development. The program may become so large that the programmer may forget what one part of the code does. Commenting helps to straighten this memory loss as well as help a programmer to know what is going on. Documentation of the code is also used to explain to a person reading the code why the programmer went one route verses another. In the end, the finished product is a well tested, commented, and understandable piece of code easy to modify.

RESULTS

My results were positive. The programs ran well and followed the specifications given to me by Mr. Hicks. Overall, the results of the entire summer were also positive. I completed all my C programs successfully, and learned how to use UNIX. I went into the apprenticeship hoping to learn alot, and I can say I learned alot.

CONCLUSION

I started this program with little experience on a UNIX workstation. As soon as the first day of work began, I was working, and I mean working hard. Much was expected of me due to the successful summer I had last year. The first day I showed up, I was greeted by a tall stack of books on my desk. If that wasn't enough, I was told of the many things I would learn, like C programming language and UNIX. I was in disbelief in the amount of work and knowledge that was expected of me. However, I was able to do all of it, and I learned much in the process of doing it. In addition, I learned to budget my time and energy. In conclusion, I can comfortably say that I learned one new thing every single day.

DEVELOPMENT OF ASTROS, VERSION 11
FOR A PERSONAL COMPUTER

George P. Choung

Beavercreek High School
2660 Dayton-Xenia Rd.
Beavercreek, OH 45434

Final Report for :

High School Appretice Program
Wright Laboratories

Sponsored by:

Air Force Office of Research
Bolling Air Force Base, DC

and

Wright Laboratories

September 1994

DEVELOPMENT OF ASTROS, VERSION 11
FOR A PERSONAL COMPUTER

George P. Choung
Beavercreek High School

Abstract

This subject concerns the development of the computer program called ASTROS. This program currently is being used on several different types of computers, mostly the industry's best UNIX workstations. The source code of ASTROS is written in FORTRAN 77. Although FORTRAN 77 is a standard, there are some differences between the many different FORTRAN compilers. The task at hand was then to find these differences, and create options to bypass the difficulties.

DEVELOPMENT OF ASTROS, VERSION 11
FOR A PERSONAL COMPUTER

George P. Choung
Beavercreek High School

Introduction

ASTROS, the Automated STRuctural Optimization System is a program that aids in the design of aircraft through various processes of analysis and optimization. Although ASTROS was first developed for the purpose of evaluating air and space vehicles, it turns out that ASTROS can be used to represent a wide variety of mechanical structures. ASTROS has been and currently is being used on a smaller scale for commercial and research applications. Many situations have occurred in which ASTROS was implemented for a non-military purpose. The Structures and Optimization Group of the Flight Dynamics Directorate of Wright Laboratories has been asked to evaluate the maximum torque and stress that could applied to a certain socket wrench that a local company was developing. Also this group has used ASTROS to undertake such projects as analyzing the inner components, mostly gears, of an electrically powered car, which was being developed by a local university. Organizations such as these often need the automated and computerized analytical methods of ASTROS, but lack the necessary resources. Currently, the concentration of the use of ASTROS is occurring here on the UNIX-based CONVEX workstations. Because of the large jobs that ASTROS is capable and often forced to undertake, and the temporary memory requirements of this vast application, minicomputers have

provided the best combination of cost-effectiveness and efficiency. Due to the relative affordability of personal computers-ones that are becoming faster at an accelerating pace- the situation of porting ASTROS to a personal computer becomes a feasible and real possibility. The PC solves many of the shortcomings of using a minicomputer. First, for small businesses, a personal computer is financially within reach, while a multi-user workstation might not be. Many people are already familiar with the MS-DOS computing environment so personnel training time could be kept to a minimum. And finally, the difference in processing times between a PC and a workstation are relatively negligible for small tasks.

Discussion of Problem

The conversion of ASTROS from a UNIX platform to a DOS operating system can be described as translating the different dialects of a single language. Because the different types of operating systems FORTRAN is available on, the problem of compatibility comes up when moving from one system to another. Although FORTRAN is basically the same wherever it is produced, there are some instances in the code that needs to be changed. Some machines allow for commands not recognized by a standard FORTRAN 77 compiler. Also some of the code that needed to be changed was machine dependent and had little to do with the variations of FORTRAN.

One of the more outstanding attributes that is unique to ASTROS is its built in flexibility. Because of the archive libraries that are created, different users can produce their own source code,

compile it separately, and link it to the main program.

Methodology

There were seven basic steps to achieve the goal of having ASTROS running on a PC. The first of these steps was to obtain the source code from the CONVEX workstation that it was originally running on. These text files, approximately 1,800 of them taking up 12.1 megabytes of memory, were transferred using standard file transfer software. Then various file attributes had to be changed so that the could be properly accessed by the compiler. The next step was to initially compile all the subroutines. Because of the vast number of subroutines, in excess of 1,800, compiling one by one would be a tedious and time consuming project. To overcome this, a batch program was created that implemented the Microsoft Portable Linker. This program went through the list of source files and created object files of all that contained no errors. During this process, a file was created that contained all errors that were flagged. The next step was to edit the file that contained the errors and warnings. Some of the errors that were found were mostly trivial and either would not effect the executable file or would disappear when linked with other files. Debugging is the fourth step and was where the majority of the time was spent. This consisted of going through the list of errors, finding its corresponding place in the source code, and correcting it. Step five was creating archive libraries. In creating archive libraries, subroutines that call each other must be grouped together.

All the source files can be found in a total of 114 different

sub-directories; each grouped with other subroutines that combine to perform specified tasks. Since each individual subprogram already has a corresponding object file, one only needs to link the object files together to form the archive library. After creating the archive libraries, creating the executable file was the next step. Since the archive libraries are basically huge consolidated object files, they are linked in the same manner as normal object code. The final step in the process is testing. This step is one of the more important steps in any type of project. Testing would have involved considering many basic situations. Also projects with previously calculated results would be tested to show that the values calculated matched.

Results

Because of the time constraints involved, only the first four steps in the process were fully completed. Experimentation with different methods of archiving and linking were also explored. One of the two ways of archiving and linking was using the Microsoft FORTRAN Powerstation integrated development environment for Windows. The other way was again using the Microsoft portable linker in DOS. Although for a small amount of code, it was easier to use the Windows interface, the DOS based compiler proved to be more efficient in real time for larger projects.

The nature of the errors that were flagged fell into four general categories. The first type of error, which was already discussed, was the machine dependent code. Surprisingly much of the CONVEX specific routines, located in a directory especially created for machine

dependent code, was expected to cause errors, but compiled initially without trouble. Another problem that was encountered was the fact that UNIX allows for longer filenames that DOS. In UNIX filenames can be eleven characters long with multiple extensions possible. DOS on the other hand only allows for filenames to be eight characters long with a three character extension. There were several syntactic errors that needed to be addressed. Among these included the fact that some of the more obscure non-standard FORTRAN was not being recognized by the Microsoft compiler. Semantic errors, such as mismatched data types were picked up by the Microsoft compiler as well. These were purposely left in because the CONVEX compiler allowed this originally. There was one instance of a typographical error. In one subroutine two variable identifiers were typed incorrectly. This however did not effect the results of the program, because FORTRAN does not force the programmer to declare his variables before referencing them, which is why it probably was never found.

Conclusion

Although the importance of ASTROS in thee efficient development of air and space structures is unquestioned, its soon to be proven usefulness for small, commercial applications remains to be shown. Coupled with the fact that microprocessors for personal computers are closing the performance gap with larger, more expensive workstations, the availability of ASTROS becomes easier. This experiment of porting ASTROS not only had practical uses, but gains were also made in the area of converting UNIX FORTRAN code to MS-DOS FORTRAN code.

Nick D. DeBrosse

Kettering Fairmont High School
3301 Shroyer Road
Kettering, Ohio 45429

Final Report for:
High School Apprentice Program
Wright Laboratory

Sponsored by:
Air Force Office of Scientific Research
Bolling Air Force Base, DC

and

Wright Laboratory

August 1994

ADVANCED GAS TURBINE ENGINE COMPRESSOR DESIGNS

Nick D. DeBrosse
Kettering Fairmont High School

Abstract

Advanced gas turbine engine compressor designs and design tools were studied. A MathCAD processor was used to calculate compressor thermodynamics. The results from the MathCAD processor were used to enhance a baseline fighter engine with a growth fan using program TERMAP. From TERMAP the enhanced engine was placed in a flight simulator in a F-16 to compare the old engine's flight envelope with the enhanced engine's flight envelope. With this theoretical engine and it's data, a preliminary design program to see an advanced compressor.

ADVANCED GAS TURBINE

ENGINE COMPRESSOR DESIGNS

Nick D. DeBrosse

Introduction

The compressor is a fundamental piece of the gas turbine engine. The compressor's job is to provide the combuster with the highest pressure possible. The efficiency of the compressor is the key to a highly efficient engine. If the compressor efficiency is high then the combuster puts out more energy creating higher thrust. Since a highly efficient compressor is a key to the gas turbine engine, much time and money is invested in compressor research and technology.

Tradeoffs create problems when trying to design a more efficient compressor. One problem is when the pressure ratio (pressure leaving compressor/ pressure entering compressor) goes up the temperature rises also. If the temperature is too high, the heat will melt the engine. To create better fuel consumption the bypass ratio could be raised, but if the bypass ratio is raised then the size of the engine becomes larger increasing wind drag which worsens fuel consumption. There are no simple answers to designing a better compressor.

Methodology

The process of designing a more efficient compressor began with studying the topic. Studying the topic was reading the books Aircraft Gas Turbine Technology and The Aircraft Gas Turbine Engine and its Operation. It was essential to know as much

as possible about the gas turbine engine before getting started because without the proper background the next steps would be impossible.

The next step involved taking what was learned and seeing how it was used inside the engine. This helps better understand the mechanics of the gas turbine engine. Variables such as pressure ratio, horsepower, temperatures, and efficiencies were entered into a MathCAD processor which would calculate other variables such as final thrust, energy used, and specific fuel consumption. All equations were entered into the program by hand found in the books that were studied. A typical equation would be as follows: horsepower needed = Pressure constant of air * the change in temperature * the weight of air * 778 / 550 and net thrust = weight of air/gravity * the change in velocity + weight of fuel/gravity * speed of sound. The user could change independent variables and the computer would show how the dependent variables changed with respect to the independent variables. This helped to understand the complexity of the tradeoffs inside the gas turbine engine. There were many variables that could not be included in the MathCAD processor due to length of study was insufficient for the variables needed to add so the next step occurred.

To obtain more precise information a computer program designed for evaluating engines was used, TERMAP. In TERMAP there was many more variables including coolant and bleed factors which were unencountered in the MathCAD processor. The already existing fighter engine was used first to ensure correct results, then the theoretical engine was used. A considerable higher thrust was recorded at same altitudes and velocities as the fighter engine. Unfortunately no pitfalls were

entered into the program, so it was impossible to tell if the new engine would actually succeed in a flight setting. (A sample output has been included.)

The data from TERMAP was then put into a F-16 in a flight simulator to see how the engine behaved in flight. The F-16 was flown at certain altitudes and velocities and until it would stall. The stall points were then connected to make a flight envelope. The flight envelope with the new engine was then compared with the flight envelope of the F-16. While the overall envelope was better, there were certain areas where there should have been greater speed. With the data from TERMAP and the flight envelope from the flight simulator, a new program was used to give more graphic detail of what the compressor was doing. Unfortunately, the program was unable to reach a solution because of the technological advances that were made unto the engine. No conclusions were reached because the aerodynamic breakthroughs desired were too far ahead of the design program, and the shortness of my tour would not allow time for the program to be edited.

Acknowledgments

During my eight week tour I have had help from many people. Mostly from my mentor, Marvin Stibich, and my fellow workers John Lueke, Ellen Mayhew, Scott Richardson, and Sara Bryant. They withstood my lack of skill in their field and helped me along. For that and their good advice I thank them. I thank RDL for the opportunity to see real intelligence in action. I would also like to thank my high school geometry and programming teacher, Mr. Kramer, for excellent recommendation as well as excellent teaching. And finally I would like to thank my parents for forcing me to take the job that has been one of the most educational experiences in my life.

Sample output

```
TERMAP (VERS 10)                TITLE             DATE=            PAGE     1

MTF4

   ALT DTAMB      VEL    XM       KTAS    KIAS  DEFF    ERAM      RPR     CASE
    0.   0.0    0.000 0.000      0.0     0.0 0.0000 1.0000    1.000     1.0

P-AMB    P1-ID TAMB-R TAMB-F   T1-F RC-OA EFF-OA EFF-TH     WA    WA-COR
14.696  14.696 518.67  59.00  59.00 31.04 0.7869 0.3779  248.00  248.00

1
 ....................             RC=  3.900  EFF= 0.8500  WCOR= 248.00
 .  FAN              .            HP=24401.7
 ....................
2                                 NTC =     0  BETA=   0.0  AREA=  409.5
   DELP                           R = 0.9950  SF1=  0.118  SF2 = 0.0000
3
 ..........
 . HPC    .                       RC=  8.000  EFF= 0.8080  WCOR=   58.61
 ..........                       HP=49436.3         84
        12         12
         ...........
         .SPLITTER1.              R-TIP=  3.900           SR-TIP= 0.000
         ...........
        12
            COOL                  NTC =    62  WC =  0.912
        13                        NTC =     0  BETA=   0.0  AREA=  364.7
             DELP                 R = 0.9800  SF1=  2.888  SF2 = 0.0000
4                                 NTC =     0  BETA=   0.0  AREA=   80.3
 ..........                       R = 0.9600  SF1=  1.510  SF2 = 0.0000
 . BURNER .                       EFF= 0.9950  BOT = 2660.0
 ..........
5
  COOL                            NTC =    12  WC =  9.118
6
 ..........
 . HPT    .                       RIT= 2607.  RE =  4.566  EFF = 0.8800
 ..........                       WCOR= 13.538             HP = 49436.3
7
  PWORK                           NTC =    22  WC =  3.647  SF = 0.09000
8
  COOL                            NTC =    32  WC =  2.735
9
 ..........
 . LPT    .                       RIT= 1910.  RE =  2.452  EFF = 0.9000
 ..........                       WCOR= 54.542             HP = 24401.7
10
  COOL                            NTC =    42  WC =  1.824
11                 14
 ....................
 .     MIXER-1      .             ANGMIX=1.00  GAINMX=0.500  RMIX=1.436
 ....................
15                                NTC =     0  BETA=   0.0  AREA= 1301.7
   DELP                           R = 0.9900  SF1=  0.377  SF2 = 0.0000
16                                NTC =     0  BETA=   0.0  AREA= 1314.9
   DELP                           R = 0.9900  SF1=  0.377  SF2 = 0.0000
  REHEAT1                         NRHT(1)= 16  SW=  0.900  EFF = 0.9500
18
  COOL                            NTC =    52  WC =  0.912
19
```

```
 ..........
 .NOZZLE-7.                          RJ=  2.700  A8 =  446.8  WG =  250.98
 ..........
21
1TERMAP (VERS 10)            TITLE            DATE=           PAGE     2

 MTF4

     ALT DTAMB     VEL   XM     KTAS   KIAS  DEFF   ERAM     RPR    CASE
      0.   0.0   0.000 0.000    0.0     0.0 0.0000 1.0000   1.000    1.0

 P-AMB   P1-ID TAMB-R TAMB-F   T1-F RC-OA EFF-OA EFF-TH    WA    WA-COR
14.696  14.696 518.67  59.00  59.00 31.04 0.7869 0.3779  248.00  248.00

                    DESIGN POINT CONSTANTS AND FACTORS

 (N)   ID    SF(N,1)  SF(N,2)     SN(N)     SR(N)      SW(N)    XMNDP  (N)
 ---   --   -------  -------     -----     -----      -----    -----  ---
  1   FAN   1.02657   0.0000    1.00000   1.45000    2.47997   0.000   1
  2   DELP  0.11818   0.0000    0.00000   0.00000    0.00000   0.250   2
  3   HPC   0.94725   0.0000    0.80174   1.00000    0.58612   0.000   3
  4   BURN  1.50982   0.0000    0.00000   0.00000    0.00000   0.200   4
  5   COOL  0.00000   0.0000    0.00000   0.00000    0.00000   0.000   5
  6   HPT   1.11211   0.0000    0.45306   1.00000    0.13538   0.000   6
  7   PWRK  0.09000   0.0000    0.00000   0.00000    0.00000   0.000   7
  8   COOL  0.00000   0.0000    0.00000   0.00000    0.00000   0.000   8
  9   LPT   1.02238   0.0000    0.52755   1.00000    0.54542   0.000   9
 10   COOL  0.00000   0.0000    0.00000   0.00000    0.00000   0.000  10
 11   MIXH  0.00000   0.0000    0.00000   0.00000    0.00000   0.000  11
 12   COOL  0.00000   0.0000    0.00000   0.00000    0.00000   0.000  12
 13   DELP  2.88800   0.0000    0.00000   0.00000    0.00000   0.100  13
 14   MIXC  0.00000   0.0000    0.00000   0.00000    0.00000   0.000  14
 15   DELP  0.37705   0.0000    0.00000   0.00000    0.00000   0.200  15
 16   DELP  0.37705   0.0000    0.00000   0.00000    0.90000   0.200  16
 17   REHT  0.00000   0.0000    0.00000   0.00000    0.00000   0.000  17
 18   COOL  0.00000   0.0000    0.00000   0.00000    0.00000   0.000  18
 19   NOZZ  0.00000   0.0000    0.00000   0.00000    0.00000   0.000  19
 20    TH8  0.00000   0.4202    0.00000   0.00000    0.00000   0.000  20
 21    EX9  0.00000   0.0000    0.00000   0.00000    0.00000   0.000  21
 ---   --   -------  -------     -----     -----      -----    -----  ---

ICONF(1-15)    1  -7   2   8   5   7   3   5   4   5   5   4   5   9   7
     (16-30)   6   5  10   0   0   0   0   0   0   0   0   0   0   0   0

NTC ( 1-10)     0     0     0     0    12     0    22    32     0    42
    (11-20)     0    62     0     0     0     0     0    52     0     0
    (21-30)     0     0     0     0     0     0     0     0     0     0

NFAN :  1    NHPT :  6   NCOMP : 2   NPB  :  4   KSPLTR :  0   NGP-1 : 11
NLPC :  1    NIPT :  0   NTURB : 2   N7   : 19   IDES   :  1   NBP-1 : 14
NIPC :  0    NLPT :  9   ISEPFL: 1   N17  :  0   NBYP-1 : 12   NGP-2 :  0
NHPC :  3    NPT  :  0   MIXFLG: 1   N27  :  0   NBYP-2 :  0   NBP-2 :  0
NTIP :  0

NO. MAX. LIMITS = 0      NO. MIN. LIMITS = 0

COMPONENT MAP ID'S :  N   ID   MAPTYP   FLOW ID     EFF ID   SMRELL ID
                      1  FAN      1      0.  0.     0.  0.      0.  0.
                      3  HPC      1      0.  0.     0.  0.      0.  0.
                      6  HPT      1      0.  0.     0.  0.      0.  0.
```

9	LPT	1	0.	0.	0.	0.	0.	0.

NOZZLE MAP ID'S :	N	NOZTYP	MAPTYP	CFGT ID		CDT ID	
PRI (8-9)	19	2	1	0.	0.	0.	0.

MTF4

ALT	DTAMB	VEL	XM	KTAS	KIAS	DEFF	ERAM	RPR	CASE
0.	0.0	0.000	0.000	0.0	0.0	0.0000	1.0000	1.000	1.0

P-AMB	P1-ID	TAMB-R	TAMB-F	T1-F	RC-OA	EFF-OA	EFF-TH	WA	WA-COR
14.696	14.696	518.67	59.00	59.00	31.04	0.7869	0.3779	248.00	248.00

N	ID	T-R	P	W-COR	WD	R	EFF	FAR	AREA	XMN	NSI
1	FAN	519.	14.70	248.00	248.00	3.900	0.8500	0.0000	0.0	0.00	0
2	DELP	807.	57.32	58.32	182.35	0.995	0.0000	0.0000	409.5	0.25	0
3	HPC	807.	57.03	58.61	182.35	8.000	0.8080	0.0000	0.0	0.00	0
4	BURN	1562.	456.23	9.12	163.21	0.960	0.9950	0.0000	80.3	0.20	0
5	COOL	2660.	437.98	12.63	166.19	0.000	0.0000	0.0183	0.0	0.00	0
6	HPT	2607.	437.98	13.54	175.31	4.566	0.8800	0.0173	0.0	0.00	0
7	PWRK	1916.	95.92	51.62	175.31	0.000	0.0000	0.0173	0.0	0.00	0
8	COOL	1915.	95.92	52.68	178.95	0.000	0.0000	0.0169	0.0	0.00	0
9	LPT	1910.	95.92	54.54	181.69	2.452	0.9000	0.0167	0.0	0.00	0
10	COOL	1569.	39.12	118.69	181.69	0.000	0.0000	0.0167	0.0	0.00	0
11	MIXH	1568.	39.12	119.88	183.51	0.000	0.0000	0.0165	1234.1	0.17	0
12	COOL	807.	57.32	20.99	65.65	0.000	0.0000	0.0000	0.0	0.00	0
13	DELP	818.	57.32	21.43	66.56	0.980	0.0000	0.0000	364.7	0.10	0
14	MIXC	818.	56.17	21.87	66.56	0.000	0.0000	0.0000	67.5	0.76	0
15	DELP	1379.	40.49	147.98	250.07	0.990	0.0000	0.0121	1301.7	0.20	0
16	DELP	1379.	40.09	149.48	250.07	0.990	0.9500	0.0121	1314.9	0.20	0
17	REHT	1379.	39.69	149.48	250.07	1.000	0.0000	0.0121	1314.9	0.20	0
18	COOL	1379.	39.69	150.99	250.07	0.000	0.0000	0.0121	0.0	0.00	0
19	NOZZ	1378.	39.69	151.50	250.98	2.700	0.0000	0.0120	1.1	0.00	0
20	TH8	1170.	21.21	261.20	250.98	1.872	0.0000	0.0120	446.8	1.00	0
21	EX9	1060.	14.70	358.85	250.98	1.000	0.0000	0.0120	475.2	1.29	0

C O M P R E S S O R   B L E E D   I N F O R M A T I O N

	BLEED NO.	1	2	3	4	5	6	TOTALS
COMPR 2	BLEED	0.0500	0.0200	0.0150	0.0100	0.0050	0.0050	0.1050
NO. ID	DEL-H	1.0000	1.0000	1.0000	1.0000	0.5000	1.0000	
2 HPC	FLOW	9.118	3.647	2.735	1.824	0.912	0.912	19.147
2 HPC	TEMP	1561.9	1561.9	1561.9	1561.9	1193.1	1561.9	
2 HPC	PRESS	456.23	456.23	456.23	456.23	192.30	456.23	
2 HPC	IBF	1	1	1	1	1	1	
	NTC(N) N=	5	7	8	10	18	12	

C O M P O N E N T   P E R F O R M A N C E

N	ID	BETA	XN	XN-MAP	H.P.	HPX/PHP	EFF-MAP	R-MAP	W-MAP
1	FAN	1.000	100.0	100.0	24401.7	0.0	0.828	3.000	100.000
3	HPC	1.000	100.0	100.0	49436.3	0.0	0.853	8.000	100.000
6	HPT	0.000	100.0	100.0	49436.3	418.0	0.791	4.566	100.000
9	LPT	0.000	100.0	100.0	24401.7	0.0	0.880	2.452	100.000

N O Z Z L E   P E R F O R M A N C E

NOZZLE	(N)	TYP	FG	FN	RJ	CFG	CD	AREA-TH	V-EXIT
PRI(8-9)	19	2	15626.7	15626.7	2.700	0.9850	1.0000	446.8	2033.7

F I N A L   E N G I N E   P E R F O R M A N C E

BPR-1	RMIX-1	GAINMX-1	ANGMIX-1	BPR-2	RMIX-2	GAINMX-2	ANGMIX-2
0.3600	1.4358	0.5000	1.0000	0.0000	0.0000	0.0000	0.0000

FG	FG-R1	WFE	WFE/P3	FHV	F-RAM	DEFTIP	DTAMTP
15626.7	15626.5	10734.0	23.527	18400.0	0.0	0.0000	0.0

FN	SFC	WFT	FN-R1	WFT-R1	FN/WA	EPR	ERAMTP
15626.7	0.6869	10734.0	15626.5	10733.8	63.011	2.7004	0.0000

1TERMAP (VERS 10) TITLE DATE= PAGE 4

TERMAP DATA SET MTF4 - MIXED-EXH., NON-SPLIT 2-SPOOL TURBOFAN - IDES=0

ALT	DTAMB	VEL	XM	KTAS	KIAS	DEFF	ERAM	RPR	CASE
0.	0.0	0.000	0.000	0.0	0.0	0.0000	1.0000	1.000	2.0

P-AMB	P1-ID	TAMB-R	TAMB-F	T1-F	RC-OA	EFF-OA	EFF-TH	WA	WA-COR
14.696	14.696	518.67	59.00	59.00	31.04	0.7869	0.2024	248.00	248.00

N	ID	T-R	P	W-COR	WD	R	EFF	FAR	AREA	XMN	NSI
1	FAN	519.	14.70	248.00	248.00	3.900	0.8500	0.0000	0.0	0.00	0
2	DELP	807.	57.32	58.32	182.35	0.995	0.0000	0.0000	409.5	0.25	0
3	HPC	807.	57.03	58.61	182.35	8.000	0.8080	0.0000	0.0	0.00	0
4	BURN	1562.	456.23	9.12	163.21	0.960	0.9950	0.0000	80.3	0.20	0
5	COOL	2660.	437.98	12.63	166.19	0.000	0.0000	0.0183	0.0	0.00	0
6	HPT	2607.	437.98	13.54	175.30	4.566	0.8800	0.0173	0.0	0.00	0
7	PWRK	1916.	95.92	51.62	175.30	0.000	0.0000	0.0173	0.0	0.00	0
8	COOL	1915.	95.92	52.68	178.95	0.000	0.0000	0.0169	0.0	0.00	0
9	LPT	1910.	95.92	54.54	181.69	2.452	0.9000	0.0167	0.0	0.00	0
10	COOL	1569.	39.12	118.69	181.69	0.000	0.0000	0.0167	0.0	0.00	0
11	MIXH	1568.	39.12	119.88	183.51	0.000	0.0000	0.0165	1234.1	0.17	0
12	COOL	807.	57.32	20.99	65.65	0.000	0.0000	0.0000	0.0	0.00	0
13	DELP	818.	57.32	21.43	66.56	0.980	0.0000	0.0000	364.7	0.10	0
14	MIXC	818.	56.17	21.87	66.56	0.000	0.0000	0.0000	67.5	0.76	0
15	DELP	1379.	40.49	147.98	250.07	0.990	0.0000	0.0121	1301.6	0.20	0
16	DELP	1379.	40.09	149.48	250.07	0.990	0.9500	0.0121	1314.9	0.20	0
17	REHT	3986.	39.69	243.77	237.45	0.932	0.0000	0.0678	1314.9	0.44	0
18	COOL	3772.	36.98	281.28	262.45	0.000	0.0000	0.0622	0.0	0.00	0
19	NOZZ	3764.	36.98	281.98	263.36	2.516	0.0000	0.0620	1.1	0.00	0
20	TH8	3334.	20.44	480.13	263.36	1.809	0.0000	0.0620	854.3	1.00	0
21	EX9	3113.	14.70	645.25	263.36	1.000	0.0000	0.0620	904.1	1.27	0

MODE=1152= T (5) PLA= 2660.000 PLA LIMIT= PLA MATRX= 0 LOOP= 10

C O M P R E S S O R   B L E E D   I N F O R M A T I O N

	BLEED NO.	1	2	3	4	5	6	TOTALS
COMPR 2	BLEED	0.0500	0.0200	0.0150	0.0100	0.0050	0.0050	0.1050
NO. ID	DEL-H	1.0000	1.0000	1.0000	1.0000	0.5000	1.0000	
2 HPC	FLOW	9.118	3.647	2.735	1.824	0.912	0.912	19.147
2 HPC	TEMP	1561.9	1561.9	1561.9	1561.9	1193.1	1561.9	

2 HPC	PRESS	456.23	456.23	456.23	456.23	192.30	456.23
2 HPC	IBF	1	1	1	1	1	1
	NTC(N) N=	5	7	8	10	18	12

C O M P O N E N T   P E R F O R M A N C E

N	ID	BETA	XN	XN-MAP	H.P.	HPX/PHP	EFF-MAP	R-MAP	W-MAP
1	FAN	1.000	100.0	100.0	24401.7	0.0	0.828	3.000	100.000
3	HPC	1.000	100.0	100.0	49436.3	0.0	0.853	8.000	100.000
6	HPT	0.000	100.0	100.0	49463.4	418.0	0.791	4.566	100.000
9	LPT	0.000	100.0	100.0	24414.7	0.0	0.880	2.452	100.000

N O Z Z L E   P E R F O R M A N C E

NOZZLE	(N)	TYP	FG	FN	RJ	CFG	CD	AREA-TH	V-EXIT
PRI(8-9)	19	2	26593.4	26593.4	2.516	0.9850	1.0000	854.3	3298.3

TERMAP DATA SET MTF4 - MIXED-EXH., NON-SPLIT 2-SPOOL TURBOFAN - IDES=0

F I N A L   E N G I N E   P E R F O R M A N C E

BPR-1	RMIX-1	GAINMX-1	ANGMIX-1	BPR-2	RMIX-2	GAINMX-2	ANGMIX-2
0.3600	1.4358	0.5000	1.0000	0.0000	0.0000	0.0000	0.0000

TRHEAT-1	PCTRH-1	WFR-1	TRHEAT-2	PCTRH-2	WFR-2
4400.0	1.0000	44578.5	0.0	0.0000	0.0

FG	FG-R1	WFE	WFE/P3	FHV	F-RAM	DEFTIP	DTAMTP
26593.4	26593.0	10734.0	23.527	18400.0	0.0	0.0000	0.0

FN	SFC	WFT	FN-R1	WFT-R1	FN/WA	EPR	ERAMTP
26593.4	2.0799	55312.4	26593.0	55311.5	107.232	2.5160	0.0000

CHARACTERIZATION OF CORE SOIL SAMPLES AND PLANTS FROM TEST AREA A-22 TO DETERMINE CONTAMINATION

Nancy H. Deibler
High School Apprentice
Environmental Assessment Branch

Wright Laboratory Armament Directorate
WL/MNSE
Eglin AFB, Florida 32542-5434

Final Report for:
High School Apprenticeship Program
Wright Laboratory Armament Directorate

Sponsored by:
Air Force Office of Scientific Research
Bolling Air Force Base, Washington DC.

August 1994

CHARACTERIZATION OF CORE SOIL SAMPLES AND PLANTS FROM TA A-22 TO DETERMINE CONTAMINATION

Nancy Deibler
Choctawhatcheee High School

ABSTRACT

Metal contamination in soil is a hazard to the environment. Testing of surface soil samples for heavy metal contamination has shown possible aluminum and iron contamination in some soil at Test Area (TA) A-22, which is a ground aircraft gun test area on Eglin Air force Base. Further investigation of metal contamination on TA A-22 was investigated. Core soil samples were taken 40 centimeters deep in the ground from TA A-22. The metal content of each soil sample was determined with a Portable X-ray Fluorescence Spectrometer. The pH of each soil sample was taken with the Expandable Ionanalyzer 940. The elements present, amount of each, and the pH of each soil sample was found and compared to controls of similar texture. The results show no detectable heavy metal contamination leaching into the ground. A second test was conducted to determine heavy metal uptake of plants on TA A-22. Persimmon leaves, Turkey Oak leaves, and Yucca plants were collected from TA A-22. The plant samples were processed for analysis with the Inductively Coupled Plasma Spectrophotometer (ICP) Analysis. Due to a malfunction of the ICP, analysis of the plants was not completed. Once the ICP analysis is conducted, heavy metal uptake of plants on TA A-22 will be determined.

CONTENTS

INTRODUCTION

The characterization of surface soil samples at TA A-22 has shown possible aluminum and iron contamination of the soils. The purpose of my project this summer was to conduct further testing on TA A-22 to determine the extent of heavy metal contamination on TA A-22. The results of my project will show The impact that munitions testing on TA A-22 has on the environment will be shown with the results of my project. With the conclusions from my testing proper action can be taken for contamination if needed.

BACKGROUND

Soil is a the surface layer of the earth which supports plant life. From soil, plants get mechanical support, essential element, water, and oxygen. Soil is needed for the survival of plants, and plants provide oxygen which is essential for animals. Soil is the original source of most nutrients for plants and animals. Consequently, soil is an essential part of natural life on this earth. The physical and chemical conditions of soil must be adequate for plants and life. Since it is so important to keep this natural resource in it's proper condition, it is necessary to be aware of any disturbances from man that are hurting the soil.

PROCEDURES

Core soil samples were collected at TA A-22 which is the site of munitions testing of a large range of metals. Control samples were collected at TA C-52A which is the site of non release testing of EO, IR, laser, and MMW seekers. The two control core soil samples are undisturbed; therefore, they represent the normal metal content of soils. The control samples had the same texture as the trial samples from TA A-22. The control samples are free of any heavy metal contamination. All samples were taken 40 centimeters

deep into the ground with a post hole digger. Samples were collected in the areas that surface soil samples were collected in last summer. One sample was taken along the shore of Choctawhatchee Bay. One sample was taken in Target Butt 413 where munitions are first deposited after being fired at the target. Another samples was collected approximately 36 meters in front of Target Butt 413 in a wetland area.. The last sample was taken from a target butt near the Ballistics Experimental Facility (BEF). After all samples were collected, they were brought to the chemistry lab for processing and analysis. First the soil samples were dried to release any moisture. Then all samples were evenly homogenized with a ball jar roller mill. Five grams of each soil sample were weighed. The measured amounts of soil were poured into small spectra cups for analysis.

The first analysis was done using the Metallurgist XR which is a Portable X-ray Fluorescence Spectrometer. The soil samples collected at TA A-22 were analyzed using the Portable X-ray. This instrument uses two radioisotope sources, cadmium 109 and iron 55. These sources excite the electrons causing an electron displacement. The X-ray reads the displacement energy levels of each element peak. The Portable X-ray has the capability to simultaneously measure and analyze 21 of the common alloying elements in a full range of Fe, Ni, Co, Cu, and Al based alloys in any size or shape material. Depending on the type of surface on the sample, the instrument will read the sample using two different settings: universal, for samples with rough or ridged surface, and special flat, for samples with a flat surface. Then the instrument prints out the percentage of each element present in the sample placed on the probe, with the exception of calcium, silicon, sulfur, potassium, carbon, hydrogen, and oxygen that can not be detected by the Portable X-ray. Although the instrument can not detect the element Aluminum, it will give you the nearest Aluminum alloy.

Next the pH of each soil sample was measured. The pH is the logarithm of the reciprocal of the active hydrogen ions in grams per liter. The pH of soil can help determine if the soil is normal. Many natural factors, such as rain, sulfur, and plants, can

change the pH of soil. If the soil becomes too acidic, plants may develop an increase in solubility of such elements as aluminum and manganese and develop a nutrient imbalance. Since the availability of many of the micronutrients is influenced by the acidity of the soil, it is imperative that the pH of the soil is normal. Most crops do not yield their maximum potential in soils that are strongly acidic. If it is known that a disturbance is causing the soil too be too acidic for plant life, than the disturbance can be stopped or treatments like liming can be done. For pH testing, 10 grams of each core soil sample was mixed with 10 milliliters of distilled water. The pH of each core soil sample was measured with the Expandable Ionanalyzer 940. The pH meter is calibrated with a standard that has a pH of 7 and a standard with a pH of 10. The pH meter than automatically calculates the pH level of the samples.

The last test done to characterize the core soil samples was Inductively Coupled Plasma Spectrophotometer (ICP) analysis. For ICP analysis, 50 grams of each soil sample was weighed. Then 25 milliliters of a 25 percent nitric acid and 75 percent distilled water solution was mixed with the each sample. The samples and the nitric acid solution were allowed to digest for extended period of time. The samples were then filtered with number 2 qualitative filter paper. The remaining liquid was to be used for ICP analysis. The ICP works by comparing the wave length of light of a standard or known substance to the wave length of light of your sample. Using a standard or known substance you calibrate the ICP so it reads the standard's element parts per million (ppm). The ICP uses the calibrated peak for reference to read the ppm of your sample.

For analysis of heavy metal uptake of plants on TA A-22, 3 different types of plants that are common to this area were collected. Yucca aloifolia l. (Yucca plant), Diospyros virginiana L. (common Persimmon leaves), Quercus Laevis Walt. (Turkey Oak leaves) were collected from areas of TA A-22. Control samples that would represent the normal heavy metal content of these plants were collected from TA C-52A. After the plant samples were collected, they were brought to the lab for analysis. The plant samples

were cut and ground to fit in crucibles. The plants were then ashed in the muffle furnace to eliminate any remaining organics. The plant samples were then weighed. Twenty five milliliters of a 25 percent nitric acid and 75 percent distilled water solution was added to each sample. After the plant samples and nitric acid solution had digested, the samples were filtered. The remaining liquid will be used for ICP analysis.

RESULTS

The results from the Portable X-ray Fluorescence Spectrometer analysis of core soil samples collected from TA A-22 are shown in Figure 1. Iron and titanium are elements that are naturally found in our soil. There presence in the samples are normal. As you can see in the chart, the trial samples from TA A-22 contain no elevated amounts of heavy metals compared to the normal represented by the controls.

X-ray Analysis Of Core Soil Samples from Range 22				
SAMPLE	**Fe (%)**	**Mo (%)**	**Ti (%)**	**Zr (%)**
TA A-22				
shore	----------	----------	**0.2**	----------
TB 1	**0.49**	----------	**0.14**	----------
TB 413	**0.64**	----------	**0.33**	----------
wetlands	----------	**0.01**	----------	----------
TA C-52A				
control 1	**0.85**	----------	**0.56**	----------
control 2	**0.48**	----------	**0.42**	**0.03**

FIGURE 1

The results from pH are shown on Figure 2. In humid regions such as Florida, normal pH of soils ranges from 5 to 7. In the specific area that Eglin Air Force Base is in the average pH of the soil is 5.5. As you can see in the chart, the pH of the core soil samples from TA A-22 are close to the average pH of this area and vary little from the pH of the controls. Since the soils' pH are closer to the neutral range, the possibility of heavy metal contamination leaching into the soil is less.

CORE SOIL SAMPLE'S pH

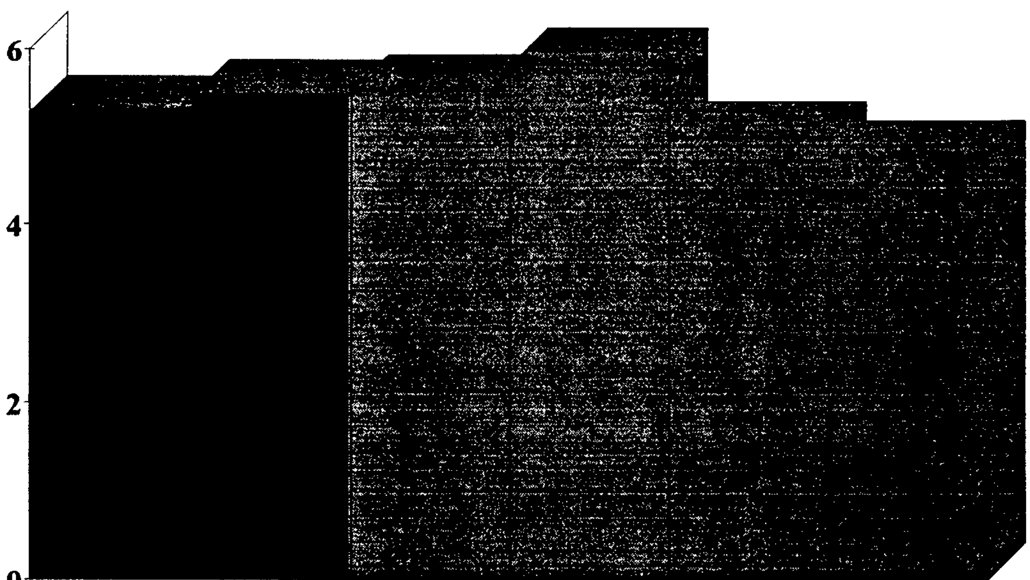

Control 1	Control 2	Shore	TB 1	Tb 413	Wetland
5.27	5.46	5.52	5.82	4.97	4.75

FIGURE 2

CONCLUSION

Previous testing of surface soil on TA A-22 showed possible aluminum and iron contamination, further testing of the soils has given us more information of the extent of the heavy metal contamination. Results from the Portable X-ray analysis showed no evidence of heavy metal contamination leaching into the soil. The pH of the soil is normal. Once ICP analysis of the core soil samples can be conducted, heavy metal contamination leaching into the soil can be determined. The plant samples from TA are prepared for ICP analysis. The results from ICP analysis of the plant samples from TA A-22 will determine if there is any heavy metal contamination uptake of plants from TA A-22. Though with the results from the core soil testing, there probably will not be any heavy metal contamination in the plants, since their soil shows no contamination.

MISCELLANEOUS

In addition to conducting my project, I experienced field work for contractors project. I went with a group seining in the creeks on the ranges for brown darters. It was interesting to see the collecting of live samples for experimentation. I also helped the lab prepare for disposal of all the expired chemicals in the labs. We bar-coded and took inventory on over 2,000 chemicals in the Environmental Assessment Branch's labs. We were preparing for records in the HAZMAT IMMS program in the computer. The system will be keeping track of all the hazardous chemicals on the base. I took part in the packaging of all the expired chemicals in the labs.

ACKNOWLEDGMENTS

I could not have accomplished anything this summer without the help off others. I would like to first thank my mentor, Mr. Luis Santana. He lead me through the process of my project and was there to help me with my other accomplishments of this summer's apprenticeship. I truly appreciated all the support that was given to me from the other members of the Environmental Assessment Branch. Lt. Brad Noland was gracious enough to drive us out to the test areas to collect our samples. I would like to also thank Lt. Noland for his time and effort. I thank Don Harrison and Mike Deiler for handling the High School Apprenticeship Program. Glenda Apel helped me alot in the office and contributed much to the program. Last I would like to thank Melissa Griffiths and Mary Pletcher for all their support and friendship this summer. It wouldn't have been as enjoyable with out them. I also thank the Wright Lab for allow high school students to become a part of their scientific research.

BIBLIOGRAPHY

Donahue, R. L., J. C. Shickluna, and L. S. Robertson, "Soils: An Introduction to Soils and Plant Growth," Prentice-Hall, Inc., Englewood Cliffs, New Jersey, 1971, 1965, 1958.

Elias, Thomas S., "The Complete Trees of North America," Book Division, New York, 1980.

Lyon, T. L., H. O. Buckman, and N. C. Brady, "The Nature and Properties of Soils," The Macmillian Company, New York, 1950.

Platt, Rutherford, "Discover American Trees," Dodd, Mead &Company, New York, 1968.

Thompson, L. M. and F. R. Troeh, "Soils and Soil Fertility," Fourth Edition, McGraw-Hill, Inc., 1978.

AEROSPACE ENGINEERING:

The Building of Computer Programs and Inexpensive, Simple Machines

Timothy G. Donohue

Carroll High School
4524 Linden Ave.
Dayton, OH 45432

Final Report for:
High School Apprentice Program
Wright Patterson Air Force Base

Sponsored by:
Air Force Office of Scientific Research
Bolling Air Force Base, Washington DC

and

Wright Patterson Air Force Base

August 1994

Forward

I worked under the guidance of Lt. Michael Meyer, Aircrew Protection Branch, Wright Patterson Air Force Base.

AEROSPACE ENGINEERING:

The Building of Computer Programs and Inexpensive, Simple Machines

Timothy G. Donohue
Carroll High School

Abstract

Two of the most important jobs of the aerospace engineer include the building of computer programs that analyze and simplify data obtained in testing, and the designing and building of simple machines used to test the capabilities of certain airplane parts. During my eight weeks acting as an apprentice aerospace engineer, I took part in both of those jobs. The first program I built numerically integrates the angular rate data from the AMIT (ADAM MACE Integration Test) ejection test at Holloman AFB, New Mexico, on April 15, 1994, to obtain orientation data throughout the ejection event. The second program was used with a data file (20 columns wide and over 100,000 rows long) from three F-111 ejection tests that measured pressure on the escape capsule throughout the ejection event. This program opens 19 new data files, each containing column #1 (time in seconds) and one of the other 19 columns of data. Finally, I designed a simple, inexpensive, efficient machine that holds an ejection seat and allows it to yaw and pitch to a certain angle. It can then be locked in place so that forces upon the seat can be measured.

AEROSPACE ENGINEERING:

The Building of Computer Programs and Inexpensive, Simple Machines

Timothy G. Donohue

Introduction

If someone were to ask you what an aerospace engineer's job is, chances are you would answer, "Building, designing, and testing airplanes." Even though this is true, there are two other jobs that are just as important: Analyzing and simplifying of data obtained in testing through the use of computer programs, and the building and designing of the machines used to test the airplanes and ejection seats.

In many experiments conducted by the U. S. Air Force Aircrew Protection Branch, the aerospace engineers are unable to readily analyze the data without first modifying it. This modification is done by computer programs created by the aerospace engineers. These programs will format the data needed and rearrange, integrate, and/or convert the data to the correct units to make the data easier to analyze.

Another important job of an aerospace engineer is creating a simple, inexpensive, efficient machine to test the capabilities of certain parts of an airplane. To design these machines, the engineer must first find the forces and stresses upon the machine during testing. These forces will give the engineer an idea of the type and amount and type of structure needed to build a machine that will withstand these forces.

Discussion of Problem

During my eight weeks acting as an apprentice aerospace engineer in the Aircrew Protection Branch, I created two computer programs that allowed data to be analyzed more readily, and designed a simple machine that would allow an ejection seat to yaw and pitch to a certain angle and be locked in place. The first program had to be able to integrate the angular rate data from the AMIT test (April 15, 1994) and obtain orientation data throughout the ejection event. The second program was to be used with a data file 20 columns wide and over 100,000 rows long. The first of the columns was time (in seconds),

while the other columns contained pressure data. The problem was to open 19 new files, each containing column #1 and one of the other 19 columns of data; so that each pressure trace could be analyzed separately.

Methodology

In order to build the programs needed, I first had to learn the FORTRAN computer language. I built a program titled Timsprog.2 to integrate the angular rate data from the AMIT (ejection seat) test on April 15, 1994, and obtain orientation data throughout the ejection event. In this program, the computer inputs the angular rate data into the Trapezoidal Rule numerical integration scheme (Reference 1). The Trapezoidal Rule separates the angular rate data into the time (in seconds) and the angle of orientation (in radians).

To allow for a more accurate analysis, I simplified the data after running it through the program. Because the ejection event began at 7.14 seconds, I threw out all data before that time period. Since there was no angular movement before this point, the angle of orientation at 7.14 seconds should have been equal to the initial conditions of the ejection seat, which were 20 degrees yaw and 30 degrees pitch. However, since the angular rate sensors used were very sensitive to linear acceleration, the angle of orientation data was not equal to the known initial conditions. Subsequently, I subtracted the angle of orientation at 7.14 seconds from every other angle of orientation. Finally, to complete the simplification process, I converted all of the angles from radians to degrees.

The second program I made was Transdat. This program accepts any file 20 columns wide and separates it into 19 separate files, each containing column #1 and one of the other 19 columns. This program will allow each column of data to be independently analyzed (A copy of both programs can be found in the Results).

Finally, I had to design a simple machine that would allow an ejection seat to yaw and pitch to the necessary angle and be locked in place for wind blast and wind tunnel testing. The first step was to

design the general shape and features of the machine (See preliminary design of machine in Results). Next, it was necessary to calculate the forces upon the ejection seat and the machine during testing. I determined these aerodynamic forces using the formula: F= 1/2 (PV^2)*ACd, where F= force, P= density of air, V= velocity, A= area, and Cd= coefficient of drag. I calculated the area of five sections of the seat (head, chest, waist and knees, left leg, right leg), and determined the force upon each section (I used five different coefficients of drag: 0.75, 1.00, 1.25, 1.50, 1.75). Once the forces were discovered, I calculated the moment about each section of the seat using the equation: M= F*D (M= moment, F= force, D= distance from center of section to the bottom of the machine). Next, I determined the stress upon each of the roller pins (see drawing in Results) using the equation: S= [(−1/3)F(x) *c]/[π(c^4 – r^4)/4], where S= stress, x= distance from point of the moment, c= outer radius of rod, r= inner radius of rod (Reference 2). Using this equation, I determined the stress on both the vertical and horizontal rods (see drawing of machine), for selected outer and inner radii. By analyzing the stresses, I was able to select the appropriate metal to be used to construct the machine.

Results

All final results can be found in the next 12 pages, in the form of drawings, charts, and computer programs.

References

1. Mizrahi, Abe and Michael Sullivan. Calculus and Analytic Geometry, Wadsworth Publishing Company: Belmont, California, 1982; pp. 475- 476

2. AIAA Aerospace Design Engineers Guide, American Institute of Aeronautics and Astronautics, Inc.: Washington, DC, 1993

Timsprog.2

```
THIS PROGRAM INTEGRATES ANGULAR RATE DATA FROM THE ADAM DATA ACQUISITION SYSTEM TO
OBTAIN ORIENTATION DATA THROUGHOUT THE EJECTION EVENT.

OPEN DATA FILE FROM ADAM TESTING

WRITE (*,*) 'ENTER INPUT FILE NAME'

OPEN (2, FILE = ' ' )

OPEN OUTPUT FILE

WRITE (*,*) 'ENTER OUTPUT FILE NAME'

OPEN (8, FILE = ' ', STATUS = 'NEW')

READ IN FIRST TWO TIME AND DATA VALUES

READ (2, *) T0, H0

READ (2, *) T1, H1

CHECK THE TIMESTEP TO ASSURE THAT IT IS GREATER THAN ZERO

TIMESTEP = T1 - T0

IF (TIMESTEP .LE. 0.0) THEN

    WRITE (*, *) 'TIMESTEP IS LESS THAN OR EQUAL TO ZERO'

IF TIMESTEP IS LESS THAN OR EQUAL TO ZERO END THE PROGRAM

    GOTO 100

END IF

INITIALIZE THE COUNTER

COUNTER = 1

INITIALIZE THE SUM ACCUMULATOR WITH THE 2ND INPUT VALUE

SUM = H1

ENTER LOOP BY CHECKING IF WE ARE AT END OF FILE

DO WHILE (.NOT. EOF (2))

READ IN THE NEXT VALUE FROM THE INPUT

READ (2, *) TN, HN

CALCULATE TRAPEZOIDAL RULE

AREA = ((TN - T0) / (COUNTER + 1)) * (H0 / 2.0 + SUM + HN / 2.0)

PRINT OUT THE RESULTS

WRITE (8, 10) TN, AREA

IF (TN.EQ.8.72)GOTO100

10 FORMAT (F14.6,'  ',F14.6)

INCREMENT COUNTER

COUNTER = COUNTER + 1

INCREMENT THE SUM ACCUMULATOR

SUM = SUM + HN

END DO

100 END
```

Transdat.

```
      CHARACTER FILENAME*30
      WRITE(*,*) 'ENTER INPUT FILE NAME'
      READ(*,'(A)') FILENAME
      WRITE(*,5) FILENAME
    5 FORMAT(A)
      OPEN(2, FILE=FILENAME)
      WRITE(*,*) 'ENTER OUTPUT FILE NAME'
      READ(*,'(A)') FILENAME
      WRITE(*,6) FILENAME
    6 FORMAT(A)
      OPEN(8, FILE=FILENAME)
      WRITE(*,*) 'ENTER COLUMN NUMBER (BETWEEN 2 AND 20)'
      READ(*,*) COLUMN
      WRITE(*,*) 'ENTER THE NUMBER OF ROWS IN DATA FILE'
      READ(*,*) IMAX
      WRITE(*,*) 'ENTER THE NUMBER OF ROWS TO SKIP'
      READ(*,*) NUMBER
      DO 10 I= 1, NUMBER
      READ(2,*)
   10 CONTINUE
      IF(COLUMN.EQ.2) THEN
      DO 12 I= 1, IMAX
      READ(2,*) DTN,DAN
      WRITE(8,300) DTN,DAN
   12 CONTINUE
      END IF
      IF(COLUMN.EQ.3) THEN
      DO 13 I= 1, IMAX
      READ(2,*) DTN,DAN,DBN
      WRITE(8,300) DTN,DBN
   13 CONTINUE
      END IF
      IF(COLUMN.EQ.4) THEN
      DO 14 I= 1, IMAX
      READ(2,*) DTN,DAN,DBN,DCN
      WRITE(8,300) DTN,DCN
   14 CONTINUE
```

```
      END IF
      IF(COLUMN.EQ.5) THEN
      DO 15 I= 1, IMAX
      READ(2,*) DTN,DAN,DBN,DCN,DDN
      WRITE(8,300) DTN,DDN
   15 CONTINUE
      END IF
      IF(COLUMN.EQ.6) THEN
      DO 16 I= 1, IMAX
      READ(2,*) DTN,DAN,DBN,DCN,DDN,DEN
      WRITE(8,300) DTN,DEN
   16 CONTINUE
      END IF
      IF(COLUMN.EQ.7) THEN
      DO 17 I= 1, IMAX
      READ(2,*) DTN,DAN,DBN,DCN,DDN,DEN,DFN
      WRITE(8,300) DTN,DFN
   17 CONTINUE
      END IF
      IF(COLUMN.EQ.8) THEN
      DO 18 I= 1, IMAX
      READ(2,*) DTN,DAN,DBN,DCN,DDN,DEN,DFN,DGN
      WRITE(8,300) DTN,DGN
   18 CONTINUE

      END IF
      IF(COLUMN.EQ.9) THEN
      DO 19 I= 1, IMAX
      READ(2,*) DTN,DAN,DBN,DCN,DDN,DEN,DFN,DGN,DHN
      WRITE(8,300) DTN,DHN
   19 CONTINUE
      END IF
      IF(COLUMN.EQ.10) THEN
      DO 20 I= 1, IMAX
      READ(2,*) DTN,DAN,DBN,DCN,DDN,DEN,DFN,DGN,DHN,DIN
      WRITE(8,300) DTN,DIN
   20 CONTINUE
      END IF
```

```
      IF(COLUMN.EQ.11) THEN
      DO 21 I= 1, IMAX
      READ(2,*) DTN,DAN,DBN,DCN,DDN,DEN,DFN,DGN,DHN,DIN,DJN
      WRITE(8,300) DTN,DJN
21    CONTINUE
      END IF
      IF(COLUMN.EQ.12) THEN
      DO 22 I= 1, IMAX
      READ(2,*) DTN,DAN,DBN,DCN,DDN,DEN,DFN,DGN,DHN,DIN,DJN,DKN
      WRITE(8,300) DTN,DKN
22    CONTINUE
      END IF
      IF(COLUMN.EQ.13) THEN
      DO 23 I= 1, IMAX
      READ(2,*) DTN,DAN,DBN,DCN,DDN,DEN,DFN,DGN,DHN,DIN,DJN,DKN,DLN
      WRITE(8,300) DTN,DLN
23    CONTINUE
      END IF
      IF(COLUMN.EQ.14) THEN
      DO 24 I= 1, IMAX
      READ(2,*) DTN,DAN,DBN,DCN,DDN,DEN,DFN,DGN,DHN,DIN,DJN,DKN,DLN,DMN
      WRITE(8,300) DTN,DMN
24    CONTINUE
      END IF
      IF(COLUMN.EQ.15) THEN
      DO 25 I= 1, IMAX
      READ(2,*) DTN,DAN,DBN,DCN,DDN,DEN,DFN,DGN,DHN,DIN,DJN,DKN,DLN,DMN
     A,DPN
      WRITE(8,300) DTN,DPN
25    CONTINUE
      END IF
      IF(COLUMN.EQ.16) THEN
      DO 26 I= 1, IMAX
      READ(2,*) DTN,DAN,DBN,DCN,DDN,DEN,DFN,DGN,DHN,DIN,DJN,DKN,DLN,DMN
     A,DPN,DQN
      WRITE(8,300) DTN,DQN
26    CONTINUE
      END IF
```

```
      IF(COLUMN.EQ.17) THEN
      DO 27 I= 1, IMAX
      READ(2,*) DTN,DAN,DBN,DCN,DDN,DEN,DFN,DGN,DHN,DIN,DJN,DKN,DLN,DMN
     A,DPN,DQN,DRN
      WRITE(8,300) DTN,DRN
   27 CONTINUE
      END IF
      IF(COLUMN.EQ.18) THEN
      DO 28 I= 1, IMAX
      READ(2,*) DTN,DAN,DBN,DCN,DDN,DEN,DFN,DGN,DHN,DIN,DJN,DKN,DLN,DMN
     A,DPN,DQN,DRN,DSN
      WRITE(8,300) DTN,DSN
   28 CONTINUE
      END IF
      IF(COLUMN.EQ.19) THEN
      DO 29 I= 1, IMAX
      READ(2,*) DTN,DAN,DBN,DCN,DDN,DEN,DFN,DGN,DHN,DIN,DJN,DKN,DLN,DMN
     A,DPN,DQN,DRN,DSN,DUN
      WRITE(8,300) DTN,DUN
   29 CONTINUE
      END IF
      IF(COLUMN.EQ.20) THEN
      DO 30 I= 1, IMAX
      READ(2,*) DTN,DAN,DBN,DCN,DDN,DEN,DFN,DGN,DHN,DIN,DJN,DKN,DLN,DMN
     A,DPN,DQN,DRN,DSN,DUN,DVN
      WRITE(8,300) DTN,DVN
   30 CONTINUE
      END IF
      IF(COLUMN.GT.20) THEN
      WRITE(*,*) 'COLUMN NUMBER MUST BE BETWEEN 2 AND 20'
      END IF
      IF(COLUMN.LT.2) THEN
      WRITE(*,*) 'COLUMN NUMBER MUST BE BETWEEN 2 AND 20'
      END IF
  300 FORMAT(F14.6,'   ',F14.6)
 1000 END
```

Front View of
Machine Design

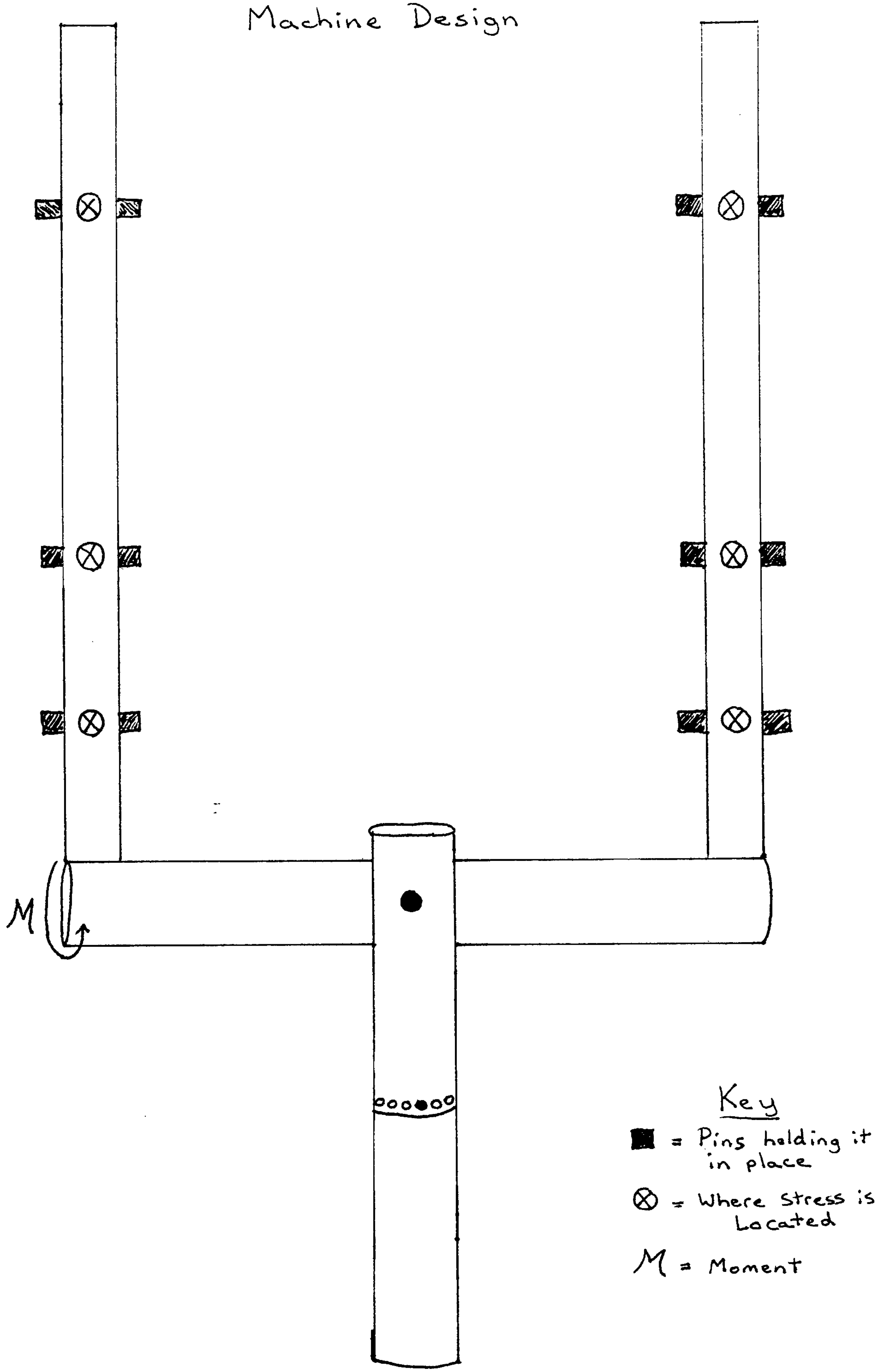

Side View of
Machine Design

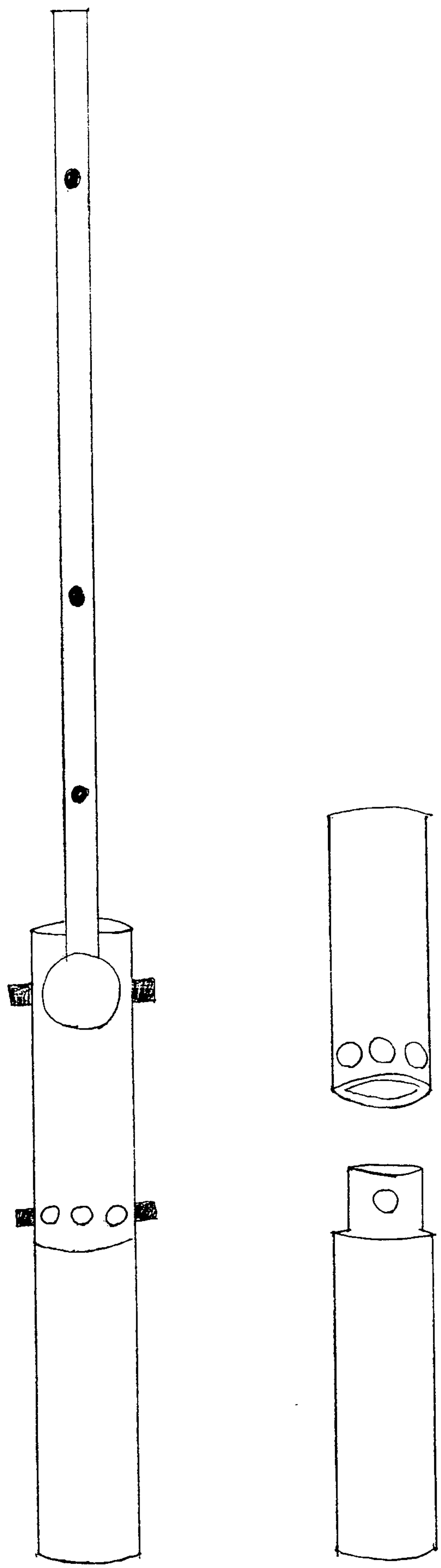

Forces on each Section of Seat

Example: $F = qACd$ $\quad q = \frac{1}{2}\rho v^2$

Total $A \approx 5.033\ ft^2$
$V = 928.27\ ft/s$
$\rho = 23.77 \times 10^{-4}\ \frac{slugs}{ft^3}$

$$F_{Total} = \left(\frac{1}{2}\right)(23.77\times10^{-4})(928.27)^2(5.033)(1.00) = 5,154.46$$

	$Cd = 0.75$	$Cd = 1.00$	$Cd = 1.25$	$Cd = 1.50$	[illegible] 1.75
F_{head}	431.98 lbs	557.3[illegible] lbs	696.74 lbs	836.09 lbs	975.44 lbs
F_{Chest}	2,142.24 lbs	2,856.31 lbs	3,570.39 lbs	4,2[illegible] lbs	[illegible]
$F_{waist + knees}$	1,036.86 lbs	1,382.49 lbs	1,723.11 lbs	2,073.73 lbs	2,419.35 lbs
$F_{L\ Leg}$	134.35 lbs	179.13 lbs	223.91 lbs	268.70 lbs	313.48 lbs
$F_{R\ Leg}$	134.35 lbs	179.13 lbs	223.91 lbs	26[illegible] lbs	313.48 lbs
F_{Total}	3,865.84 lbs	5,154.46 lbs	6,443.07 lbs	7,73[illegible] lbs	[illegible],020.30 lbs

Ejection Seat

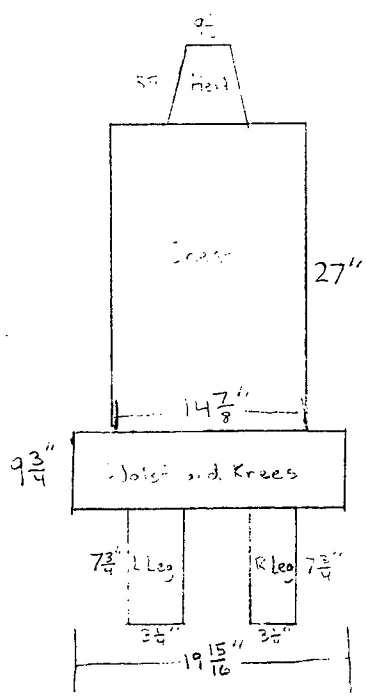

Moment at each section of the Seat and total Moment

$M = F \cdot d$ $\quad$ d= distance from center of section to ground

Example: $C_d = 0.75$, $F_{head} = 431.98\ lbs$

$$M = (431.98)(6.906) = 2,983.36\ lbs$$

	Cd=0.75	Cd=1.00	Cd=1.25	Cd=1.50	Cd=1.75
M_{head}	2,[illegible]83.3[illegible] lb·ft	3,849.47 lb·ft	4,811.86 lb·ft	5,774.25 lb·ft	6,736.63 lb·ft
M_{chest}	11,648.73 lb·ft	15,531.19 lb·ft	19,414 lb·ft	23,[illegible].81 lb·ft	27,179.[illegible] lb·ft
$M_{Waist + [illegible]}$	4,050.[illegible] lb·ft	5,400.25 lb·ft	6,750.43 lb·ft	8,100.51 lb·ft	9,450.59 lb·ft
$M_{L\ Leg}$	426.84 lb·ft	569.11 lb·ft	711.38 lb·ft	853.65 lb·ft	995.95 lb·ft
$M_{R\ Leg}$	426.84 lb·ft	569.11 lb·ft	711.38 lb·ft	853.68 lb·ft	995.95 lb·ft
ΣM	19,535.7 lb·ft	25,919.23 lb·ft	32,399.05 lb·ft	38,878.93 lb·ft	45,358.74 lb·ft

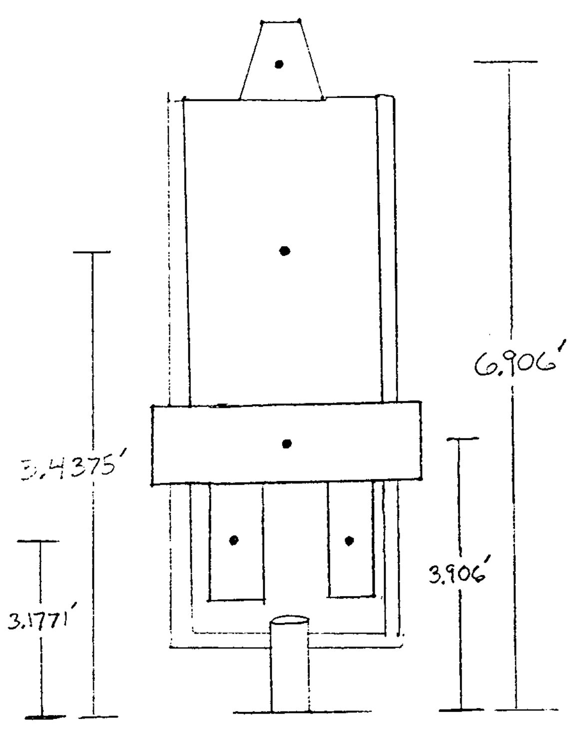

Stresses (top rod)

$$S = \frac{\frac{1}{3}F(x+y+d)c}{\frac{\pi(R^4-r^4)}{4}}$$

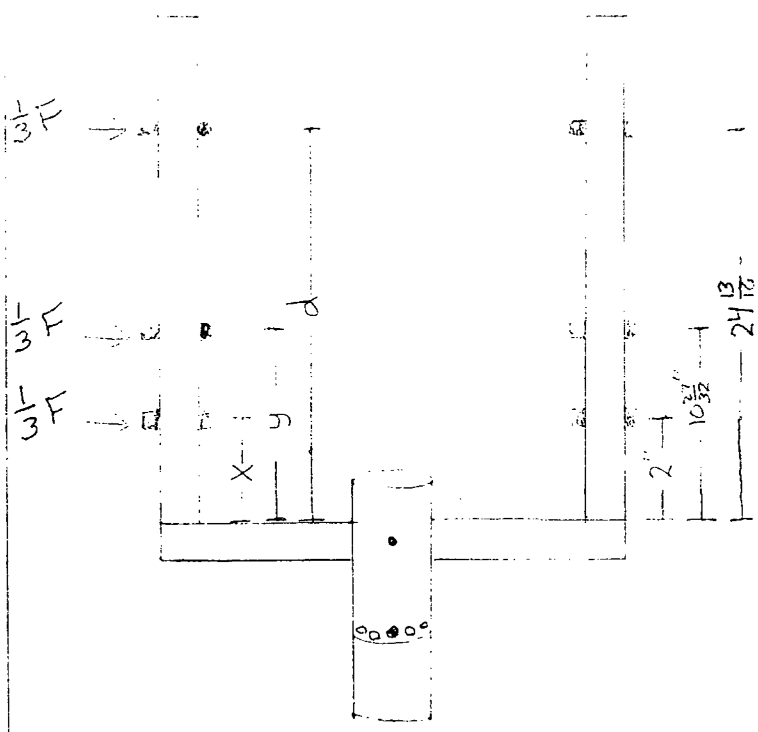

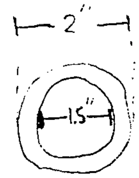

Example: diameter (inner diameter) = 2"
t (thickness) = .25"
d = .75
F = 3,865.84

$$S = \frac{\frac{1}{3}(3865.84)(2+10\frac{27}{32}+24\frac{13}{16})(1)}{\pi(1^4-.75^4)} = 57{,}747.79$$

Stresses (top rod)

$$\sigma = \frac{\frac{1}{3}F(x+y+d)c}{\frac{\pi(R^4-r^4)}{4}}$$

diameter = 2" t = .25"

	Cd = 0.75	Cd = 1.00	Cd = 1.25	Cd = 1.50	Cd = 1.75
σ	57,747.79 psi	76,997.15 psi	96,246.36 psi	115,495.72 psi	134,744.94 psi

diameter = 3" t = .25"

	Cd = 0.75	Cd = 1.00	Cd = 1.25	Cd = 1.50	Cd = 1.75
σ	26,276.57 psi	35,035.43 psi	43,794.31 psi	52,553.22 psi	61,312.05 psi

diameter = 3", t = .5"

	Cd = 0.75	Cd = 1.00	Cd = 1.25	Cd = 1.50	Cd = 1.75
σ	12,524.36 psi	16,699.17 psi	20,873.94 psi	25,048.75 psi	29,223.53 psi

diameter = 3", t = .75"

	Cd = 0.75	Cd = 1.00	Cd = 1.25	Cd = 1.50	Cd = 1.75
σ	7,937.61 psi	10,583.49 psi	13,229.35 psi	15,875.23 psi	18,521.1 psi

Key

σ = Stress

R = c = outer radius

t = thickness

r = inner radius

Cd = Coefficient of Drag

F = Force

x = distance from moment

Stresses [illegible]

$$\sigma = \frac{Mc}{I} \qquad I = \frac{\pi(R^4 - r^4)}{4} \qquad 2'' \quad t = .25''$$

$$M = \tfrac{1}{2}P(x)$$

diameter = 2" t = .25"

	Cd = 0.75	Cd = 1.00	Cd = 1.25	Cd = 1.50	Cd = 1.75
σ	34,217.36 psi	45,623.21 psi	57,028.97 psi	68,434.81 psi	79,183.78 psi

diameter = 3" t = .25"

	Cd = 0.75	Cd = 1.00	Cd = 1.25	Cd = 1.50	Cd = 1.75
σ	15,569.69 psi	20,759.61 psi	25,949.5 psi	31,139.42 psi	36,329.3 psi

diameter = 3" t = .5"

	Cd = 0.75	Cd = 1.00	Cd = 1.25	Cd = 1.5	Cd = 1.75
σ	7,421.07 psi	9,894.78 psi	12,368.46 psi	14,[illegible].17 psi	17,315.55 psi

diameter = 3" t = .75"

	Cd = 0.75	Cd = 1.00	Cd = 1.75	Cd = 1.50	Cd = 1.75
σ	4,703.28 psi	6,271.05 psi	7,838.8 psi	9,406.57 psi	10,974.33 psi

Investigation of Programming and UNIX Utilities in Support of Computational Mechanics

Michael J. Dooley
High School Apprentice
Warheads Branch, Computational Mechanics Section

Wright Laboratory Armament Directorate
WL/MNMW
Eglin AFB, FL 32542-5434

Final Report for:
High School Apprenticeship Program
Wright Laboratory Armament Directorate

Sponsored by:
Air Force Office of Scientific Research
Bolling Air Force Base, Washington, DC

August 1994

Investigation of programming and UNIX applications in support of Computational Mechanics

Michael J. Dooley
High School Apprentice
WarHeads Branch, Computational Mechanics Section
WL/MNMW

Abstract

Computational Mechanics, designated MNMW was established to support in engineering analysis of defense experiments done at Eglin Air Force Base, Florida. I was given two assignments, first to explore several UNIX utilities and report on their benefits to Computational Mechanics under the direction of my mentor Mr. Michael E. Nixon. Next I was to manipulate a result file from an EPIC 94 calculation of an experiment performed at Range C-64 on Eglin, A.F.B. To accomplish this, I first used the UNIX script language awk, then Lahey, F77, and Microsoft FORTRAN. This would benefit my section in several regards. First, it would introduce me to the processes and applications of this section and prepare me for larger projects next year. Next, I would gain useful knowledge in UNIX utilities that I could then brief my section on, and they could decide which would be useful to their work. Next, the manipulation of the time history data file mentioned earlier would allow my section to gain a clearer understanding of the data collected.

Section 1.1

My initial assignment was to explore UNIX and several of its utilities and discover how those utilities would benefit Computational Mechanics. First, I explored explore the UNIX system and learn the various commands I would need to master to successfully manipulate a UNIX based computer system. Some of these utilities being vi, jot, Korn shell, and also explored C Shell and had written several C Shell scripts. Once I had a firm grasp of these utilities and knew the basic UNIX commands I was ready to explore some of the more complicated UNIX operations, the first of these utilities being user communications. To do this, I first experimented with the commands: /usr/bin/talk and the network configuration files of this command and how it could be applied to internet communications. It was soon discovered that unless these options were specified in your network configuration, they could not be successfully used. I then began to research network setups for IRIX in an attempt to discover how the system can be configured to allow these options to be properly used. I could not however, change the network configuration myself, as that would be a violation of section security. So the procedure was discussed with the sectional network supervisor the communications utilities I researched and security was then given to implement these network changes.

Section 1.2

The next application I investigated was UNIX sendmail. UNIX sendmail relays information through a UNIX LAN via a network host on that LAN to another host or the Internet. To accomplish this, sendmail uses two main configuration files, sendmail.fc and sendmail.cf. The sendmail.fc stores all the essential configurations necessary for a network to operate while sendmail.cf stores all optional configurations to specify the file to each individual network's needs, in MNMW's case, to a VAX computer in the adjoining math lab. However, this system also posed a possible breach in security to sensitive files on the network, so until better security measures could be implemented, the project was put on hold.

Section 1.3

On completing UNIX sendmail, I then moved onto the time history data file mentioned earlier. My first attempt at manipulating this file came in the UNIX script language awk. Awk was developed in the mid 1970's as a utility for UNIX. Awk is a useful utility for simple file and database management. It can extract data and create reports for users by use of its C like script programming language. This script language allows a non or beginning programmer to successfully manipulate data in a manner that will be useful to others without spending several weeks learning the complex set of syntax and grammatical assignments the traditional languages use. Awk can also successfully handle tedious database management and sorting with but the smallest amount of work for the programmer. However, awk was primarily developed as a text manipulation script language, was job was to see how well it could manipulate numerical data in the timehis.dat file. An example of the timehis.dat file setup is available in appendix F. As a database manager can see, a complex database can be quickly and easily manipulated by Awk script file. In the timehis.dat file, I was required to write a program that would perform the following operations to the file: First, separate the file into the individual nodes, second take the maximum and minimum of the x, y, z, and pressure column along with their corresponding times. This is the program created:

```
BEGIN {  printf (" The data is as follows \n"); count=0; old_count=1;low=99999.;high=99999.}
    {
# The above assigns the initial count to 0 and the high and low to 0
        if ( $1 == "XYDATA,")   {
                count+=1;
            printf($2);
                printf($3) }
         if(count != old_count) {
                printf("High,Low %d %d \n",high,low);
           old_count=count;
           low=999999.;
           high=-999999. }
# It determines the lowest value for each set of data nodes
         if ($2 < low )  { low=$2 }
      printf($1)
         if ($2 > high )  { high=$2}
         printf($1)
        }
END {printf("High,Low %d %d \n",high,low);}
```

Awk is divided into three program blocks. The begin, main program, and end block. The begin block establishes initial values in the program's execution. The main program, through a series of if loops, calculates the maximum and minimum of the four node segments and the end program block outputs this data to a file specified at the UNIX command line. Although there are many examples of how Awk can make long hours of database management much easier, there are several disadvantages to Awk and its usage.

Section 1.4

First and paramount in its disadvantages is it did not work correctly. The result, located IN appendix A is confusing, difficult to read, and some of the results were corrupted. The next problem with awk is its long debugging time. Awk is very unforgiving in syntax. Awk, unless programmed exactly to its specified boundaries will produce unpredictable, and even dangerous results. Because of this and the fact that awk has no compiler, careful monitoring of your Awk script file's progress would be a good idea despite programming experience. Another disadvantage of Awk is its limited manipulation capabilities. Awk cannot manipulate data specified in multifield input columns unless taken one at a time, which can split data beyond the bounds of what the user wishes to accomplish (which means it can't manipulate any data type larger than one column unless the program is redesigned manually to collect the data the programmer wishes to manipulate into one column). This can also lead to problems with databases in other formats such as Excel, DBase, etc. because these programs do not use straight ASCII formats in their data files. Despite these disadvantaged Awk remains a useful UNIX tool for data management and manipulation for text based data files, however, with the continued improvement of database and spreadsheet programs as well as the UNIX utility perl, the need for awk has seemed to diminished and the language will soon become obsolete.

Section 2.1

Even though a great deal was learned from awk, my timehis.dat file still needed to be manipulated to suit the needs of Computational Mechanics. The answer came in the FORTRAN programming language. FORTRAN was chosen because my proceeding apprenticeship tour will be

spent creating and manipulating large FORTRAN programs, so it would be a good idea to begin learning now. FORTRAN was developed in the 1950's as a programming language to aid in the manipulation of that day's modern computers. Over the next thirty years, FORTRAN has been challenged by many other languages in speed and performance but remains one of the premier language for use in engineering development and design. Computational Mechanics has used FORTRAN for many years in the development and results of collected data from preliminary weapons testing. Although some of the tasks from my awk program will be performed in my FORTRAN, many of the requirements were reevaluated and modified. The new program's requirements were to separate the nodes, find the x, y, and z values at time 0, to find the maximum and minimum values of each pressure segment along with their corresponding times, to find the two and three dimensional values of each node from the center, to divide each maximum and minimum of each pressure segment by the overall maximum and minimum of all the nodes. The first step in the creation of my program was to establish my logic. I approached this problem by using a systematic analysis of the data to retrieve the needed results requested by my mentor. Appendix B-D of my report give a more clear demonstration of my approach. There you will find a commented version of my program to better understand my logic. FORTRAN was a good selection as a backup to AWK. It allowed for easy manipulation of the file and the data to be written out in a clean readable manner. I was successful, by using FORTRAN to manipulate the data and to come up with the correct results. Asample of the correct results can be found under appendix E.

Section 2.2

The use of both AWK and FORTRAN to manipulate the file timehis.dat compelled me to compare the advantages of AWK as a database management program. Although FORTRAN is primarily an engineering and number crunching language, it did seem to perform its job quite well in a database management role. However, AWK did not seem to live up to established expectations as a dedicated database language. As mentioned before, AWK does have its uses, but those uses are limited to how the data in the database is set up. In more traditional languages like FORTRAN, Pascal, and C, those limitation can be simply bypassed with a few extra instructions. AWK is an excellent tool in managing

data in a similar format, but deviate from that format, and AWK becomes a tedious and unpredictable language that is not easy to work with.

Other Projects

In addition to working on the UNIX utilities, the UNIX sendmail and the time history program, I performed several other duties for MNMW. First we reassembled and set up a Zenith i286 for E-mail and editing, I repaired a malfunctioning drive on one of the section's computers, installed new drives on several computers and workstations in the section and provided logistics assistance to the various active duty, civil service, and contractors in Computational Mechanics.

Equipment Used

Throughout my summer, I used a plethora of hardware, software, and equipment to accomplish my projects. First, I used a Zenith 286, a Unisys 386, a Gateway DX-2, 66, an SGI Indigo, and an SGI Indy. I also used Windows 3.11, Word 2.0, Powerpoint 3.0, Lahey FORTRAN, F77, Microsoft FORTRAN, Excel 4.0, X-Windows, and IRIX driven menu program.

What I learned

During my tour at Wright Labs, I have learned many useful UNIX utilities as well as the basic commands of UNIX and workstations. I am now well versed in the awk script language as well as have a working knowledge of FORTRAN. However, I think several greater lessons have been learned. First, I have learned a lot about a professional work environment and the responsibilities in such and environment. I have also learned a better understanding of people who work in MNMW and have adapted myself to better understand their way of thinking. This will benefit me as I progress through my life and supply knowledge of the "real world' that will remain with me throughout my life.

Summary

My summer working in the High School Apprenticeship program has been very rewarding and educational. I Have gained valuable knowledge and experience in FORTRAN and UNIX that will benefit me as my computer career broadens to college. I have been very pleased with my assignments and my mentor, Michael Nixon. This program has been a great experience that will sere me well into adulthood.

AWK RESULTS

0.101287E-040.101287E-040.202161E-040.202161E-040.300403E-040.300403E-040.401008E-040.401008E-040.500972E-040.500972E-040.600411E-040.600411E-040.700775E-040.700775E-040.800190E-040.800190E-040.901363E-040.901363E-040.100050E-030.100050E-030.110136E-030.110136E-030.120164E-030.120164E-030.130069E-030.130069E-030.140124E-030.140124E-030.150060E-030.150060E-030.160109E-030.160109E-030.170062E-030.170062E-030.180105E-030.180105E-030.190068E-030.190068E-030.200056E-030.200056E-030.210158E-030.210158E-030.220080E-030.220080E-030.229695E-030.229695E-030.239785E-030.239785E-030.249732E-030.249732E-030.259799E-030.259799E-030.269719E-030.269719E-030.279726E-030.279726E-030.289782E-030.289782E-030.299758E-030.299758E-030.309730E-030.309730E-030.319734E-030.319734E-030.329750E-030.329750E-030.339765E-030.339765E-030.349784E-030.349784E-030.359721E-030.359721E-030.369721E-030.369721E-030.379782E-030.379782E-030.389802E-030.389802E-030.399803E-030.399803E-030.409789E-030.409789E-030.419568E-030.419568E-030.429595E-030.429595E-030.439655E-030.439655E-030.449654E-030.449654E-030.459605E-030.459605E-030.469619E-030.469619E-030.479578E-030.479578E-030.489587E-030.489587E-030.499652E-030.499652E-030.509590E-030.509590E-030.519596E-030.519596E-030.529600E-030.529600E-030.539569E-030.539569E-030.549607E-030.549607E-030.559606E-030.559606E-030.569671E-030.569671E-030.579587E-030.579587E-030.589569E-030.589569E-030.599616E-030.599616E-030.609619E-030.609619E-030.619582E-030.619582E-030.629644E-030.629644E-030.639600E-030.639600E-030.649646E-030.649646E-030.655711E-030.655711E-030.665736E-030.665736E-030.675751E-030.675751E-030.685752E-030.685752E-030.695733E-030.695733E-030.705803E-030.705803E-030.715739E-030.715739E-030.725752E-030.725752E-030.735721E-030.735721E-030.745742E-030.745742E-030.755790E-030.755790E-030.765764E-030.765764E-030.775815E-030.775815E-030.785725E-030.785725E-030.795715E-030.795715E-030.805789E-030.805789E-030.815721E-030.815721E-030.825742E-030.825742E-030.835736E-030.835736E-030.845812E-030.845812E-030.855751E-030.855751E-030.865768E-030.865768E-030.875749E-030.875749E-030.885805E-030.885805E-030.895721E-030.895721E-030.905805E-030.905805E-030.915786E-030.915786E-030.925776E-030.925776E-030.935741E-030.935741E-030.945782E-030.945782E-030.955797E-030.955797E-030.965793E-030.965793E-030.975799E-030.975799E-030.985788E-030.985788E-030.995763E-030.995763E-030.100571E-020.100571E-020.101576E-020.101576E-020.102577E-020.102577E-020.103579E-020.103579E-020.104580E-020.104580E-020.105575E-020.105575E-020.106577E-020.106577E-020.107579E-020.107579E-020.108581E-020.108581E-020.109581E-020.109581E-020.110579E-020.110579E-020.111577E-020.111577E-020.112574E-020.112574E-020.113581E-020.113581E-020.114574E-020.114574E-020.115576E-020.115576E-020.116575E-020.116575E-020.117573E-020.117573E-020.118579E-020.118579E-020.119573E-020.119573E-020.120576E-020.120576E-020.121579E-020.121579E-020.122581E-020.122581E-020.123572E-020.123572E-020.124573E-020.124573E-020.125573E-020.125573E-020.126572E-020.126572E-020

□

APPENDIX A

```
C Program statement
   Program Sort
CCCCCCCCCCCCCCCCCCCCCCCCCCCCCCCCCC
C Sets the numerical size limitsC
CCCCCCCCCCCCCCCCCCCCCCCCCCCCCCCCCC
   real x(100), y(100), z(100)
   real pmin(200), pmax(200)
   real max(200), min(200)
   real pmina(200),pmaxa(200)
   real dimtwo(200),dimthe(200)
   integer node(100)
CCCCCCCCCCCCCCCCCCCCCCCCCCCCCCCCCCCCCC
C Sets the size limits of the arraysC
CCCCCCCCCCCCCCCCCCCCCCCCCCCCCCCCCCCCCC
   character*40 dummy
   character*30 hdummy
   character*14 hdum
CCCCCCCCCCCCCCCCCCCCCCCCCCCCCCCCCCCCCCCCCCCCCCCCCCCCCCCCCCCCCCC
C Sets the icount to 0.The icount is used when when counting C
C how many elements are in each segment of timehis.dat     C
CCCCCCCCCCCCCCCCCCCCCCCCCCCCCCCCCCCCCCCCCCCCCCCCCCCCCCCCCCCCCCC
   icount=0
CCCCCCCCCCCCCCCCCCCCCCCCCCCCCCCCCCCCCCCCCCCCCCCCCCCCCCCCCCCCCCCCCCCCCCC
C Opens timehis.dat for analysis and creates duh.dat to store those  C
C result analysis.  Timehis.dat will be set up in four segments,    C
C indicated by a header and set up in andx, y, z and a pressure     C
C segment made up by two columns of data                       C
CCCCCCCCCCCCCCCCCCCCCCCCCCCCCCCCCCCCCCCCCCCCCCCCCCCCCCCCCCCCCCCCCCCCCCC
   OPEN (UNIT=25, file='timehis.dat')
   OPEN (UNIT=26, file='duh.dat')
CCCCCCCCCCCCCCCCCCCCCCCCCCCCCCCCCCCCCCCCCCCCCCCCCCCCCCCCCCCCCCCCCCCCCC
C Reads the header and ignores it. Line 102 sets the format for the C
C read statement as an array 30 characters long                C
CCCCCCCCCCCCCCCCCCCCCCCCCCCCCCCCCCCCCCCCCCCCCCCCCCCCCCCCCCCCCCCCCCCCCC
   read (25,102) hdummy
 102  format (a30)
CCCCCCCCCCCCCCCCCCCCCCCCCCCCCCCCCCCCCCCCCCCCCCCCCCCCCCCCCCCCCCCCCCCCCCCC
C Reads through the above segment, counts how many rows there are. If C
C runs out of rows, it jumps to line 500.  Line 101 sets the format  C
C for the read.  Icount will increment the number of rows it counts  C
C The goto statement returns the scan to line 1 where it will read   C
C and continue to look for rows of the specified format            C
CCCCCCCCCCCCCCCCCCCCCCCCCCCCCCCCCCCCCCCCCCCCCCCCCCCCCCCCCCCCCCCCCCCCCCCC
 1   read (25,101,err=500) xdum, ydum
 101  format (2E15.6)
   icount = icount + 1
   goto 1
CCCCCCCCCCCCCCCCCCCCCCCCCCCCCCCCCCCCCCCCCCCCCCCCCCCCCCC
C Line 500 rewinds the scan back to the header C
CCCCCCCCCCCCCCCCCCCCCCCCCCCCCCCCCCCCCCCCCCCCCCCCCCCCCCC
 500  rewind 25
CCCCCCCCCCCCCCCCCCCCCCCCCCCCC
C Begins the node count C
CCCCCCCCCCCCCCCCCCCCCCCCCCCCC
   ncount=1
CCCCCCCCCCCCCCCCCCCCCCCCCCCCCCCCCCCCCCCCCCCCCCCCCCCCCCCCCCCCCCCCCCCCCC
C Reads the header and using format 105 to extract the node number  C
C from the header.                                     C
CCCCCCCCCCCCCCCCCCCCCCCCCCCCCCCCCCCCCCCCCCCCCCCCCCCCCCCCCCCCCCCCCCCCCC
 2     read (25,105,err=999) hdum, node(ncount)
 105  format(a13,i5)
CCCCCCCCCCCCCCCCCCCCCCCCCCCCCCCCCCCCCCCCCCCCCCCCCCCCCCCCCCCCCCCCCCCCCCCC
C Reads the first row of the x segment, takes the x value or column 2 C
C value found above and does nothing with it by using a do loop.  The C
C next few lines proceed to increment the scan by using the icount   C
C found above and does nothing with it by using a do loop.          C
CCCCCCCCCCCCCCCCCCCCCCCCCCCCCCCCCCCCCCCCCCCCCCCCCCCCCCCCCCCCCCCCCCCCCCCC
 3   read(25,101) xdum, x(ncount)
```

APPENDIX B

```
          do ic=1, icount -1, 1
          read (25,101) xdum, ydum
          enddo
CCCCCCCCCCCCCCCCCCCCCCCCCCCCCCCCCCCCCCCCCCCCCCCCCCCCCCCCCCCCCCCCCCC
C Performs the same function on the y segment as on the x segment    C
CCCCCCCCCCCCCCCCCCCCCCCCCCCCCCCCCCCCCCCCCCCCCCCCCCCCCCCCCCCCCCCCCCC
          read(25,102) hdummy
           read (25,101) xdum, y(ncount)
            do ic=1, icount -1
            read (25,101) xdum, ydum
            enddo
CCCCCCCCCCCCCCCCCCCCCCCCCCCCCCCCCCCCCCCCCCCCCCCCCCCCCCCCCCCCCCCCCCCCC
C Performs the same function on the z segment as on the x and y segment C
CCCCCCCCCCCCCCCCCCCCCCCCCCCCCCCCCCCCCCCCCCCCCCCCCCCCCCCCCCCCCCCCCCCCC
                   read (25,102) hdummy
                   read (25,101) xdum, z(ncount)
                    do ic = 1, icount - 1
                    read (25,101) xdum, ydum
                    enddo


CCCCCCCCCCCCCCCCCCCCCCCCCCCCCCCCCCCCCCCCCCCCCCCCCCCCCCCCCCCCCCCCCCC
C Assigns a high value to pmin and a low value to pmax for easy      C
C manipulation                               C
CCCCCCCCCCCCCCCCCCCCCCCCCCCCCCCCCCCCCCCCCCCCCCCCCCCCCCCCCCCCCCCCCCC
Pmax(ncount) = -999999999.
   pmax(ncount) = -999999999.
   Pmin(ncount) = 999999999.
CCCCCCCCCCCCCCCCCCCCCCCCCCCCCCCCCCCCCCCC
C Reads and ignores the pressure heading C
CCCCCCCCCCCCCCCCCCCCCCCCCCCCCCCCCCCCCCCC
   read (25, 102) hdummy
CCCCCCCCCCCCCCCCCCCCCCCCCCCCCCCCCCCCCCCCCCCCCCCCCCCCCCCCCCCCCCCCCCCCCCC
C This section of the program begins by incrementing icount same as above C
C Then it will read each row adn assign the temporary variables values of C
C time and pres. Then it will proceed to analyze the maxes and mins of   C
C column 2 of the pressure segment using 'if' blocks t oscan the columns. C
C If during the program's scan it finds a value higher or lower than the  C
C current pmax and pmin respectively, it will repace that value for the   C
C variable along with its correlating time.                  C
CCCCCCCCCCCCCCCCCCCCCCCCCCCCCCCCCCCCCCCCCCCCCCCCCCCCCCCCCCCCCCCCCCCCCCC
          do ic=1, icount
          read (25, 101) time, pres
           if (pres.gt.Pmax(ncount)) then
            pmax(ncount) = pres
            max(ncount)= time
            else if (pres.lt.pmin(ncount)) then
             pmin(ncount) = pres
             min(ncount)= time
             endif
    enddo
CCCCCCCCCCCCCCCCCCCCCCCCCCCCCCCCCCCCCCCCCCCCCCCCCCC
C Calculates the xy and xyz distances for each node C
CCCCCCCCCCCCCCCCCCCCCCCCCCCCCCCCCCCCCCCCCCCCCCCCCCC
   Dimtwo(ncount)=sqrt(x(ncount)*x(ncount)+y(ncount)*y(ncount))
   dimthe(ncount)=sqrt(x(ncount)*x(ncount)+y(ncount)*y(ncount)+
   &z(ncount)*z(ncount))
CCCCCCCCCCCCCCCCCCCCCCCCCCCCCCCCCCCCCCCCCCCCCCCCCCCCCCCCCCCCCCCCC
C increments the node counter when all the scans are completed for C
C each node                          C
CCCCCCCCCCCCCCCCCCCCCCCCCCCCCCCCCCCCCCCCCCCCCCCCCCCCCCCCCCCCCCCCC
   ncount = ncount +1
CCCCCCCCCCCCCCCCCCCCCCCCCCCCCCCCCCCCCCCCCCCCCCCCCCCCCCCCCCCCCCCCCCC
C If the ncount has scanned all 68 nodes, this statement directs the C
C program to line 999                       C
CCCCCCCCCCCCCCCCCCCCCCCCCCCCCCCCCCCCCCCCCCCCCCCCCCCCCCCCCCCCCCCCCCC
   if(ncount.eq.68) goto 999
```

```
CCCCCCCCCCCCCCCCCCCCCCCCCCCCCCCCCCCCCCCCCCCCCCCCCCCCCCCC
C Returns the program to line two for the next node scan C
CCCCCCCCCCCCCCCCCCCCCCCCCCCCCCCCCCCCCCCCCCCCCCCCCCCCCCCC
   goto 2
CCCCCCCCCCCCCCCCCCCCCCCCCCCCCCCCCCCCCCCCCCCCCCCCCCCCCCCCCCCCCCCC
C Write the result data to file 26, ncount - 1 times. This data C
C are the results from my program thus far          C
CCCCCCCCCCCCCCCCCCCCCCCCCCCCCCCCCCCCCCCCCCCCCCCCCCCCCCCCCCCCCCCC
 999 do i=1, ncount-1
   write(26,110)node(i),x(i),y(i),dimtwo(i),z(i),dimthe(i),
   &pmin(i),min(i),pmax(i),max(i)
 110 format (i5,e15.7,e15.7,e15.7,e15.7,e15.7,e15.7,e15.7,e15.7,e15.7)
   enddo
CCCCCCCCCCCCCCCCCCCCCCCCCCCCCCCCCCCCCCCCCCCCCCCCCCCCCCCCCCCCCCCCCCCCCCCCCC
C Closes timehis.dat and creates derg.dat to store the final manipulations C
C of duh.dat                                 C
CCCCCCCCCCCCCCCCCCCCCCCCCCCCCCCCCCCCCCCCCCCCCCCCCCCCCCCCCCCCCCCCCCCCCCCCCC
    CLOSE (UNIT=25)
    OPEN  (UNIT=27,file='derg.dat')
C Rewinds file 26 to the beginning C
   rewind 26
CCCCCCCCCCCCCCCCCCCCCCCCCCCCCCCCCCCCCCCCCCCCCCCCCCCCCCCCCCCCCCCCCCCCCCCCCCCC
C Sets apmax and apmin low and high values respectively for easy manipulation C
 CCCCCCCCCCCCCCCCCCCCCCCCCCCCCCCCCCCCCCCCCCCCCCCCCCCCCCCCCCCCCCCCCCCCCCCCCCC
   apmin=999999999.
   apmax=-999999999.
   ncount=1
   do ic=1,67
   read(26,110)node(ncount),x(ncount),y(ncount),dimtwo(ncount),
   &z(ncount),dimthe(ncount),pmin(ncount),min(ncount),pmax(ncount)
   &max(ncount)
 CCCCCCCCCCCCCCCCCCCCCCCCCCCCCCCCCCCCCCCCCCCCCCCCCCCCCCCCCCCCCCCCCCCCCCCC
 C Scans the pmaxes and pmins to find the max pmax and min pmin by using C
 C if blocks                                C
 CCCCCCCCCCCCCCCCCCCCCCCCCCCCCCCCCCCCCCCCCCCCCCCCCCCCCCCCCCCCCCCCCCCCCCCC
   if(pmax(ncount).gt.apmax) then
   apmax=pmax(ncount)
   endif
   if(pmin(ncount).lt.apmin) then
   apmin=pmin(ncount)
   endif
113  format(i5,11e15.7)
CCCCCCCCCCCCCCCCCCCCCCCCCCCCCCCCCCCCCCCCCCCCCCCCCCCCCCCCCCCCCCCCCCCCCCCCC
C Uses a do loop to perfrom a scalar operation on duh.dat and store      C
C those results in derg,dat or file unit 27.  First, it divides all the  C
C pmax and pmins by the max pmax and min pmin and then writes those      C
C Results along with the results from previous node scans in the assigned C
C format                                    C
CCCCCCCCCCCCCCCCCCCCCCCCCCCCCCCCCCCCCCCCCCCCCCCCCCCCCCCCCCCCCCCCCCCCCCCCC
 120 enddo
   rewind 26
   do jc=1,67
   pmina(jc)=pmin(jc)/apmin
   pmaxa(jc)=pmax(jc)/apmax
   read(26,113)node(ncount),x(ncount),y(ncount),z(ncount)
   &,dimtwo(ncount),dimthe(ncount),pmina(ic),min(ncount),pmaxa(ic)
   &max(ic)
   write(27,113)node(ncount),x(ncount),y(ncount),dimtwo(ncount)
   &,z(ncount),dimthe(ncount),pmina(ic),min(ncount),
   &pmaxa(ncount),max(ic)
   enddo
CCCCCCCCCCCCCCCCCCCCCCCCCCCCCCCCCCC
C Stops the program and ten ends C
CCCCCCCCCCCCCCCCCCCCCCCCCCCCCCCCCCC
   stop
   end
```

APPENDIX D

FORTRAN RESULTS

6755 -0.1445580E+02 0.5927380E+01 0.0000000E+00 0.1562383E+02 0.1562383E+02 -
0.4412880E+03 0.4097890E-03 0.3495905E-01 0.1045800E-02
7079 -0.1659480E+01 0.1702430E+01 -0.3155260E+00 0.2377423E+01 0.2398270E+01
0.0000000E+00 0.5596060E-03 0.3495905E-01 0.1401240E-03
7117 -0.1990350E-01 0.2107360E+01 -0.3155260E+00 0.2107454E+01 0.2130943E+01 0.3674500E-
01 0.1135810E-02 0.3495905E-01 0.1801050E-03
7201 -0.3087680E+01 0.5503170E+00 -0.3155260E+00 0.3136338E+01 0.3152170E+01
0.0000000E+00 0.1155760E-02 0.3495905E-01 0.1700620E-03
7204 -0.3145790E+01 0.1386680E+00 -0.3155260E+00 0.3148845E+01 0.3164614E+01
0.1215000E+02 0.1175730E-02 0.3495905E-01 0.1700620E-03
7425 0.1238270E+01 0.3316620E+01 -0.3155260E+00 0.3540237E+01 0.3554271E+01
0.8422590E+02 0.5009720E-04 0.3495905E-01 0.2697190E-03
7482 0.3350330E+01 0.1382440E+01 -0.3155260E+00 0.3624342E+01 0.3638050E+01 -
0.7231570E-07 0.2021610E-04 0.3495905E-01 0.3998030E-03
27207 0.3757930E+01 0.3842530E+01 -0.5022270E+01 0.5374670E+01 0.7355968E+01 -
0.5393700E+03 0.9857879E-03 0.3495905E-01 0.1700620E-03
27960 -0.3901140E+01 0.1464930E+02 -0.5022270E+01 0.1515984E+02 0.1597010E+02 -
0.2851580E+03 0.4895870E-03 0.3495905E-01 0.1025770E-02
27995 -0.1445580E+02 0.5927380E+01 -0.5022270E+01 0.1562383E+02 0.1641119E+02 -
0.1847850E+03 0.4496540E-03 0.3495905E-01 0.1045800E-02
28319 -0.1659480E+01 0.1702430E+01 -0.5588910E+01 0.2377423E+01 0.6073554E+01 -
0.2361040E+03 0.1900680E-03 0.3495905E-01 0.6757510E-03
28357 -0.1990350E-01 0.2107360E+01 -0.5588910E+01 0.2107454E+01 0.5973046E+01 -
0.2037820E+03 0.1045800E-02 0.3495905E-01 0.6496460E-03
28389 0.1796520E+01 0.0000000E+00 -0.5588910E+01 0.1796520E+01 0.5870553E+01 -
0.5264730E+03 0.2200800E-03 0.3495905E-01 0.1201640E-03
28441 -0.3087680E+01 0.5503170E+00 -0.5588910E+01 0.3136338E+01 0.6408786E+01 -
0.8601480E+02 0.1900680E-03 0.3495905E-01 0.7357210E-03
28444 -0.3145790E+01 0.1386680E+00 -0.5588910E+01 0.3148845E+01 0.6414916E+01 -
0.7205790E+02 0.1900680E-03 0.3495905E-01 0.7357210E-03
28665 0.1238270E+01 0.3316620E+01 -0.5588910E+01 0.3540237E+01 0.6615829E+01 -
0.3970210E+03 0.9857879E-03 0.3495905E-01 0.6396000E-03
28722 0.3350330E+01 0.1382440E+01 -0.5588910E+01 0.3624342E+01 0.6661214E+01 -
0.4439850E+03 0.9857879E-03 0.3495905E-01 0.4496540E-03
41367 0.3757930E+01 0.3842530E+01 -0.1043320E+02 0.5374670E+01 0.1173621E+02 -
0.3304800E+03 0.1115770E-02 0.3495905E-01 0.1601090E-03
42120 -0.3901140E+01 0.1464930E+02 -0.1043320E+02 0.1515984E+02 0.1840306E+02 -
0.1216230E+03 0.1215790E-02 0.3495905E-01 0.7157390E-03
42155 -0.1445580E+02 0.5927380E+01 -0.1043320E+02 0.1562383E+02 0.1878711E+02 -
0.5474490E+01 0.2000560E-03 0.3495905E-01 0.1085810E-02
42479 -0.1659480E+01 0.1702430E+01 -0.1127040E+02 0.2377423E+01 0.1151842E+02 -
0.4961180E+03 0.3497840E-03 0.3495905E-01 0.9357410E-03
42517 -0.1990350E-01 0.2107360E+01 -0.1127040E+02 0.2107454E+01 0.1146574E+02 -
0.2863400E+03 0.3497840E-03 0.3495905E-01 0.8257420E-03
42549 0.1796520E+01 0.0000000E+00 -0.1127040E+02 0.1796520E+01 0.1141269E+02 -
0.5346080E+03 0.3497840E-03 0.3495905E-01 0.1601090E-03

TIMEHIS.DAT

XYDATA, Node 2230 X pos

0.000000E+00	0.000000E+00
0.101287E-04	0.474797E-14
0.202161E-04	-0.962954E-04
0.300403E-04	0.455302E-03
0.401008E-04	0.939425E-03
0.500972E-04	0.895718E-03
0.600411E-04	0.102596E-02
0.700775E-04	0.127013E-02
0.800190E-04	0.994788E-03
0.901363E-04	0.826996E-03
0.100050E-03	0.110099E-02
0.110136E-03	0.182676E-02
0.120164E-03	0.130632E-02
0.130069E-03	0.207676E-02
0.140124E-03	0.286416E-02
0.150060E-03	0.459770E-02
0.160109E-03	0.605534E-02
0.170062E-03	0.757888E-02
0.180105E-03	0.103257E-01
0.190068E-03	0.139823E-01
0.200056E-03	0.136242E-01
0.210158E-03	0.142114E-01
0.220080E-03	0.199824E-01
0.229695E-03	0.268318E-01
0.239785E-03	0.266440E-01
0.249732E-03	0.260139E-01
0.259799E-03	0.323658E-01
0.269719E-03	0.394489E-01
0.279726E-03	0.433307E-01
0.289782E-03	0.444036E-01
0.299758E-03	0.444821E-01
0.309730E-03	0.472006E-01
0.319734E-03	0.526952E-01
0.329750E-03	0.582189E-01
0.339765E-03	0.587497E-01
0.349784E-03	0.568690E-01
0.359721E-03	0.544854E-01
0.369721E-03	0.586950E-01
0.379782E-03	0.631144E-01
0.389802E-03	0.619737E-01
0.399803E-03	0.605279E-01
0.409789E-03	0.584462E-01
0.419568E-03	0.551935E-01
0.429595E-03	0.542276E-01
0.439655E-03	0.577584E-01
0.449654E-03	0.647625E-01
0.459605E-03	0.673285E-01

A STUDY OF POLYMER DISPERSED LIQUID CRYSTALS

Ajay Goel

Centerville High School

500 E. Franklin St.

Centerville, OH 45459

Final report for:

High School Apprentice Program

Wright Patterson Air Force Base

Electro-Magnetic Materials Division

Sponsored by:

Air Force Office of Scientific Research

Bolling Air Force Base, DC

September 1994

A STUDY OF POLYMER DISPERSED LIQUID CRYSTALS

Ajay Goel

Centerville High School

Abstract

Polymer dispersed liquid crystal films were studied. Films were made by mixing a monomer, a liquid crystal, a coinitiator, and a photosensitive dye. In some situations, a cross-linker was added. And in other cases, a surfactant was added. After the "syrup" was dissolved using an ultrasonic tip, a thin film of the mixture was exposed to different intensities of different kinds of light. After regular phase separation of the liquid crystal was observed, Bragg gratings were also produced in the film by exposing it with two laser beams simultaneously.

A STUDY OF POLYMER DISPERSED LIQUID CRYSTALS

Ajay Goel

Introduction

Liquid crystals are playing an increasingly important role in today's technological world. Their valuable properties can be seen when observing watches and calculators (LCD's-liquid crystal displays), and TV screens. Very recently, however, liquid crystals have come to use in car winshields--so that the operator can have the window clear when driving or cloudy when parked to block sunlight. The technology that allows this to happen revolves around polymer-dispersed liquid crystal films. The liquid crystal phase is a phase in between the liquid phase and the solid phase--that is it possesses properties of both. The liquid crystal phase itself has different sub-phases such as smectic A, smectic B, smectic C, nematic, and cholesteric. They are very flexible. Their rodlike molecules can be oriented along a director using an electric field of low voltage. When placed in a polymer matrix, however, it is more different to control the molecules' properties and orientations. PDLC films were observed along with films in which diffraction gratings were written. This is also known as a hologram. An image, or simply even the spot of a laser beam was diffracted by the grating. The liquid crystal separates out of the polymer matrix--known as phase separation. It has a cloudiness to it so that the film is not transparent. These kinds of holograms and optical images are much different and advantageous to industries which utilize optical data storage or similar holographic imagery. In traditional holographic images, the properties are "fixed"--once the hologram is developed its properties cannot be changed. With PDLC's however, voltage can be applied to the film to switch the image on and off. Producing images using PDLC films is also advantageous because it employs a one step developing process. When using ordinary holographic film to produce images, the film must first be exposed to laser light reflected off the image; then the film must be submerged in a variety of chemicals to develop it. This also applies to photographic cameras. Using PDLC's requires only for the film to be exposed to light in order for the image to be visible to the human eye. Also, gratings involving liquid crystal have a definite higher diffraction efficiency because the difference in the refractive index between high density polymerization areas and high density liquid crystal areas is greater than the difference between high density polymerization areas and low density polymerization areas.

Methodology

Different "syrups" were made using different amounts of E-7 liquid crystal, none and some cross linker (N-vinylpyrrollidone), different combinations of 2 monomers (penta-erythritol triacrylate and dipentaerythrol hydroxy penta acrylate), a coinitiator of n-phenyl glycene, and a photo initiator of Rose Bengal dye. The syrup was uniformely dissolved using an ultrasonic tip. A couple of drops of a syrup would then be placed on a glass slide. Thin strips of Handi-Wrap (kind of like Seran Wrap) were placed on the two ends of the

slide to serve as spacers to allow the liquid crystal E-7 to phase separate. Another piece of glass was then placed on top of the other, smooshing the syrup into a thin film. Binder clips were then placed on the ends of the sample to keep the sample together and control the shrinkage of the liquid crystal droplets. Primarily, six samples were made using each syrup. High and low intensities of 3 different kinds of lights were used to photopolymerize the sample: an incandescent floodlit lamp, a floodlit laser beam, and a split laser beam to produce a diffraction grating in the sample. Once the feasibility and potential of the syrup was determined, new samples were made using special glass slides coated with conducting indium tin oxide (ITO). This made it possible to apply voltage to the sample to make the cloudiness of the liquid crystal diappear. When the cloudiness of the sample disappears, so does the diffraction gratings ability to diffract the light. Therefore the diffracted spot or image disappears, while making the transmitted spot brighter (since the light is not split up anymore between the diffracted and transmitted images, most of the light is transmitted).

Liquid crystal molecules are rodlike. When phase separated, they point in all random directions, making the film opaque. When voltage is applied, however, all the rods become oriented in the direction of the electric field and align in the direction of the director of the liquid crystal. All pointing in the same direction, they make it possible for the viewer to see through the film. The goal with the ITO samples was to get the diffracted image to switch at the lowest possible voltage while maximizing the diffraction efficiency at the beginning. Only then will the films be of use to the electro-optical image processing industry.

Results and Discussion

To begin with, a table is shown of the different syrups' compositions.

Syrup	% monomer	% liquid crystal	% surfactant	% crosslinker	% coinitiator	% photoinitiator
RB63A	96.1 % PETA	0	0	0	3.59	.285
RB64A	75.5% PETA	21.3	0	0	3.01	.237
RB65A	65.7% PETA	31.3	0	0	2.76	.228
RB66A	60.2% PETA	31.5	0	5.07	3.01	.194
RB67A	56.5% PETA	34.1	6.44	0	2.73	.285
RB68A	67.3% DPHDA	30.4	0	0	1.91	.342
RB69A	43.4% DPHDA	39.9	8.16	6.17	2.17	.235
RB70A	97.0% PETA	0	0	0	2.67	.292
RB71A	91.9% PETA	0	0	5.56	2.38	.156
RB72A	97.1% DPHDA	0	0	0	2.71	.241

RB73A	91.2% DPHDA	0	0	5.78	2.71	.359
RB74A	26.5% PETA and 35.8% DPHDA	30.8	5.10	0	1.61	.207

Each syrup was tested in a variety of ways. The liquid crystal component of the syrup was the main concern however. The right percentage of the liquid crystal in the total syrup was the most important determinant of the switchability of an image using that syrup. Each syrup was used in floodlit lamp and laser samples, as well as grating samples. Each syrup, once its feasibility was shown, was sandwiched between glass plates coated with ITO. After all the samples were made, select samples were scraped off the glass or ITO and run through a differential scanning calorimeter (DSC). This instrument is used extensively in the chemical engineering/materials science arena. It measures the heat flow in and out of a particular sample, showing important phase transitions as a function of time or temperature. As stated before, liquid crystals have subphases within the liquid crystal phase: smectic A, smectic B, smectic C, nematic, and cholesteric. A liquid crystal, need not have all of the phases, however. The liquid crystal used in this experiment, E-7, only has a nematic phase. A phase diagram of E-7 would show a transition from the nematic liquid crystal phase to the isotropic liquid phase at about 58 degrees Celcius. Part of this experiment also determined whether the transition point from nematic to isotropic liquid was affected by placing the liquid crystal in a polymer matrix. Referring to the previous table, it was observed that the percentage of coinitiator (n-phenyl glycene) is not important in determining the quality of the syrup as long as there is plenty there for the syrup to fully react when being photopolymerized. The same goes for Rose Bengal dye, the photoinitiator. Three to four miligrams is generally sufficient when making small samples of syrup. The only problem occured when too much dye was added (8 to 9 miligrams); this created problems because when the syrup would be ultrasonicated, some Rose Bengal particles would remain undissolved. The first set of experiments were done simply to observe the difference in a photopolymerized sample with and without liquid crystal, using syrups RB63A and RB64A.

SAMPLE	TYPE	COMMENTS
RB63A1	floodlit lamp, 11.8 mw/cm^2	no phase separation due to absence of liquid crystal
RB64A1	floodlit lamp, 11.8 mw/cm^2	some phase separation apparent
RB63A2	floodlit lamp, 11.8 mw/cm^2	no phase separation due to absence of liquid crystal
RB64A2	floodlit lamp, 11.8 mw/cm^2	some phase separation apparent
RB63A3	floodlit laser, 50.2 mw/cm^2	no phase separation

SAMPLE	TYPE	COMMENTS
RB64A3	floodlit laser, 50.2 mw/cm^2	more phase separation than floodlit lamp samples
RB63A4	floodlit laser, 5.10 mw/cm^2	no phase separation
RB64A4	floodlit laser, 5.10 mw/cm^2	more phase separation than lamp samples but less than higher intensity laser samples
RB63A5	grating, 50.2 mw/cm^2 total	grating is okay, nothing special
RB64A5	grating, 50.2 mw/cm^2 total	grating has a much higher diffraction efficiency than RB63A5
RB63A6	grating, 5.4 mw/cm^2 total	diffraction efficiency appears to be same as RB63A5
RB64A6	grating, 5.4 mw/cm^2 total	diffraction efficiency higher than RB63A6 but no difference between this sample's and RB64A5's, but phase separation is greater
RB64A7	grating on ITO, 5.4 mw/cm^2	initial D.E of 30%, but diffraction spot does not switch at any voltage
RB64A8	grating on ITO, 58 mw/cm^2	lower diffraction efficiency, does not switch with voltage at all
RB65A1	floodlit lamp, 110 mw/cm^2	lots of beautiful phase separation
RB66A1	floodlit lamp, 110 mw/cm^2	hardly any phase separation at all
RB65A2	floodlit lamp, 11 mw/cm^2	not much phase separation initially, but later postcuring developed phase separation
RB66A2	floodlit lamp, 11mw/cm^2	not much phase separation at all
RB65A3	floodlit laser, 5.04 mw/cm^2	more phase separation than lamp samples
RB66A3	floodlit laser, 5.04 mw/cm^2	not nearly as much phase separation as RB65A3
RB65A4	floodlit laser, 50.8 mw/cm^2	a little less phase separation than previous sample
RB66A4	floodlit laser, 50.8 mw/cm^2	much less phase separation than previous sample
RB65A5	grating, 50.1 mw/cm^2	none
RB66A5	grating, 50.1 mw/cm^2	none
RB65A6	grating, 5.0 mw/cm^2	more phase separation than RB65A5
RB66A6	grating, 5.0 mw/cm^2	none

DISCUSSION OF RB63A AND RB64A

In the RB63A floodlit samples, there was clearly no cloudiness because of the absence of liquid crystal. Gratings were written, but not with a high diffraction efficiency as in the RB64A samples. This was the first set of experiments showing that liquid crystal in a sample increases the diffraction efficiency. ITO samples were made, but none of them switched very well at all with voltage.

DISCUSSION OF RB65A AND RB66A

Generally, it seems that RB66A, the syrup with cross linker, does not show as much phase separation as RB65A. This is because crosslinker speeds up the polymerization process and does not allow as much time for liquid crystal droplets to separate from the polymer matrix. Also generally, using lower intensity light produced more phase separation because a higher intensity also speeds up the polymerization process. These trends were more evident in samples 3 and 4 due to kinetics. With the #2 samples, none of them showed much phase separation until the next day. The next day, the #2 samples showed more phase separation than with the #1 samples. This is consistent with the theory that more phase separation occurs with lower power and without cross linker. ITO samples were also made as shown by the following table.

SAMPLE	LASER POWER	COMMENTS
RB65A7	68 mw/cm^2 total	about 32 % DE, but does not switch
RB65A8	5 mw/cm^2 total	with the addition of a drop of surfactant (octanoic acid), sample switched wonderfully at only 15 volts, initial DE is 40%
RB65A9	30 mw/cm^2 total	with the addition of a drop of surfactant, sample switches at 70 volts, initial DE only 10%
RB65A10	30 mw/cm^2 total	none
RB65A11	15 mw/cm^2 total	with addition of a drop of surfactant, sample shows maximum switching at 72 volts
all RB66A	differing powers	none of them switched very well at all under 200 volts

ANALYSIS OF ITO SAMPLES CONTAINING RB65A AND RB66A

The RB65A samples switched very well with a fair diffraction efficiency while the RB66A samples were poor in all areas. This is due to the addition of the cross-linker in the RB66A syrup. Crosslinker "tightens" the polymer matrix and therefore reduces the amount of phase separated liquid crystal as well the size of the liquid crystal droplets. This results in higher switching voltages. When a drop of surfactant is added to the

sample before photopolymerizing, the viscousity is decreased as well as the size of the liquid crystal droplets. It is shown, however, that crosslinker shrinks the droplets more than the surfactant. If droplets are too big, switching does not occur at low voltages. Surfactant also lowers the amount of phase separation which reduces the amount of scattered light. This ususally increases the diffraction efficiency also. The next syrup, RB67A, contained a fixed amount of surfactant as well as 34% liquid crystal.

Here are the samples:

SAMPLE	TYPE	COMMENTS
RB67A1	floodlit lamp, 44 mw/cm^2	nice phase separation
RB67A2	floodlit lamp, 11.8 mw/cm^2	nice phase separation
RB67A3	floodlit lamp, 118 mw/cm^2	nice phase separation
RB67A4	laser floodlit, 50 mw/cm^2	more phase separation than lamp samples
RB67A5	laser floodlit, 5 mw/cm^2	initially, sample RB67A4 had more, nicer phase separation than this one, but after postcuring time, both samples appeared to be the same.
RB67A6	laser grating, 5 mw/cm^2 total	grating is good
RB67A7	laser grating, 50 mw/cm^2 total	grating is no different than previous one
RB67A8	laser grating on ITO, 50 mw/cm^2 total	sample shows maximum switching at 22-30 volts with initial diffraction efficiency at 10%
RB67A9	laser grating on ITO, 50 mw/cm^2 total	sample shows maximum switching at 30 volts with an initial diffraction efficiency of 35%
RB67A10	laser grating on ITO, 50 mw/cm^2	sample shows maximum switching at 30 volts with an initial diffraction efficiency at 12 volts
RB67A11	laser grating on ITO, 50 mw/cm^2	sample shows maximum switching at 22 volts with an initial diffraction efficiency of 18%
RB67A12	laser grating on ITO, 50 mw/cm^2	sample does not do much
RB67A13	laser grating on ITO, 5 mw/cm^2	sample shows maximum switching at 40 volts with an initial diffraction efficiency of 30%
RB67A14	laser grating on ITO, 5 mw/cm^2	initially sample shows maximum switching at around 30-40 volts, poor diffraction efficiency of only 15%

DISCUSSION OF RB67A SAMPLES

Generally, a lower intensity laser produces more, uniform phase separation. RB67A4 and RB67A5 were surprises since 4 was the higher power, but had nicer phase separation initially. After time, however, both samples, 4 and 5, appeared to have grown the same amount of phase separation and displayed the same amount of uniformity. Time is often a big factor with PDLC's as will be discussed further later on. The ITO samples generally switched well. Initially samples done under the high and low intensity showed switching voltages of 30 to 40 volts. Samples done under the higher power did show on the average a higher diffraction efficiency. Time was a disturbing factor in this experiment. After two days, samples were tested again. Switching voltages went up by factors of four to five. They increased from 20-30 volts to 190-250 volts. Most likely, this is a result of further polymerization over time. Fresh samples are not 100% polymerized, but after a few days, they are. The next syrup, RB68A, was a repeat of an earlier syrup tried before I arrived but without crosslinker. No test samples were done on this. ITO was used from the beginning.

SAMPLE	TYPE	COMMENTS
RB68A1	laser grating on ITO	10 minute exposure, bad sample, too much phase separation
RB68A2	laser grating on ITO	5 minute exposure, drop of surfactant added, still too much phase separation, weak grating
RB68A3	laser grating on glass	5 minute exposure, drop of surfactant added, still too much phaser separation for a good grating
RB68A4	laser grating on glass, 10 mw/cm^2 total	2 drops of surfactant added
RB68A5	laser grating on glass, 14 mw.cm^2 total	terrible sample, many airholes in sample
RB68A6	laser grating on ITO, 30 mw/cm^2 total	drop of surfactant added, high diffraction efficiency, switches well at 200 volts
RB68A7	laser grating on ITO, 30 mw/cm^2	three drops of surfactant added, initial DE of 60%, switches at 52 volts

DISCUSSION OF RB68A SAMPLES

At the beginning of this syrup's experiments, the intensity of the laser was not measured. The main difference between this syrup and the others was the use of the pentacrylate monomer instead of the triacrylate monomer. Pentacrylate is more viscous, and therefore required more surfactant too be effective. RB68A7 was the best sample, having the most surfactant in it. Data was taken on this sample immediately after it was made. Initial diffraction efficiency was 50%. It went down to 0% with the application of 95 volts. A few of the

samples were tested again in the later days. The switching voltages did increase, but not significantly as in the previous triacrylate experiment. In general, it seems that triacrylate samples' switching voltages increase by factors of four to five over time, while pentacrylate samples' switching voltages increase by only factors of one to two. This means that the pentacrylate monomer is polymerizing faster and more readily than the triacrylate monomer. The next syrup, RB69A, contained a high 40% liquid crystal. This did not prove to be an effective syrup. Samples were made on ITO, but when voltage was applied, the sample would short out. This much liquid crystal in the sample simply did not allow for a strong electric field to be applied. The next four syrups, RB70-73A were all control samples. DSC's were run on these and compared to the other samples. This will be discussed later. After compiling all the results, one more syrup was made. This turned out to be the "super syrup" that I had been waiting for. It was composed of an unusual combination of both monomers, triacrylate and pentacrylate. The final "super" syrup was RB74A.

SAMPLE	TYPE	COMMENTS
RB74A1	laser grating on glass, 30 mw/cm^2	initial diffraction efficiency of about 55%
RB74A2	laser grating on ITO, 30 mw/cm^2	initial diffraction efficiency of 25%, switches at 125 volts
*RB74A3	laser grating on ITO, 30 mw/cm^2	initial diffraction efficiency of 62.5%, at 63 volts DE is down to 4%
RB74A4	laser grating on ITO, $30mw/cm^2$, with drop of surfactant	initial DE of 50%, DE goes down to 0.5% with the application of only 40 volts
RB74A5	laser grating on ITO, ummeasurable high power, drop of surf.	maximum DE is 38%, minimum DE is 0% with application of 14 volts
RB74A7	laser grating on ITO, unmeasurable high intensity	one drop of surfactant added to entire syrup and mixed before making syrup, maximum DE is 10%, goes down to .1% with the application of 55 volts
RB74A8	laser grating on ITO, unmeasurable high intensity	one more drop of surfactant was added to entire syrup and mixed before making syrup, maximum DE is 50%, minimum DE is 2% with the application of 75 volts

DISCUSSION OF RB74A, THE "SUPER" SYRUP

Clearly, this is the best syrup. Diffraction efficiencies upwards of 60% were reached while switching voltages as low as 15 volts were reached. Surfactant was necessary to reduce the droplet size and the amount of phase separation, but the monomer was still stable enough to make a high diffraction efficiency grating.

THE DSC

A Differential Scanning Calorimeter was used to measure heat flow through the PDLC films. As stated before, the transition from nematic to isotropic of the liquid crystal E-7 occurs at 58 degrees Celcius. The DSC was primarily used to see if the transition temperature would be changed when the liquid crystal is placed in a polymer matrix. It revealed more than was expected. The measurement of heat flow shows peaks to depict phase transitions. A down peak indicates an endothermic phase transition (ex: solid to liquid or liquid to gas), while an up peak indicates an exothermic phase transition (ex: liquid to solid). Abnormally huge peaks appeared with the first several samples at around 100 degrees Celcius regardless of their composition. It was determined that these are actually polymerization peaks. This indicated that samples still have not been 100% fully polymerized, even after photopolymerization with the lamp or laser and after postcuring with weeks of time. When the areas around the 50 to 60 degree range were zoomed in on, the E-7 transition peaks were revealed. There were, however, continuous polymerization disturbances in the graph--it was such an annoyance that proper conclusions could not be drawn. To take care of this problem, the remaining samples were placed in an oven at 110 degrees Celcius for several days. After this was done, clearer peaks were shown regarding the E-7 transition. A general trend which was observed is that whether the sample was a floodlit or a grating, if it was exposed at a low intensity, the E-7 transition point was lower than 58 degrees C, and if it was exposed at a higher intensity, then the E-7 transition point was higher than 58 degrees C.

Conclusion

After experimenting with many types of PDLC films, the ones with the most pentacrylate with little triacrylate produced the films with the highest diffraction efficiency and lowest switching voltage. Octanoic acid definitely needs to be present to reduce E-7 droplet sizes and also reduce switching voltages. Over a period of time, samples made with triacrylate monomer had their switching voltages increase by a factor of four to five, while samples made with pentacrylate monomer had their switching voltages go up by a factor of approximately two. The ideal mass percentage of liquid crystal E-7 turned out to be 30% to 32%. Too much liquid crystal resulted in too much phase separation. As a result too much laser light scattering would occur, giving a lower diffraction efficiency. In a polymer matrix, a liquid crystal is still able to maintain its properties of birifringence and its transition points. The properties' defining values are, however, altered by the type of polymer matrix in which they are in.

Acknowledgements

I would like to thank Dr. Natarajan, Mr. V.P. Tondiglia, Dr. T.J. Bunning, and Colin McHugh for all their help and support during my 8 week tour.

AUTOMATED INTEGRATION OF LADAR IMAGERY AND TIFF STRUCTURE FOR FLEXIBLE SENSOR ANALYSIS

Christie W. Gooden
High School Apprentice
Seeker Technology Evaluation Branch

Wright Laboratory Armament Directorate
WL/MNGI
Eglin AFB, FL 32542-5434

Final Report for:
High School Apprenticeship Program
Wright Laboratory Armament Directorate

Sponsored By:
Air Force Office of Scientific Research
Bolling AFB, Washington D.C.

August 1994

Automated Integration of LADAR Imagery and TIFF Structure for Flexible Sensor Analysis

Christie W. Gooden
High School Apprentice
Seeker Technology Evaluation Branch
WL/MNGI

Abstract

Last year, an existing program was modified to decrease man-in-the-loop hours and increase the output of pertinent data. Future plans included automation of the complete obtaining and displaying process of LADAR data written in the C programming language as opposed to the Pascal language utilized beforehand. Due to extenuating circumstances, a better way of displaying data was used to complement last years project; Tag Image File Format, better known as TIFF.

AUTOMATED INTEGRATION OF LADAR IMAGERY AND TIFF STRUCTURE FOR FLEXIBLE SENSOR ANALYSIS

Christie W. Gooden

Introduction

The MNG branch of Wright Laboratories has continued its work on sensor technology. This work aspires to make the United States tactical weapons a one of a kind fighting machine that maximizes the enemy's casualties while minimizing the United States' losses. The race for weapon supremacy is still on and the Sensor Technology Branch is at the forefront of air-to-land sensor expertise. To keep this position, the researches at Eglin constantly upgrade their display, speed, and efficiency capabilities.

Background LADAR's multiple display capabilities are very useful in a reconnaissance setting. It displays the range, doppler, and reflectivity of the same target area independently of each other. Work has been done to fuse the data from the reflectivity data, called intensity, and the range data to bring about an enhanced image. While working on this puzzle, problems with the header, the leading 256 bytes of the image, arose. The header

contains a lot of information useful to a sensor, such as flight time, and target. However, this information is not standardized enough for a graphics processing unit to understand. Documentation of the image proved impossible due to the header. To solve this problem, TIFF was introduced.

Tag Image File Format, is a special format with a detailed header. The header contains a plethora of information including width, length, compression of an image, and total number of bytes. TIFF was introduced by the Aldus Corporation in 1986. Since then, it has had many revisions and enhancements. All of these changes have served to make TIFF a better format for storing and interchanging raster images. According to the manual, "TIFF describes image data that typically comes from scanners, frame grabbers and paint- and photo-retouching programs." TIFF is designed to be almost universal in the scanning world and is easily adaptable for the changing times ahead. Even though Aldus produced this format, it is not limited to other Aldus systems. TIFF can be used with almost any type of graphics processing unit. It also has a wide range of color displays. Bi-level (black and white), grayscale, and color imagery are easily placed into a TIFF format.

The structure of the header was found to be the key to TIFF imaging capabilities. In TIFF the header consisted of image file directories. These directories were arranged by tags, 2 byte short integers that tell the computer information about the image. The importance of tags was due to the way the images were accessed. The actual bytes that make up the images were stored in strips and each strip consisted of rows. The location of a strip varied with each particular image, which made it difficult for a computer to find. Therefore, the designers of TIFF made up tags that explained the necessary information for display. The tag StripOffsets told

the computer where the first strip was located, StripByteCounts told the number of bytes in a strip, and RowsPerStrip told the number of rows in a strip. Tags like these were required. Other tags, such as Model and Software, were extensions to the basic TIFF format, and consequential not required.

Procedure

The first step in understanding the TIFF format is to research the 121 page manual. The manual goes through more than everything needed for a basic TIFF file. In fact the first forty-five pages are devoted to baseline, or basic, format while the rest deals with multiple extensions. The research process took approximately a week and a half of perusal. After a complete study, already created TIFF files were placed in the *Norton Advanced Utilities* program to be poked and prodded. *Norton Advanced Utilities* was the perfect tool because it has the capability to display the individual bytes of an image. The first TIFF file opened was a black and white image named balloon.tif. The image was basically three balloons with smiley faces. Due to the nature of the image, an initial hypothesis was introduced. The file was expected to have an uncomplicated header with very few bytes and the image bytes itself was expected to be a few hundred bytes. On the contrary the header was approximately 722 bytes long and the image data contained 66,861 bytes. Challenged yet undaunted, the study began.

The TIFF manual provided a sample header for a bi-level image, the least complicated file. The plan was to use this sample to compare with balloon.tif. The contrasts were expected to be minimal due to the similarity in structure. Width and length were expected to be the only changes. Before

the two could be compared, another problem arose. The byte scheme looked nothing like the sample in the manual. Before pushing the panic button, however, further inspection began. What was discovered was very interesting. Somehow the *Norton Advanced Utilities* program inverts the bytes on the display screen. In other words, a four byte sequence that should read "00030001", read like this "03000100". The header was also displayed in hexadecimal format. After manually inverting the bytes and converting back and forth from base 16 to base 10, the header of the balloon.tif file was carefully decoded and studied. The header for the LADAR images needed to be very similar in structure to a regular TIFF image. The sensor images that were about to undergo conversion had a few differences from the bi-level structure that were studied. For instance, Photometric Interpretation is a field that describes the colors of an image. Since the LADAR images are in grayscale and the images studied were in black and white, Photometric Interpretation had to be changed. Of course, width and length contrasted, as well as RowsPerStrip and StripOffsets.

Pursuing the knowledge needed to produce a header was the first step in producing a Pascal program to do the same. Last year's Pascal knowledge was utilized to automate the process of conversion. In Turbo Pascal, two windows were opened. One window carried the program to be modified and the other window contained the actual changes. The intensity and range of the same target area were to be converted to the TIFF format. The original LADAR files contained both range and intensity imagery. The goal was to find the different offsets of the images and separate them into two files utilizing the TIFF format. The program that was modified could already access both range and intensity separately. This made it easier to find the

offsets and create two files for each target area. After a week of modification the goal was achieved.

Results The new program effectively placed a TIFF format onto a formerly unstructured file. The process creates an intensity TIFF and a range TIFF file for every target area accessed. Documentation of past work became possible due to this program. A surprise development also occurred. The TIFF pictures were clearer than the original. The reason for this phenomenon was the sophistication of the graphics processing units that were utilized. The processing units that had to be used before the change scaled the picture causing certain elements to be lost. For instance a tank in the original pictures would look like a box. The barrel of the tank was barely visible. In the TIFF files, the barrel was easily seen. Even though the process was done in grayscale, colors can be added quite easily. In short, the new TIFF format created wonderful improvements to an old picture.

Conclusions C programming would be very useful to this process. Since C is more widely used, this program could be added to another program more easily if it was in C. The program worked beautifully and has an unlimited use.

Acknowledgments

Acknowledgments

My mentor, Emily Martinez, was a wonderful influence on me and I appreciate everything she did for me. I learned more than I ever thought I could and it's all due to her. Emily is the best. I would also like to thank my parents, my friends and especially my fellow HSAPers. They have made the past two summers the best in the world. I wish them all the best. The whole MNG branch was wonderful to me and treated me like an adult which I appreciate more than words can say. Lastly, I would like to thank this program and its coordinators for everything. Without this program I would be working at a grocery store over the summer turning my brain into putty instead of sharpening my thinking skills. Thanks to all.

HEAT PIPE COMPATIBILITY WITH AIRCRAFT

Gary Lee Grogg

Carroll High School
4524 Linden Ave.
Dayton, OH 45432

Final Report For:
High School Apprenticeship Program
Wright Laboratory
Wright-Patterson Air Force Base

Sponsored by:
Air Force Office of Scientific Research
Bolling Air Force Base, DC

and

Wright Laboratory

August 1994

HEAT PIPE COMPATIBILITY WITH AIRCRAFT

Gary Lee Grogg
Carroll High School

Abstract

Heat pipes are being tested for coolant systems on aircraft. Experiments are being conducted to evaluate the heat transport capabilities and stability of a single pore capillary pumped heat pipe loop. Variables considered for the heat pipe loop included heat load, vibration frequency, and the capillary tube ID (inner diameter). Data was obtained using thermocouples spaced along the pipe, and a pressure transducer. Results showed that increased activity and instability followed an increase in heat content. Additional instability was a result of vibrational forces; however, meniscus stability appears to be enhanced when the effects were used in conjunction.

Additional testing is also being conducted on a Russian developed capillary pumped loop heat pipe. The flexible design allows the evaporator and condenser sections to be oriented at various angles and height differences. At steady-state, evaporator and condenser temperatures, as well as the temperature difference determines the efficiency and limitations of the pipe. From the acquired data, conclusions can be drawn about the compatibility on aircraft.

HEAT PIPE COMPATIBILITY WITH AIRCRAFT

Gary Lee Grogg

CHAPTER 1: INTRODUCTION

Heat transfer principles and heat pipes have been in use for quite some time, yet applications continue to expand and improved methods of cooling are needed now more than ever. The heat pipe may soon be seen on high speed turbine blades, leading edges of aircraft and inside the aircraft. However, not enough is known about heat pipes to predict how they will work in these new conditions. Previous studies on the subject are inadequate and contradictory. Thus experimentation detailing the effects on capillary forces, the evaporating meniscus, and a loop heat pipe under dynamic conditions similar to future uses will produce vital information.

Heat transfer? Heat pipes? Sounds hot, but what is it? Well... heat transfer is self explanatory, but a heat pipe might sound confusing. A heat pipe is a self contained apparatus capable of transporting large amounts of heat through the incorporation of phase change heat transfer. The working fluid (in liquid form) absorbs the applied heat and evaporates, gaining energy proportional to the heat of vaporization. The vapor flows through the pipe to the condenser section of the pipe where it is returned to liquid form as energy is removed. The fluid then returns to the evaporator section to repeat the cycle. Methods may vary between centripetal force, force of gravity,

electrostatic and magnetic forces, and capillarity. The last of these is the most common, used in passive heat pipes because no energy is needed to keep it running.

Figure 1.1: The schematic of a typical heat pipe

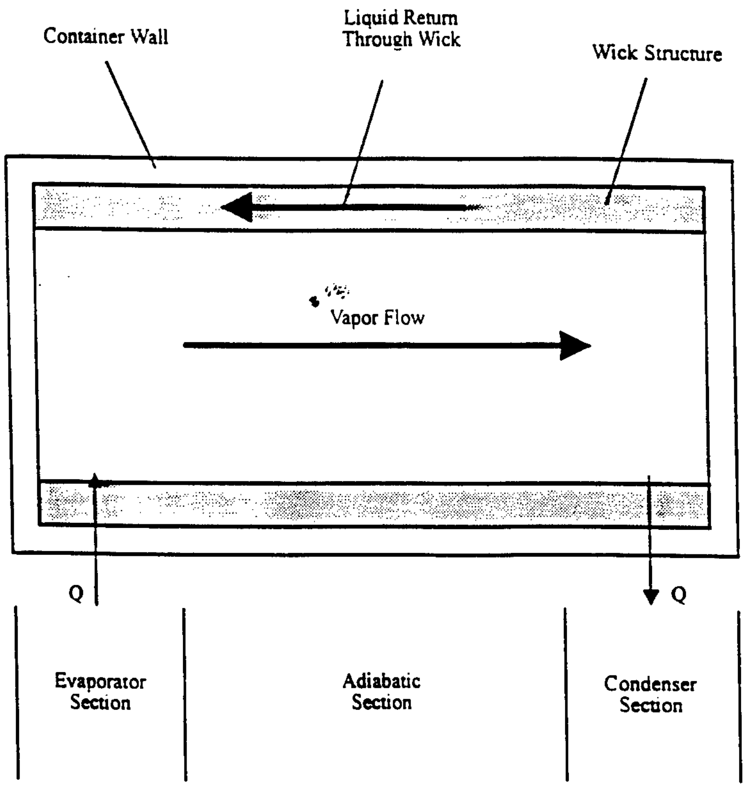

The porous "wick" makes use of capillary forces by producing the necessary liquid-vapor interfaces. Some wick structures include meshes, groves, or other porous structures. Everyone has seen a wick structure and capillary forces in action. A sponge absorbs water and water flows through a tree by these same capillary forces that cool the newest electronics. Heat pipes are also at work on gas turbine blade tips, rocket engines, microelectronic arrays, and hot fuel element surfaces in

hypothetical nuclear reactor accidents. (Bankoff,10)

A derivation of the traditional heat pipe was developed in the 1980's by Yury F. Maidanik and his associates at the Laboratory of Heat Transfer Devices, Institute of Thermal Physics, Ural Branch of the USSR Academy Of Sciences. The Russians patented the "Heat Transfer Apparatus", which is now known as the Loop Heat Pipe. On the following page is a diagram of the loop heat pipe.

In the capillary pumped loop heat pipe the vapor line and liquid line are separated. The vapor is collected by a system of grooves and headers that lead it through the vapor line to the condenser section. The vapor pressure forces the condensate up the central pipe where it refills the reservoirs in the evaporator. The annulus connects the reservoirs and feeds the liquid to the wick, thus completing a passive cycle.

The effects of heat transfer can be seen mainly through the study of thermocapillarity. Since surface tension has a tendency to decrease with rising temperature, liquid is convected away from the warmer troughs to the cooler crests, thus destabilizing the film. (Bankoff, 10) Another cause of destabilization noticed by Bankoff(1971) is the more rapid vaporization of the troughs as compared to the crests. In some instances, for very thin film layers, both effects may be present. Another cause of destabilization may be vibration at the harmonic frequency of the working fluid.

SELF PRIMING LOOP HEAT PIPE

From U.S. Patent 4,515,209.

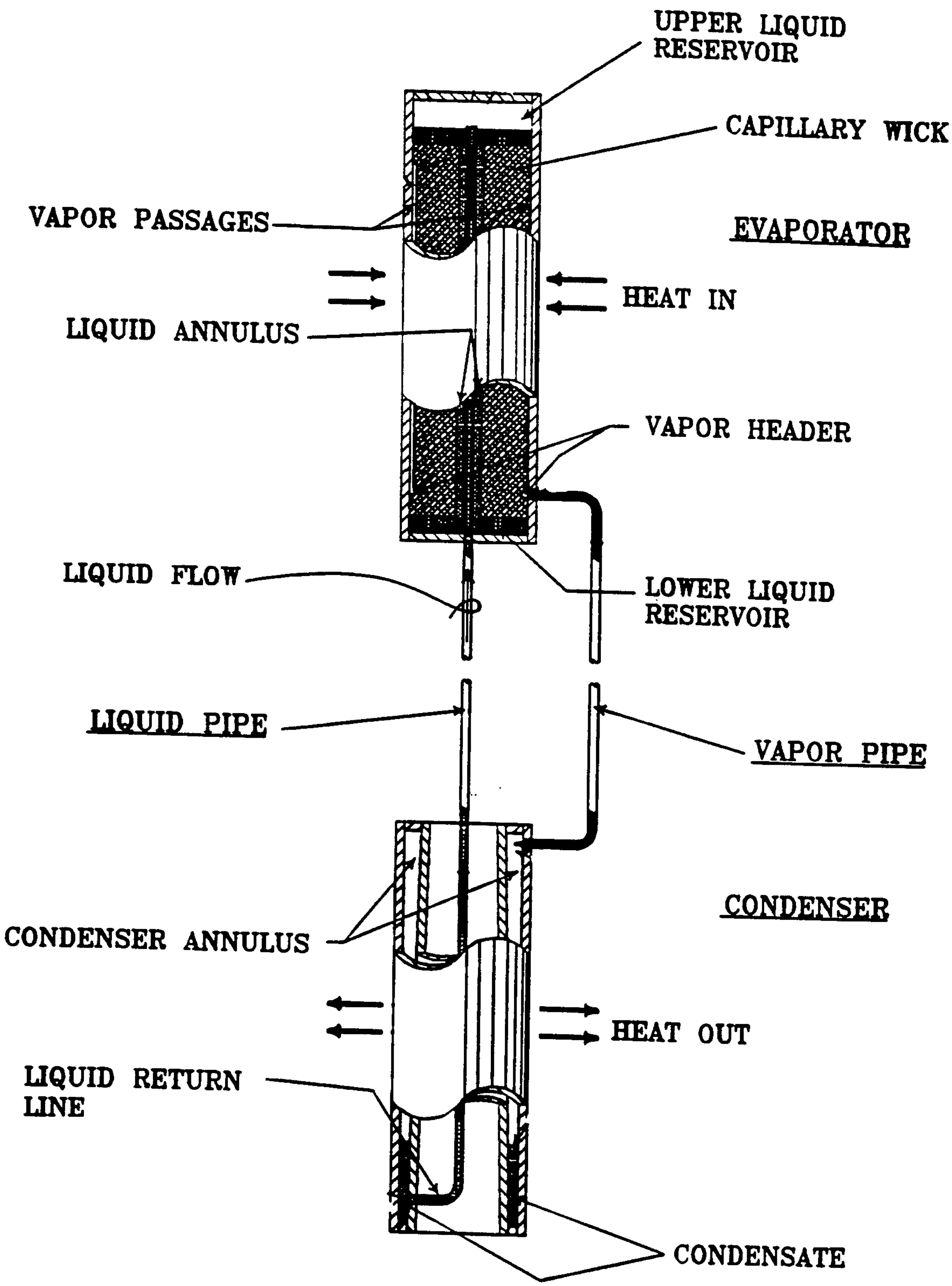

12\1969\1969 FG 53 .DWG

Previous research of thin film evaporating menisci has concentrated under static conditions. However, new applications will inherently subject heat pipes to dynamic conditions: vibrations and acceleration forces. Understanding in this area is inadequate. The majority of testing done was on entire heat pipes, leaving only guesses as to the activity and effects on the working fluid at the liquid-vapor interfaces. Therefore tests concentrating on the evaporating meniscus under dynamic conditions may lend substantial understanding to the future of the heat pipe. Previous testing in this area showed mixed results, ranging from the proposal that vibrations "may improve the performance of heat pipes," to ,"results indicated that the vibrations caused the maximum heat transfer capability to decrease. The fact that these studies were contradictory lays ground for further testing.

CHAPTER 2 : METHODOLOGY

Vibration Effects on Evaporating Meniscus

The experimentation was concerned with the heat transport and activity of an evaporating meniscus under dynamic conditions. Therefore the interface had to be visible during testing. A single pore glass pipe loop was constructed for the experiment. A precision bore capillary tube, fused to glass tubing produced an enclosed transparent system. A transparent gold film around one end of the tube provided the resistance heating element for the evaporator section. Electric leads were attached to silver bands painted at either end of the film, approximately two centimeters apart. Three openings to the tube allowed for access to the pressure transducer, and vacuum pump through the top of the loop, and a vacuum septum through which the working fluid, n-pentane, was injected. Digital readings obtained from the Sensotech STJE/1835-05 electronic pressure transducer, and five 32 gauge, type T thermocouples provided the objective data. Four of the thermocouples, attached along the outer wall of the capillary tube, showed the temperature gradients along the tube during experimentation. A hole drilled through the pipe and into the vapor space incorporated the fifth thermocouple for a vapor temperature reading. Thermal epoxy, used on all the thermocouples, provided a strong vacuum seal.

Figure 2.1: Schematic of capillary pumped heat pipe loop

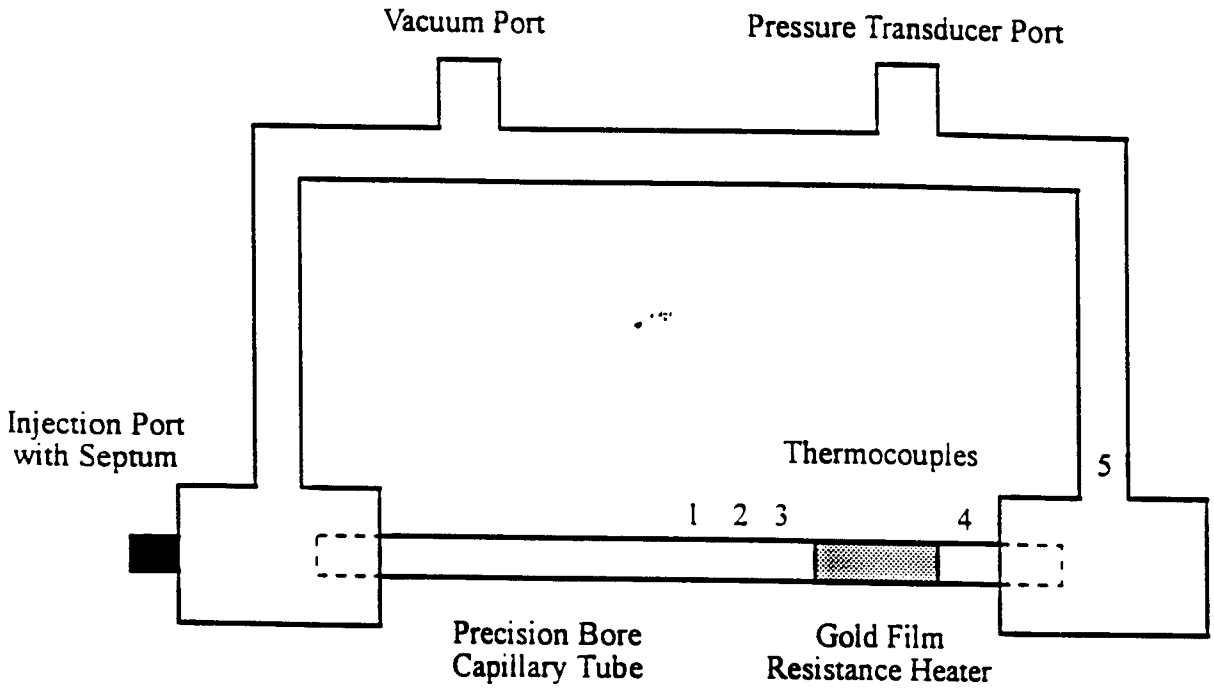

To control the experimental variables and set up a dynamic environment, more equipment was incorporated into the setup. A Vibration Test Systems electrodynamic vibration generator interfaced with a P.C. created a periodic sine mode of vibration. The heat pipe loop, attached to a specially constructed platform, moved in a plane perpendicular to the vibrational field. A typical laboratory mechanical vacuum pump evacuated the loop initially, and then the pipe was vacuum sealed through the use of a union-valve-union assembly. This provided an ideal saturated environment once the working fluid was injected. The pipe maintained the seal through the use of Teflon furrels within the union. Two DC power supplies ran the

pressure transducer and the other for the gold film heating. The gold film resistance heater was part of a circuit incorporating the shunt resistor and useful for determining the power input to the test cell from the gold film heater.

All of the information from the thermocouples and pressure transducer, as well as the voltage drop across the heater and shunt resistor, was monitored by a Hewlett Packard data acquisition unit. These data points were converted to useable information as a function of time.

Figure 2.2 : Schematic of experimental setup

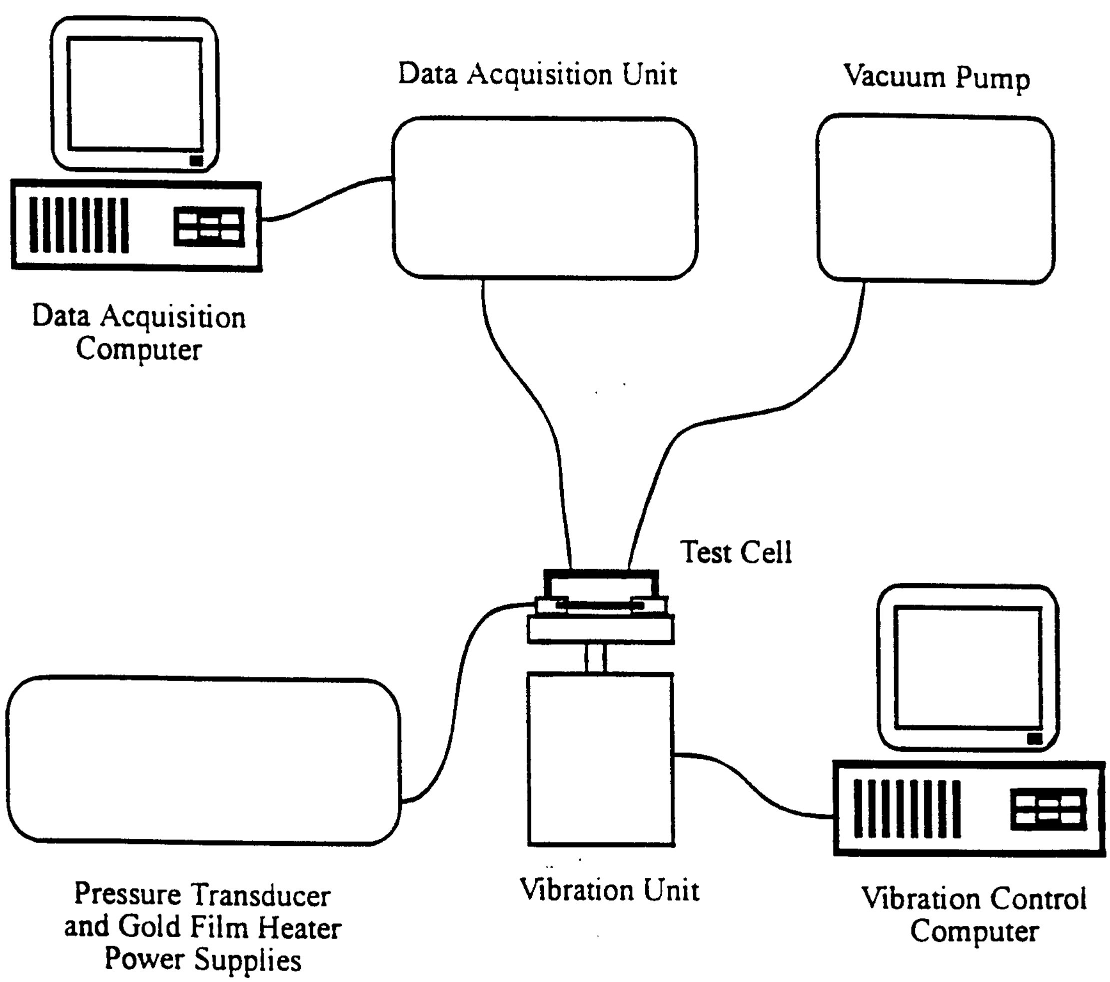

Russian Loop Heat Pipe

While testing was not in progress on the capillary meniscus, experiments were conducted on the Russian loop heat pipe. The flexible design spanned a total length of thirteen feet, however, for testing purposes the evaporator and condenser sections were attached 110 inches apart, at pivot points along a beam. This allowed them to be rotated to specific angles. Variable height difference was attained by rotating the beam about a central axis. Thermocouples spaced along the pipe and at the evaporator and condenser fed into a Fluke data logging system. The Fluke sent measurements from these thermocouples, as well as heat input and heat flow out, to disk and printer. A flowmeter recorded the flow of the deionized water into the heat pipe from a temperature regulated bath. Heat was applied by a Sorenson 600-1.5B power supply.

Figure 2.3: Schematic of Loop Heat Pipe Setup

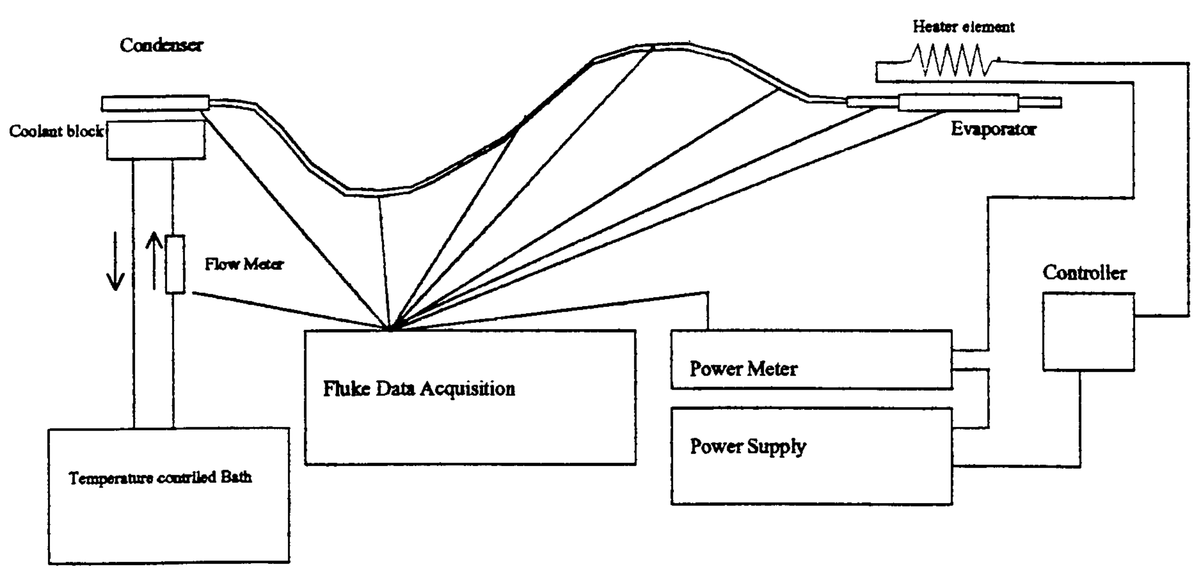

CHAPTER 3 : PROCEDURE

Vibration Effects on Evaporating Meniscus

The vibration unit was rotated to an angle of fifteen degrees to the horizontal. This was necessary to maintain a reservoir at the condenser end of the tube, after filled with the working fluid. The platform with the loop was then mounted and the other test equipment connected to it. The fluid was injected into the pipe with a gas tight syringe. Approximately 2.4 ml of n-pentane was injected and left to stabilize before testing began.

Now for the testing. The data acquisition unit ran for one minute before heat or vibrations were applied. Various levels of heat were applied in an instantaneous voltage step across the gold film. Vibrations varied in both frequency and acceleration. The data taken from the test was first run through a fortran program that read out the averages for the thermocouples. Next, those averages were input into another fortran program that output the derivative. From this data, graphs were made to show the slope spikes, which corellated to pressure and temperature jumps.

The number of pulses was recorded by the experimenter by observations through the glass capillary tube. The observations were recorded with the time they were taken so they could be matched against the graphs. The following pages show the different temperature and vibration gradients that the pipe was tested at and the data received with those factors.

Data Table 3.1: Test Results for .991 mm ID tube

Test	h(mm)	P(psi)	aprox V	Freq(Hz)	Acc(g)	start	end	#osc
June 1A	7.80	9.68	5	0	0	0.83	0.50	0
June 1B	7.30	9.69	10	0	0	0.63	0.38	0
June 1C	8.30	9.70	15	0	0	0.50	below	1
June 1D	8.10	9.77	20	0	0	0.86	unstable	2
June 1E	7.60	9.77	18	0	0	0.50	below	0
June 3A	11.50	9.59	15	250	2	0.88	0.25	slight
June 3B	8.60	9.69	15	250	20	1.10	0.38	0
June 3C	9.02	9.87	15	200	2	0.95	0.25	1 big??
June 3D	10.09	9.00	15	200	20.2	0.75	0.50	big sporadic
June 3E	7.91	9.53	15	0	0	0.50	0.06	0
June 3F	7.80	9.57	15	125	2	0.95	0.25	3 big
June 3G	8.00	9.55	15	125	20	0.50	0.00	osc in resevoir
June 7A	8.60	9.58	18	250	2	0.88	below	pulse/5sec
June 7B	7.30	9.75	18	200	2	0.63	0.00	pulse/2sec
June 7C	8.80	9.67	18	0	0	0.44	below	0
June 7D	8.10	9.73	18	0	0	0.88	below	0
June 7E	9.10	9.88	18	125	2	0.63	above	0
June 7F	8.00	9.90	18	250	20	0.88	below	5
June 7G	9.60	9.78	18	200	20	0.50	below	0
June 7H	8.30	9.78	18	125	20	0.50	below	sloshing
June 9A	9.40	9.45	20	0	0	0.63	below	much
June 9B	8.60	9.49	20	250	2	0.88	below	>30big&30small
June 9C	9.40	9.50	20	200	2	0.63	below	slight
June 9D	8.90	9.58	20	125	2	0.44	TC3	0
June 9E	8.80	9.63	20	250	20	0.63	below	some in resevoir
June 9F	8.80	9.80	20	0	0	0.90	0.13	>50 big & sm.
June 9G	9.20	9.74	20	200	20	0.44	below	0
June 9H	8.70	9.78	20	125	20	0.75	below	0
June 9I	8.70	9.83	15	125	20	0.89	below	0
June 15A	7.90	9.62	15	0	0	0.75	0.13	slight
June 15B	7.80	9.77	15	250	2	0.90	0.25	1 big
June 15C	8.10	9.80	15	200	2	0.63	below	0
June 21A	8.43	10.03	15	0	0	0.90	0.13	3
June 21B	9.05	10.03	15	0	0	0.75	bolow	0
June 21C	8.35	10.17	15	125	21.7	0.90	0.17	0

Data Table 3.2: Thermocouple and pressure transducer data

Test	T1 avg	T1 max	T2 avg	T2 max	T3 avg	T3 max	T4 avg	T4 max	T5 avg	T5 max	P1 avg	P1 max
June 1A	0.258	0.873	0.368	1.183	0.589	1.817	0.736	2.225	0.236	0.728	0.068	0.204
June 1B	0.600	1.909	0.976	2.992	1.776	5.181	2.901	9.173	0.327	0.923	0.108	0.301
June 1C	0.966	3.380	1.698	5.600	3.250	10.074	6.631	20.887	0.569	2.755	0.110	0.302
June 1D	0.897	3.657	1.784	6.639	4.097	12.872	11.411	34.728	0.923	4.152	0.196	0.653
June 1E	1.316	4.345	2.397	7.451	4.701	13.801	10.000	29.811	0.827	3.713	0.121	0.342
June 3A	0.792	2.628	1.479	4.638	2.946	8.803	5.106	15.072	0.777	2.435	0.192	0.665
June 3B	0.854	2.742	1.536	4.855	3.001	9.264	4.989	14.757	0.972	2.954	0.219	0.723
June 3C	0.828	2.548	1.496	4.516	3.073	8.782	4.926	14.328	0.945	2.795	0.165	0.541
June 3D	0.775	2.882	1.459	4.943	2.924	9.150	5.568	17.121	0.361	1.046	0.125	0.357
June 3E	0.775	2.882	1.459	4.943	2.924	9.150	5.568	17.121	0.361	1.046	0.125	0.357
June 3F	0.847	2.679	1.569	4.706	3.138	8.942	5.165	16.369	0.561	1.720	0.172	0.575
June 3G	0.774	2.756	1.376	4.835	2.667	9.254	6.338	20.921	0.893	3.948	-0.310	9.165
June 7A	1.001	3.379	1.894	6.022	3.905	11.485	7.877	23.322	0.386	1.273	0.154	0.488
June 7B	0.901	3.363	1.751	5.958	3.726	11.618	7.868	23.760	0.381	1.248	0.130	0.467
June 7C	1.103	3.824	2.065	6.592	4.142	12.617	8.088	24.757	0.332	1.829	0.141	0.374
June 7D	1.017	3.327	1.964	6.023	4.017	11.655	8.173	24.308	0.316	1.312	0.155	0.383
June 7E	1.090	3.582	2.050	6.351	4.123	12.186	8.080	24.496	0.687	1.813	0.230	0.597
June 7F	0.893	2.940	1.728	5.411	3.642	10.804	7.510	21.567	0.701	2.069	0.228	0.741
June 7G	1.142	2.451	2.123	7.294	4.223	13.582	8.124	26.228	0.441	1.389	0.181	0.536
June 7H	1.052	3.522	1.977	6.241	3.962	11.949	9.059	26.492	1.246	4.158	0.346	0.976
June 9A	0.950	3.331	1.888	6.261	4.131	12.649	9.199	27.370	0.609	1.814	0.185	0.646
June 9B	0.692	2.442	1.143	5.067	3.326	10.842	8.649	25.337	0.659	1.865	0.226	0.680
June 9C	1.176	4.150	2.298	7.443	4.717	14.239	9.349	28.510	0.396	2.233	0.111	0.290
June 9D	1.368	5.102	2.575	8.853	5.158	16.323	10.044	31.321	0.502	2.851	0.148	0.441
June 9E	1.296	4.795	2.457	0.378	4.962	15.665	9.742	30.382	0.405	1.647	0.198	0.513
June 9F	0.727	2.620	1.506	5.216	3.575	11.603	8.828	27.313	0.488	1.502	0.180	0.616
June 9G	1.250	4.755	2.348	8.049	4.701	14.876	9.117	28.480	0.490	2.648	0.168	0.465
June 9H	1.141	4.174	2.123	7.210	4.281	13.611	9.874	31.142	1.258	4.926	0.339	0.957
June 9I	0.780	2.923	1.410	4.846	2.775	8.816	6.251	24.837	1.100	4.792	0.326	3.020
June 15A	0.755	2.427	1.452	4.334	2.919	8.238	5.331	15.725	0.345	1.043	0.168	0.476
June 15B	0.716	2.647	1.357	4.594	2.752	8.731	5.252	16.628	0.466	1.459	0.192	0.578
June 15C	0.807	2.596	1.505	4.530	2.990	8.561	5.606	17.225	0.296	0.927	0.142	0.405
June 21A	0.756	2.371	1.410	4.323	2.830	8.416	5.449	16.264	0.540	1.650	0.217	0.653
June 21B	0.830	2.890	1.543	4.955	3.048	9.270	5.575	17.596	0.283	0.864	0.150	0.408
June 21C	0.884	3.090	1.608	5.091	3.171	9.226	6.140	19.871	1.040	4.010	0.333	1.009

Russian Loop Heat Pipe

At the beginning of an experiment, the heat pipe was arranged for the particular test. Height and angular measurements were taken along the pipe for reference. Next the bath temp was allowed to reach proper temperature, while the flow rate, and heat input were set. The scan on the data logger was started which routinely scaned the inputs every two minutes. Once the data logger detected steady state, defined by a temperature change of less than 0.15 degrees for the thermocouples along the condensor, it begen dumping the data to the disk and printer at the two minute intervals. The heat input, heat flow out, average evaporator temp, average condenser temp, and difference of condensor and evporator temp, were all recorded from the printout. The actual heat input, flow rate, and outside evaporator temperature, were also recorded. Once steady state was attained for ten minutes, the heat input was increased fifteen watts and allowed to reach steady state.

CHAPTER 4 : DISCUSSION OF RESULTS

Vibration Effects for evaporating Meniscus

Fluid was injected into the tube until it stabilized in the upper half of the gold film and allowed to sit until equilibrium was reached. Then the experimental conditions were enacted upon the pipe. A general tendency of the interface to drift down toward the lower band was visible in all of the tests. If the liquid remained stable it tended to continue to recess until it neared the lower silver band. Instability was defined as oscillations or pulses at the interface. During the tests in which the meniscus became unstable, the oscillations would range from 3 mm to 10 mm and the pulses would range from 10 mm to the entire length of the pipe. Pressure rose gradually throughout the tests because of evaporation of the working fluid due to the external heat input. In addition, pressure spikes accompanied the dramatic pulses most likely as a direct result of accelerated evaporative rate. This could be the result of increased interface surface area due to the vibrations. Temperature differences also related to the pulsing and instability. Large decreases in temperature at thermocouple three coincided with instability. This is most likely caused by the mixing of the cooler fluid in the reservoir and the warmer fluid near the liquid-vapor interface. Thus, instability accelerates heat transfer under these circumstances. Further instability can result from the correlation of the vibration frequency with the

working fluids natural frequency, or a subharmonic. Even though the greater vibrations produced more instability, some combinations of heat input and vibrations dulled the activity. The resultant effect was a more stable trial than either of the variables when isolated.

Russian Loop Heat Pipe

Testing is still in progress so no conclusions can be established.

CHAPTER 5 : CONCLUSION

Vibration Effects on Evaporating Meniscus

The results of this project relate directly to working heat pipes because the heat input levels reflect the general heat loads on current heat pipes.(Valociek, 47) However the data recovered from this experiment was inconsistent. The vibrational instabilities were sometimes related to the harmonics of the fluid, yet for many of the experiments, no relation was discovered. The pulsations increased relative to heat input in the tests yet at the highest heat content, stability increased when vibrations were imposed. Thus, to some extent, the coupling of heat and vibration seem to have canceling affects.

The test provided valuable information concerning the effects of destabilization on efficiency of heat pipes. The decrease in temperature at the interface following instability, points toward improved heat transport, and the increasing vapor pressure reflects an increased evaporation at the interface. The combined effects of destabilization support the theory of increased heat transport efficiency as a result of destabilization.

WORKS CITED

Bankoff, S.G. "Significant Questions in Thin Liquid Film Heat Transfer". Journal of Heat Transfer. Vol. 116. February 1994, pp 10-16.

Valociek, David A. "The effect of low frequency vibrations on an evaporating meniscus for a near perfect wetting fluid". August 1994, 61 pp.

Gernet, Nelson J. and Richard L. Weidner III. "SBIR Phase 1 Development for: Improved Flexible Heat Pipe Cold Plate". February 21, 1994. 26 pp.

The Analog Systems In Test Cell 22

Matthew T. Gudorf

Carroll High School
4524 Linden Ave.
Dayton, OH 45440

Final Report for:
High School Apprentice Program
Wright Laboratories

Sponsored by:
Air Force Office of Scientific Research
Bolling AFB, Washington DC

August 1994

The Analog Systems In
Test Cell 22

Matthew T. Gudorf
Wright Laboratories Test Cell 22

Abstract

The data acquisition systems of Test Cell 22 are comprised of two Sun Workstations. One works as analog in and the other is analog out. The Suns drive two Creates again one as analog in the other as analog out. Each Create contains cards. These cards use pressure and voltage to control the experiments and gather the data from the experiments run in Cell 22. One card will control one input or output such as a valve or thermocouple. At the present time the system is set up to accommodate a compact heat exchanger with a single catalyzed or uncatalyzed tube. All of the data to be gathered will enter through the input Create. All of the controls of the experiment are handled through the output Create. The data from the Test Cell, Creates, and Suns is all transferred on fiber optic cable. The speed at which all of the information from each input source is gathered is very critical in reducing the time that a correction can be made to keep the controls in there proper ranges. Due to this the speed is pushed to its maximum collection rate at about one cycle per second. This generates very large amounts of numbers in a very short amount of time with the problem being that if the input computer generating possibly faulty numbers the output computer will attempt to correct the numbers to there given ranges, and from that point generation of faulty data begins to occur. The proposed plan is to write a program to read predetermined output with the input computer and generate the same numbers every time the program is run. (see fig 1)

Fig 1

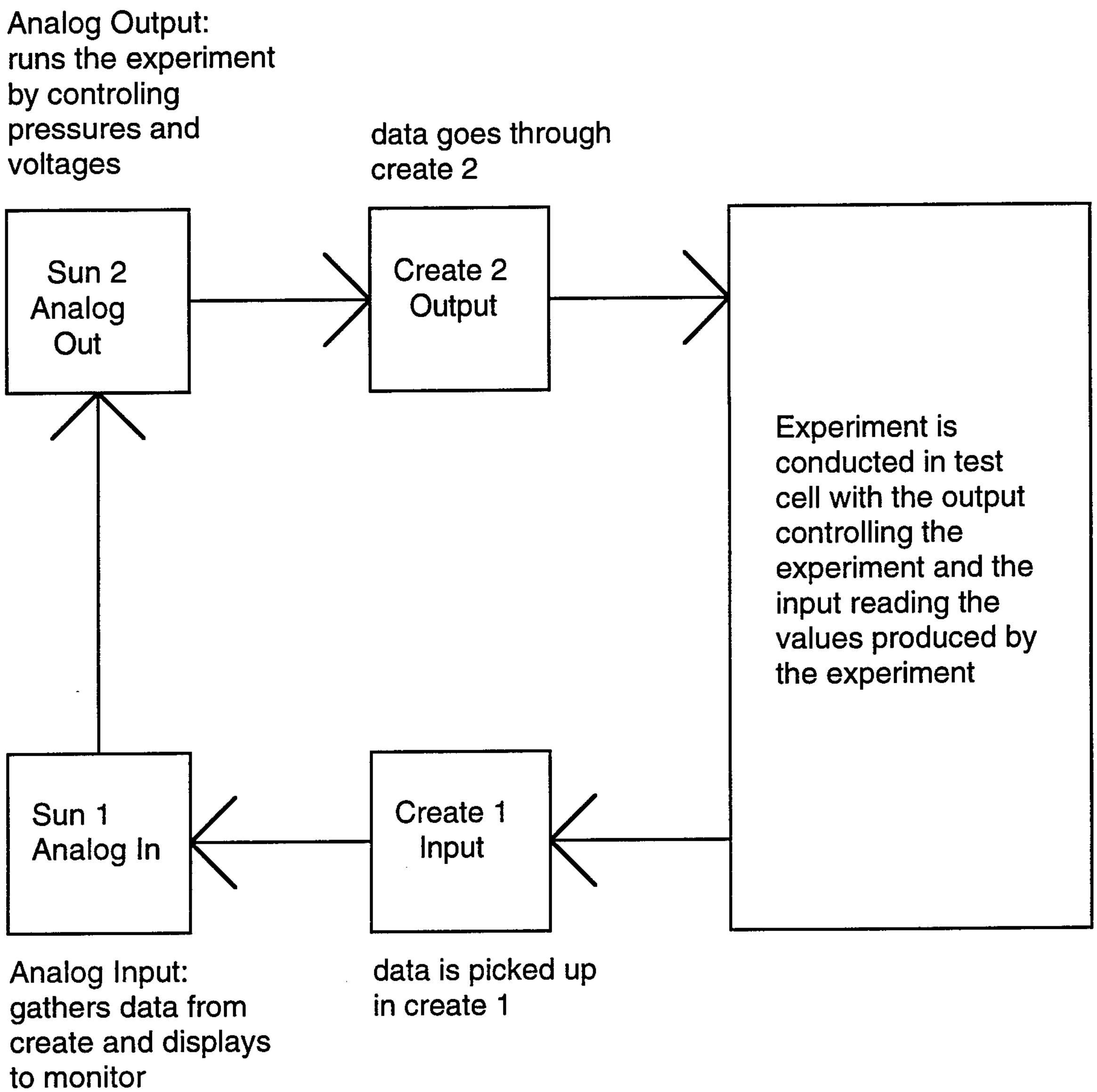
Analog Output:
runs the experiment
by controling
pressures and
voltages
data goes through
create 2
Sun 2
Analog
Out
Create 2
Output
Experiment is
conducted in test
cell with the output
controlling the
experiment and the
input reading the
values produced by
the experiment
Sun 1
Analog In
Create 1
Input
Analog Input:
gathers data from
create and displays
to monitor
data is picked up
in create 1

The Analog Systems In Test Cell 22

Matthew T. Gudorf

Introduction

The changes over the past thirty years in data collection have been extraordinary. Researchers not only developed new and diverse experimental designs, but also developed new and extremely complex ways of gathering the data from the experiments. The best means of data collection to date is through the development and use of computers.The computer has allowed researchers to collect data at ever increasing rates. Which makes the experiment run more beneficial because of the amount of data that can be recorded, processed, and analyzed. Today data is analyzed even while the experiment is still underway. These systems are being used in the labs now, with technology trying to push the data collection rate faster and faster. The problems begin to arise when computers generate numbers at extreme rates that can no longer be easily checked by humans to make sure faulty data is not being produced.

Discussion of the Problem

In Test Cell 22 data acquisition is not only extremely fast, but thousands of different numbers are produced by an input computer. These numbers are displayed on a monitor and processed by another computer at the same time. The second computer reads the data and makes adequate changes to the experiment being run to keep the constant numbers in there given ranges. The problem is that there is no way to check to see if the data from the input computer is accurate. The proposed solution was to write a program to read predetermined data from the output computer to the input computer and see if each time this was done the numbers generated would remain constant.

Method

The method to be used was to use old data that would be hand checked for accuracy so the output would be known prior to running the program. The output computer would be told what file to acquire, then it would process it and send the

information straight to the input computer which would read the data as if it were reading it from the active Test Cell just like normal it would gather the data and display the numbers to be checked. (see fig 2) The fallowing pages are an exert from the program. This is written in the computer language FORTRAN for a UNIX based machine.

Results

The program is only half completed. The amount of data to be read and channeled correctly requires a long program that is difficult to write. The program has been broken into six separate programs that in the end will work as a whole. Two of the smaller programs have been compiled and are ready for use. However without all of the programs working the system will not function.

The program so far is very straight forward and should be continuable by anyone who has written in the FORTRAN language before.

Conclusion

The rate at which a computer can process data is ever increasing and this will help in the long run, but as the rate increases developers need to have ways to check the computer instead of letting it just analyze numbers at speeds that numbers are uncontrollable. It is important to remember that data is only valuable as long as percent error can be kept to a minimum and the data can be trusted as true. As far as the collection of data in room 22 the six programs need to be completed but should become a valuable asset to the test facility in checking the computer for data that has become corrupted.

Fig 2

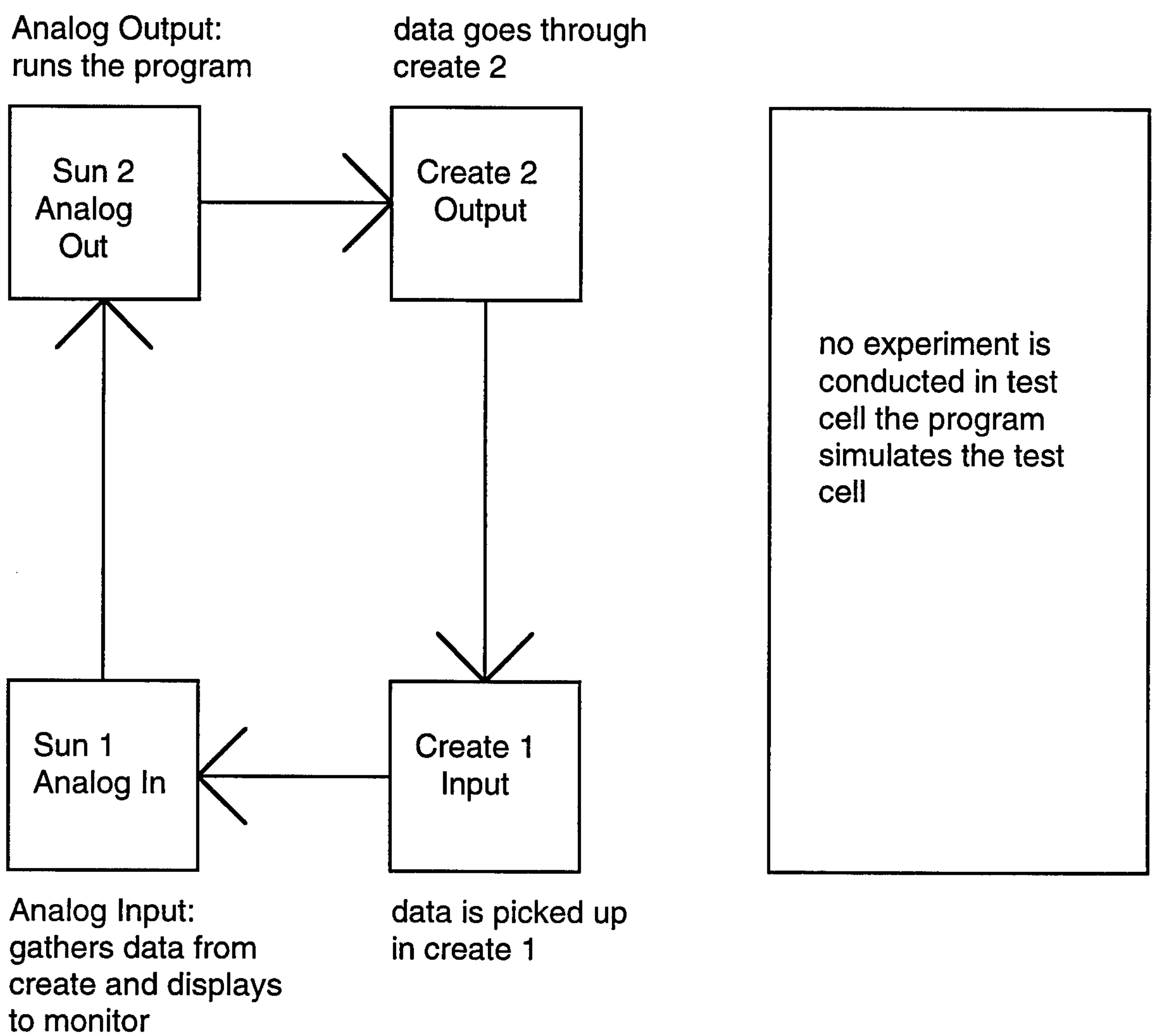

Analog Output:
runs the program
data goes through
create 2
Sun 2
Analog
Out
Create 2
Output
no experiment is
conducted in test
cell the program
simulates the test
cell
Sun 1
Analog In
Create 1
Input
Analog Input:
gathers data from
create and displays
to monitor
data is picked up
in create 1

```
C              SECTION 1
C      ADIABATIC FLOW WITH FRICTION
C
       A=PI*D1**2/4.
       RHO1=P1/R/T1*144.
       C1=SQRT(GC*GAM*R*T1)
       V1=WDOT/RHO1/A*144.
       M1=V1/C1
       WRITE(8,3030)M1
       WRITE(*,3030)M1
3030   FORMAT('  M1= ',F8.5)
       IF(M1.GE..95)THEN
          WRITE(8,3038)
          WRITE(*,3038)
3038      FORMAT(/,5X,'FLOW IS CHOKED USE A LARGER PIPE')
          GO TO 4080
       ENDIF
       RE=4.*WDOT/(3.1416*D0/12.*U)          !2 Feb 94
       WRITE(8,3040)RE
3040   FORMAT('  RE= ',E12.5)

       Calculation of friction factor in section 2 (d = D1)

       IF(RE.Ge.2300.)THEN

          Turbulent Flow

          FF1=.001
          FZ=1.
          J=0
          DO WHILE(FZ.GT..0001.AND.J.LT.1000)
            J=J+1
            FF=.25*(LOG10(K*12./D1/3.7)+2.51/RE/SQRT(FF1))**(-2)
            FZ=ABS(FF1-FF)
            FF1=FF
          END DO
       ELSE

          Laminar flow

           FF=64./RE
       ENDIF
       WRITE(8,3050)FF
       WRITE(*,3050)FF
3050   FORMAT('  FF= ',F7.5)


       PSTAR=M1*SQRT(2.*(1.+(GAM-1.)/2.*M1**2)/(GAM+1.))*P1
       WRITE(8,3060)PSTAR
3060   FORMAT('  P*= ',F8.4,' psia')
       LSTAR=D1/12./FF*((1.-M1**2)/GAM/M1**2+(GAM+1.)/2./GAM*
      *ALOG((GAM+1.)*M1**2/2./(1.+(GAM-1.)/2.*M1**2)))
       WRITE(8,3070)LSTAR
       WRITE(*,3070)LSTAR
3070   FORMAT('  L*= ',E10.4,' ft')
       TSTAR=T1*2.*(1.+(GAM-1.)/2.*M1**2)/(GAM+1.)
       VSTAR=SQRT(GC*GAM*R*TSTAR)
       WRITE(8,4040)VSTAR,TSTAR
4040   FORMAT('  V*= ',F6.1,' ft/s',/,'  T*= ',F6.1,' R')
```

```
C
C     PROGRAM TO CALCULATE PRESSURE LOSSES GAS PIPING SYSTEMS
C
      CHARACTER*11 GS
      CHARACTER*20 file,outfile
      INTEGER GAS
      REAL K,LSTAR,M1,M2,L,I1,MIN,K0,KB,KV,KT,M2i,M2gl,temp(20),vis(20)
      WRITE(*,*)'ENTER OUTPUT FILE NAME'
      READ(*,*)outfile
      OPEN(UNIT=8,FILE=outfile,STATUS='UNKNOWN')
      WRITE(*,22)
   22 FORMAT(/,'    PROGRAM TO CALCULATE PRESSURE LOSSES IN GAS PIPING',
     */,'    SYSTEMS ASSUMING SAME DIAMETER PIPE AND K=.00015 FT')
    1 WRITE(*,2)
    2 FORMAT(/,5X,'ENTER GAS #',/,8X,'1. AIR',/,8X,'2. METHANE',/,8X,
     *'3. ETHLYENE',/,8X,'4. PROPANE',/,8X,'5. OXYGEN',/,8X,'6. NITROGEN
     *',/,8X,'7. HYDROGEN',/,8X, '8. MCH @ 1000 F 1000 PSI',/,8X,'9. OTH
     *ER')
      READ(*,*) GAS
      WRITE(*,3)
    3 FORMAT(/,'     INPUT THE MASS FLOW (lbm/s)')
      READ(*,*)WDOT
      WRITE(*,4)
    4 FORMAT(/,'     INPUT THE GAS TEMPERATURE (R)')
      READ(*,*)T1
      WRITE(*,5)
    5 FORMAT(/,'     INPUT THE GAS PRESSURE (psia)')
      READ(*,*)P0
      WRITE(*,6)
    6 FORMAT(/,'     INPUT THE PIPE DIAMETER (in)')
      READ(*,*)D0
      WRITE(*,7)
    7 FORMAT(/,'     INPUT THE PIPE LENGTH (ft)')
      READ(*,*)L
      K=.00015
      WRITE(*,8)
    8 FORMAT(/,'     INPUT NUMBER OF RESTRICTIONS')
      READ(*,*)LR
      IF(LR.NE.0)THEN
      WRITE(*,9)
    9 FORMAT(/,8X,'SECTION #1',//,8X,'1. NUM. OF ELBOWS',/,8X,
     *'2. NUM. VALVES',/,8X,'3. NUM. TEES')
      READ(*,*)EP,NV1,NT1
      IF(EP.GT.0)THEN
      WRITE(*,11)
   11 FORMAT(' 1. NUM. OF 90 DEG. ELBOWS',/,' 2. NUM. OF 45 DEG. ELBOWS'
     *,/,' 3. NOMINAL PIPE DIA. (in)')
      READ(*,*)EN,EF,DI
C
      KB=ELB(FT,DI,EN,EF)
      ELSE
      KB=0
      ENDIF
C
      IF(NV1.GT.0)THEN
      KV=VAL(FT,V1,V2,V3,V4,V5,V6,V7)
      ELSE
      KV=0
      ENDIF
```

```
                ELSEIF(GAS.EQ.8) THEN

    DATA FOR 100% CONVERSION MCH

    GS=' MCH'
    RHOIN=1.54018
    GAM=1.1157
    U=1.3339e-5
    R=P0*144/RHOIN/T1
                ELSEIF(GAS.EQ.9) THEN
    WRITE(*,*)' ENTER ABSOLUTE VISCOSITY (lbm/ft-s), gamma, and densit
   *y'
    READ(*,*)U,GAM,rhoin
    R=P0*144/RHOIN/T1
    END IF

    ENTRANCE SECTION

 10 D1=D0
    D2=D0
    PI=3.14159
    GC=32.17

    PIN=P0
    if(rhoin.eq.0)then
    RHOIN=P0*144./R/T1
    endif
    AIN=PI*D0**2/4.
    T0=T1
    C0=SQRT(GC*GAM*R*T1)
    V0=WDOT/RHOIN/AIN*144.
    MIN=V0/C0
    WRITE(8,3000)GS,MIN,RHOIN
3000 FORMAT('  GAS=',A10,//,'  MIN=',F8.5,/,'  RHOIN=',F6.3,'lbm/cuft')
    PV0=K0*RHOIN*V0**2/288/GC
    P1=P0
    P1=P1-PV0
    WRITE(8,3005)U
3005 FORMAT('  MU=',E12.5,' lbm/(ft-s)')
    WRITE(8,3010)GAM
3010 FORMAT('  GAMMA= ',F8.4)
    WRITE(8,3015)P1
3015 FORMAT('  P1= ',F7.2,' psia')

             SECTION 1
    ADIABATIC FLOW WITH FRICTION

    A=PI*D1**2/4.
    RHO1=P1/R/T1*144.
    C1=SQRT(GC*GAM*R*T1)
    V1=WDOT/RHO1/A*144.
    WRITE(8,3020)V1,RHO1
3020 FORMAT('  V1= ',F8.3,' ft/s',/,'  RHO1= ',F6.3,' lbm/cuft')
    M1=V1/C1
    WRITE(8,3030)M1
    WRITE(*,3030)M1
3030 FORMAT('  M1= ',F8.5)
    IF(M1.GE..95)THEN
    WRITE(8,3038)
```

```
      WRITE(*,3038)
 3038 FORMAT(/,5X,'FLOW IS CHOKED USE A LARGER PIPE')
      GO TO 4080
      ENDIF
      RE=V1*D1*RHO1/12./U
      WRITE(8,3040)RE
 3040 FORMAT('  RE= ',E12.5)
C
C     Calculation of friction factor in section 2 (d = D1)
C
      IF(RE.Ge.2300.)THEN
C
      FF1=.001
      FZ=1.
      J=0
      DO WHILE(FZ.GT..0001.AND.J.LT.1000)
        J=J+1
        FF=.25*(LOG10(K*12./D1/3.7)+2.51/RE/SQRT(FF1))**(-2)
        FZ=ABS(FF1-FF)
        IF(FZ.LT.0)THEN
          FF1=FF
        ELSE
          FF1=FF
        END IF
      END DO
      ELSE
C
C     Laminar flow
C
       FF=64./RE
      ENDIF
      WRITE(8,3050)FF
 3050 FORMAT('  FF= ',F7.5)
C
C
      PSTAR=M1*SQRT(2.*(1.+(GAM-1.)/2.*M1**2)/(GAM+1.))*P1
      WRITE(8,3060)PSTAR
 3060 FORMAT('  P*= ',F8.4,' psia')
      LSTAR=D1/12./FF*((1.-M1**2)/GAM/M1**2+(GAM+1.)/2./GAM*
     *ALOG((GAM+1.)*M1**2/2./(1.+(GAM-1.)/2.*M1**2)))
      WRITE(8,3070)LSTAR
 3070 FORMAT('  L*= ',E10.5,' ft')
      TSTAR=T1*2.*(1.+(GAM-1.)/2.*M1**2)/(GAM+1.)
      VSTAR=SQRT(GC*GAM*R*TSTAR)
      if(lstar.le.l)then                                  !9 April 93
        M2=1.
        WRITE(8,3085)
        WRITE(*,3085)
 3085   FORMAT(/,5X,'FLOW IS CHOKED USE A LARGER PIPE',//)
        GOTO 4080
        ELSE
        PV1=K0*RHO1*V1**2/288./GC
C
C       Darcy Equation
c
        PFF=FF*L*12./D1*RHO1*V1**2/288./GC
c
        pls=PV1+PFF
        P2B=P1-pls
        WRITE(8,3090)P2B
```

CAD: A TESTING OF THE EFFECTIVENESS OF PROCESS DESIGN

Brian J. Guilfoos

Kettering Fairmont High School
2201 Shroyer Road
Kettering, OH 45429

Final Report for:
High School Apprentice Program
Wright Laboratory

Sponsored by:
Air Force Office of Scientific Research
Bolling Air Force Base, DC

and

Wright Laboratory

September 1994

CAD: A TESTING OF THE EFFECTIVENESS OF PROCESS DESIGN

Brian J. Guilfoos
Kettering Fairmont High School

Abstract

The purpose of this paper is to briefly review the activities of my summer, most specifically in the areas of process design and it's applications. My primary projects over the summer were the entry of data into a Macintosh for a program the lab was developing, and the machining of some parts by using a process design enhanced CAD program.

CAD: A TESTING OF THE EFFECTIVENESS OF PROCESS DESIGN

Brian J. Guilfoos

Introduction

During my HSAP apprenticeship at Wright Patterson Air Force Base I participated in several projects at my assigned lab: Wright Lab/Materials Lab. I exposed myself to some great minds and was able to use the experience to further my education and broaden my horizons. A brief summary of the summer experience follows.

Computer Aided Design

The main project I worked on during the summer was the testing and implementation of a CAD program (AML) for a UNIX environment that assisted in design of a part. For example, when you designed a part, the software would allow you to easily change extruded parts (orientation of cuts, etc.). The software also would assist in the cost estimation of a part, and suggest the most cost effective method of machining the part.

After wallowing through the incomplete user interface, I mastered enough of the features to be able to produce a design. A colleague provided me with a blueprint of the part that needed machining. The first result was not exactly of high quality, but with some new tricks the second time through produced a very accurate computer model of the part. After successfully creating the first part, I then created the second component part. We then used the program to evaluate the parts and suggest the most efficient order of cuts. This allows us to produce the part with the fewest cuts and the lowest possible cost for the current material.

The ability to have the computer calculate the most efficient method of machining the part *significantly* reduces the material waste and time necessary to move a part from the drafting table to the machining process. The concepts of process design can be applied to any procedure that must be accomplished.

See the attached sheet *RDS (Rapid Design System)* for more detailed information.

Crystallographic Database

One current development involves the development of a Macintosh-based platform for the researching of crystalline structures. The program, called KnowBE (Knowledge-Based Elicitation), is a Hypercard stack that takes numerical data on elemental and crystallographic structures and uses it as a knowledge-base to allow further research into the field. The information in the database consists of data from *Pearson's Crystallographic Database*, which the computer uses to create a three-dimensional electronic model of the crystal structure. The computer then allows the user to manipulate the model in a simulated three-dimensional viewer. My primary role in the development of the program was the entry of the data from *Pearson's Crystallographic Database* into a text format database. A typical entry, in this case $AgCu_4Er$, would look like this:

$AgCu_4Er$

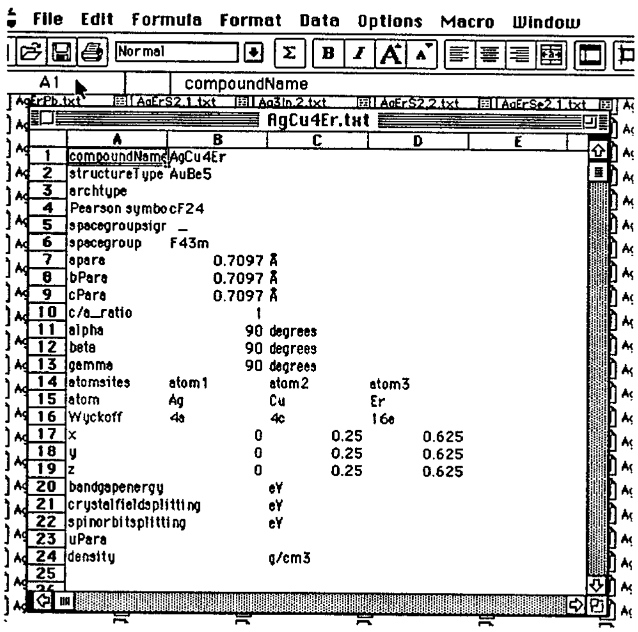

During my time on this project I compiled entries on approximately 1000 compounds. Please see the attached sheet *KnowBE* for more detailed information.

Internet

During my stay I also learned about the power and resources available on the Internet. I learned how to use the Archie and Veronica searches to find xcmds (x-commands) for use in KnowBE. However,

balancing the diversity of resources was the sheer volume of data online. The amount is truly overwhelming. It is *easily* possible to forget exactly what it is you are looking for and become sidetracked by something interesting you see during your search. The Internet is a valuable resource, and when used properly can provide a wealth of information.

Conclusions

Although I did not do true research, I did do some learning about my interests. Going into the summer I felt fairly certain of my major. Now, while still relatively certain, I have found other interests, and have learned to keep my options open and explore other fields. For example, I am now planning to at least *look* into Computer Science, possibly as a change of major if I enjoy it. I found my HSAP experience to be educational and enjoyable.

RDS

Rapid Design System

A Next Generation Engineering Design System

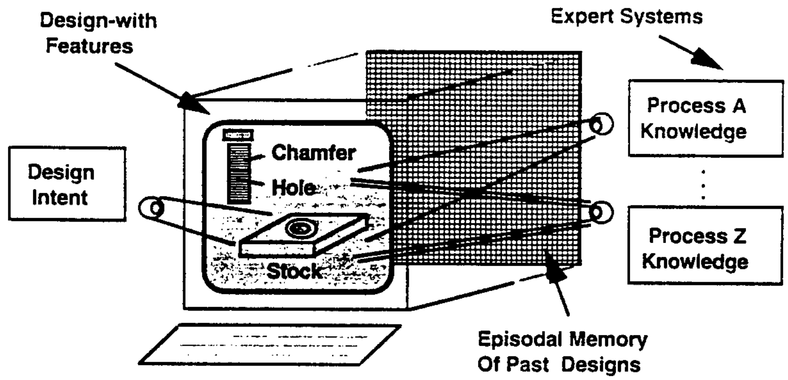

The Challenge

Why is the size of an automobile's cooling system a certain capacity, the pitch of the roof on a house a certain angle, or the hydraulics system on a commercial aircraft operated at a certain pressure? Each of these parameters is clearly specified by the design engineer on a drawing or, in the case of CAD, on a computer screen. What is not specified is "the why."

For centuries engineers have used drawings in various forms to render and document their designs. But nowhere, except in the mind of the engineer(s), are the design constraints, regarding "the why," captured. The automotive example is likely a weight-performance tradeoff, while the house roof is constrained by regulations or codes and the aircraft's hydraulic pressure is a combination of the above. Regardless of the type of constraint(s), the cost of not capturing "the why" is the time wasted in rediscovering design intent both for product upgrades and next generation designs.

The technological result has been the perpetual stagnation of design expertise from generation to generation. The time lost to retraining, together with product complexity and personnel turnover, has led to continued erosion of design quality and customer satisfaction.

The Rapid Design System

In a cooperative endeavor, a unique team of Government, Industry and University personnel developed a NEXT GENERATION design system referred to as the Rapid Design System or RDS.

At the heart of the RDS is a parametric design system which enables the coupling of design intent directly to the product geometry. To achieve this coupling the RDS emphasizes the use of 'features' which serve as templates to organize and capture design information. One set, referred to as form features, such as block, cylinder, hole, and slot, etc. is used by an engineer to capture product form and attach information such as product function, performance, or requirements. Another set of features, such as datum, flatness, or cylindricity, capture dimensions and tolerances related to the product form. Together, these two sets of features capture the geometric design of a product in a feature-based format.

The central purpose of the RDS project has been the integration of product and process design across materials and processes. To effect this integration, product features were associated with process design to capture information about product processing. The coupling of process and product information through features enables the RDS to automatically evaluate a design and generate a process plan. To date, two fabrication processes have been addressed: metal machining (to include inspection) and pattern making for metal castings. Soon to be added will be the curing of fiber reinforced polymeric composites.

A dimension of the RDS which clearly establishes it as a NEXT GENERATION engineering design system is an 'episodal associative memory' or EAM. Coupled with the use of features, the RDS utilizes a neural network technology to associatively cluster designs as episodes. In addition to storing and retrieving designs based on similarity, the memory is also being used in the pursuit of discovering new design axioms.

The EAM functions much like a human designer in storing and recalling designs. New designs are stored in reference to their associativity with past designs. Previous designs are recalled on the basis of their similarity to the designers perception of a new design.

The RDS is a feature-based, memory-driven engineering design system aptly suited to the demands of today's simultaneous or concurrent engineering environments. Not only does the RDS integrate product and process design but when coupled to rapid prototyping technology such as stereolithography or, more recently, selective laser sintering it is the ultimate weapon in 'time compression manufacturing.'

KEY PARTICIPANTS

LEAD ORGANIZATION

U.S. Air Force, Wright Laboratory*
Wright-Patterson AFB, Ohio

RESEARCH TEAM

Materials Directorate, Wright Laboratory
Wright-Patterson AFB, Ohio (Team Leader)

Case Western Reserve University
Cleveland, Ohio

Cornell University*
Ithaca, New York

Manufacturing Technology Directorate
Wright Laboratory
Wright-Patterson AFB, Ohio

University of Cincinnati***
Cincinnati, Ohio

University of Dayton***
Dayton, Ohio

Wright State University***
Fairborn, Ohio

PRODUCT & SUPPORT TEAM

AI WARE, Inc.**
Cleveland, Ohio

Institute for Advanced Manufacturing Sciences
Cincinnati, Ohio

ITASCA, Inc.
Minneapolis, Minnesota

Universal Technology Corporation
Dayton, Ohio

Wisdom Systems, Inc.
Pepper Pike, Ohio

XOX Corporation
Minneapolis, Minnestoa

CO-DEVELOPMENT & USER TEAM

4950th Test Wing
Wright-Patterson AFB, Ohio

Department of Energy (Allied-Signal Aerospace)
Kansas City, Missouri

San Antonio Air Logistics Center
Kelly AFB, Texas

ASC/SMEE Subsystem SPO
Wright-Patterson AFB, Ohio

* With Basic Research support provided by the Air Force Office of Scientific Research, Bolling AFB, Washington, D.C.

** Portions of the RDS are available commercially through TechnoSoft, Inc. in a product called CHISELS™ (to include a University Package). Contact Dr. Chemaly at 513-528-9149.

*** Participation through the Miami Valley Research Institute, Dayton, Ohio (with support provided through the Artificial Intelligence Technology Office, Avionics Directorate, Wright Laboratory, Wright-Patterson AFB, Ohio).

**For more information, contact Dr. Steve Le Clair, WL/MLIM
Wright-Patterson AFB, OH 45433-6533. Tel. (513) 255-8786**

KnowBE

Knowledge
Base
Elicitation

A Materials & Process Discovery System

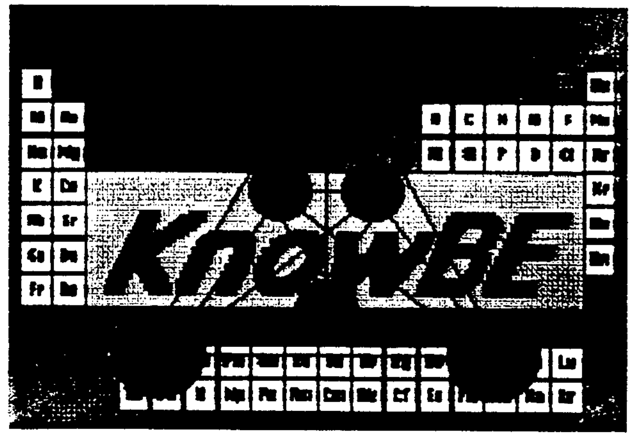

Introduction

Extracting new insights (associations and relations) from experimental data and/or databases is fundamental to the discovery process practiced by scientists and engineers for: verification of experimental results, mapping of causal (ingredients to property) relations, or synthesis of data to create new view(s) of a phenomenon. Currently this process is strongly defined by the expertise of the user. Knowledge-Bases (KBs) are helpful, because they reduce the amount of tedium required in hunting for data and rules about the phenomena, but they are also static, i.e., limited to the initial set of rules included in them. Evolutionary, pattern-directed methods for searching KB's are being developed that can take the process a step further by assessing the data for regularities and singularities present, KnowBE is a first step in this direction.

Data Bases/Knowledge Bases

Data bases are typically passive entities that wait for users to send queries regarding a subset of the stored data but do not provide a means of finding patterns present. Knowledge bases do enable pattern matching and classification, but in a severely limited sense defined by a rule set inserted along with the database. KB's are thus semi-active in nature. When searches are required that lie outside the domain of the rules, the search fails.

KnowBE Features

The coupling of pattern-directed methods which are evolutionary in their storage and recall enables an active system that provides a means of generating associations and functional mapping. KnowBE contains features of a simple database in which calculations can be accomplished on certain parameters, results of searches on data can be plotted to provide visual opportunities for the user to observe patterns and suggestions about the data patterns. In addition, concepts can be generated autonomously or via human intervention to build an evolving memory in the form of mappings between data. Thus, KnowBE's knowledge base can grow in two ways - each new experience can be used to 1) refine existing associations or clusters of similar experiences, and 2) evolve existing and enable new functional mappings or causal relations.

KnowBE's opening screen shows a periodic table from which the user chooses elements of interest and then moves to the next screen to where the type of search desired and any parameter bounds of interest are chosen. The results of the search are shown and displayed with the parameters and reference numbers from which the data was obtained. The user can move to other windows related to chemical-physical parameters associated with a specific material, to a reference list of parameters, to a graphics window to plot associations and relations, or to a print window for hard copy results.

A special window for creating a new type of display is also provided for those who want to create their own set of parameters. This window allows the parameters to be plotted in bar chart form or in x-y scatter plot form. Other windows allow the user to turn searches over to the system and then display the results for approval, archiving, printing, or plotting.

E-O Example

The initial domain applied to KnowBE is in electro-optical materials. A data base of semiconductor compounds has been created containing a number of parameter values obtained from the literature and experimental sources. Access to the data is direct, and the interface is specifically designed to be simple in use and to display information clearly to the user.

Illustrations

Figure 1. Screen shot taken from a Macintosh Quadra 680AV the 21 September 94 of a MicroSoft Excel file titled AgCu4Er.txt, utilized in the Hypercard stack *KnowBE*.

Reference Works

Chema... ...ing," WL-TR-94-4065, Wright Patterson AFB, Ohio, 1994.

Wood, Dan and Jack Park, ... AFB, Ohio, 1994.

Pao, Y.H., F.L. Merat, and G.M. R... Driven Feature-Based Design," WL-TR-93-402..., Wright Patterson AFB, Ohio, 1993.

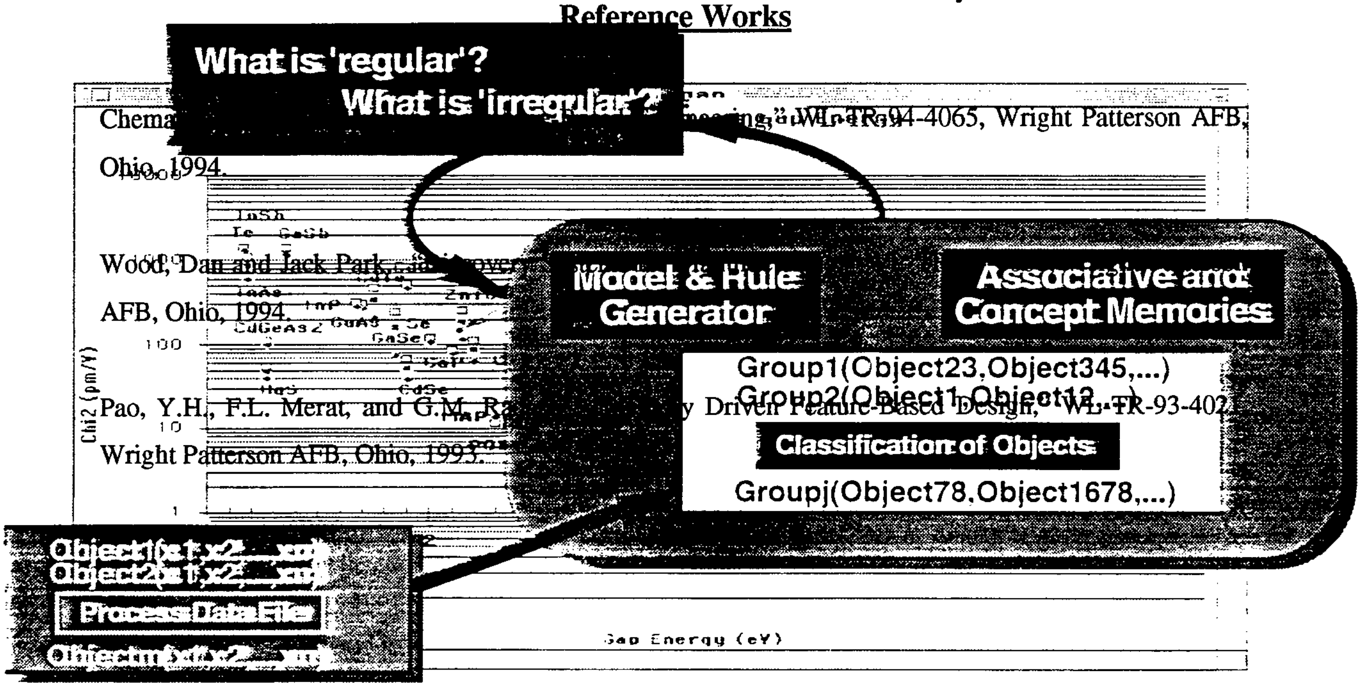

KEY PARTICIPANTS

GOVERNMENT

Materials Process Design Branch*

Mechanical and Surface Interactions Branch

Electronic and Optical Materials Branch

from the
U.S. Air Force Wright Laboratory
Wright-Patterson AFB, Ohio

* With Basic Research support provided by the Air Force Office of Scientific Research, Bolling AFB, Washington, D.C.

INDUSTRY

ThinkAlong Software, Inc.
Brownsville, California

Technology Assessment & Transfer, Inc.
Annapolis, Maryland

ACADEMIA

Case Western Reserve University
Cleveland, Ohio

For more information, contact Dr. Al Jackson, WL/MLIM, Bldg 653 2977 P St., Suite 13, Wright Patterson AFB, OH 45433-7746. Tel. (513) 255-8786

Illustrations

Figure 1: Screen shot taken from a Macintosh Quadra 680 A/V on 2 September 94 of a MicroSoft Excel file titled AgCu4Er.txt, utilized in the Hypercard stack *KnowBE.*

Reference Works

Chemaly, Adel. "Intellegent Knowledge-Based Engineering," WL-TR-94-4065, Wright Patterson AFB, Ohio, 1994.

Wood, Dan and Jack Park. "Discovery Systems for Manufacturing," WL-TR-94-4008, Wright Patterson AFB, Ohio, 1994.

Pao, Y.H., F.L. Merat, and G.M. Radack. "Memory Driven Feature-Based Design," WL-TR-93-4021, Wright Patterson AFB, Ohio, 1993.

PROJECTS IN PATTERN THEORY

Douglas J. Heil

Vandalia-Butler High School
600 S. Dixie Dr.
Vandalia, OH 45377

Final Report for:
High School Apprentice Program
Wright Laboratory

Sponsored by:
Air Force Office of Scientific Research
Bolling Air Force Base, DC

and

Wright Labs

August 1994

PROJECTS IN PATTERN THEORY

Douglas J. Heil
Vandalia-Butler High School

Abstract

Back propagation neural networks, software engineering, and the parity function were studied. A back propagation neural network was taught and tested. C++ code was transfer from a UNIX station to a PC. The parity function was studied.

PROJECTS IN PATTERN THEORY

Douglas J. Heil

The Neural-Net

Introduction

A neural network is a computation system made up of simple, connected processing elements, which processes information from external sources. A back propagation neural network uses the information from each processing element to influence the decisions at each processing element in the loop. The influenced information is sent through the network until the ending condition, or answer, is found.

A back propagation neural network was used to examine its performance against FLASH. A set of benchmark functions was run on both programs to test their performance.

Discussion of Problem

The objective was to get the back propagation neural network[1] to learn the set of benchmark functions. The original weights[2] were not learning many of the functions. The code for the back propagation neural network had the weights hardwired into it.

Methodology

A shell file was created so that the parameters could be changed. The shell command:

sh ("ff_train /usr/users/heil/nn/lrn_prm")

was inserted into the c_lib.c file where the fork for the back propagation neural network is located. The lrn_prm file contained:

---

[1] The program was written by Devert Wicker to support his dissertation work in the area of neural networks for recognition.

[2] Weights are the conditions within the each processing element that must be met before the network will continue to run.

execlp(" ff_train ","-a2","-1","8","15","1","-p0",".3","-p1",".1")

These parameters could be changed easily to help the performance of the back propagation neural network.

FLASH was run using the back propagation neural net option.

Results

The neural net would only learn 7 out of the 48 benchmark functions (see figures 1-2). The net did not change its performance even after the weights were changed. FLASH would not make the shell call to get the parameter file. The code in FLASH needs to be fixed to make the shell call. The weights need to be set to get optimal performance from the back propagation neural network.

Conclusion

The back propagation neural network will work. Time must be set aside to fix the code. Time also must be set aside to find the right values for the weights to obtain optimal performance.

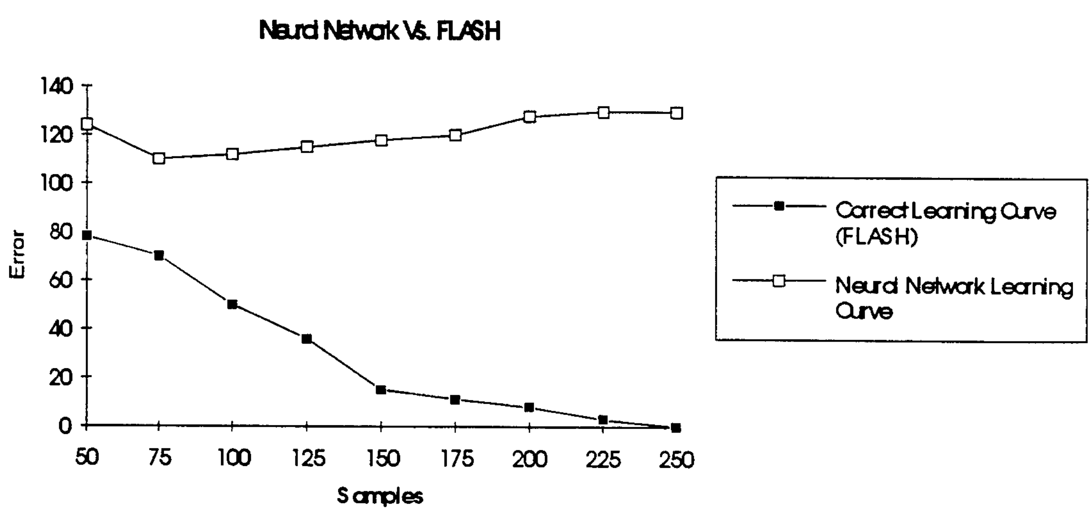

Figure 1

		dni0e300	c45-defaul	Espresso -	C4.5 m0 t	NN-DWW(041594)	
1	add4	0	39.72	2.08	3.6	13.7	
2	ch177f0	0	39.14	1.28	0		
3	kdd1	0	0.64	1.04	0.32		
4	kdd4	0	0	0	0	3.02	
5	kdd8	0	16.32	4.28	6.35		
6	subtract3	0	39.72	2.08	3.6		
7	ch176f0	0.16	20.54	4.16	5.54		
8	md_m1	2.31	1	1.59	2.38		
9	kdd2	2.4	3.76	3.72	2.76		
10	kdd3	2.72	2.56	2.56	1.28		
11	kdd6	3.72	3.84	3.76	2.48		
12	add2	5.24	64.12	29.25	27.4	34	
13	kdd9	6.55	30.56	14.56	13.79		
14	ch22f0	7	29.96	11.41	11.63		
15	md_m5	7.815	5.74	7.18	6.99		
16	kdd10	8.18	25.54	16.63	17.52		
17	greater_th	9.78	21.36	19.58	16	7.42	
18	pal	9.9	18.8	19.71	16.67		
19	ch30f0	10.29	18.18	14.53	11.54		
20	add0	10.38	22.56	20.48	16.26	16.55	
21	parity	10.45	128	83.83	86.58		
22	kdd7	10.53	26.94	6.61	20.69		
23	kdd5	11.11	15.02	8.14	10.52	14.96	
24	ch8f0	11.7	20.84	11.86	11.93		
25	ch70f3	12.04	15.5	9.21	12.18		
26	mux8	13.04	23.28	8.76	13.96		
27	md_m10	13.045	11.02	12.79	11.62		
28	modulus2	13.4	16.72	14.48	12.26		
29	ch74f1	15.85	20.9	16.8	15.79		
30	ch47f0	16.89	33.08	23.41	21.52		
31	majority_g	18.74	48.68	31.05	36.24	18.69	
32	ch15f0	19.595	47.96	27.75	27.98		
33	substr2	23	33.3	11.46	22.08		
34	substr1	24.105	41.44	13.84	30.3		
35	subtract1	24.22	64.14	45.96	41.42		
36	contains_	24.49	80.18	62.01	58.49		
37	remaindr2	25.22	31.95	27.06	25.49		
38	md_m25	25.61	29.34	28.44	25.59		
39	ch52f4	27.74	30.76	25.37	22.63		
40	ch83f2	27.885	33.42	26.1	26.03		
41	interval1	33.585	44.94	28.72	34.28		
42	interval2	35.94	62.82	34.58	44.35		
43	pal_dbl_o	38.94	73.74	47.4	50.77		
44	md_m50	42.685	54.4	44.26	42.72		
45	pal_output	58.79	84.74	58.64	58.98		
46	md1	59.125	87.84	62.53	61.5		
47	md3	59.865	85.3	59.81	60.48		
48	md2	60.055	89.04	60.07	62.25		
	Average:	17.58521	36.23646	22.30875	23.22375		

Figure 2

Flash Conversion

Introduction

FLASH[1] is a C++ program that decomposes binary functions. FLASH creates a table of possible answers for any given function. Next it samples from the table until it has enough samples to correctly guess the function. FLASH also calculates the DFC[2] of the function.

Discussion of Problem

Flash was first written to run on a PC but because of memory problems it was transferred to a UNIX station. Since on a UNIX station UNIX only commands like FORK() have been added to the code. The team needs a version of FLASH that will run on a PC. With the invention of DOS Extenders the memory problems of the PC have been solved.

Methodology

The FLASH code was put on a PC in the unxflash directory. Zortech C++ was chosen because it was the only version of C++ available that had a DOS Extender. Zortech C++ was installed on Mark Axtell's PC in the zordos directory. The workbench (C:\zwb) was used to edit and compile the code.

The code had a few errors. The UNIX only commands had to be removed for the files to compile. In the fl_main.c file there was an argument (long_bit) that was not given a value. The argument (long_bit) was defined as 0 in the tools.h file. The code compiled.

The linker would not link the compiled files because the linker said that it had found errors in the files. It kept giving this error:

BOTH 16 AND 32

---

[1] The Function Learning and Synthesis Hotbed (FLASH) was written by: T. Ross, L. Garcia, M. Axtell, D. Gadd, M. Noviskey, and J. Goldman. Wright Laboratory, WL/AART-2, WPAFB, OH 45433-6543 (513)255-3215

[2] Decomposed Function Cardinality (DFC) is a measure of a functions pattern-ness. From Pattern Theory: An Engineering Paradigm for Algorithm Design. T. Ross, M. Noviskey, T. Taylor, and D. Gadd. 1991.

The error was not documented and the makers of Zortech C++ did not know what the error meant. Unable to correct the problem with Zortech C++, GNU C++ was used instead.

GNU C++ was difficult to install onto John Jacob'sPC in the djgpp directory. The program required its own configuration and took over 100 MB to install.

Again the FLASH code was put the PC in the flash directory. The FLASH code would not compile under GNU C++. GNU's compiler did not like the syntax that the FLASH code was written in. The error received the most was:

ANSI C++ DOES NOT ALLOW THIS

Results

The FLASH code was compiled under Zortech C++ but was not linked into the executable. The FLASH code would not compile under GNU C++ because of differences between the syntax of the C++ languages.

Conclusion

The FLASH code will work on a PC. Time must be set aside to figure out the Zortech C++ linker. Time must also be set aside to learn the syntax of GNU C ++.

The Parity Function

Introduction

FLASH is believed to have a problem with combining columns with many don't cares (See figure 3).

0		x		0		x
0		0		x		x
1	=	x	=	x	=	1
1		x		x		1
1		1		1		x

figure 3

If you exchange all of the x's for either 1 or 0 you can obtain the original function but the other functions may not be the same as the original. The parity function was tested within flash to see if this was a problem. The parity function was used because it has the best properties for testing how well FLASH combines columns of many don't cares. The parity function has a column multiplicity of two[1] and any partition will yield an optimal decomposition[2].

Methodology

FLASH was run on the parity function using the dni0e300[3] decomp plan. The runs include both .bin[4] and .lst[5] formats for five through eleven vairables.

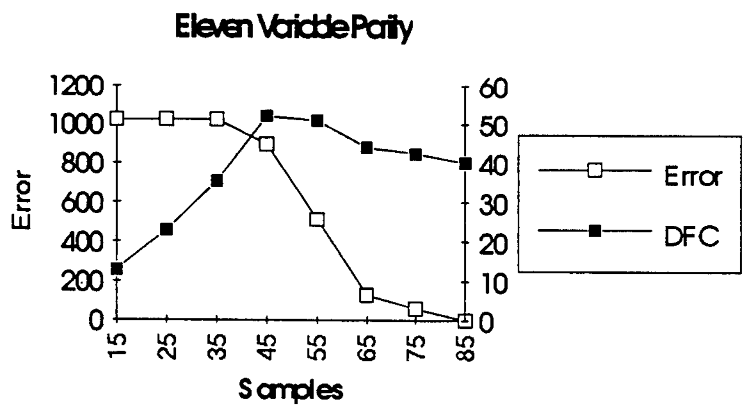

figure 4

---

[1] A column multiplicity means that any column with don't cares can only be made into two different columns.

[2] An optimal decomposition means that the answer will be the functions least compless expression.

[3] dni0e300 is the set of paremeters given to FLASH when run. dni0e300 is the benchmark values.

[4] .bin is a file format for FLASH. It is a string representing outputs in order of increasing inputs.

[5] .lst is a file format for FLASH. It is a list of imput-output pairswith the binary input.

Results

Eleven variable is where FLASH starts to make noticiable mistakes in combining columns (see figure 4). The bubble in the DFC line shows that FLASH has made a mistake. A correct DFC line would never go over the maximum DFC.

This experiment also can be used to compare the run time of FLASH. As the number of varibles increases the run time also increases exponetialy (see figure 5). The .bin and .lst methods were compared.

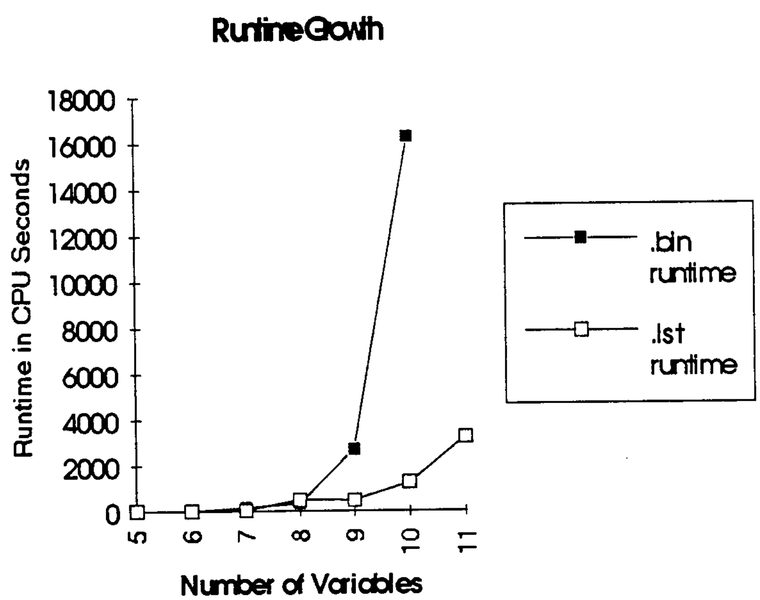

figure 5

The data shows that the .lst method does better then the .bin method for up to eleven varialbes (see figure 6-7). This is true for a low number of vairables because the table size of the .lst method are small. As the table size increases to over 500 the .bin method is faster.

.bin

Number of Vairiables	Runtime
5	2.1671
6	19.9969
7	153.0114
8	338.6403
9	2721.441
10	16289.496

figure 6

.lst

Number of Variables	Runtime
5	2.5912
6	14.885
7	37.5636
8	497.5417
9	473.6629
10	1269.1293
11	3244.2357

figure 7

Conclution

FLASH has a problem combining columns. A new method for combining columns must be found in order to improve preformance. The .lst method is faster then the .bin method up to eleven variables but a new method might show better preformance then both the .lst and the .bin methods.

HIGH SURFACE AREA CONDUCTIVE POLYMER FILMS USING

ABEX EP-110 DOPED POLYPYRROLE

Laura Hemmer
High School Apprentice
Fuzes Branch

Wright Laboratory Armament Directorate
WL/MNMF
Eglin AFB, FL 32542-5434

Final Report for:
High School Apprentice Program
Wright Laboratory Armament Directorate

Sponsored by:
Air Force Office of Scientific Research
Bolling Air Force Base, Washington, D.C.

August 1994

HIGH SURFACE AREA CONDUCTIVE POLYMER FILMS USING ABEX EP-110 DOPED POLYPYRROLE

Laura Hemmer
High School Apprentice
Fuzes Branch
Wright Laboratory Armament Directorate

Abstract

In recent years, researchers have found numerous applications for conductive polymers. For example, polymer films can serve as electrodes in capacitors [1]. The goal of this project was to increase the surface area of conductive polymer electrodes thereby increasing their capacitance. The method tested was to increase the surface area by electrochemically depositing a textured film of ABEX EP-110 doped polypyrrole. These textured polymer electrodes were then used to make a double layer capacitor [2]. The capacitance of the textured electrode capacitor was compared to a capacitor made from smooth polypyrrole electrodes to determine the effectiveness of this deposition method.

HIGH SURFACE AREA CONDUCTIVE POLYMER FILMS USING ABEX EP-110 DOPED POLYPYRROLE

Laura Hemmer

INTRODUCTION

Conductive polymers have become a growing interest for scientists in recent years. Many experiments have been undertaken to determine uses for these "organic metals." Past work has determined that conductive polymers have numerous applications. Conductive polymers are used in "smart windows," which are light sensitive devices. In addition, conductive polymers can be fabricated into rechargeable batteries or serve as electrodes in capacitors [1]. They are used as electrodes since they can sustain higher voltages than other materials commonly used in capacitors [3]. Their versatile nature has opened up many new possibilities.

DISCUSSION OF PROBLEM

One way to increase the capacitance of a double layer capacitor is to increase the surface area of the electrodes. This creates more interaction along the interface between the electrolyte and the electrodes. The objective of this project was to make high surface area conductive polymer electrodes to be used in a double layer capacitor. This was done by electrochemically depositing a textured film of polypyrrole doped with ABEX EP-110 [4].* It is possible to alter the physical and electrical properties of polypyrrole films by changing the conditions at which the films are deposited [5]. Therefore, it was necessary to test polypyrrole films made at optimum deposition conditions. The textured film has

*ABEX EP-110 courtesy of Rhone-Poulenc Surfactants. (Chemical Structure- Figure1)

increased surface area when compared to smooth polypyrrole films and thus should have increased capacitance. The PPY/ABEX EP-110 films were used as the electrodes in the double layer capacitors. It has been shown that polpyrrole that contains a polyether side chain in the 3-position has a significant advantage in charge storage ability (Chemical Structure- Figure 1 [6]). This feature, combined with the use of the new surfactant dopant ABEX EP-110, would account for any improvements in charge storage [7]. The dopant molecule does not bond to any particular position of the polypyrrole structure in a covalent fashion; however, its presence is felt electrostatically via ionic or dipole bonding since the molecular charge centers tend to be unbalanced.

METHODOLOGY

The first step in this project was to make the textured polypyrrole films. All variables that affect the quality of the polypyrrole films were tested with the exception of temperature of the system. The effects of temperature on the quality of the polypyrrole films were researched previously and the results have already been determined [8]. Those variables tested in this project include the molarities of the chemicals in the solution, the volume of the solution, agitation to the system, the type of electrodes used for depositions, the current density, the distance between the electrodes, and the time length of the deposition. Two 8x15 cm electrodes were placed in a container for the experiments. The distance between the electrodes varied from 14 or 15 cm to approximately 23 cm. Stainless steel electrodes were used for the majority of the experimentation. Zirconium and silicon electrodes were also tested. The films deposited on the silicon electrodes were preliminary tests for depositions in a plasma CVD deposition system [9]. A solution of polypyrrole doped with ABEX EP-110 was used to

electrochemically deposit a conductive polypyrrole film onto the anode (Figure 2). Molarities tested include .005M PPY mixed with .005M ABEX; .05M PPY mixed with .005M ABEX; .01M PPY mixed with .001M ABEX. Volumes of solution used were one liter and two liters. For the deposition, currents applied to the electrodes varied as such: 20, 35, 40, 45, 50, 55, 60, 65, and 70 mA. The time lengths of the depositions included 45 min., 55 min., 1 hour, 1 hour 5 min., 1 hour 15 min., and 1 hour 30 min. Agitation was also applied to the deposition system for some of the experiments. Settings tested were 50, 100, and 200 rpm.

Following the depositions, the films were tested to measure resistance. Film sheet resistance was determined using a four point probe and displayed by a precision LCR meter (Hewlett Packard 4284A). This figure was then used to calculate the resistivity of the textured polypyrrole films. The formula, resistivity equals film sheet resistance multiplied by film thickness, was for the calculations. At times this was precluded by extreme surface roughness. I then proceeded to use the best textured polypyrrole films as electrodes in double layer capacitors (Figure 3). The electrolyte for these capacitors was created using strips of Whatman filter paper soaked in a solution of nitromethane and potassium iodide at the solubility limit [10, 11]. Once the capacitors were constructed, they were charged for five minutes and the steady state voltage was measured by a multimeter to be 0.5 volt. A coulometer (Princeton Applied Research Model 379) was then used to measure the charge stored in the capacitors. Following voltage and charge measurements, the capacitance of the capacitors could be calculated using the equation $C=Q/V$ [12]. Since surface area is directly proportional to capacitance, comparison of the calculations would be indicative of the increase in surface area [13]. We were then be able to determine the effectiveness of our deposition techniques.

RESULTS

My first objective was to establish the optimum conditions for the deposition of ABEX EP-110 doped polypyrrole. After completing numerous experiments, I determined the following conditions to produce the best films: time length of deposition, 1 hour; molarity of polypyrrole, .05M; molarity of ABEX EP-110, .005M; current density, .50mA/cm^2; volume of solution, 1 Liter; type of electrode, stainless steel foil; distance between electrodes, 14 cm; agitation to the system, none. After this objective was accomplished, I began constructing several double layer capacitors. The textured film capacitors made with ABEX EP-110 had capacitances ranging from 0.4180 to 0.7028 farad. This is a remarkable increase from the textured film capacitors made previously with ammonium chloride; the best ammonium chloride capacitor had a capacitance of only .05844 farad. Smooth film capacitors stored even less charge with a capacitance of 2.00×10^{-7} farad [14].

CONCLUSION

Through careful experimentation, I was able to achieve both of my original objectives. I determined the optimum deposition conditions for polypyrrole doped with ABEX EP-110. After accomplishing this, I was able to construct several double layer capacitors with increased capacitances. These improvements will hopefully guide later research with textured polypyrrole films.

REFERENCES

1. M.G. Kanatzidis, "Conductive Polymers," *Chemical and Engineering News*, Dec 3, 1990.

2. D. Finello, "Solid Laminated Double Layer Capacitor," AFATL-TR-90-72, Air Force Armament Directorate, July 1990.

3. S. DiStefano, "Conducting Polymers for Thermoplastic Electrodes," JPL Task Plan No. 80-3201, Air Force Armament Laboratory, August 1991.

4. R. K. Bunting, "Electronic Polymer Capacitors," Task 7 Prototype Design Final Report, March 1994.

5. Same as 3.

6. D. Delabouglise, "Control of the Interface Properties of Conducting Polypyrrole," *Synthetic Metals*, 1992.

7. Same as 4.

8. D. Harrison, "Factors Influencing the Deposition of Polypyrrole Film," High School Apprenticeship Program Final Report, August 1993 (Wright Laboratory Armament Directorate, Eglin AFB, FL)

9. D. Meyer and J.A. Woollam, "Diamondlike Carbon Hermetic Encapsulants," SBIR Phase II Contract No. F08630-91-0047, Wright Laboratory Armament Directorate, July 1993.

10. J.C. Philip and H.B. Oakley, "Conductivity and Ionization of Solutions of Potassium Iodide in Nitromethane," J. Chemical Soc. 125, (1924), 1189 - 1195.

11. D.J. Anderson, "General Review of Electrolytes," J. Electrochemical Soc.124, (1977), pp. 401C - 409C.

12. M. E. Van Valkenburg, *Network Analysis*, Prentice-Hall, Inc., Englewood Cliffs, New Jersey, 1974, pp. 7-19.

13. V. Del Toro, *Principles of Electrical Engineering*, Prentice-Hall, Inc., Englewood Cliffs, New Jersey, 1972, pp. 41.

14. L. Hemmer, "High Surface Area Conductive Polymer Films Using An Ammonium Chloride Aqueous Solution," High School Apprenticeship Program Final Report, August 1993, (Wright Laboratory Armament Directorate, Eglin AFB, FL).

ABEX EP-110 (Rhone-Poulenc)
abbreviated structure

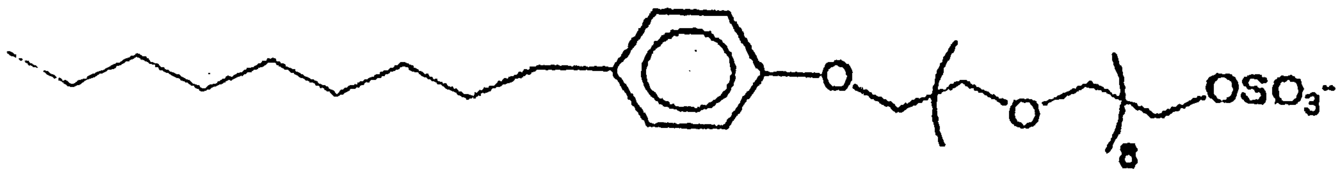

Figure 1

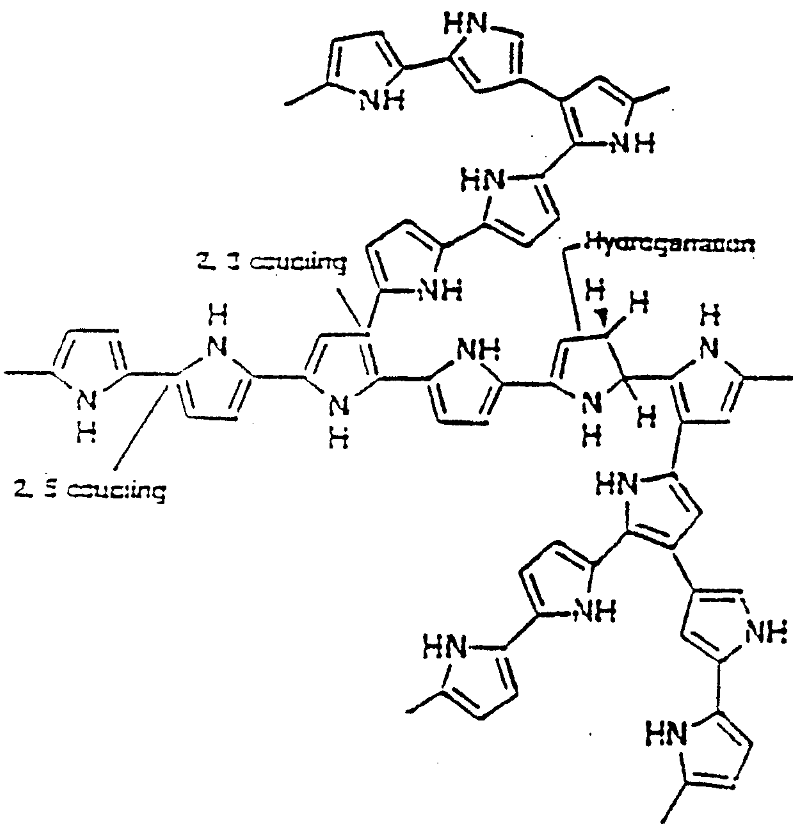

Proposed disordered stuctural model for polypyrrole

DEPOSITION OF POLYPYRROLE

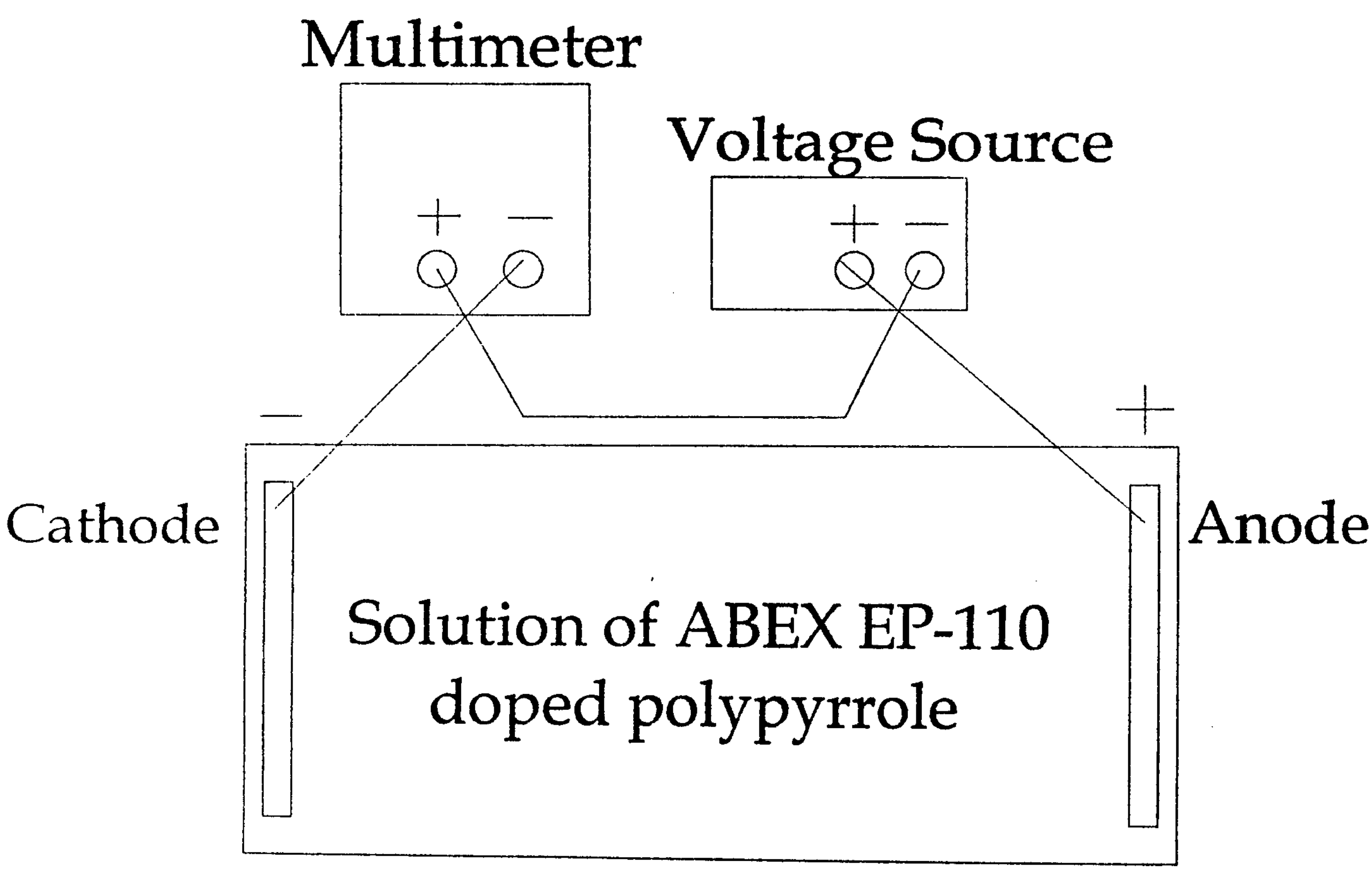

Figure 2

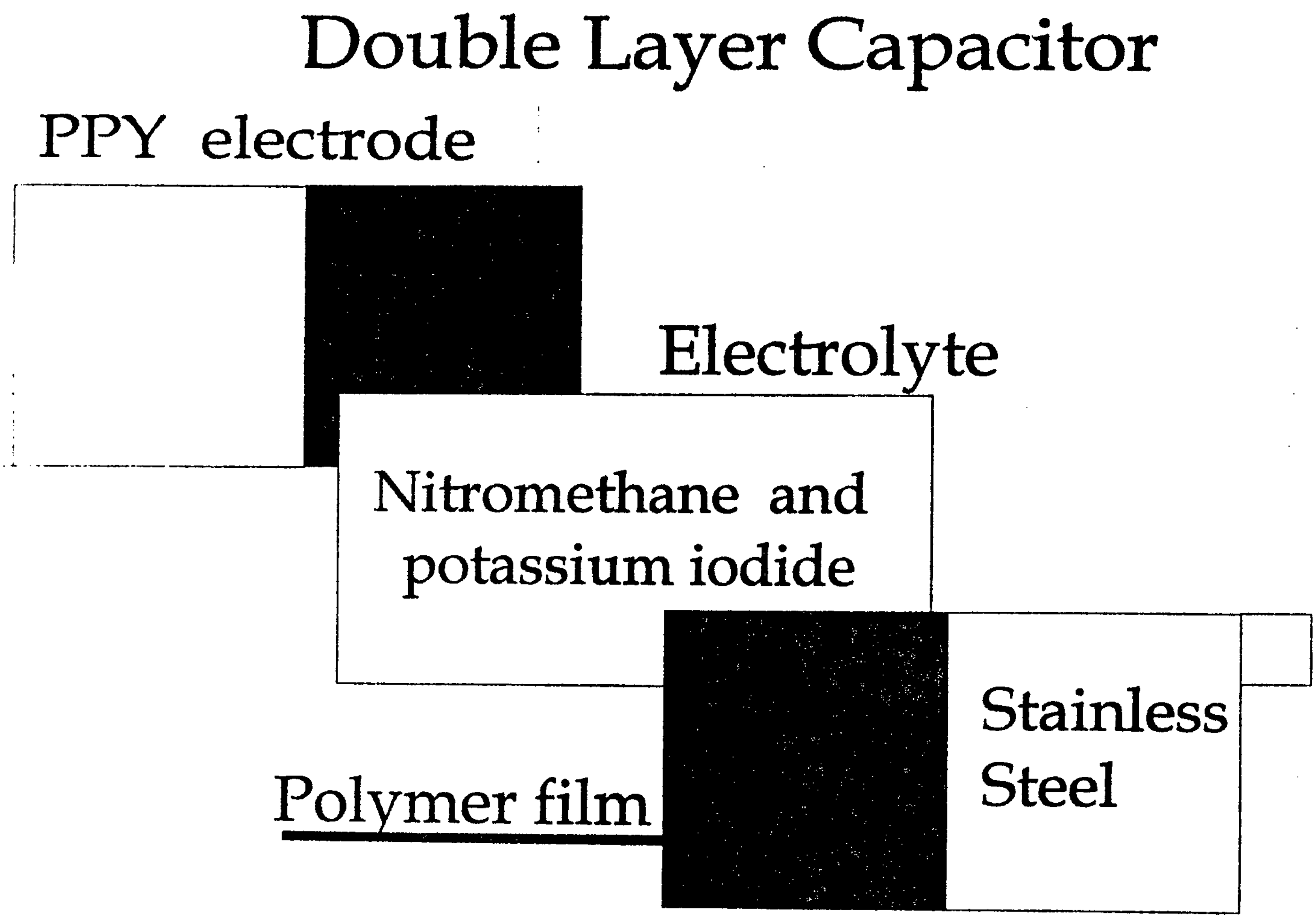
Double Layer Capacitor
PPY electrode
Electrolyte
Nitromethane and potassium iodide
Stainless Steel
Polymer film

Figure 3

PRELIMINARY STUDY FOR APPLICATION OF IRMA SYNTHETIC SIGNATURE TO MODEL HAZARDOUS WASTE SITES

David B. Hernandez
High School Apprentice
Seeker Technology Evaluation Branch

Freeport High School
Kylea Laird Dr.
Freeport, FL 32439

Wright Laboratory Armament Directorate
WL/MNGI
Eglin Air Force Base, FL 32542-5434

Final Report for:
High School Apprenticeship Program
Wright Laboratory Armament Directorate

Sponsored by:
Air Force Office of Scientific Research
Bolling Air Force Base, DC

and

Wright Laboratory

August 1994

PRELIMINARY STUDY FOR APPLICATION OF IRMA SYNTHETIC SIGNATURE TO MODEL HAZARDOUS WASTE SITES

David B. Hernandez
High School Apprentice
Seeker Technology Evaluation Branch
WL/MNGI

Abstract

This project involved technology transfer from military use to civilian use specifically to detect and cleanup hazardous waste sites. The sensors that the military uses to detect enemy outposts can be used to detect hazardous chemicals and can give valuable information as to the cause of the environmentally unsafe chemicals and how best to dispose of them in a safe, clean fashion. This process would save numerous man hours in trying to detect a waste site and in trying to clean it up. Even small traces of a hazardous chemicals would show up using Irma. This helps to minimize the area of treatment and maximize the time available for cleanup. Currently, WL/MNGI is working on the application of Irma to automatic target recognition. The goal of this project is to see if it is possible to apply those same techniques to locate hazardous waste sites and what those sites are composed of.

PRELIMINARY STUDY FOR APPLICATION OF IRMA SYNTHETIC SIGNATURE TO MODEL HAZARDOUS WASTE SITES

David B. Hernandez
High School Apprentice
Seeker Technology Evaluation Branch
WL/MNGI

Introduction

In recent years the United States has been making the move from a military oriented country to a more civilian oriented country. There have been programs developed to convert military technology and knowledge to civilian use. One of the country's largest problems is that of hazardous waste. Some of the country's largest waste sites, which are on the Superfund list, were old military bases that produced chemical and nuclear warfare during the Cold War. It is only natural then that the military assist in cleaning up these sites. This project will help with that task by examining what military technology would be best suited to detecting a Superfund site and how it could bring the best results. This project looks at how well Irma can synthesis the signature of hazardous waste sites and how practical and effective it would be to implement it as a means of selecting detection methods for hazardous waste.

Background

One way in which military technology can be applied to civilian use is by using Irma, a synthetic signature model. One can give it a set of conditions about the weather, the terrain, the time of day and Irma will produce an image in either visual, infrared, LADAR or passive millimeter wave. Each scene can be generated in all wave lengths to show multiple characteristics of that scene. Visual will give one a visual picture of what is in the image, infrared will show heat signatures, LADAR or Laser RADAR will show range, reflectivity and doppler, which displays kinetic information, and passive millimeter wave will give one what is man-made in the image. The same way one would be able to replicate a launcher that had just

fired a missile early in the morning with a clear breeze one can replicate a hazardous waste site that was composed of lead, oil, gas and asbestos that had been leaking into the ground water for over a year from a factory built on a low hill. The chemicals would have a different signature than the surrounding environment and would be visible in one or more different wavelengths that Irma is capable of producing.

Procedure

The first step to this project was to gather information on what constituted a hazardous waste site and any relevant information that could be used with this compilation. Articles and other literature pertaining to this were retrieved from Eglin Air Force Base Library and the Technical Library on Eglin AFB for use in this project and for background information. This information was used to accurately define what a hazardous waste site is and what would be the best and most accurate way to model a hazardous waste site.

The information was acquired using Pro-Quest on a Zenith 248, at Eglin Air Force Base's Library and IHS on an IBM 386, at the Technical Library. The categories to find the information were Hazardous/Toxic Waste Sites. Twenty articles on topics ranging from detection and clean-up to disposal and preventive action were collected for the research. Next, an extensive referencing and listing of the articles was made using Microsoft Word. Notes were taken and cross-referenced by category to later be put in a database for analysis.

Notes and information from the twenty articles were listed in five categories: hazardous traits, detection, simulation and modeling, disposal, and miscellaneous data. Notes were taken on these articles and were organized and compiled into Microsoft Word. These notes were then printed out and were placed with the articles into a three-ring binder.

A short synopsis of the information found within some of the articles is listed below:

"Currently, there are unmanned vehicles being developed to better monitor Earth's environment. Unmanned air vehicles (UAV's), unmanned undersea vehicles (UUV's), and

unmanned ground vehicles (UGV's) have many advantages over manned systems. High-altitude, long-endurance (HALE) UAV's can fly days or months at a time, taking air samples and monitoring the atmosphere, ground and seas. UUV's and UGV's can remain stationary for long periods and then move on to new observation areas." (Shaker, Stevan M., 1992, p. 21-26)

"Submerged Quench Incineration (SQI) - SQI is a high-powered gas flame incineration process that uses water to cool and wash combustion products and gases. It destroys most organics and ammonia, and it produces a brine, or salty water, containing small quantities of heavy metals. The brine can be dried into a salt and disposed of in a hazardous waste landfill. The brine also can be treated to remove the metals and discharged as waste water at an appropriate metals recovery facility." (Gascoyne, Stephen, 1993, p. 33-37)

"Today, four main methods are used for safely disposing of hazardous waste:

Burial - The materials are buried in carefully constructed hazardous waste landfills.

Chemical & Physical Treatment - Chemical & Physical treatment to change the substance so that it eliminates or reduces toxicity.

Deposit - The materials are placed in safe underground spaces such as abandoned salt mines.

Incineration - The materials are put through a combustion process to break down the molecular bonds.

Scientists have discovered that certain microorganisms such as bacteria and fungi literally feed on hazardous waste. In the process, they make it less harmful. Bacteria contain enzymes that break down the complicated carbon-based molecules that make up many hazardous waste materials. The bacteria absorb the broken-down waste, further reducing its chemical structure to make food for the bacteria. The end result is more harmless bacteria, some carbon dioxide, and a lot less waste. This entire process is known as bioremediation.

Bioremediation can be used to attack such hazardous substances as wood preservatives, pesticides, solvents, and toxic petrochemicals. It can even be used to change radioactive materials to clean up contaminated ground water. Several types of bacteria have shown that they

remove the radioactive uranium and other materials from polluted ground water near nuclear facilities. The resulting sludge is still radioactive, but it is easier to control and store safely.

Today, there are four main traits of hazardous waste that scientists use to recognize and classify hazardous waste:

Corrosivity - The substance has a pH of less than 2 (extremely acidic) or greater than 12 (extremely alkaline). Includes many chemicals used in industrial processes.

Ignitability - The substance ignites when exposed to air or water or could explode when the temperature drops below 140 degrees Fahrenheit. Includes fuels and solvents.

Reactivity - Includes all materials that react violently with themselves, water, or air by exploding or generating dangerous fumes or gases. Includes volatile chemicals like phosphorus.

Toxicity - Substances that induce illness, death, or otherwise impacts the health of living things. Includes some medical wastes, asbestos, pesticides, and heavy metals like lead and cadmium." (Scott, Geoff, 1993, p. 17-19)

"Lead is one of the troublesome volatile metals that cause emission problems during incineration of metal-contaminated organic wastes. Toxic metals were listed as contaminants at 21 of the 28 State of Texas Superfund sites. (1), The most common contaminants were lead (13 sites) and chromium (12 sites), with lesser numbers of sites contaminated with arsenic, mercury, zinc, and cadmium. Soil contamination at lead battery recycling sites (LBRS) was a primary reason for the predominance of lead. At the national level also, these lead battery recycling sites are recognized as a significant problem." (Clifford, A., Shen-Sin Chen, and Carmen Reznik, 1993, p. 467-479)

"A new software system for carrying out the assessments of hazardous waste sites has been developed by ConSolve Inc., Lexington Mass. Commercially released the system , called SitePlanner is a computer-added engineering system designed to help environmental managers and engineers manage, evaluate, and visualize the huge quantity of data collected from such things as surface features, geological data, sample boring locations and analytical data.

SitePlanner is designed it integrate all the data and tasks typically used to characterize a waste site." (Krieger, James, 1992, p. 30-31)

The following is a list of several hazardous chemicals found in some of the articles:

Chemical Formula	Chemical Name
CH_2Cl	methyl chloride (chloromethane)
CH_2Cl_2	methlene chloride (dichloromethane)
$CHCl_3$	chloroform (trichloromethane)
CCl_4	carbon tetrachloride (tetrachloromethane)
C_2H_5Cl	ethyl chloride (chloroethane)
C_2H_3Cl	vinyl chloride (chloroethene, chloroethylene)
1,1-$C_2H_4Cl_2$	1,1-dichoroethane
1,2-$C_2H_4Cl_2$	ethylene dichloride (1,2-dichloroethane)
1,1-$C_2H_2Cl_2$	vinylidene chloride (1,1-dichloroethene, 1,1-dichloroethylene)
1,2-$C_2H_2Cl_2$	1,2-dichloroethylene (1,2-dichloroethene)
C_2Cl_2	dicholoracetylene (dichloroethyne)
1,1,1-$C_2H_3Cl_3$	methyl chloroform (1,1,1-trichloroethane)
1,1,2-$C_2H_2Cl_2$	1,1,2-trichloroethane
C_2HCl_3	trichloroethylene (trichloroethene, trichloroethylene)
C_2Cl_4	perchloroethylene (tetrachloroethene)
HCl	hydrogen chloride
Cl_2	chlorine
CCl_2O	phosgene

The following is a list of companies and organizations working on the problem of hazardous waste:

Ames Research Laboratory	Argonne National Laboratory
BioTrol Inc.	CH2M Hill
ConSolve Inc.	Earth Observation Systems

Edison Electric Institute	Emerging Technology
Wash Laboratories of the Battelle Memorial Inst	Department of Energy
Gray Freshwater Biological Institute	EPA
Idaho National Engineering Laboratory	NIST
National Oceanic & Atmospheric Administration	FreezeWall Inc.
Oak Ridge National Laboratories	Pyrolysis Systems Inc.
Sandia National Laboratories	Scientific Ecology Group Inc.
Dept of Environmental Protection and Energy	Westinghouse Electric
National Inst for Chemical Studies	Wallops Flight Center

Results and Conclusions

From this study it has been concluded that Irma is able to model hazardous waste signatures. All the research and study done on hazardous waste leads one to conclude that Irma can effectively model hazardous waste signatures. Now the question is how well Irma can model hazardous waste signatures and if it can model them accurently enough to make it feasible to be used on a regular basis. It is recommend that this study be continued to evaluate the full potential of Irma's application to modeling hazardous waste signatures. In the future Irma may be used to assist in modifying sensor algorithms to not only detect hazardous waste signatures, but also what chemicals make up the waste and exactly how far it penetrates into the ground. That is why it is important that this study be continued. The full potential of applying Irma to the problem of hazardous waste has not yet been looked into and it would make an excellent project for next year.

Acknowledgments

There are a number of people that helped with this project. In particular Emily Martinez, mentor; Don Harrison, HSAP coordinator; Mike Deiler, HSAP coordinator; John Provine, WL/MNGI Branch Chief; Alice McRae, secretary; Glenda Apel, secretary; Christie Gooden, apprentice; Robyn Carley; apprentice and all the members of WL/MNGI for their help and support during this project.

References

Bishop, Gordan. "Firms, Legislaters Bristle at DEPE's 'Non-Product Output' Regulations" [Newark] Star-Ledger 22 Feb. 1994, sec. B: 4.

Clifford, A., Shen-Sin Chen, and Carmen Reznik. "Volatizing Toxic Metals From Soil" Waste Management Vol.13 1993: 467-479.

Daniels, Steve, and Debra K. Rubin. "Firm Pushes Process to Deep-Freeze Wastes" Engineering News Record 15 Nov. 1993: 53.

Egorova, L.E., P.V. Roslyakov, A.V. Burkova and Chung Beijing. "Mathematical Simulation and Calculation of Emissions of Toxic Combustion Products From Fossil Fuels" Thermal Engineering Vol.40, No.7 1993: 560-566.

Evans, Daniel J., Rob Coppock. "Hazardous Waste Cleanup" Environment Vol.35, No.1: 3-4 & 42.

Fisher, Elizabeth M., Catherine P. Koshland. "Numerical Simulation of the Thermal

Destruction of Some Chlorinated C_1 and C_2 Hydrocarbons" Journal of the Air and Waste Management Association Vol.40 Oct. 1990: 1384-1390.

Fitzgibbon, Joe. "Company Uses Microbe to Clean Contaminated Dirt" [Portland] The Oregonian 19 Jan. 1994, sec. B: 5.

Gascoyne, Stephen. "Slipcovering a Superfund Site" The Bulletin of the Atomic Scientist Sept. 1993: 33-37.

Hull, J.R., K.V. Liu, W.T. Sha, Jyotti Kamal and C.E. Nielson. "Dependence of Ground Heat Loss Upon Solar Pond Size and Perimeter Insulation" Solar Energy Vol.33, No.1: 25-33.

King, Chris W., Alan J. Witten and Gregory D. Reed. "Detection and Imaging of Buried Wastes Using Seismic Wave Propagation" Journal of Environmental Engineering Vol.115 June 1989: 527-540.

Krieger, James. "System Software Aids Waste-Sites Analysis" Environmental Progress Feb. 1992: 30-31.

"Old Horrors" The Economist 29 May 1993: 12-13.

Pomice, Eva. "Cleaning Up after Industry's Slobs" Science and Technology Apr. 1991: 31.

Rhee, Seung-Whee, Danny D. Reible, W. David Constant. "Stochastic Modeling of Flow and Transport in Deep-Well Injection Disposal Systems" Journal of Hazardous Materials Oct. 1993: 313-333.

Scott, Geoff. "Tackling the Oozing Monster Hazardous Waste" Environment Sept. 1993: 17-19.

Shaker, Stevan M. "Unmanned Sensor Systems for Earth Observation and Environmental Cleanup" Sensors Apr. 1992: 21-26.

Ward, Ken Jr. "Toxic Emissions Decline While Chemical Production Rises" Engineering News Record Feb. 1994: 13-16.

"Wastewater Management Rises to Top Priority" Power Engineering Oct. 1992: 21-26.

Wireback, Taft. "Cloud Returns to Puzzle Experts" [Greensboro] News and Record 8 Feb. 1994, sec. G: 6.

PARALLEL GASEOUS FUEL INJECTION INTO A MACH 2 FREESTREAM

Melanie L. Hodges
Research Apprentice
Advanced Propulsion Division

Wright-Patterson Air Force Base
Area B, Building 18
WL/POPT
Wright-Patterson AFB, OH 45433-6563

Final Report for:
Summer Research Program
Wright Laboratory

Sponsored by:
Air Force Office of Scientific Research
Bolling Air Force Base, Washington, D.C.

August 1994

PARALLEL GASEOUS FUEL INJECTION INTO A MACH 2 FREESTREAM

Melanie L. Hodges
Research Apprentice
Advanced Propulsion Division
Wright Laboratory
Wright-Patterson Air Force Base

Abstract

Planar Rayleigh/Mie scattering and Acetone Planar Laser Induced Fluorescence (PLIF) flow visualization are presented for helium injected at sonic velocities from an extended strut into a Mach 2 freestream. The turbulent structure and penetration characteristics of the helium injected parallel into the flow at three different nozzle-to-freestream air pressure ratios were examined. Typical features of the flow, including a barrel shock, Mach disk, recompression shock, and recirculation zones were evident in Rayleigh/Mie and Acetone PLIF images taken from three different views along the flow. Mie scattering images reveal the presence of a conical shock in the near flowfield, upstream of the recompression shock in the highly overpressurized cases. Jet spread was insignificant for all case studies. This investigation will be used as a baseline study for comparison in future mixing enhancement studies utilizing different injector geometries.

Acknowledgments

I would like to thank the following people for their time and patience during my summer research at Wright-Patterson AFB: Capt. Lou Carreiro, Dr. Diana Glawe, Mr. Charlie Smith, Mr. Gary Haines, Dr. Tzong T. Chen, Mr. Dave Schommer , Dr. A.S. Nejad, Lt. Jeffrey Fillmore, Dr. Anna E.S. Creese, Mr. James Summit, Mrs. Beverly Chaffin, Ms. Virginia Reynolds, and the members of the Advanced Propulsion Division of Wright Laboratory.

PARALLEL GASEOUS FUEL INJECTION INTO A MACH 2 FREESTREAM

Melanie L. Hodges

Introduction

Goals for the National AeroSpace Plane (NASP) and its derivatives include flight velocities in the hypersonic regime. In order to achieve such velocities, a fundamental knowledge of the fuel injection, mixing, and combustion processes carried out within the combustion chamber of these hypersonic engines is necessary. These processes will take place in a supersonic stream and therefore, must occur quickly since the residence time within such combustors will be minimal. Numerous fuel injection concepts have been proposed for such combustors, including injection from an extended strut in the upstream portion of the combustion chamber.[1] This concept is the basis for this investigation.

Due to the demanding space and time constraints of a supersonic combustor, it is imperative to produce optimal mixing and penetration of the fuel within the chamber. Though injection normal to the freestream creates better mixing, strong bowshocks formed during injection cause major thrust losses within the flow.[2] Therefore, it would be beneficial to increase the mixing and penetration attained by parallel injection, which would eliminate the thrust losses associated with normal injection. In the past, modified nozzle geometries, selective initial conditions, and acoustic excitation have been proven to enhance fuel/air mixing in subsonic flows. However, due to the high flight velocities of hypersonic planes, injection and combustion must occur at supersonic speeds and the mixing characteristics are naturally different under supersonic conditions than subsonic conditions.

The goal for this research is to investigate flow characteristics of gaseous parallel fuel injection into a supersonic freestream. Acetone Planar Laser Induced Fluorescence (PLIF) and planar Rayleigh/Mie scattering are used to examine flow parameters. The injection configuration was of vital importance to this research. To eliminate any extraneous factors from the experiment the strut needed to be mounted inside the supersonic tunnel with minimal upstream disturbances. The strut provided a rigid support for the injector nozzles and a recirculation zone at the base, ideal for flameholding in future

combustion applications. For these studies a simple circular converging injector nozzle was used to provide a baseline study for future mixing technique comparisons, and helium was used as the injectant to simulate hydrogen, the fuel proposed for several scramjet engine concepts.

Experimental Methods

The new supersonic combustion facility at Wright Laboratory offered an environment specifically designed for the type of injection studies reported in this paper. The combustion tunnel and the fuel injector used for study, along with the diagnostic techniques employed in these experiments, are discussed below. For further details concerning the combustion tunnel, see Gruber and Nejad[3].

The state of the art research facility at Wright Laboratory is a result of a collaborative in-house design effort. The preliminary planning began in 1990 and the facility was completed by the end of 1992. It offers a wide range of flow capabilities, including:

- Variable Mach number capability (1.5 to 5.0)
- Continuous flow operation
- Stagnation conditions up to 400 psig at 1660 ^{o}R
- 5-inch by 6-inch test section
- Peak air flow rate of 34 lb_m/sec
- Optical access to the test section from four sides including the end.

The results of their efforts are shown in a schematic of the facility (Figures 1 & 2). The test section allows optical access on three sides and the end for the use of nonintrusive diagnostic techniques. The windows are made of fused silica, which allows exceptional UV laser penetration for diagnostic techniques such as Acetone PLIF or Rayleigh/ Mie scattering.

The 0.5 in (1.27 cm) thick strut extends through the nozzle section into the test section of the tunnel to eliminate leading edge shock waves. In addition, the Mach 2.0 tunnel nozzle was designed to provide a uniform Mach 2.0 freestream flow prior to reaching the end of the strut where injection occurs. The 0.138 in (3.5 mm) diameter circular injector nozzle is located at the end of the strut. Helium is supplied to the injector through the sidewall of the tunnel into the strut and is directed through a 90

degree bend to enter the converging circular nozzle. Helium exits the circular injector at sonic velocities into the Mach 2 freestream. Figure 3 provides a schematic of the strut and injector configuration within the tunnel.

The diagnostic methods used in this study include Rayleigh/Mie scattering and Acetone PLIF. Mie scattering was used to identify positioning of injectant in the freestream and to provide a visual representation of the flowfield characteristics. Helium was injected into the test section and allowed to mix with the freestream. A Lambda Physik EMG 150 Excimer laser produced 248 nm wavelength ultra-violet radiation for Rayleigh/Mie scattering. The laser beam was passed through a series of lenses and prisms to create an approximately 0.5 mm thick ultraviolet laser sheet which was projected into the tunnel at several different angles as shown in Figures 4-6. Naturally occurring water vapor within the test section effectively scattered the UV radiation and the signal was collected by a Princeton Instrument Intensified Charge Coupled Device (ICCD) camera using a UV telephoto lens. The instantaneous digital images were then stored in a central processing unit (CPU) for analysis at a later time. The Rayleigh/Mie images highlight the shock waves in the freestream and mixing with the injected helium. Figure 7 provides a schematic representation of features of the flowfield visible in Rayleigh/Mie images. Future work will include particle measurement. However, for this study, the size of the scattering particles is not important. The information in these images is the same whether the scattering is Mie or Rayleigh as long as the particles follow the flow.

Acetone PLIF was used in conjunction with Rayleigh/Mie scattering in this investigation. A frequency doubled Spectra-Physics Quanta-Ray DCR-4 Nd: YAG laser (532 nm wavelength beam) along with a Quanta-Ray wavelength extender (WEX-1) produced the 266 nm ultra-violet radiation for acetone PLIF. The same optical and imaging system as the Rayleigh/Mie setup (Figure 4) was used, except that the Excimer laser was replaced by the Yag/WEX system and an ordinary camera lens replaced the UV telephoto lens. An ordinary camera lens can be used because of the visible fluorescence of the acetone. In this diagnostic system, the injected helium was seeded with acetone. When the laser sheet passes through the tunnel the acetone is excited to a higher energy level in the (255-320 nm) wavelength band and then fluoresces in the (350-600 nm) wavelength band. As in Rayleigh/Mie system, the images are collected

and stored in the CPU. The acetone PLIF images reveal the internal shock structure of the injected helium as shown in Figure 8.

Results and Discussion

The helium was injected at nozzle-to-freestream air pressure ratios of 1 (pressure matched), 2, and 4. Rayleigh/Mie scattering images were taken from three different planes of view: streamwise, planar, and face on (as shown in Figures 4-6). Note that the face-on images are slightly elongated along the horizontal axis due to a 27 degree angle between the camera axis and flow axis. Though an optical access was available downstream of the injector for capturing face-on images, it was necessary to situate the camera at this angle along the side window due to focusing difficulties with the camera. Figure 4 shows a schematic drawing of the srtreamwise view of the PLIF images. In all images helium is represented by the dark regions, while the freestream is represented by the light areas.

Figure 9 presents Mie scattering images for all four case studies: no injection, pressure matched, and nozzle-to-freestream pressure ratios 2 and 4. Helium appears as dark regions in the images and the flow direction is left to right. Recompression shock angles are comparatively the same for all pressure ratios and no injection. However, the image taken at 4x pressure reveals a second shock not apparent in the other cases upstream of the recompression shock (Figure 9d).

Figure 10 shows Rayleigh/Mie scattering face-on images taken for the pressure matched and pressure ratio 4 cases. As noted earlier, the images are slightly elongated due to the angle from which they were taken. 'Lobed' structures located along the boundary of the jet contour suggest areas of large scale mixing with the freestream in the transverse direction, and are most apparent in the pressure ratio 4 case (Figure 10b). Images taken in the other two views (streamwise and planar) also exhibit these structures. Figure 11 illustrates planar cut images for the pressure matched and 4x pressure case. This view reveals consecutive sets of helium lobes (dark regions) and the entrained freestream fluid layer between them (bright regions). These lobes are especially distinct in the pressure matched case images.

Acetone PLIF streamwise images (Figure 12) reveal the barrel shock and Mach disk features of the over pressurized jet flowfield. The over pressurized helium leaves the injector and accelerates,

expanding through a barrel shock/Mach disk mechanism which acts to raise the pressure of the injectant to the required freestream value. A schematic representation of these structures is presented in Figure 8.

Bending of the freestream fluid as it flows over the end of the strut and encounters the side region of the barrel shock is believed to be the cause of the second shock upstream of the recompression shock seen in Figure 9d. This shock also appears in the face-on view images (Figure 10b) as an ellipse surrounding the helium jet. Comparing these two images reveals that the shock is cone shaped. This conical shock is clearly apparent in the over pressurized cases but does not appear in the pressure matched or 2x pressure cases. One possible explanation for this inconsistency is that the shock unites with the recompression shock in these cases. However, the more likely explanation is that the barrel shock influence does not extend far enough to create this shock in the 2x pressure case, and the pressure matched injectant case does not produce a barrel shock.

Conclusions

This study represents a preliminary investigation into the behavior of parallel injected helium into a supersonic freestream. Results of the Mie scattering and Acetone PLIF images provide a visible representation of the flowfield characteristics. PLIF images accent the barrel shock and Mach disk seen in the over pressurized jet. Mie scattering images reveal a recirculation zone at the base of the extended strut and the presence of a conical shock in the highly over pressurized cases. Jet spread was insignificant for all nozzle-to freestream pressure ratios. However, the jet does spread predominantly along the spanwise direction creating a oblong jet contour with large scale 'lobed' structures in the transverse direction. This study will serve as a baseline study to be used for comparison in future mixing enhancement studies using different injector geometries. Future investigations will involve other diagnostic techniques such as LDV (Laser Doppler Velocimetry) which will allow more precise determination of the jet width and the boundary layer thickness as well as providing velocity measurements.

References

1. Northam, G.B., Trexler, C.A., and McClinton, C., "Flame-holding Characteristics of a Swept Strut Hydrogen Fuel Injector for Scramjet Application, " NASA TR A81-10711, 1981.

2. King, P.S., Thomas, R.H., Schetz, J.A., Billig, F.S., "Combined Tangential-Normal Injection Into a Supersonic Flow," AIAA Paper 89-0622, 1989.

3. Gruber, M.R. and A.S. Nejad, "Development of a Large-Scale Supersonic Combustion Research Facility; Volume 1-Design and Fabrication," Wright Laboratory Report No. WL-TR-93-2052, 1993.

4. Glawe, D.D., Donbar, J.M.,et al. "Parallel fuel Injection from the Base of an Extended Strut into Supersonic Flow" AIAA Paper 94-0711, 1994.

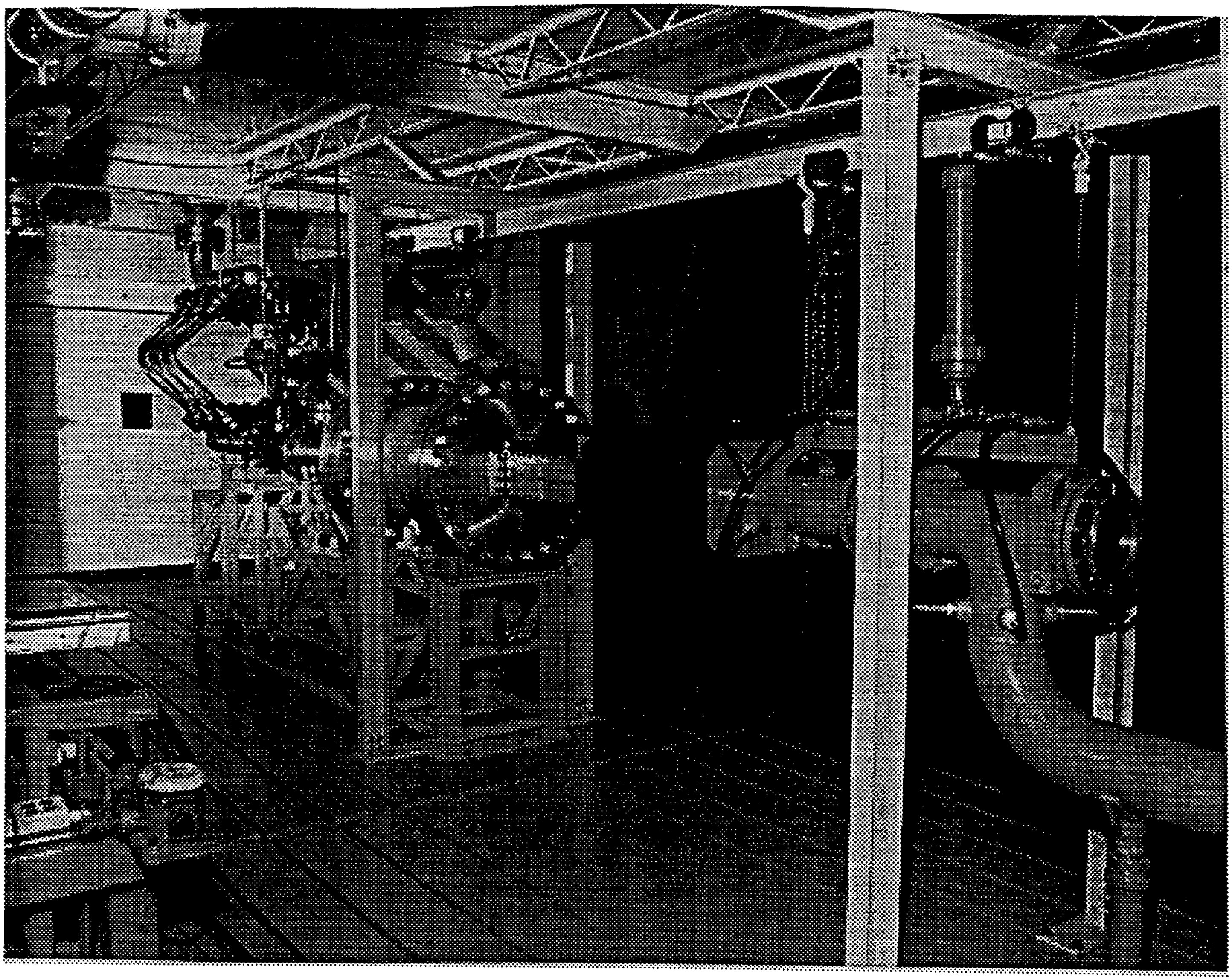

Figure 1. Supersonic Combustion Research Facility

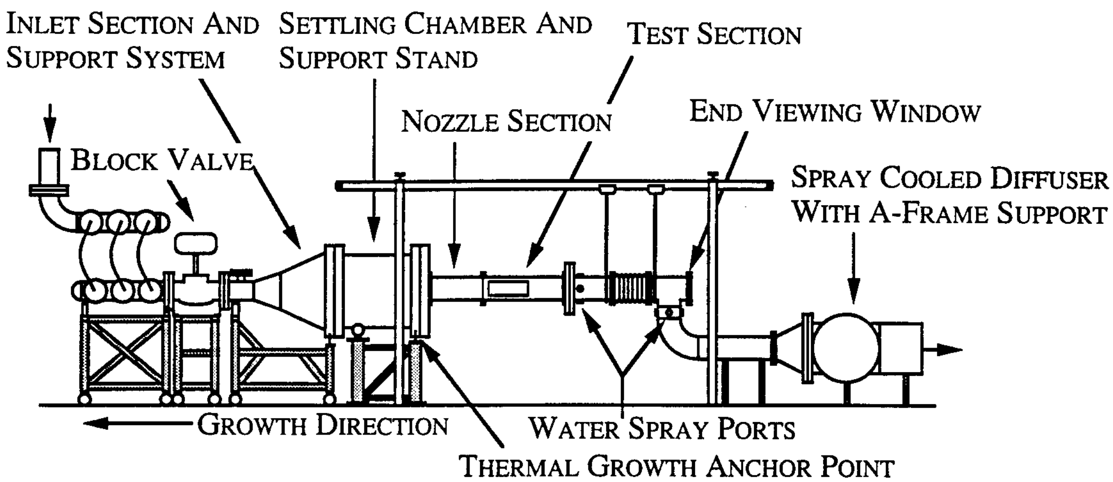

Figure 2 Schematic of Supersonic Combustion Tunnel

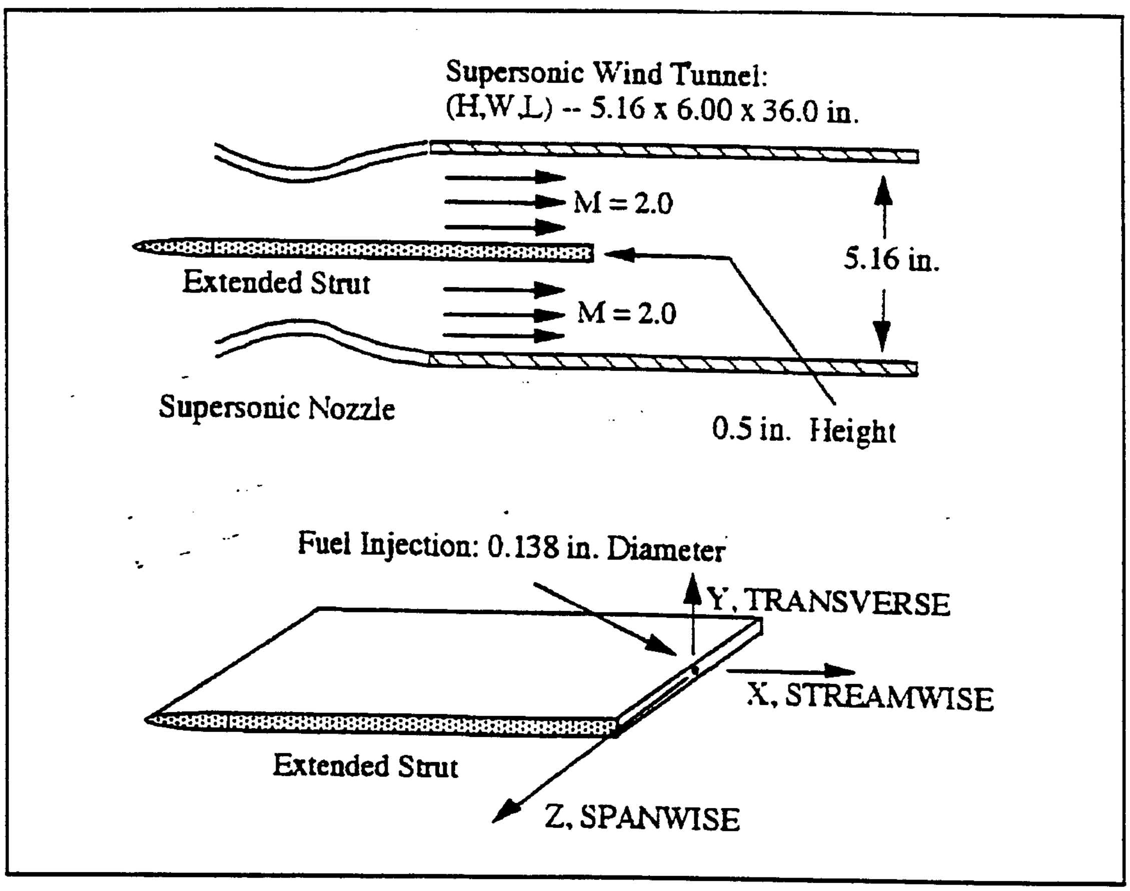

Figure 3 Schematic of the extended strut and Mach 2 nozzle

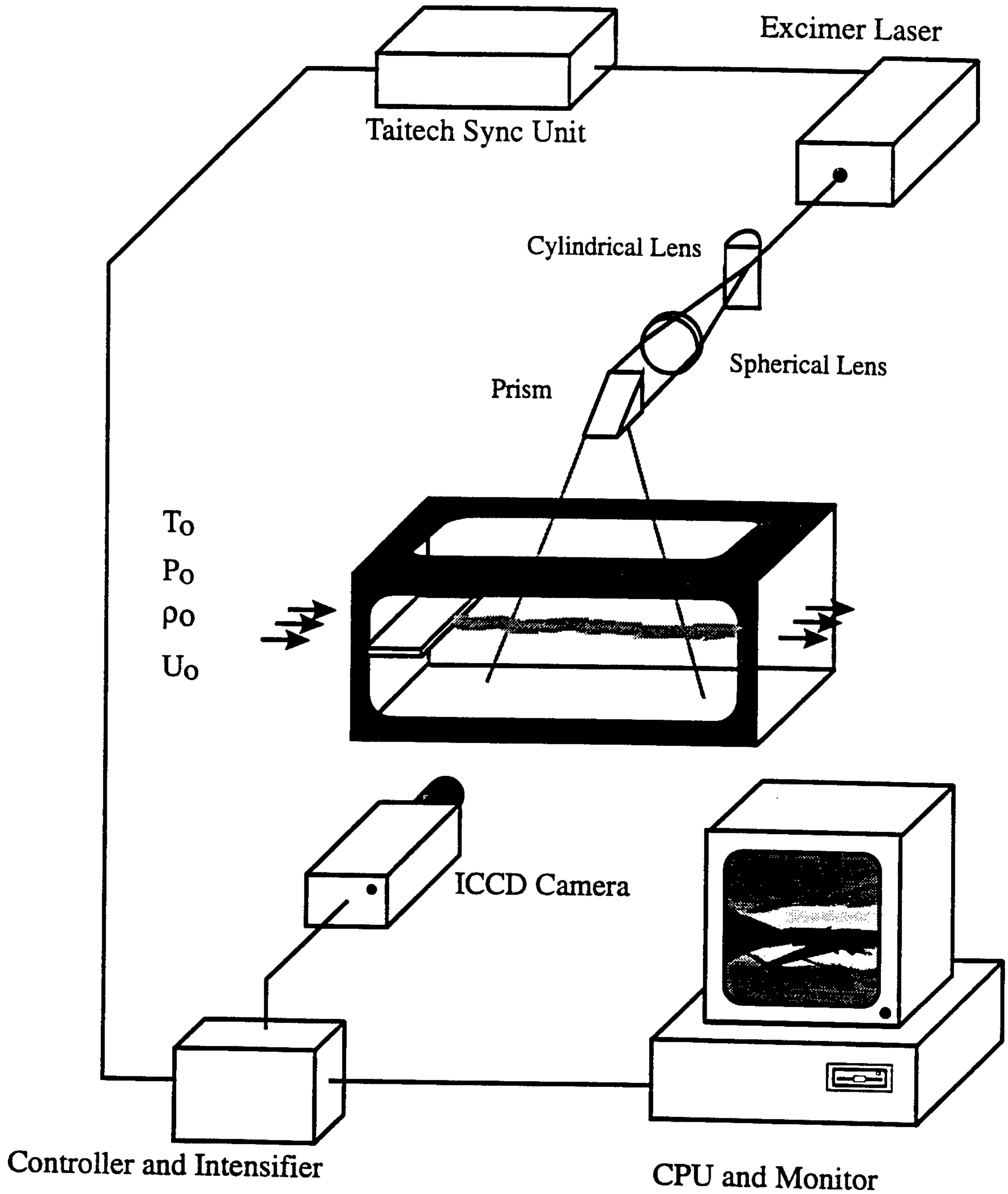

Figure 4 Rayleigh/Mie laser configuration for streamwise view

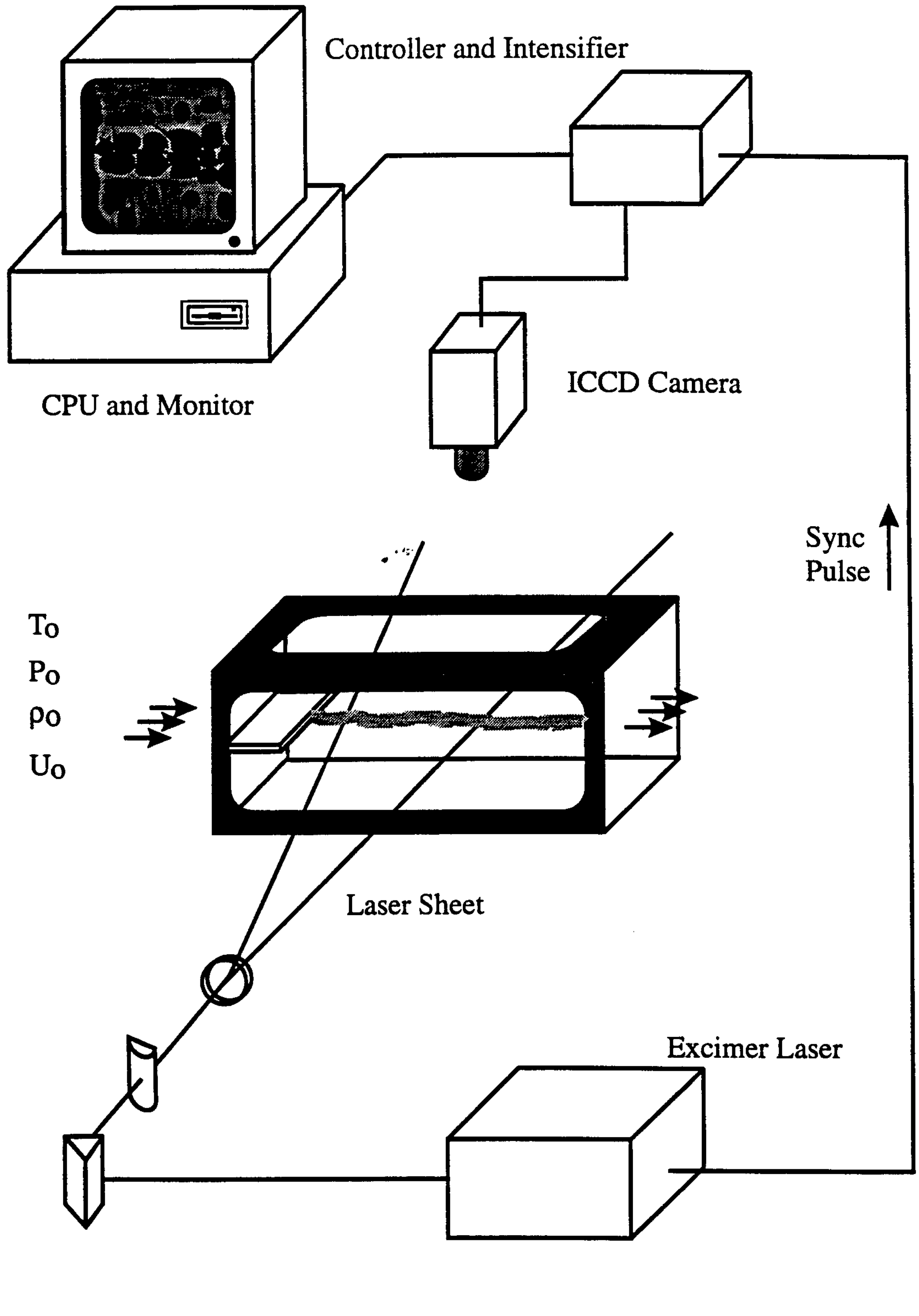

Figure 5 Rayleigh/Mie laser configuration for planar view

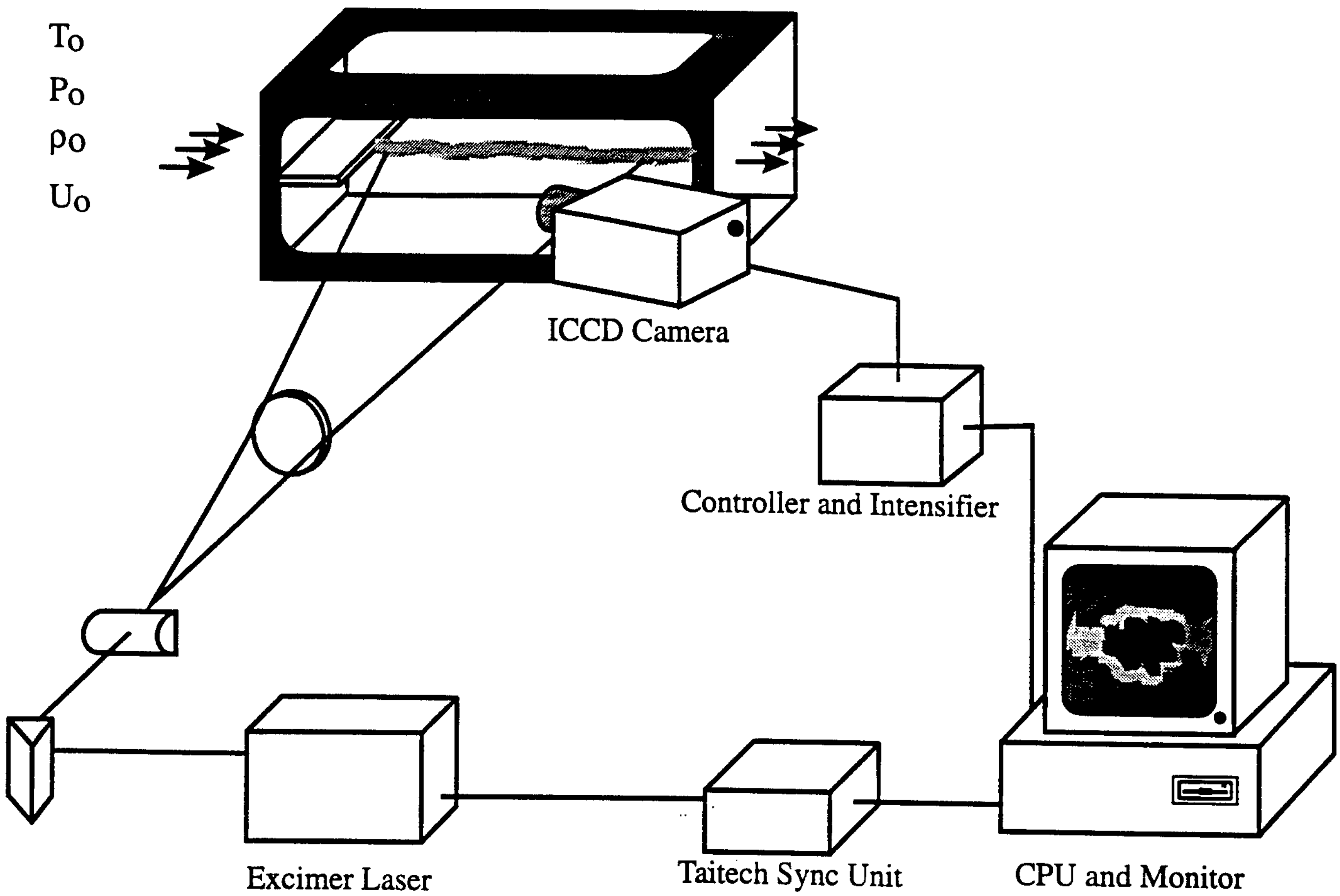

Figure 6 Rayleigh/Mie laser configuration for face-on view

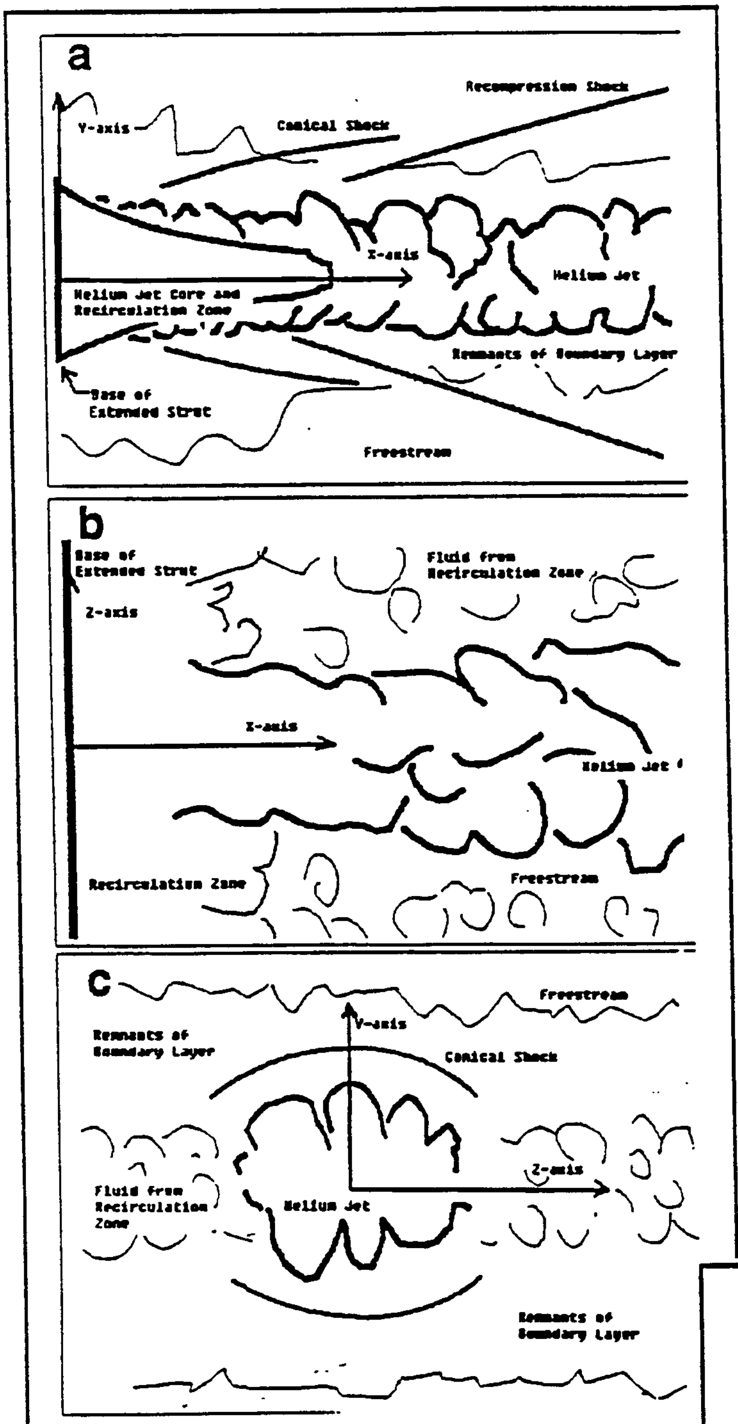

Figure 7 Schematic of Rayleigh/ Mie images
a) streamwise b) planar c) face-on views

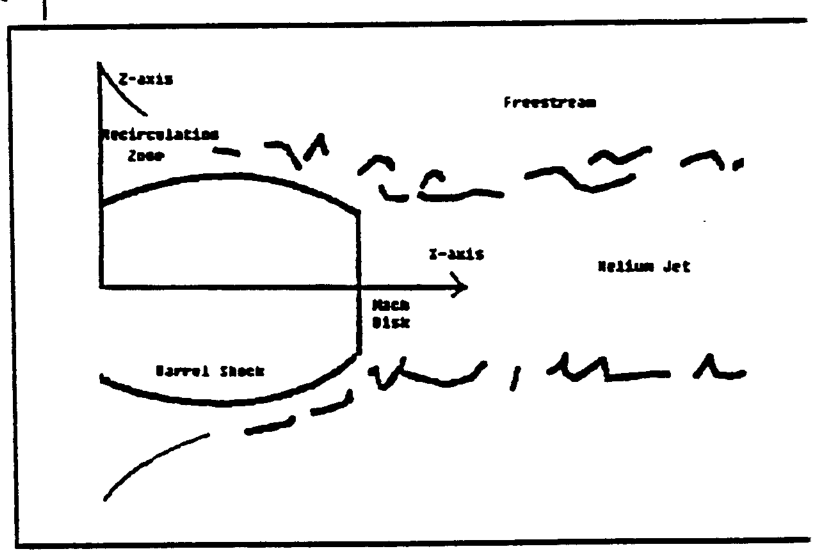

Figure 8 Schematic of PLIF image, streamwise view

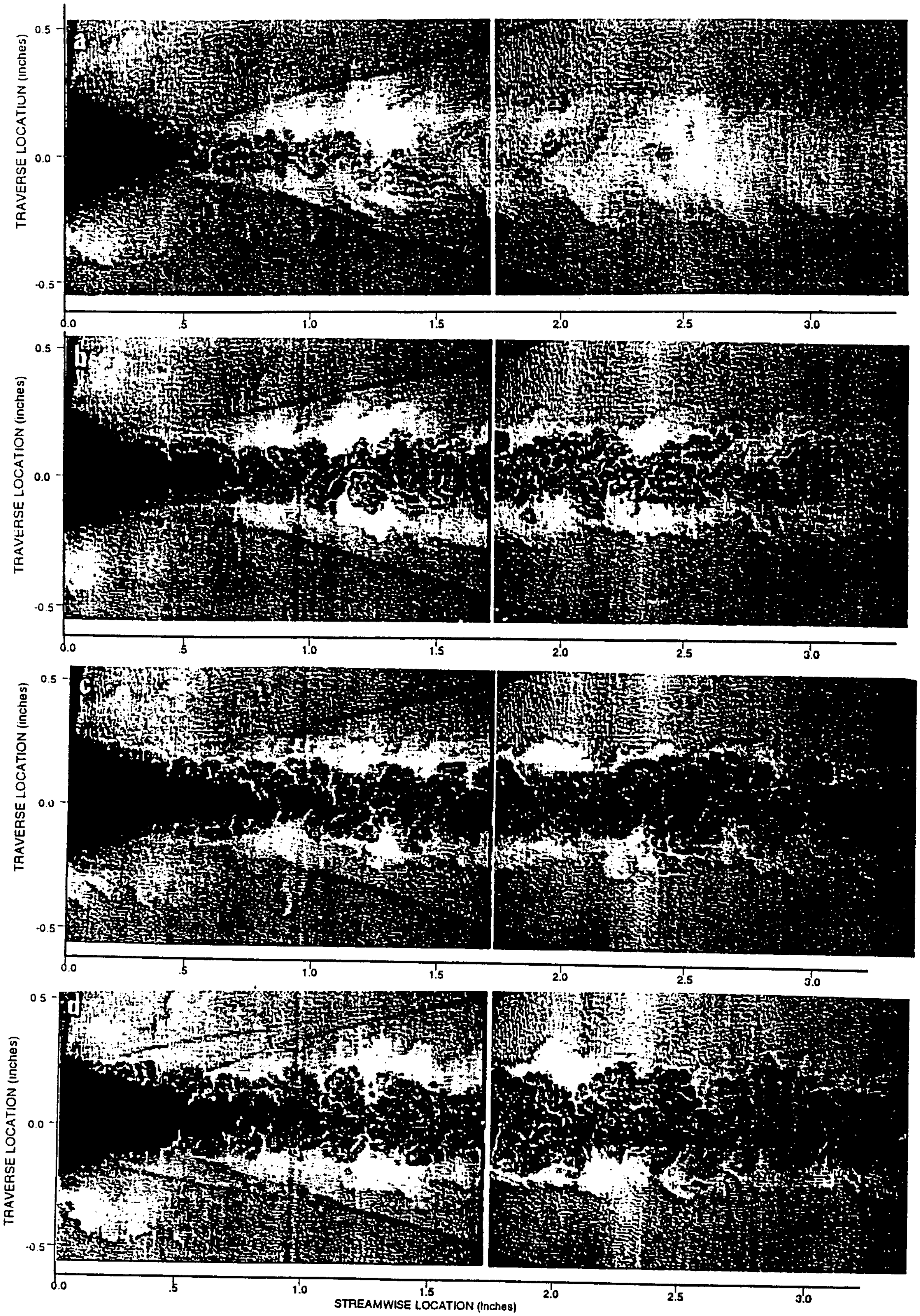

Figure 9 Streamwise Mie scattering images
a) no injection b) pressure matched c) 2x presssure case d) 4x pressure case

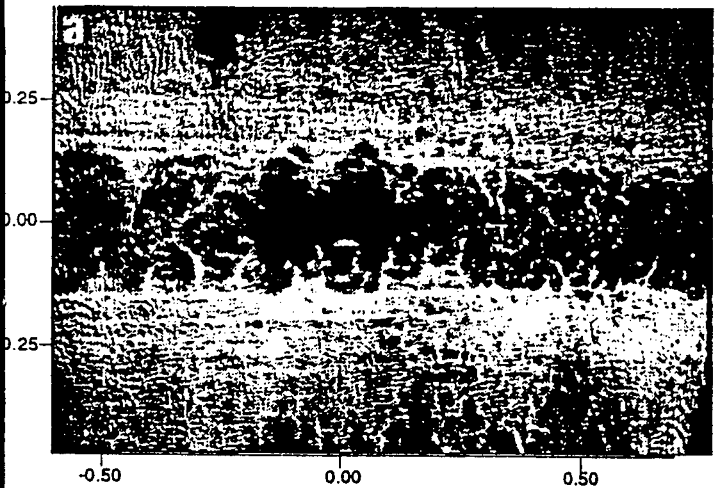

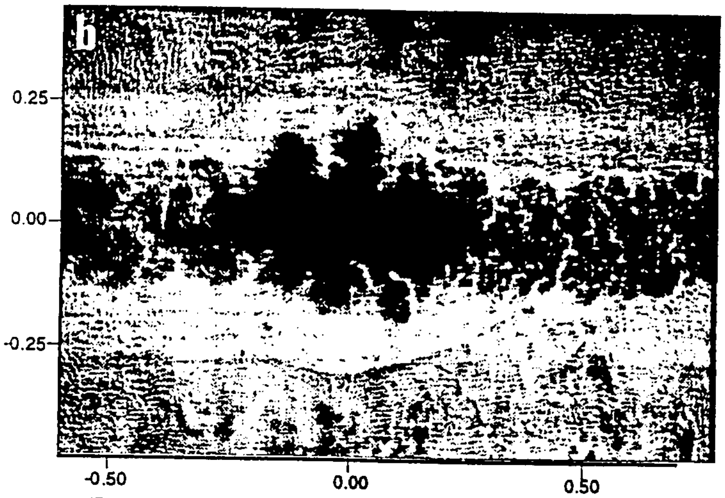

Figure 10 Face-on Mie scattering images
a) pressure matched b) 4x pressure case

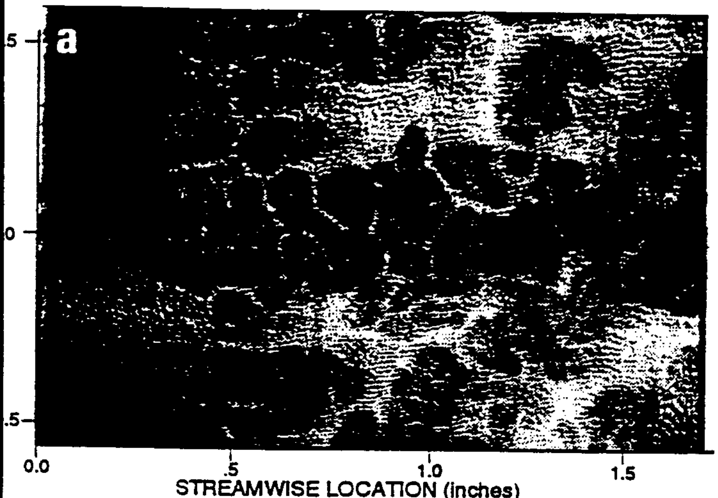

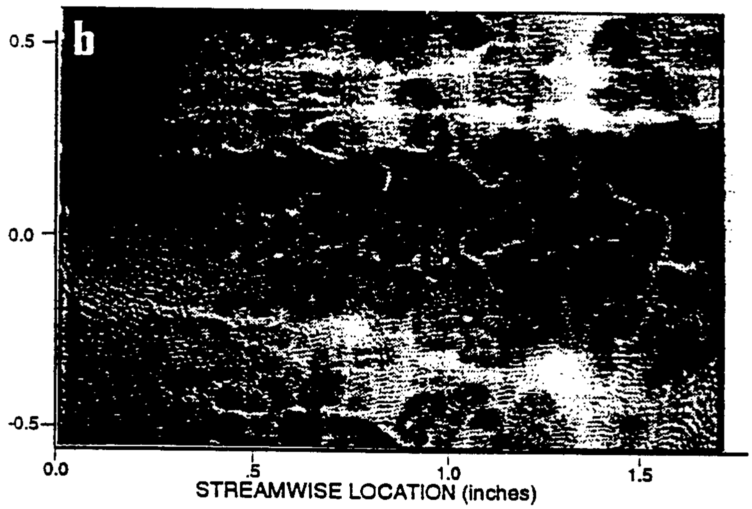

Figure 11 Planar Mie scattering images
a) pressure matched b) 4x pressure case

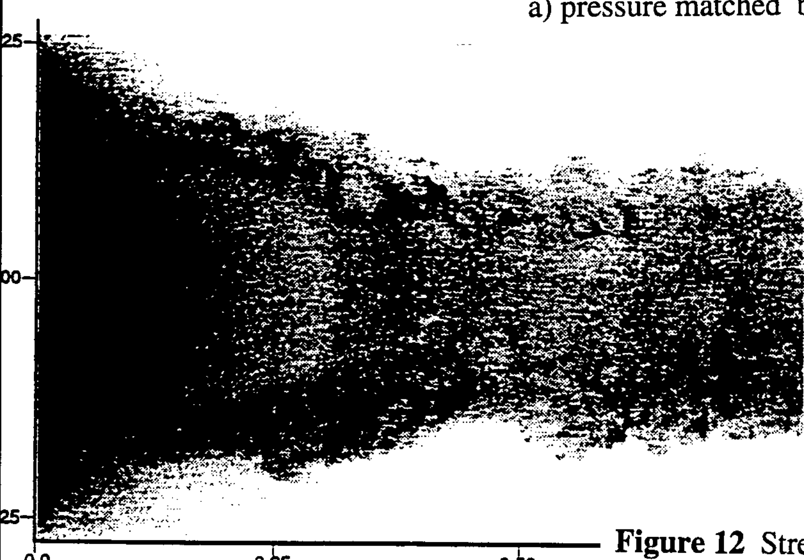

Figure 12 Streamwise Acetone PLIF image at 4x pressure case

FLUORODENITRATION OF AROMATIC SUBSTRATES

Venessa L. Hurst
High School Apprentice
High Explosive Reaserch and Develpoment Lab

Write Laboratory Armament Directorate
WL/MNMW
Eglin AFB, FL. 32542-5434

Final Report For:
High School Apprenticeship Program
Write Laboratry Armament Directorate

Sponsored By:
Air Force Office of Scientific Research
Bolling Air Force Base, Washington D.C.

August 18, 1994

FLUORODENITRATION OF AROMATIC SUBSTRATES

Venessa L. Hurst

Abstract

During this summer while in the HSAP program, I tried to demilitarize four different explosives. They were dinitrobenzene, nitrobenzonitrile, trinitrobenzene, and trinitrotoluene. They were each reacted with tetramethylammonium fluoride in the solvent dimethyl sulfoxide. I tested them after the experiment had taken place and looked to see if I could find the product that I was looking for. I found that product and this was proof that I did demilitarize the explosives.

FLUORODENITRATION OF
AROMATIC SUBSTRATES

Venessa L. Hurst

Introduction:

This prodject was done to see if it was possible to demilitraize different explosives. There would be great advantages to doing this. One of the advantages was that it would be safer to dispose of the explosives if they were dimilitarized. There are possibly others but this was reason that I was doing this project.

Methodology:

The method that this was carried out by used tetramethylammonium fluoride. However the first thing that had to be done was that the tetramethylammonium fluoride had to be synthesised. This was a three step process. The first step was an acid base neutralization. When this was done tetramethylammonium chloride was created. After the tetramethylammonium chloridewas made, it was then possible to do a haylid displacement between the tetramethylammonium chloride and the potassium fluoride. The fluoride

and chloride switched places. Through this procedure tetramethylammonium fluoride was synthesized.

Now that the tetramethylammonium fluoride was synthisized the experiments could take place. The first thing that was tested was dinitribenzene. The way that this was done was by taking .5g of tetramethylammonium fluoride and 1g of dintrobenzene and dissolving them together in a dimethyl sulfoxide solution. It was then heated at 100 degrees C in a water bath. Samples were taken every four hours. This procedure was repeated for every experiment that was performed. There were three other explosives tested; nitrobenzonitrile, trinitrobenzene, and trinitrotoluene. After the actual experiment was carryed out there had to be a way to exstract the product. This was done by using a distillation set up. Then after the prospective product was extracted test were run so that there could be an identification of what it was. I used four different tests to do this. They were High Pressure Liquid Chromatograph, Gass Chromatograph / Mass Spectrometer, Nuclear Magnetic Resonace, and the IR.

Due to the amount of time that was left before the presentation there was not time to test all of the experiments so therefor the dinitrobenznene and the trinrobenzene were the only two that got tested extensivly. Here are some of the different graphs that were taken from the tests that were run.

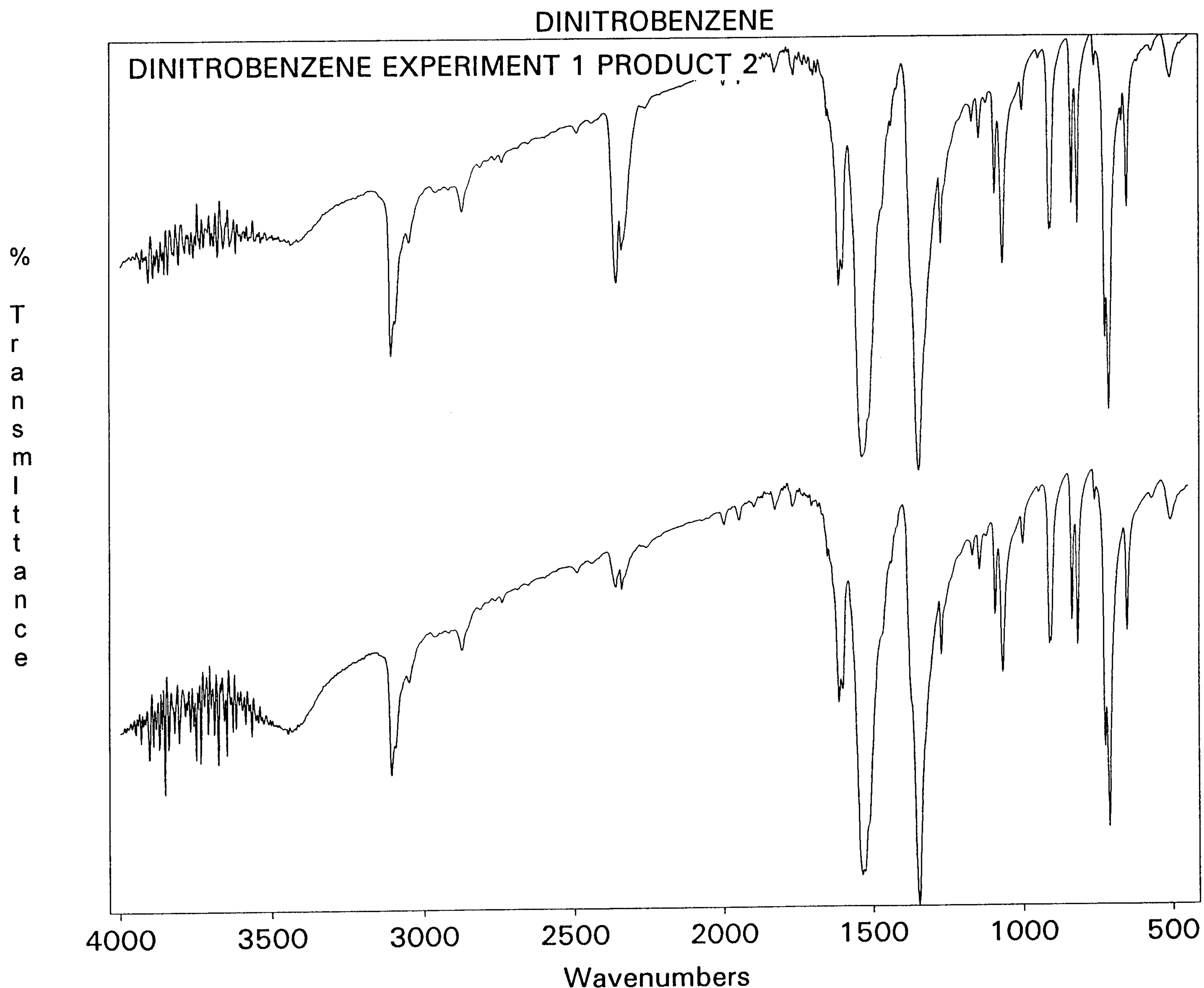
DINITROBENZENE
DINITROBENZENE EXPERIMENT 1 PRODUCT 2
% Transmittance
4000
3500
3000
2500
2000
1500
1000
500
Wavenumbers

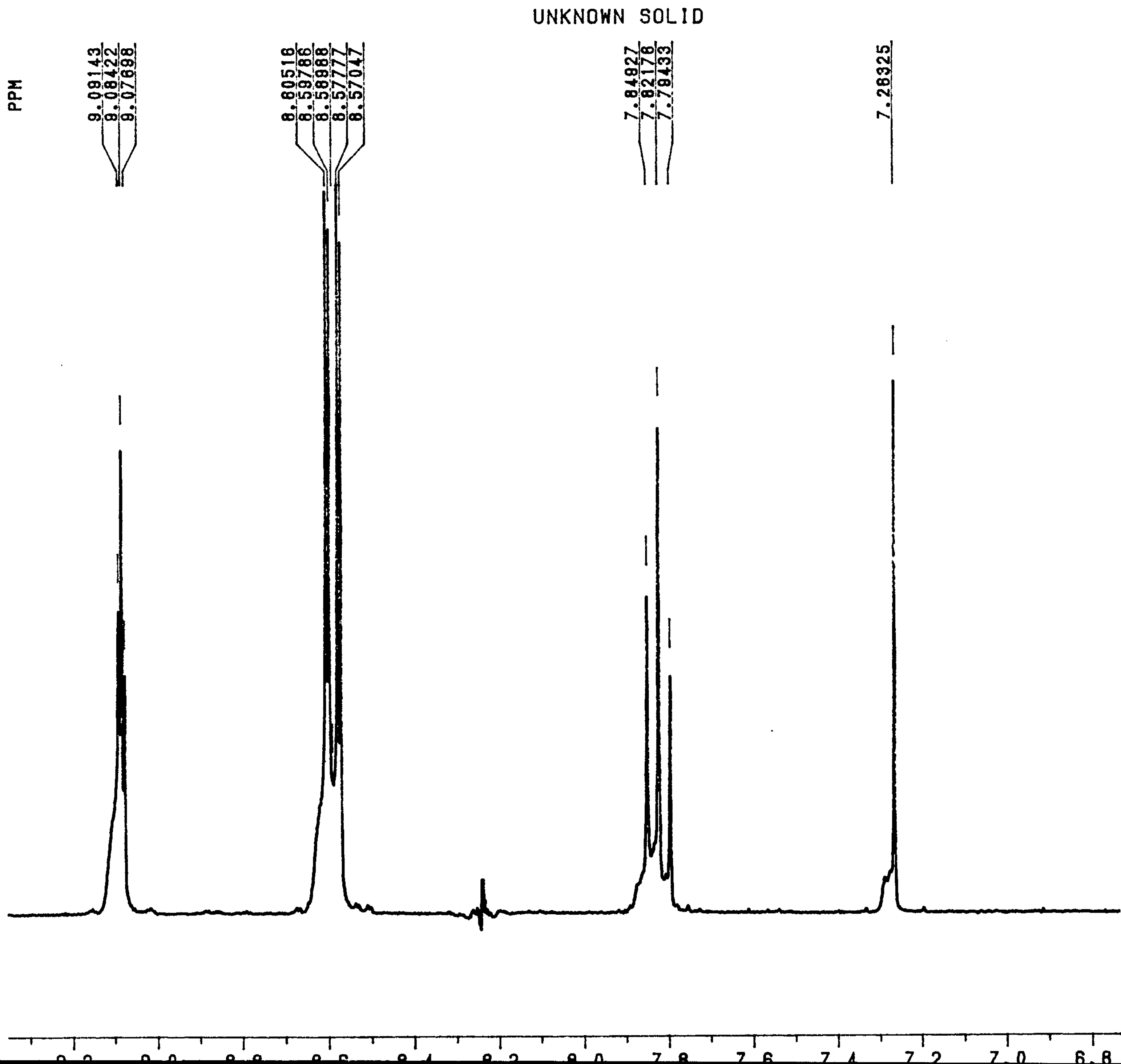

BRUKER

DATE 21-7-94

SF 300.133
SY 210.0
O1 5000.000
SI 32768
TD 32768
SW 4504.505
HZ/PT .275

PW 1.0
RD 3.000
AQ 3.637
RG 1
NS 1200
TE 297

FW 5700
O2 3200.000
DP 63L PO

LB .100
GB 0.0
CX 20.00
CY 13.00
F1 2806.52H
F2 2021.03H
HZ/CM 39.274
PPM/CM .131
SR 3366.07

Results and Conclusions

After looking at the test results I was able to say that I did dimilitsize the dinitrobenzene. However when I was looking at the test results from the trinitrobenzene I noticed that the trinitrobenzene was not even showing up on the tests. This ment that the test would be inconclusive.

Aknowledgements

I would like to thank Mr. Harrison and Mr. Dieler for run the program so that we could have this wonderful oppratunity. I would also like to thank Doctor Robert McKenney for taking time out of his busy schedul and being my mentor. I would like to thank everyone at the HEARD for helping my any time that I need so. I would like to thank all of the fellow HSAP students because of all of their support.

EXPERIMENTS IN FUEL RESEARCH

Ryan A. Jasper

Carroll High School
4524 Linden Avenue
Dayton, OH 45432

Final Report for:
High School Apprentice Program
Wright Laboratory

Sponsored by:
Air Force Office of Scientific Research
Bolling Air Force Base, DC

And

Wright Lab

August 1994

EXPERIMENTS IN FUEL RESEARCH

Ryan A. Jasper

Abstract

The importance of fuel in the military is only second to the safety level afforded to the pilots of military aircraft by making sure the fuel used is at the best possible performance levels. Numerous tests were run in the effort to analyze the performance of fuels in conditions similar to those found in aircrafts and to test the effectiveness of fuel additives and fuel additive packages.

EXPERIMENTS IN FUEL RESEARCH

Ryan A. Jasper

The JP-8 fuel is a kerosene-based fuel that is similar to the Jet A-1 fuel. For a long while, the Army and Air Force have used the JP-4 fuel but are currently in an effort to switch to JP-8 because of the engine problems caused by the JP-4 fuel coupled with the fact that the JP-8 fuel is less flammable.

Jet fuel is the chief coolant in military aircraft. The JP-8+100 program is a united effort by the Air Force, the Navy, and the engine manufacturers Pratt Whitney and General Electric to find and test additive packages that will increase the heat absorbancy (thermal stability) of the fuel. Additive packages are tested in the Isothermal Corrosion Oxidation Tester (ICOT) and the Microcarbon Residue Tester (MCRT). If propitious results are achieved, the Quartz Crystal Microbalance is used for further testing. At Wright Lab, the ICOT and MCRT are run to test the fuels at higher temperatures.

In the ICOT, both the neat fuel and the fuel with additives are stressed. A 100-ml sample of each fuel is taken, placed in a glass tube, and lowered into an aluminum heating block. The fuel is stressed for five hours at 180 C with 1.3-L/hr of air supplied through a blower tube. The fuel is removed at the end of the five hours and then allowed to cool overnight. It is then filtered through a .6-micron filter that is consequently rinsed with hexane. The filter is heated at 100 C to drive off any residual fuel and hexane. It is then weighed and the amount of solid collected on the filter is reported in milligrams of deposit per liter of fuel. The effectiveness of an additive stressed in the ICOT is based on its ability to reduce or eliminate bulk deposits.

In the MCRT, a .85-g sample of fuel is weighed into six pre-weighed glass vials. These vials are placed into a chamber and then heated to 250 C for three hours with 9-L/hr of air flowing from twelve equidistant holes at the top of the chamber. This air sweeps downward, taking the evolved gas with it through a hole at the bottom of the chamber. That which remains in the glass vials, the residue, is not soluble in most organic solvents and is the solid reported as

a percentage of the original fuel weight in that vial. The condensate collected in the traps is soluble in acetone. It is a gum reported as a percentage of the total fuel weight. Low molecular weight compounds tend to form the gum while high molecular weight compounds tend to form the solids adhering to the glass vials. This test is attempting to imitate the temperatures of a typical fuel nozzle. The effectiveness of an additive in this test is based on its ability to reduce solid and gum formation.

Some other tests that were run that were independent of the JP-8+100 program are kinematic viscosity tests and the ball-on-cylinder lubricity evaluator (BOCLE) test.

There are numerous petroleum products that are used as lubricants for bearings, gears, hydraulic equipment, etc. The proper operation of the affected equipment depends on the proper kinematic viscosity of the liquid. The kinematic viscosity is a measure of the resistive flow of a fluid under gravity. The kinematic viscosity of several petroleum fuels is important for proper use such as flow of fuel through pipe lines, injection nozzles, and the determination of the temperature range for proper operation of the fuel in burners. When testing for kinematic viscosity, the time is measured in seconds for a fixed volume of liquid to flow under gravity through a capillary tube of a calibrated viscometer under a reproducible driving head at a closely controlled temperature. The kinematic viscosity is measured in centistokes and is derived by multiplying the calibration constant of the viscometer by the measured flow time.

The lubricity of a fuel is used to describe the boundary lubrication properties of a fluid. Wear due to excessive friction resulting in a shortened life of engine components such as fuel controls and pumps has sometimes been attributed to a lack of lubricity in a fuel. When testing for a fuel's lubricity, the fuel is placed in a test reservoir that maintains a 10% relative humidity. A non-rotating steel ball is held in a vertically mounted steel ring with an applied load. The test cylinder is partially immersed in the reservoir where the fuel is located and the cylinder rotates through the reservoir at a

fixed speed. The cylinder remains wet with fuel while the fuel is continuously applied to the ball/cylinder interface region. The wear scar generated on the stationary ball is measured in millimeters and is a measure of the fuel's lubricating qualities.

All of the tests mentioned are run in an effort to discover how close to ideal a fuel is when measured against a derived set of specs. The numerous factors affecting a fuel's performance must always be tested to continually place the safety factor on a pedestal. Whether the tests are being run to probe for compounds in a fuel, to analyze gum formation, or to look at the volatility to certain types of reactions, they are all being done to ensure that such dangers, such as the extreme case of engine failure, are avoided.

WORKS CITED

ASTM Method D445-88, "Standard Test Method for Kinematic Viscosity of Transparent and Opaque Liquids," 1992 Annual Book of ASTM Standards Vol. 05.01, pp. 154-159.

ASTM Method D5001-90a, "Standard Test Method for Measurement of Lubricity of Aviation Turbine Fuels by the Ball-on-Cylinder Lubricity Evaluator (BOCLE)," 1992 Annual Book of ASTM Standards Vol. 05.03, pp. 757-762.

Grinstead, Rebecca. "Evaluation of JP-8+100 Additives by the Isothermal Corrosion Oxidation Test and the Microcarbon Residue Test." UDR-TR-94-85, May 1994.

SEGMENTATION OF AN M-60 TANK FROM A HIGH-CLUTTER BACKGROUND

Mark E. Jeffcoat
High School Apprentice
Advanced Guidance Branch

Wright Laboratory Armament Directorate
WL/MNGA
Eglin AFB, Florida 32542-5434

Final Report for:
High School Apprenticeship Program
Wright Laboratory Armament Directorate

Sponsored by:
Air Force Office of Scientific Research
Bolling Air Force Base, Washington, D.C.

SEGMENTATION OF AN M-60 TANK FROM A HIGH-CLUTTER BACKGROUND

Mark E. Jeffcoat
High School Apprentice
Advanced Guidance Branch

Abstract

This paper discusses three methods used in the attempted automation of the segmentation of M-60 tanks from a highly cluttered background. The first and least successful procedure used standard image processing tools. The second method, by neural networks, was not conclusively demonstrated to perform any better. The third method, segmenting pixels by comparing them to an ideal, proved to be most effective, but requires further processing to complete the segmentation.

Introduction

Pictures of an M-60 tank were taken from 360 different angles and declinations. The tank was resting on a turntable covered by a black tarpaulin, which was mounted on railroad tracks, and was surrounded by vegetation. The black tarp was intended to make the processing of the image easier; it did so, but the tracks and vegetation outside the tarp still created serious problems. Most projects using the images needed them without the background. The tarp made manual separation fairly simple, though time consuming, but the tracks and vegetation made automated separation extremely difficult. Three different methods of image segmentation were attempted, with varying degrees of success.

Apparatus

The implementation of each segmentation algorithm was done either in the C programming language or in Khoros, a visual image

processing language from the University of New Mexico. Khoros also provided standard image processing tools. The software ran on a Sun SPARCstation 2, in a UNIX environment.

A Macintosh IIx did the word and neural network processing. NeuralWare's NWorks Professional II/PLUS did all the neural network testing.

Methodology

The first method attempted was to use standard image processing tools to extract the tank. The basic tool was an algorithm that would label regions in an image; the problem was to clearly define the regions. In some cases a gradient function could sharpen the borders, especially if the tank had a very simple outline, as in figure 1. The labeling routine is rather simpleminded, and needed all the help it could get. It attempts to place pixels into regions by comparing the values of a pixel to its neighbors. As the shape of the tank gets more complicated, or does not fall into an easily defined block (figure 2), such tools tend to become even less effective.

Figure 1.

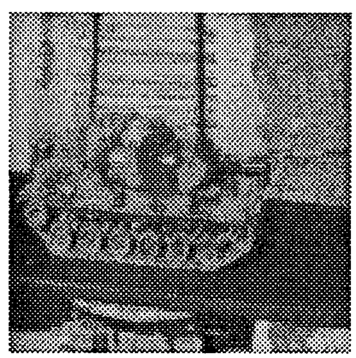

Figure 2.

Segmentation procedure that worked well on one image tended not to work well on others, especially when the differences were significant (Figures 1 and 2). Procedures had to be designed

for a small class of images, and would not apply generally. Automation would be of little benefit in such a situation.

Data for each of the last two methods was also taken from routines provided spatial and fractal information about an image. The spatial routine performs feature extraction by comparing pixels with the mean pixel value. The fractal routine assigns a fractal dimension to each pixel using the Hurst Dimensional Estimate. Fractal dimension data is usually useful in distinguishing artificial from natural objects, a quality very useful in this sort of problem.

The second approach to the problem was the backpropagation-trained neural network. The nets used data from the original, fractal, spatial, and labeled images. Simple networks did not perform well in classifying the pixels, so more complicated ones attempted the problem. Some of the more complicated networks were also given data about the surrounding pixels as well as the pixel itself. However, the processing power of the Macintosh was not quite up to the task, and UNIX software that would meet the specifications of this project did not exist. The software written specifically for this purpose never quite made it into existence, and further neural network testing will need to wait until software is available.

The final method, the most promising, was rather simple. The values of the pixels in the image were summed to find a mean value. Mean values were also found for the fractal, spatial, and labeled images. These were the values for an ideal tank pixel. Pixels in the image to be segmented were compared to the ideal by finding the square of the Euclidean distance in 4-space from the ideal. This error was assigned to each pixel, producing figure 3.

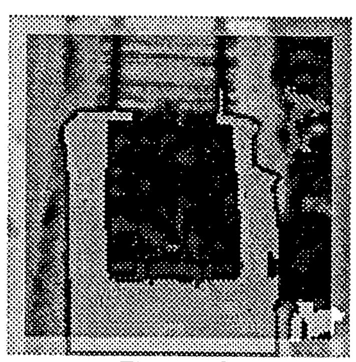

Figure 3.

The image was then segmented with a threshold, cutting out pixels whose error value was too high to be a tank. The result (after overlaying the original image onto pixels identified as part of the tank) was figure 4.

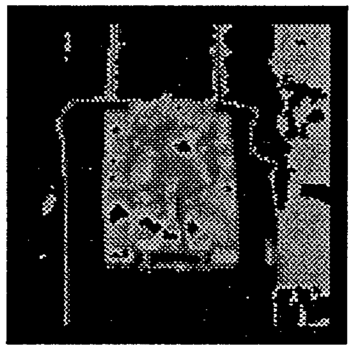

Figure 4.

The outline of the tank is very well distinguished from the background, and the large area that managed to convince the threshold that it really was part of the tank should be removable by conventional techniques.

Further Research

Neural networks have shown enough promise that their effectiveness should be tested further. The third method may also improve by being provided more data, e.g. values for the surrounding pixels, or by dragging in actual statistical methods and using pixel deviation from the mean tank pixel to classify. Also, tests should be conducted to determine what information about the tank pixel is most important in classifying it as such.

CARBON-CARBON PRIMARY STRUCTURES TEST

Andrew J. Konicki

Kettering-Fairmont High School
3301 Shroyer Road
Kettering, Ohio 45429

Final Report for:
High School Apprenticeship Program
Wright Labs

Sponsered by:
Air Force of Scientific Research
Bolling Air Force Base, Washington D.C.

and

Wright Labs

August 1994

CARBON-CARBON STRUCTURES TEST

Andrew J. Konicki
Kettering-Fairmont High School

Abstract

The application of heat and pressure to Carbon-Carbon (C-C) is being studied. The primary objective of this test is to demonstrate the application of advanced C-C materials to full-scale, high temperature, hypersonic vehicle primary structures, such as aircraft.

CARBON-CARBON STRUCTURES TEST

Andrew J. Konicki

Introduction

C-C was first used years ago in and around the exhaust area in aircraft where intense heat and pressure would build up. C-C can take this type of heat and pressure because it is a very strong material made of graphite yarn, similar to the pattern of plywood. The only problems with C-C is that it is expensive and oxidizes easily without a special coating.

Today the Air Force is using C-C on wings and other parts of an aircraft because of the high speeds some aircraft can reach. With high speeds comes friction and with friction comes heat.

The tests we are running will tell us just how much heat and pressure C-C can handle before breaking apart.

Problem

The Air Force needed some sort of material that could withstand the intense heat and pressure that friction was causing. They

came up with C-C. C-C would be used in aircraft that could reach speeds of Mach 3 or higher.

The Air Force needs us to test their new material to find out just how much heat and pressure this material could take.

Methodology

First we put strain gages and thermocouples on the C-C and then heat the specimen up to 2200°F. We get readings from the strain gages and thermocouples attached to the specimen; which tells us how much heat and pressure the specimen is under. After that, we compare those readings with the predicted readings from Boeing Aerospace Corporation. The comparison of the readings will tell us if the specimen is under too much or too little heat and or pressure.

By running the C-C through this test, we will find how much heat and pressure an aircraft made from C-C can withstand.

Results

There are no results or conclusions at this point in time because the test will not be completed until sometime next

year.

THE EFFECTIVENESS AND ACCURACY OF CADRA SOFTWARE

BARRY KRESS

WRIGHT LABORATORY
101 W EGLIN BLVD
EGLIN AFB, FL. 32542-6810

FINAL REPORT FOR:
HIGH SCHOOL APPRENTICESHIP PROGRAM
WRIGHT LABORATORY

SPONSORED BY:
AIR FORCE OFFICE OF SCIENTIFIC RESEARCH
BOLLING AIR FORCE BASE, WASHINGTON, D.C.

AUGUST 1994

THE EFFECTIVENESS AND ACCURACY OF CADRA SOFTWARE

BARRY KRESS
HIGH SCHOOL APPRENTICESHIP PROGRAM
AEROBALLISTICS SECTION
WRIGHT LABORATORY ARMAMENT DIRECTORATE

ABSTRACT

The purpose of these tests is determine the accuracy and effectiveness of software that locates the spatial position and angular orientation of a free-flight projectile. This software system is referred to as Cadra. The Cadra software is designed to decrease the time it takes to reduce the trajectory data received from testing projectiles at the Aeroballistic Research Facility(ARF). Results indicate that the Cadra software tested, which is still in its' developmental stage, needs to have some corrections made to it. However, these tests suggest that the logic behind the system is sound, and once a few errors are corrected the system should be operational.

THE EFFECTIVENESS AND ACCURACY OF CADRA SOFTWARE

BARRY KRESS

INTRODUCTION

The Aeroballistic Research Facility(ARF) is used to test free-flight projectiles in order to extract their trajectory data. This data is acquired through the use of 100 infra-red activated cameras that take pictures focused on the shadows of free-flight projectiles cast on a screen(see figure 1). These pictures are referred to as shadowgraphs. There are 50 stations in the ARF, each containing two cameras and two screens. One camera rests in the pit and takes its picture against a screen placed on the ceiling. The other camera is situated in the hall and takes its picture against a screen placed on the wall directly in front of it. In front of the each screen are two parallel wires that are kept in constant alignment. These two wires each contain two "reference" beads. Under the current system the film of these shadows is taken to the Math Lab where the projectile's movement is determined by recording its orientation with respect to the four reference beads. This data is then placed in a file called a tunnel file. It is then possible to take that tunnel file into another software program and determine the aerodynamic properties of that projectile. Currently it takes over a week to get this tunnel file back from the Math Lab.

The Cadra software tested is really a combination of several different programs. The first part of the Cadra system consists of a digitizer(ccd camera) that is used to transform a scanned in piece of film into a computer data file containing a grid of pixels. After scanning in the film from all the stations, another part of the Cadra system takes the pixel data and translates that into the trajectory data. The current Cadra system requires the manual scanning in of each piece of film on a EKTRON scanner and clicking onto the four reference beads as well as four reference points on the shadow. Eventually digital cameras will be utilized that will electronically send all the necessary data to an updated, fully automatic Cadra version that will not require any manual input of reference points. This new version would reduce the time needed to receive aerodynamic results down to a few minutes. Even the current manual Cadra version significantly reduces the time it takes to receive a tunnel file.

METHOD OF EVALUATION

To evaluate the Cadra system, we took a set of projectile flights we had previously analyzed by our old system and reanalyzed them using the new Cadra system. Thus, all projectiles chosen for the evaluation of the Cadra software already had tunnel files from the Math Lab. Also, all the projectiles chosen had their trajectory data reduced to determine their aerodynamic coefficients in a software program called ARFDAS. In each case, the film that the Math Lab used to make its tunnel file was the same film scanned into the Cadra program. These previously made tunnel files from the Math Lab were used in all comparisons unless otherwise noted. The first projectiles chosen for evaluation were a series of cone cylinder flares. Ten shots were manually scanned into the Cadra program, and 10 tunnel files were created. These tunnel files were then run through ARFDAS. Using the Cadra tunnel files as an input, ARFDAS computed a mach number very close to the one received from the Math Lab's tunnel file. However, there was a difference in the angle outputs received from the two tunnel files. At this point, we thought one possible cause for the angle error was the unique shape of the projectiles in conjunction with very small angle changes. Therefore, a new projectile was chosen to test the accuracy of the Cadra software. A 20mm bullet was chosen because of its relatively straight shape. The film from this one shot was scanned in twice, and was saved separately in order to test the repeatability of Cadra. We wanted to see if Cadra's repeatability was going to be at least equal to that of the Math Lab, necessitating a "double reading". Once again after running the Cadra tunnel file there was a noticeable difference between the angles calculated by ARFDAS using the Math Lab tunnel file, and the Cadra tunnel file. We then decided to test one more projectile in order to find the origin of the angular problems. The criteria we used for choosing the next projectile was broadened to not only consider the projectiles overall shape, but also to consider large angular changes for easier comparison. The PGU-38 was chosen because it was felt that it matched the criteria very well. One shot was scanned into Cadra and the subsequent tunnel file was created. Again a difference in output angles was discovered.

DISCUSSION OF RESULTS

The resulting differences in angle outputs definitely was found to be originating from the process of going from the shadowgraphs to the tunnel file. In order to determine if the error occurred when manually scanning in the film, or in a computer calculation within the Cadra program, a FORTRAN program was written that prints the difference between each respective value found in the Math Lab and Cadra tunnel files. This comparison was made between the spatial positions(x,y,&z) and the angular orientations(m&n) using time as the reference point(see figure 2). The output of this FORTRAN program reveals that the x,y,and z values of both tunnel files were relatively close(see figure 3). However, the difference between the two tunnel file angular orientations(m&n) is sometimes greater than the angles themselves, and of course far exceeds our measuring accuracy. In order to be sure that there was only a problem with the Cadra angular calculations and not repeatability, we sent the 20mm film back to the Math Lab to have a new tunnel file made. We then took the two Math Lab tunnel files for the 20mm shot and ran them through the same FORTRAN comparison program. The repeatability of the x,y,and z is very similar to that of Cadra's repeatability of x,y, and z. However, the repeatability of the angles from the Math Lab tunnel files is far greater than that of the repeatability of the angle outputs within the Cadra program. At this point we are fairly certain of an angular calculation problem within Cadra, but are still unsure of its exact origin. The new Math Lab tunnel file angles were found to be within our measuring accuracy of their original counterparts, therefore convincing us that the Cadra angle errors were a product of incorrect calculations. A raw data plot of theta and psi(which are directly related to m&n) was then printed using a Cadra tunnel file as the input. The resulting graph pinpointed an angular problem. All of Cadra's theta's were negative and all the psi's were positive (see figures 4&5). Figure 4 shows the raw data plot of the 20mm bullet with the Math Lab angles represented in the top graph and Cadra's angles shown in the bottom graph. Figure 5 shows the raw data plots of the PGU-38 25mm bullet with the Math Lab values again shown in the top graph, and Cadra's angles displayed in the bottom graph. The true angles (theta and psi) should each encompass two quadrants(like the Math Lab raw data plots demonstrate). Also, because the two graphs in each figure represent angle data from the same exact shot, then the angular values would be exactly the same. Therefore, since the angular differences far exceed our

measuring accuracy, angle calculation errors must be present. To satisfy ourselves that the only problem with the Cadra software was with the angle calculations and not also in the digitizing process we converted the "spreadsheet" of the scanned in pixel values from the Cadra digitizer into the same format the Math Lab uses as the input for its tunnel file program. This conversion was then sent to the Math Lab to be run through their tunnel file calculations. We hope that when compared to the original Math Lab tunnel file, the values from the new tunnel file will be found to only differ within our measuring accuracy. If so, then the problem was definitely narrowed down to the angular calculations.

CONCLUSIONS

The current Cadra software cannot be used to make accurate tunnel files from the film of free flight projectiles because of problems with angular calculations. Once the calculations are corrected, further testing will be required to determine the accuracy and effectiveness of Cadra software. If found to be reliable, the Cadra software will greatly reduce the cost and time it takes to evaluate free-flight projectiles.

ACKNOWLEDGMENTS

First of all I would like to thank the Department of Defense for the opportunity to work in this program. Secondly, I would like to thank Don Harrison, Mike Deiler, and especially Glenda Apel for sponsoring this program and for always ready to lend a hand to help. Thirdly, I would like to thank all the guys at MNAA for making my summer really enjoyable. Thank you: Greg, Clay, Jerry, Wayne, AL, John, John, Tim, JJ, and Patty, for helping me whenever I needed it. Fourth, I would like to thank Mike Valentino for helping me all summer with my project and answering any questions I had. Most of all I would like to thank all the other apprentices for two summers of great fun and friendship. Thank you all for making work so enjoyable.

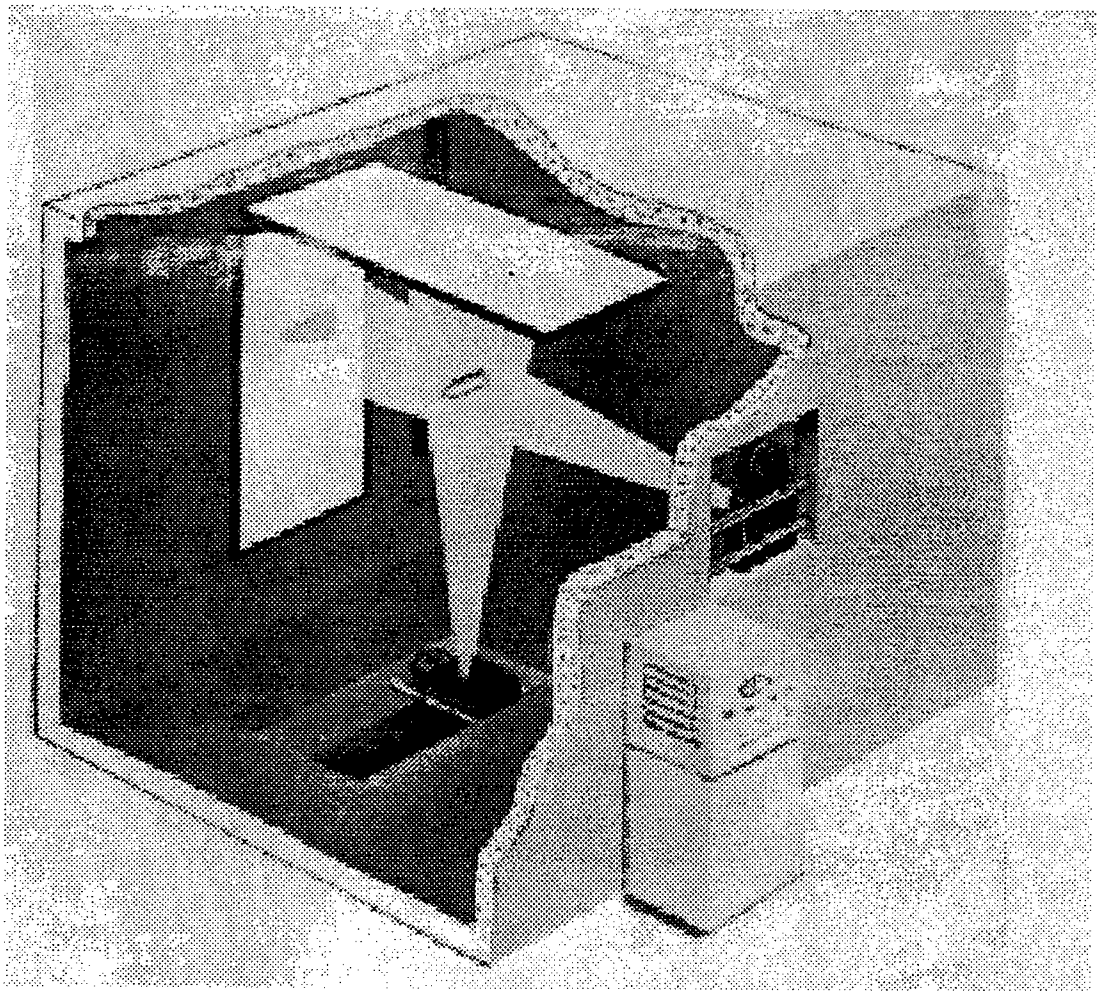

Figure 1. Typical Shadowgraph Station

```
      PROGRAM BARRY

c *** this program compares the math lab tunnel files with cadras
c     tunnel file; compares time,x,y,z,m,n ***

CHARACTER SNAME*20
      CHARACTER SNAME2*20
      OPEN (1,FILE='c:\abk\930914.org', STATUS='UNKNOWN')
      OPEN (2,FILE='C:\ABK\M55RERED.DAT',STATUS='UNKNOWN')
      OPEN (3,FILE='C:\ABK\compare.dat',STATUS='UNKNOWN')
      READ (1,9)SNAME
      READ (2,9)SNAME2
    9 FORMAT (1X,A10)
      DO 10 I=1,50
      READ (1,8) T1,Y1,Z1,X1,A1,B1
      IF (T1 .EQ. 200.) STOP
C      IF (I .EQ. 1) THEN
C      T=T1
C      Y=Y1
C      Z=Z1
C      X=X1
C      A=A1
C      B=B1
C      ENDIF
C      T1=T1-T
C      Y1=Y1-Y
C      Z1=Z1-Z
C      X1=X1-X
C      A1=A1-A
C      B1=B1-B
      READ (2,4) T2,Y2,Z2,X2,A2,B2
    8 FORMAT (F10.7,3(F9.4),2(F8.5))
    4 FORMAT (F10.7,3(F9.4),2(F8.5))
C      IF (T1 .GT. 0) THEN
      DIFFT3=(T1-T2)
      DIFFY3=(Y1-Y2)
      DIFFZ3=(Z1-Z2)
      DIFFX3=(X1-X2)*12
      DIFFA3=(A1-A2)
      DIFFB3=(B1-B2)


C      ENDIF
      WRITE (3,7) T1,DIFFT3,DIFFY3,DIFFZ3,DIFFX3,DIFFA3,DIFFB3
    7 FORMAT( 7G12.5)
   10 CONTINUE
      END
```

Figure 2. FORTRAN Program Used in All Comparisons

930914.ORG VS. M55RERED.DAT
MATH LAB 20MM VS. MATH LAB 20MM (REREAD)

				CHANGE IN		
	T	Y	Z	X	M	N
.42989	.00000	-.29755E-03	-.22011E-02	-.72041E-02	-.94400E-02	.27000E-03
.43142	.00000	.65002E-02	-.11400E-01	-.23998E-01	.17000E-02	-.12720E-01
.43297	.00000	.60005E-02	.10300E-01	.11902E-02	-.12250E-01	.11200E-02
.43603	.00000	.15198E-01	-.16199E-01	-.19203E-01	.92000E-03	-.51900E-02
.44224	.00000	.21099E-01	.18997E-02	-.15610E-01	-.15100E-02	-.26000E-03
.44533	.00000	.16197E-01	.72002E-02	.72327E-02	-.15000E-02	-.35600E-02
.44838	.00000	.61989E-02	-.39997E-02	-.21606E-01	.26000E-03	.67800E-02
.45142	.00000	.95978E-02	.12100E-01	-.72327E-02	-.19200E-02	-.64800E-02
.45775	.00000	-.12501E-01	-.65401E-01	-.18036E-01	-.73500E-02	-.66800E-02
.46398	.00000	-.30975E-02	.11499E-01	-.60425E-02	-.42100E-02	-.50800E-02
.46716	.00000	.13199E-01	-.16699E-01	.20416E-01	-.25000E-02	-.47200E-02
.47033	.00000	.13008E-02	.23003E-02	-.10986E-02	-.58700E-02	.37900E-02
.47350	.00000	.16975E-02	.21400E-01	.10803E-01	.25300E-02	-.59200E-02
.47506	.00000	.21019E-02	-.88997E-02	.19226E-01	.27000E-02	-.33700E-02
.48141	.00000	.10399E-01	.44003E-02	.10803E-01	.15600E-02	-.20200E-02
.48461	.00000	-.19836E-03	-.10401E-01	-.17944E-01	-.34700E-02	-.28400E-02
.48621	.00000	.81978E-02	-.14500E-01	.84229E-02	-.59100E-02	.14500E-02
.49399	.00000	.57983E-02	-.65994E-02	.84229E-02	.13000E-03	.68000E-03
.49729	.00000	-.17014E-02	.33016E-02	.71411E-02	-.78000E-02	.70000E-03
.50051	.00000	.75989E-02	.18005E-02	.10803E-01	.29100E-02	-.56100E-02
.50692	.00000	.58100	-.68380	-.46875E-01	-.13300E-01	.14230E-01
.51028	.00000	-.93002E-02	.40054E-03	-.10986E-01	.54300E-02	-.51100E-02
.51512	.00000	-.14992E-02	-.12901E-01	-.46509E-01	.37400E-02	-.14500E-02
.52002	.00000	-.81978E-02	-.12999E-01	-.20508E-01	-.66700E-02	.12600E-02
.52496	.00000	-.11600E-01	-.42992E-02	-.98877E-02	.40700E-02	-.62600E-02
.52978	.00000	.14992E-02	-.22301E-01	-.69580E-02	-.59500E-02	.82300E-02
.53485	.00000	.10399E-01	-.42992E-02	-.95215E-02	.56500E-02	.56000E-03
.53986	.00000	-.10300E-01	.29945E-03	-.25635E-02	-.46100E-02	-.35000E-03
.54983	.00000	.51994E-02	.20000E-01	.22705E-01	.70200E-02	.61600E-02
.55487	.00000	-.14400E-01	.46005E-02	.15747E-01	-.22500E-02	-.36700E-02
.55986	.00000	-.32005E-02	-.67997E-02	-.25635E-02	-.26500E-02	.17300E-02
.56492	.00000	.17700E-01	.20027E-03	-.36621E-02	-.11190E-01	.55100E-02
.57004	.00000	-.85983E-02	-.79918E-03	.10620E-01	.40000E-04	.66900E-02
.57510	.00000	-.69809E-03	-.94986E-02	-.12085E-01	.89200E-02	.23700E-02
.58534	.00000	-.59967E-02	-.12300E-01	-.20508E-01	-.97000E-03	-.35000E-03
.59049	.00000	.87051E-02	-.46997E-02	-.73242E-02	.36500E-02	.26400E-02
.60607	.00000	-.78049E-02	.77000E-02	-.20508E-01	-.30300E-02	-.78400E-02
.61130	.00000	-.23041E-02	-.46005E-02	.00000	.41800E-02	.91000E-03
.62000	.15020E-04	-.27298E-01	-.16901E-01	-.19043E-01	.47500E-02	-.19600E-02
.63594	.00000	.32700E-01	-.49099E-01	-.35889E-01	.47300E-02	-.47000E-02
.64109	.00000	.69962E-02	.84000E-02	-.25635E-01	.64000E-02	-.32700E-02
.64654	.00000	.21896E-01	-.45700E-01	.13770	-.84700E-02	-.70000E-02

Figure 3. Output From FORTRAN Comparison Program

S930914

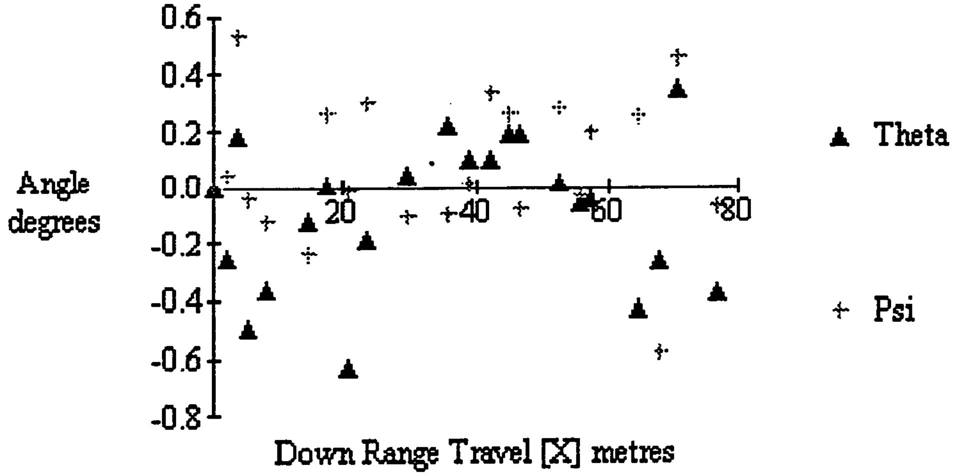

S010914

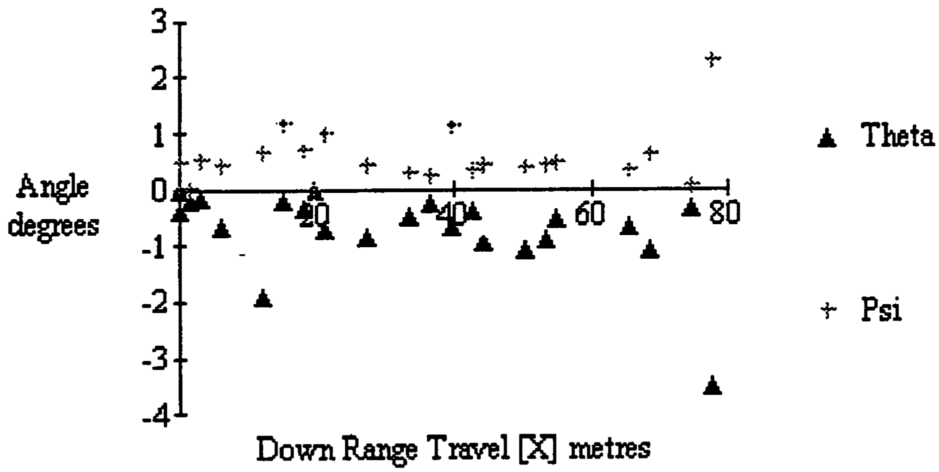

Figure 4. Raw Data Plots from 20MM Bullet Math Lab and Cadra Tunnel Files

S921183

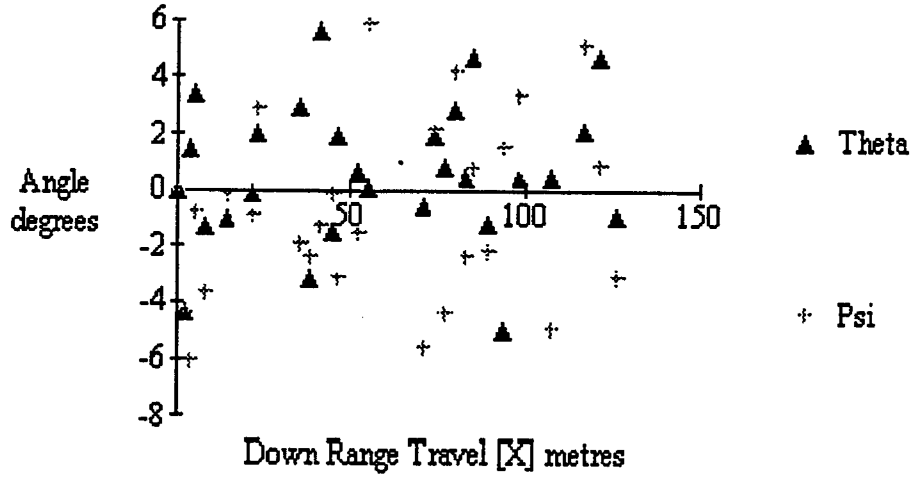

S011183

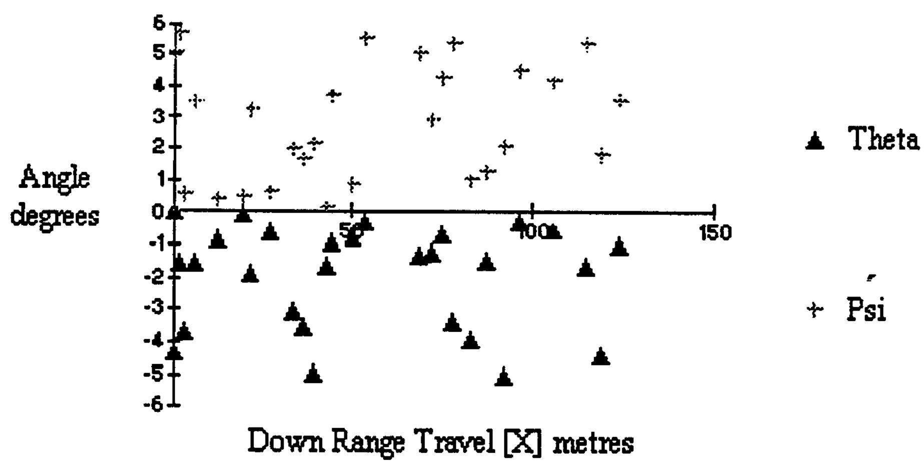

Figure5. Raw Data Plots from PGU-38 25MM bullet
Math Lab and Cadra Tunnel Files